Austrian Journal of Technical and Natural Sciences

№ 9–10 2016
September–October

«East West» Association for Advanced Studies and Higher Education GmbH

Vienna
2016

Austrian Journal of Technical and Natural Sciences

Scientific journal

№ 9–10 2016 (September–October)

ISSN 2310-5607

Editorial office European Science Review
"East West" Association for Advanced Studies
and Higher Education GmbH, Am Gestade 1
1010 Vienna, Austria

Email: info@ew-a.org

Homepage: www.ew-a.org

Austrian Journal of Technical and Natural Sciences is an international, German/English/Russian language, peer-reviewed journal. It is published bimonthly with circulation of 1000 copies.

The decisive criterion for accepting a manuscript for publication is scientific quality. All research articles published in this journal have undergone a rigorous peer review. Based on initial screening by the editors, each paper is anonymized and reviewed by at least two anonymous referees. Recommending the articles for publishing, the reviewers confirm that in their opinion the submitted article contains important or new scientific results.

East West Association GmbH is not responsible for the stylistic content of the article. The responsibility for the stylistic content lies on an author of an article.

Instructions for authors

Full instructions for manuscript preparation and submission can be found through the "East West" Association GmbH home page at: http://www.ew-a.org.

Material disclaimer

The opinions expressed in the conference proceedings do not necessarily reflect those of the «East West» Association for Advanced Studies and Higher Education GmbH, the editor, the editorial board, or the organization to which the authors are affiliated.

East West Association GmbH is not responsible for the stylistic content of the article. The responsibility for the stylistic content lies on an author of an article.

Included to the open access repositories:

Typeset in Berling by Ziegler Buchdruckerei, Linz, Austria.
Printed by «East West» Association for Advanced Studies and Higher Education GmbH, Vienna, Austria on acid-free paper.

Section 1. Biology

DOI: http://dx.doi.org/10.20534/AJT-16-9.10-3-5

Zhurlov Oleg Sergeevich,
Institute of Cellular and Intracellular Symbiosis
of the Ural Branch of the Russian Academy of Sciences,
Orenburg, Russia
E-mail: jurlov1968@mail.ru

Hydrophobic properties of bacteria: interspecific and pathovariant differences

Abctract: A comparative analysis of hydrophilic-lipophilic balance of bacteria depending on the species, ecotype and pathovariant specificity. The degree of hydrophobicity of the bacterial surface is exposed to a statistically significant influence of taxonomic and eco-variant specificity. The pathovars of bacteria isolated from the foci of pyo-inflammatory diseases of soft tissues are much less hydrophobic than the bacteria living on the mucous membranes.

Keywords: bacteria, physicochemical properties, hydrophilic-lipophilic balance.

Hydrophobic interactions causing the adhesion on the epithelium or phagocyte often do not depend on the molecular specificity between the bacterial superficial components or on the «molecular texture» of two surfaces. The process of hydrophobic interactions can be presented as a phenomenon of movement of nonpolar groups of molecules from water to hydrophobic areas created at the expense of association of nonpolar groups [1]. From the point of physical chemistry, the surface of a bacterial cell is inhomogeneous and represented with a big number of hydrophilic and hydrophobic sites [2], which can participate in both, the processes of intercellular interactions and during the interaction with different abiotic surfaces and molecules.

Today, the relevancy of the study of the phenomenon of hydrophobic interactions is related to the development of nanotechnological systems of drug delivery based on polymers and micro-particles, to the studies of non-specific adhesion of bacteria to the abiotic surface (formation of biofilms), to the modification of superficial structures of bacterial cell by the opsonins of serum [3], to the selection of bacteria with special physico-chemical properties of the surface [4].

However, despite this, the use of the indicator of hydrophobic behavior of the bacterial surface does not have a unified scale of measurement. Often, specialists of different areas of knowledge have to use different methods of measurement of hydrophobic behavior, which affects the comparison of experimental data obtained with the help of different methods of measurement of hydrophobic behavior. The disagreements with regard to both, the exact nature of hydrophobic interactions [5] and basic method of measurement of bacterial hydrophobic behavior [6; 7] remain among scientists.

In this respect, the aim of our research was the analysis of physico-chemical properties of bacteria depending on their taxonomic and pathovariant specificity with the help of division of bacteria in two-phase system «polyethyleneglycol/dextran».

Materials and methods of research

The study of the hydrophobic behavior of the surface of bacteria was conducted on the sample consisting of 311 strains of pathogenic and opportunistic gram-positive and gram-negative bacteria: 38 strains of S.aureus and 36 strains of coagulase-negative staphylococci (secreted from the air of closed space, from bacteria carrier and from wound fluid of the patients with pyo-inflammatory diseases of soft tissues); 34 strains of Enterococcus faecalis (secreted from the motions of healthy people and in diabetic conditions of the bowel, as well as wound fluid in different pyo-inflammatory diseases); 118 strains of E.coli (secreted from the motions of the patients with

dysbiotic disruptions of the bowel microflora, from wound fluid in wound infections as well as from the water of utility-drinking purpose); 11 clinical isolates of N.gonorrhoeae secreted in gonorrhea; 15 strains of K.pneumoniae, 15 strains of S.flexneri and 14 strains of S.enteritidis excreted from the motions of the patients with acute intestinal infections and bowel dysbiosis.

To measure the hydrophobic behavior of the surface of bacterial cells, the method of two-phase division of bacterial suspended material in the system «polyethylene glycol PEG 6000 — dextran T500» was applied [8]. Optical density of upper (PEG 6000) and lower (dextran T500) phases were measured on the spectrophotometer at the wavelength of (λ=540 nm). The hydrophobic behavior was expressed in the form of hydrophilic-lipophilic balance (HLB=Lg [$OD_{PEG}/OD_{Dextran}$]) of the surface. The degree of HLB was expressed in absorbance units (a. u.).

The obtained results were subject to statistical processing by the methods of variation statistics. To reveal statistically significant differences in the compared groups of observations, the parametrical criterion of Student-Fischer test, parametrical one-factor and two-factor dispersion analysis were used. The differences were considered significant at the level of error probability not exceeding 5% ($p<0.05$) [9].

Results of the research

The results of the definition of the hydrophilic-lipophilic balance in the listed groups of bacteria averaged depending on their taxonomic specificity certify that moderately expressed hydrophobic behavior of the cellular surface was typical for the bacteria E.coli (mean level of HLB is –0,003±0,062 a. u.), S.aureus (0,021±0,042 a. u.), ABB group (–0,119± 0,099 a. u.), as well as enterococci (0,144±0,033 a. u.) and Neisseria (gonococci — 0,006±0,041 a. u.). However, it could not be said in respect of a range of representatives of the family Enterobacteriaceae, which were characterized by a significantly higher degree of hydrophobic behavior. Thus, the strains of S.enteritidis (1,546±0,177 a. u.) and S.flexneri (1,271±0,122 a. u.) showed the highest hydrophobic behavior among all researched bacteria. The lowest degree of hydrophobic behavior was shown by K.pneumoniae HLB (–0,364±0,183 a. u.) secreted from the patients with acute intestinal infections and bowel dysbiosis.

In order to detect taxonomic (species) specificity of the researched bacteria with regard to their hydrophobic properties, dispersion analysis based on the comparison of intragroup and intergroup variability of features (HLB) was applied. The results of the analysis indicate expressed relation of the hydrophilic-lipophilic balance of the surface of bacteria with their taxonomic specificity (F=76,7; P<0,001).

Expressed hyper-variability of the studied feature accompanying all analyzed groups of bacteria draws attention. Such fact, related to multiple determination of HLB, in our opinion, indicates the need for a more detailed analysis of the regularities of the hydrophobic behavior expression: not only due to taxonomic specificity, but also depending on the source of bacteria excretion (pathovariant differences).

Thus, the strains of S.aureus isolated with the mucous of nasal passages of healthy bacteria carriers differed in higher degree of hydrophobic behavior (0,130±0,036 a. u.) compared with the isolates from the fluid in pyo-inflammatory diseases (–0,176±0,059 a. u.; P<0,05).

Same nature of distribution of the feature was registered for coagulase-negative staphylococci (0,214±0,088 a. u. against –0,119±0,143 a. u.; P<0,05). Similar regularity was found for the strains of Escherichia coli, the pathovars of which, inhabiting the mucous (motions and uro-pathogenic), showed significantly big hydrophobic behavior of the surface compared with the pathovars secreted from the foci of pyo-inflammatory processes of soft tissues. Enterococci, in the whole, more hydrophobic, also showed lower hydrophobic behavior of the surface if they were isolated from the wound fluid or infection focal in pyo-inflammatory diseases of soft tissues (0,117±0,073 a. u.; for the differences of other groups of enterococci F=10,72, P<0,05), compared with the strains secreted from the motions of healthy people (0,181±0,032 a. u.). However, for this group of bacteria, the lower levels of HLB were noted in the strains secreted from the motions in dysbiotic bowel disturbances (0,039±0,133 a. u.).

Described regularities related to the eco-variant differences of the bacteria in hydrophobic behavior certify about the relatively higher level of HLB of gonococci (0,006±0,041 a. u.), salmonella (1,546±0,177 a. u.), shigella (1,271±0,122 a. u.) isolated in the infections, in the pathogenesis of which, the phenomenon of adhesion to the mucous membranes of macro-organism takes an important place.

The influence of the epitope of habitation/secretion of the bacteria as well as taxonomic specificity on their hydrophobic behavior was proved in the use of the procedure of dispersion analysis and turned out to be statistically significant at the high level of accuracy (F=15.99; P<0,001).

Eco-variant differences, as it is known, are described for almost all biological properties of bacteria, in anyway related to the pathogenicity manifested by them.

These very regularities in the expressiveness of the features of pathogenic and opportunistic bacteria are frequent evidence of the contribution of this or that phenoand/or genotypical phenomenon to the appearance and development of pathological processes.

Discussion

Summarizing the description of the general regularities of variation of hydrophobic behavior of bacteria depending on taxonomic and pathovariant specificity, one can say that the application of unified methodical way (division of bacteria in two-phase system of water solutions of polymers «polyethylene glycol/dextran») and definition of hydrophobic behavior at the wide circle of cultures of pathogenic and opportunistic bacteria showed significant variability of hydrophobic behavior of the native bacterial cells. The degree of hydrophobic behavior of the bacterial surface is subject to the statistically significant effect of both, taxonomic and eco-variant specificity. The pathovars of bacteria isolated from the foci of pyo-inflammatory diseases of soft tissues, are significantly less hydrophobic compared with the pathovars inhabiting (parasitizing) the mucous membranes.

References:

1. Езепчук Ю. В. Патогенность как функция биомолекул/АМН СССР. – М., Медицина, – 1985. – 240 с.
2. Beveridge T. J. The bacterial surface: general considerations towards desing and function//Can. J. Microbiol. – 1988. – V. 34. – P. 363–372.
3. Брудастов Ю. А., Гриценко В. А., Журлов О. С., Чертков К. Л. Характеристика гидрофобных свойств бактерий при их взаимодействии с сывороткой крови//Журнал микробиологии, эпидемиологии и иммунобиологии. – 1997. – № 4. – С. 73–77.
4. Журлов О. С. Метод получения и хранения бактерий со специфическими физико-химическими свойствами поверхности//Международный журнал прикладных и фундаментальных исследований. – 2015. – № 11. – С. 249–250.
5. Hildebrand J. H. Is there a «hydrophobic effect»? Proc. Natl. Acad. Sci. USA. – 1979. – V. 76. – P. 194.
6. Israelachvili J. N., Pashley R. M. Measurement of the hydrophobic interaction between two hydrophobic surfaces in aqueous electrolyte solutions//J. Colloid Interface Sci. – 1984. – V. 98. – P. 500–514.
7. Rosenberg M., Kjellenberg S. Hydrophobic Interactions: Role in Bacterial Adhesion//Adv. Microbiol. Ecol. – 1986. – V.9. – P. 353–393.
8. Magnusson K. E., Stendahl O., Tagesson C., Edebo L., Johansson G. The tendency of smooth and rough Salmonella typhimurium bacteria and lipopolysaccharide to hydrophobic and ionic interaction, as studied in aqueous polymer two-phase systems//Acta Pathol. Microbiol. Scand. (B). – 1977. – V.85. – P. 212–218.
9. Лакин Г. Ф. Биометрия, – М.: Высш. шк., – 1990. – 352 с.

DOI: http://dx.doi.org/10.20534/AJT-16-9.10-5-8

Kiçaj Hajdar,
University of Vlora "Ismail Qemali"
Faculty of Technical Sciences; Vlora, Albania
Prof. Asoc. Dr. in zoology;
E-mail: hajdarkicaj@yahoo.it
E-mail: hajdar.kicaj@univlora.edu.al
MSc. Shkurtaj Berlinda,
University of Vlora "Ismail Qemali"

Variations of body size of testudo hermanni in the area of Vlora, Albania

Abstract: The purpose of this paper is to study the body variations of the *Testudo hermani* turtle in the Vlora area. Morphometric study is done for individuals caught in the study area and later morphometric data of these indviduals are analyzed. For each of the areas, average values, higher values and lower ones are

compared in terms of morphometric measurements of Testudo hermanni. These values include curved carapace length (CCL), straight carapace length (SCL), plastron length (CPL), carapace width (CCW), plastron width (CPW), measured in mm. Based on morphometric measurements, the length of the carapace-SCL, but not only, juvenile individuals and adult individuals have been identified concluding the structure of the population. Body mass comparisons are made for the studied individuals in accordance with the collecting areas, evaluating the factors that lead to variations.

Keywords: Testudo hermanni, Carapace, plastron, morphological features, morphometric measurements.

Introduction

The systematic status of the *Testudo hermanni* turtle is negotiable by different authors. *Testudo hermanni* is assigned in the Eurotestudo gender by many authors [6, 805–807], while others have displaced the Mediterranean *Testudo hermanni hermanni* and the Balkanic *Testudo hermanni boettgeri* forms at the level of species and have recognized Dalmatian populations as third species, *Testudo hercegovinensis*.

The Mediterranean region is an important area of research for many biological aspects of turtle gender and especially *Testudo hermanni*, according to diversity [4, 535–536], ecology sexual dimorphism and morphological variation [1, 67–69].

Body size has a significant effect on the ecology and physiology, but the attention is focused more on the effects of body size rather than its causes. The size of the studied populations has a length difference of 46 mm in males and 94 mm in females of the *Testudo hermanni* turtle. *Testudo hermanni* is a sub-specie with highlighted sexual dimorphism. This is shown in the weight of the individuals, in the change of some characters like carapace length, plastron length, tail shape and size, form and placement of supercaudal scutes etc [3, 227–231].

Material and methodology

The studied area is a part of Vlora Region. Gathering places are determined in advance, based on climatic conditions, vegetation and other representative features of the area like height above the sea level, the presence or not of vegetation, soil types etc. The study was conducted in the region of Vlora over a year, from May 2015 to May 2016. Data collection is done in four collection stations: Kanina (1), Dukat (2), Llogara (3), Vranisht (4).

For each catched individual, morphometric measurements were performed and the data are compiled in a standard form. The data collection is based on the work methodology published by local and foreign authors. Measurement techniques are implemented in the field described by Stubbs et al. (1984). Turtles are captured by hand and later measured. For the analysis of biometric elements even dead animals from natural causes were analyzed. Gender is determined on the basis of external characteristics. They were distinguished by the shape of the external skeleton, the shape of the rear lateral scutes, width at anal and supracaudal level and shape and size of the tail [1, 67–68; 2, 445–446]. Adult-sized animals are considered males over 13 cm and females over 15 cm. The length of the carapace (SCL) has been considered too. A simple tailoring meter and a scaled ruler are used for measurements and an electronic scale is used for the weight.

Figure 1. Collecting areas

Results and discussion

1 Morphological characteristics variations

Out of 81 individuals that were studied, 75 were alive individuals and six dead individuals. Morphometric data were analyzed for all the collected individuals, of which 28 male, 47 females and six dead individuals. *Testudo hermanni* tortoises are sexually dimorphic in body size and shape. Males are smaller than females (12%). The rate of sexual dimorphism size did not depend on the average body mass. There are various hypotheses about the main causes of the body size variability, but the basic cause in the fluctuation of size between countries are the differences in mortality of adults, the cooperation with the ambient temperature closely related to other factors affecting forest habitats as fires, etc.. Individuals with the greatest length of the carapace (CCL) 270 mm belong to the Vranisht area. Individuals with the smallest length of the carapace (CCL) 155 mm was found in the Kanina

area (not including juvenile individuals). Morphometric data of studied individuals in the studied area were analyzed for average values, highest values and lowest ones in terms of morphometric measurements of *Testudo hermanni*. These values include curved carapace length-CCL, straight carapace length-SCL, plastron length-CPL, carapace width-CCW, plastron width-CPW, carapace height and are expressed in mm.

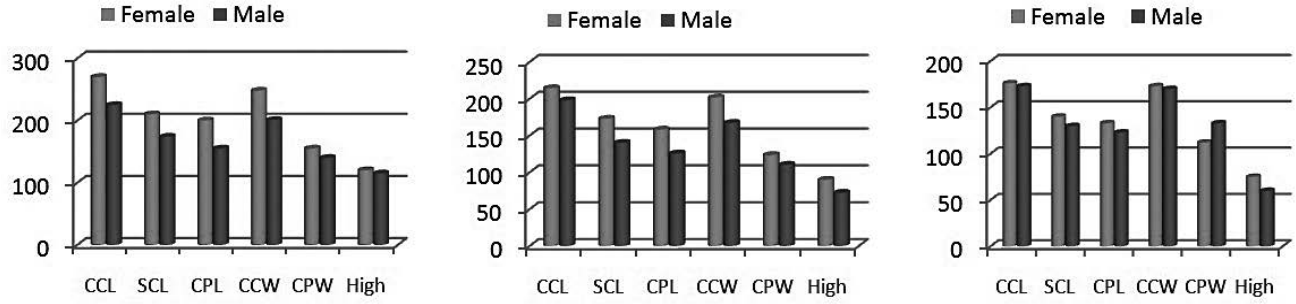

Chart 1. Comparison of the maximum, average and minimum values of the measurement characters Testudo hermanni

The graph above it shows that sexual dimorphism is visible in all biometric measurements performed on the studied individuals. These changes are also almost identical to individual groups of different areas.

Based on the length of the straight carapace -SCL, individuals are grouped in several classes: first class individuals with SCL < 15 cm for females and < 13 cm for males, second-class individuals with SCL from 15–20 cm for females and 13–18 cm for males and third class individuals with SCL > SCL 20cm for females and > 18 cm for males, which correspond respectively to juvenile individuals, adult individuals and sterile individuals.

Table 1. – Grouping of individuals by class

SCL-cm	<15	15–20	>20
Female%	14	74	12
SCL-cm	<10	13–18	>18
Male%	7.3	60.2	32.5

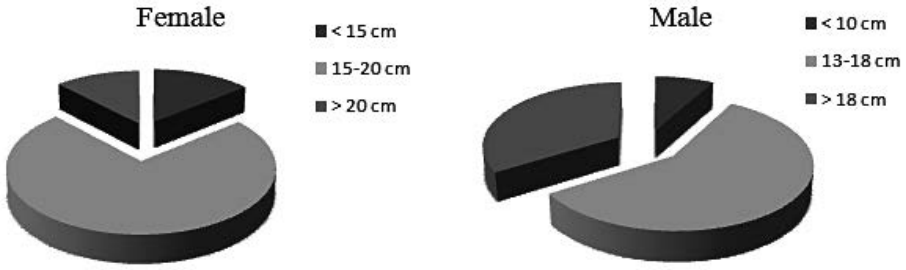

Chart 2. Male and female individuals grouping by grade%

2 Variations in body weight

From this study it is clear that in different areas there are significant weight changes in terms of the studied individuals. The following charts show the variation of body weight of the studied individuals, for minimum weight, maximum as well as their average weight by gathering places.

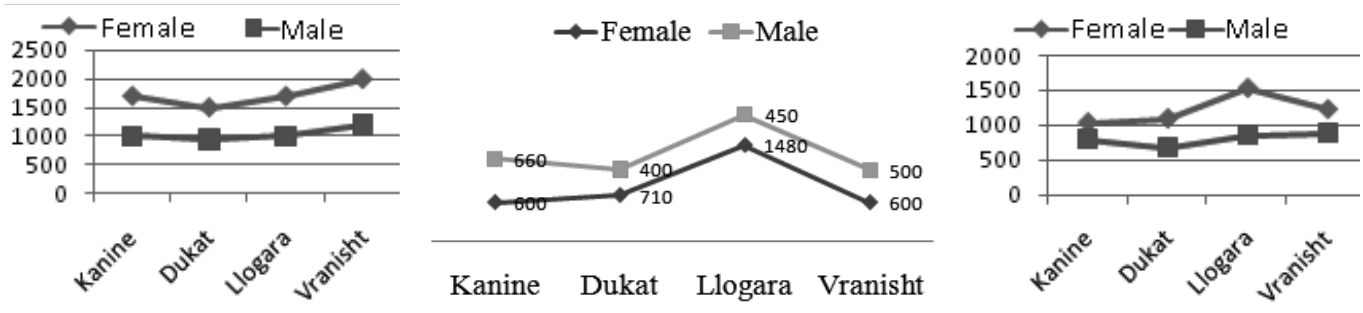

Chart 3. Variation of minimum, maximum and average body weight of the studied individuals

The data of biometric measurements are compared for all the studied individuals between different areas. It is concluded that the size of the studied individuals differs between the two study areas of Kanina and Dukat, and the two other areas, Llogara and Vranisht. The above charts show the trend for four assembly areas by comparing the smallest value, the greatest value as well as the average weight value for all the studied individuals. Based on the climate data, it's noted a tendency of increasing body mass from the first two gathering places (with mild climate and high temperatures) to the two stations (with relatively cold climate). The size of the body seems to grow in cold areas, contrary to the expected model for ectotherms. Demographic data available for the population of *Testudo hermanni* requires deeper study mechanisms.

Secondly, the body size change in *Testudo hermanni* was considerable, with a significant difference of average mass. Recent studies suggest that historical evolutionary changes are the main determinant of the size change and that selective effects are relatively small. Change of the body size is more related with temperatures and could be due to environmental factors such as food and non-evolutionary factors. Changes in adult body size can have other causes, such as: changes in growth rate of young individuals and their growth duration. A population can have great adult size, because young people are initially larger, because they grow faster, or because they grow for a longer time due to longer survival, or any combination of these factors together [5, 803–805].

4. Conclusions

In this paper were studied 75 living individuals *Testudo hermanni*, who after capture, were subjects of biometric measurements and then were released in the collecting places. Also part of this study includes data for six dead individuals from various causes.

From biometric measurements results that 37% of individuals are males and 63% females.

Based on morphological assessment it is concluded that 60% of males and 75% of females belong to reproductive individuals. This is an additional reason to evaluate carefully those biotic or abiotic factors that in a near future could endanger the population of *Testudo hermanni*. This requires deeper studies and statistical analysis.

Sexual dimorphism is quite evident in *Testudo hermani*. Some of the changing characters are CCL, SCL, CCW, PL, PW, TL, height, weight, etc.

Body size seems to grow in cold areas contrary to the expected pattern for ectotherms. Demographic data available for the population of *Testudo hermanni* mechanisms require deeper studies. Changes in adult body size may result from changes in the offspring population, growth rate of young individuals, their growth duration, etc.

References:

1. Djordjević S., Tomović L., Golubović A., Simović A., Sterijovski B., Djurakić M., Bonnet X. (2013): Geographic (in-)variability of gender-specific traits in Hermann's tortoise. Herpetological – Journal – 23: 67–74.
2. Djordjević S., Djurakić M., Golubović A., Ajtić R, Tomović L., Bonnet X. (2011): Sexual body size and body shape dimorphism of Testudo hermanni in central and eastern Serbia. Amphibi-Reptilia – 32: 445–458.
3. Dordević S. (2012): Sexual dimorphism in Testudo hermanni from the central part of the Balkan Peninsula. Dissertation. University of Conservation and Biology – 1: 227–231.
4. Fritz U. et al. A rangewide phylogeography of Hermann's tortoise, Testudo hermanni (Reptilia: Testudines: Testudinidae): implications for taxonomy© 2006. Journal compilation © 2006. The Norwegian Academy of Science and Letters Zoologica Scripta, – 35, 5, – September – 2006, – P. 531–543.
5. Kozlowski J. (1982). Sexual size dimorphisn: a life history perspective. Oikos – 54: 253–255.
6. Lapparent De Broin F. & Bour R. & Pharham J.F & Perala J. (2006 a): Eurotestudo. A new genus for the species Testudo hermanni Gmelin, – 1789 – Comptes Palevol, – Paris; – 5: 803–811.

DOI: http://dx.doi.org/10.20534/AJT-16-9.10-9-12

Nenasheva Elena Mikhailovna,
Kamchatka State technical university
Post-graduate student
E-mail: siuakoatl@gmail.com

The first studies of the structure and typology of networks of orb-weaver spiders (Aranei: Araneidae) of Kamchatka

Abstract: For the first time systematized the preliminary results of studies on the structure of networks of hunting orb-weaver spider in Kamchatka. Identified environmental aspects of changes in hunting nets, reflecting the behavioral responses of spiders.

Keywords: Kamchatka, orb-weaver spider, rotate trapping network, reference network, environmental monitoring

Introduction

The fauna of orb-web spiders (Aranei: Araneidae) of Kamchatka to date counts 14 species, belonging to 7 genera (*Aculepeira* Chamberlin et Ivie, 1942; *Araneus* Clerck, 1758; *Araniella* Chamberlin et Ivie, 1942; *Cercidia* Thorell, 1869; *Hypsosinga* Ausseraer, 1871; *Larinioides* Caporiacco, 1934; *Parazygiella* Wunderlich, 2004); dominated by spiders of *Araneus* genus. Data are given on the last faunal summaries [6; 7; 8; 10; 12].

A distinctive feature of the family *Araneidae* spiders is the construction of species-specific hunting rotate structured networks [4]. On the basis of the accounting networks of prey can be carried sparing number of methods to control spiders. The scientific study of the structure spiciform networks spiders began in the first third of the XX century with the works of Wiehle [16; 17], further work in this direction was continued by Levi [5], Eberhard [1], Tyschenko [14; 15] and a number of other researchers. The introduction to the arachnology practices the method of using the reference networks belongs to V. P. Tyschenko.

The current study of web spiders prey networks aimed primarily at identifying the environmental factors that influence the success of food-catching nets [11; 13; 18]. It should be noted that the degree of knowledge of hunting nets in Russia, despite the long history of arachnological research generally lower than in most Western European countries [4]. To date, more fully described in catching spider network of the European part of Russia, Central and Eastern Siberia. In Kamchatka, the study of this kind has not yet been carried out, and our work in this respect is a pioneer in the region.

Rotate networks inherent maximum catchability effective trapping zone at the lowest cost web (figure 1).

Figure 1. In mountain tundra in Kamchatka region the networks catchability can exceed the daily requirements in the production of spider.
Photo by Natalia Kollegova

The networks of *Araneidae* spiders species is settled vertically on the trees and shrub vegetation. Each type of network has a fixed spider structure comprising species-specific number of radii of turns in the central zone of the duct and the spiral thread. Generally, the spider movement occurring to the bottom of the network more often than on the top, so the networks always rotate at the bottom of asymmetry [3; 4; 9].

Despite the fact that the upper part of the network due to the high strength and elasticity of the arachnoid thread resistant to environmental influences (such as the wind blows more insects, the impact of atmospheric precipitation), the network as a whole is rather fragile structure and damaged by severe impacts, spiders therefore typically nightly reduced network structure (and it may be damaged as separate segments, and the entire network as a whole, which ultimately gives some deviation from the ideal circular structures). Meanwhile, we must not

forget that the greatest influence on the shape, size and network pattern render insects that spiders are the main source of food. Changes in the type of production can significantly affect the network drawing. In the literature [4] suggests that spiders have constant behavioral repertoire of their networks pattern regulation in response to the changing nutritional needs.

Material and Methods

The material for this work served as the fees of the author, which were conducted during the field research in the period from 2012 to 2016 on the Kamchatka Territory (model site "Avacha pass", a neighborhood of Petropavlovsk-Kamchatsky, azonal habitats of the eastern coast of the Pacific Ocean). Total surveyed about 200 networks of orb-weaving spiders belonging to *Araneidae* family. Catching nets measurements were carried out in adult females according to the method of reference networks [14]. Also note the presence or absence of a cover, degree of illumination and vegetable preferences. The observations were made in the early morning hours (6 to 9) and the evening (from 17 to 19), which is associated with behavioral characteristics of the object being studied. Basically we studied trapping network spiders belonging to the species *Araneus diadematus, Araneus marmoreus, Araneus quadratus* and *Larinioides cornutus* as the most typical representatives of the family in the region.

Results and discussion

Spiders *Larinioides cornutus* Clerck, 1758 prefer places with high humidity. Networks are building on the shrub and forb vegetation. Because herbs and web often build special shelters, connected to the signal thread center in shelters spend most of the day. Restoring the network (if necessary) takes place after dusk. Quite compact network is almost symmetrical structure; weaving loose network that appears to be due to the location of open spaces and scavenged on an unstable attachment of objects (grasses, herbaceous vegetation).

Spiders species *Araneus marmoreus* Clerck, 1758 weave network before dawn. In the center of the network, as a rule, can be found immatures, while mature females are hiding in shelters, arranged in rolled leaves of trees associated with the center of the signal thread network. Networks may be located in both hardwood and softwood trees. Networks are generally arranged on the medium ones portions at a height of 1–1.5 m from the surface (figure 2).

Spiders species *Araneus quadratus* Clerck, 1758 build networks at a short distance from the ground to the herbaceous vegetation. Trapping networks — large, elongated down dense, asymmetric downwards rigidly structured. A distinctive feature of the network architecture of spiders of this species — a clear asymmetry of the network down to the right.

Spiders species *Araneus diadematus* Clerck, 1758 placed the network, usually on trees growing in areas with an average brightness. Networks are large, symmetrical, slightly extended down from the clearly marked tightly braided central zone.

Figure 2. If there is a good forage base spiders are densely braided networks rather limited areas within a single bush can count up to ten network. Photo by Natalia Kollegova

In some cases, the trapping structure can be isolated network anomalies (fig. 3).

Figure 3. Typical anomalies in hunting nets orb-weaver spider in Kamchatka

As can be seen from the figure, the anomaly in the classical structure of the hunting networks can be expressed in different ways. The most characteristic of them: split hunting yarns (figure 3a), reduced the number of hunting sectors, abnormal external braiding of the network (figure 3b), the lack of the hunting yarns in the sector (figure 3c). Figure 3d shows a comparison reference network. In our opinion, abnormalities associated with the influence of external environmental factors, and this issue is still to be explored in detail.

Conclusions

The findings suggest that, since various kinds of external influences affect the behavior of spiders, this is reflected in changes in the structure and configuration of the catching nets. Thus, network-catching orb weaving spiders of *Araneidae* family may serve as a biological indicator of environmental conditions and monitoring their architecture can be used as a rapid method for assessing the quality of the state of the parameters of the medium.

Acknowledgment

The author expresses his deep gratitude to nature photographer Natalia Kollegova for providing unique photographs of architecture networking orb-weaver spider in Kamchatka and the organization of care in the field observations.

References:

1. Eberhard W. G. Behavioral characters for the higher classification of orb-weaving spiders; Evolution/W. G. Eberhard. – 1982. – 36 (5). – P. 1067–1095.
2. Eberhard W. G. Photography of orb webs in the field/W. G. Eberhard//Bull. Brit. Arachnology. – 1976. – Vol. 3, – No. 7. – P. 200–204.
3. Herberstein M. E. Asymmetry in spider orb-webs: a result of physical constraints?/M. E. Herberstein, A. M. Heiling//Animal Behaviour. – 1999. – Vol. 58, – No. 6. – P. 1241–1246.
4. Kartashev A. G. Structure-catching nets of orb weaving spiders: monograph./A. G. Kartashev, A. A. Kartasheva. – Tomsk: Tomsk State University of management and electronic systems, – 2009. – 120 p.
5. Levi H. W. Orb-webs and phylogeny of orb-weavers/H. W. Levi//Zool. Soc. Lond. Symp. – 1978. – 42 (1) – P. 1–15.
6. Marusik Yu. M. First data on spiders and harvestmen (Arachnida: Aranei, Opiliones) from Karaginski Island, Eastern Koryakia, Kamchatka Peninsula/Yu. M. Marusik, O. F. Khrulova//Arthropoda Selecta. – 2011. – Vol. 20. No. 4. – P. 232–329.
7. Marusik Yu. M. New data on spiders (Aranei) from Eastern Koryakia, Kamchatka Peninsula/Yu. M. Marusik, M. M. Omelko, A. S. Ryabukhin//Arthropoda Selecta. – 2013. – Vol. 22. No. 4. – P. 363–377.

8. Marusik Yu. M. New data on spiders and harvestmen (Arachnida: Aranei & Opiliones) from Western Koryakia, Kamchatka Peninsula/Yu. M. Marusik, A. S. Ryabukhin, G. V. Kuzminykh//Arthropoda Selecta. – 2010. – Vol. 19. – No. 4. – P. 227–236.
9. Masters M. W. Functional explanation of top-bottom asymmetry in vertical orb-webs/M. W. Masters, A. A. Moffat//Animal Behaviour. – 1983. – Vol. 31. – P. 1043–1046.
10. Mikhailov K. G. Catalogue of spiders (Arachnida, Aranei) of the territories of former Soviet Union/K. G. Mikhailov. – Moscow: Zoological museum of Moscow State University, – 1997. – 416 p.
11. Nenasheva E. M**.** The some peculiarities of feeding behavior of the orb-web spiders (Aranei: Araneidae) in the subalpic zone of the volcanic mountain systems of the Nature Park "Volcanoes of Kamchatka" (on the example of model site "Avacha Pass")/E. M. Nenasheva//Conservation of biodiversity of Kamchatka and adjacent seas. – Petropavlovsk-Kamchatsky: Kamchatpress, – 2014 a. – P. 359–363.
12. Nenasheva E. M. Survey fauna and biology of spiders (Arachnida: Araneae) on the example of Kamchatka ecosystems natural park «Volcanoes of Kamchatka»/E. M. Nenasheva, V. V. Zykov//Conservation of biodiversity of Kamchatka and adjacent seas. – Petropavlovsk-Kamchatsky: Kamchatpress, – 2014 b. – P. 79–95.
13. Sherman P. M. The orb-web: an energetic and behavioral estimator of a spider's dynamic foraging and reproductive strategies/P. M. Sherman//Anim. Behav. – 1994. – Vol. 48. – P. 19–34.
14. Tyschenko V. P. Trapping network of orb weaving spiders. 1. The justification of the reference networks on the example of two species of genus Araneus/V. P. Tyschenko//Zool. Journal. – 1984. – Vol. 63, – No. 6. – P. 839–847.
15. Tyschenko V. P.T rapping network of orb weaving spiders. 3. Geographic variation networks of Araneus marmoreus/V. P. Tyschenko, Yu. M. Marusik//Zool. Journal. – 1985. – Vol. 64, – No. 12. – P. 1816–1822.
16. Wiehle H. Araneidae/H. Wiehle//Die Tierwelt Deutsch., Spinnentiere. Jena. – 1931. – Bd 23. – 135 p.
17. Wiehle H. Beitrage zur Kenntnis des Radnetzbaues der Epeiriden, Tetragnathiden und Uloboriden/H. Wiehle//Zeitschrift fur Morphologie und Okologie der Tiere. – 1927. – Vol. 8. – P. 468–537.
18. Zshokke S. Factors influencing the size of the orb web in Araneus diadematus/S. Zshokke//In: Proceedings of the 16th European Colloquium of Arachnology (Zabka M., ed.). – 1997. – P. 329–334.

Section 2. Geodesy

DOI: http://dx.doi.org/10.20534/AJT-16-9.10-13-14

Kantur Vladimir Alexeevich,
Petrosyants Viktor Vladimirovich,
Far Eastern Federal University,
Vladivostok, Russia,
E-mail: vkantur@gmail.com,
E-mail: petrosyantsvv@gmail.com

Technology of natural environments remote testing

Abstract: The authors would like to present the technology of remote contactless testing for objects of the natural environment, which is based on the information-wave resonance of the information-wave generator, the object to be tested and the human being's field structures. The functional scheme of the experimental complex information-wave testing unit and principle of its operation are shown here. The results of a rock sample testing on detection of any precious metals are given. Thus, the above-mentioned method of information-wave testing proves the ability to identify any objects of natural environments.

Keywords: remote, information-wave test, the natural environment.

The founder of the contemporary theory of the Earth's geosphere is Academician V. Vernadskii, who pointed out that all objects in the world interact with one another. They are based in a single information space. He also suggested that the information exchange between the objects of living and non-living nature is carried out remotely at the level of information-wave interaction. His follower Academician V. Kaznacheev introduced the energy-information-sharing phenomenon that exists between the cells of individual organs, functional systems of the human body and between the organism and the external environment [1]. Due to the fact that a human being is an open energy-information system, we can assume the existence of channels inside the body providing communication with the external environment. Inside the human body acupuncture meridians with acupuncture points located on them belong to these channels. These meridians are responsible for the communication between cells and organs of the body on the whole, as well as the energy centers. Probably, field structures associated with human energy centers are able to serve as communication means between the organism and the external environment. The availability of such centers in the human body was proved by Russian and foreign researchers [2; 3; 4; 5]. In their opinion emergence of the energy blocks in the identified centers causes the violation of energy homeostasis (a state disturbing the information and energy exchange due to bioelectric potentials of the functioning cells in human body functional systems), and changes in the person's psychosomatic state. Thus, energy blocks emergence in the energy centers causes energy homeostasis breakdown in the cells of these organs. We can assume the energy blocks in the human energy centers are the result of both the processes inside the human body and the processes in the natural environment. Prof. Y. Gotovskii [6] shows that energy blocks in the energy centers of the human body are removed due to exposure to electromagnetic radiation with fixed frequencies. As a result, the cellular energy-information homeostasis, metabolic processes activity and damaged cell structure are restored. That leads to the normalization of person's psychophysical state and his recovery, as well.

We believe that any natural objects and environments can influence a person remotely through their field structures. Any object entering the area of the human structure field can cause information response in the human energy centers with subsequent change in his functional and psychosomatic state.

The purpose of this article is to do a research on the information encoding from the objects of natural environments that are within the interaction with the human field structure. We have developed an experimental unit for the study of inanimate nature objects effect on the human body.

The information-wave test (IWT) functional scheme of the experimental unit is shown in Fig. 1.

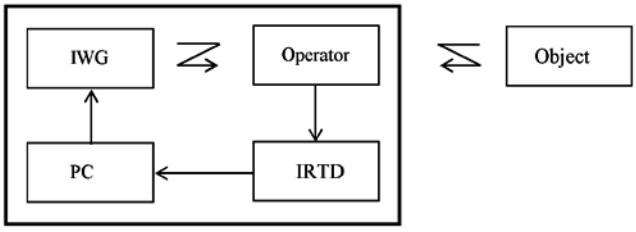

Figure1. Functional scheme of the experimental unit

The IWT experimental unit includes: information-wave generator (IWG), personal computer (PC), information reading and transformation device (IRTD) consisting of a primary transmitter, sensor and analog-to-digital transformer. The IWG output signal power is less than 0.05 watts.

The principle of the unit operation is as follows: the operator through the PC sets the so-called information marker, that enters as a pulse code modulation signal the IWG input. The electrical signal from the IWG output is converted through a special antenna into an electromagnetic signal, which affects the operator. If the testing object is within the human field structures sensitivity area, a corresponding IRTD signal is generated, which is observed by the operator on the PC screen.

As an example, a description of an experiment on testing the presence of gold in an ore piece of rock is given here 10 volunteers aged 25–35 years as operators were involved in the experiment. Each operator conducted independently 10 measurements. The average value of **X**, the average value of **M** error, reliability of the results of **P** in all dimensions.

The testing consisted of two stages: calibration and measurement. In the calibration stage each operator measured his level of psychosomatic reactions (with the skin resistance sensor and vascular conductance light sensors) on the effect of field structures formed at the IWG output with an information-wave marker. The information about gold presence was encoded in the information-wave marker. At the stage of measuring a piece of gold-bearing ore was placed into the area of field structures sensitivity and there was a repeated impact onto the operator with IWG signal which changed the operator's psychosomatic reactions. Such changes were observed only at the presence of the gold within the operator's sensitivity area. We believe this effect is caused by the resonant interaction of natural object (gold) field structures and the information-wave marker with the operator's field structures.

The result of the experiment on detecting the presence of gold according to sensitivity area IWT method is, as follows: in calibration mode (gold outside the sensitivity area) IWT indicators made 74.5 ± 0.9 relative value units (r. v.u). In the measurement mode (gold within the sensitivity area) IWT indicators made 38.2 ± 1.2 r. v.u. The reliability of the estimated values measured was at $\mathbf{P} < 0.001$. The experimental unit was able to detect the presence of the object to be tested within a 3-meter-distance from the operator.

Similar experiments with analogical results were conducted with copper, iron and other various objects proving the possibility of practical application of information-wave testing for natural environments.

Conclusions

The possibility of natural environments remote testing with the information-wave testing method was proved experimentally. This method is based on the interaction of the information-wave generator, the object to be tested and the human being's field structures.

References:

1. Kaznacheev V., Mikhailova L. Bioinformatic function of natural electro-magnetic fields. – Novosibirsk: Nauka, Sib. Dept., – 1985. – 182 p.
2. Luvsan G. Traditional and modern aspects of East-reflexive therapy. – Moscow: Nauka, – 1992.
3. Birukov V. Vibration therapy. – St. Petersburg: Krylov Publishing House, – 2010. – 185 p.
4. Gerber R. Vibration Medicine. Trans from English. – M: Sofia, – 2008. – 592 p.
5. Miller R. Bridging the Gap: An Interview with Valerie Hunt, Ed. D." Science of Mind, – Oct 1983.
6. Gotovskii Y., Kosarev L. Exogenous bioresonance therapy with fixed frequencies. Methodology Manual. – M: Imedis, – 2011.

Section 3. Mathematics

DOI: http://dx.doi.org/10.20534/AJT-16-9.10-15-14

Druzhinin Victor Vladimirovich,
Strahov Anton Viktorovich
National research nuclear University «MEPHI»
Sarov physical-technical Institute Department of mathematics
E-mail: vvdr@newmail.ru

Full integral formula for sums of generalized arithmetic progressions

Abstract: The formula given for the calculation of the sums with bases, forming an arithmetic progression, in the same degree with arbitrary first term. The results are for the degrees from "1" to "4". Differential and recurrence relations founded for such amounts and made the application.

Keywords: the sum of the terms of an arithmetic progression, the amount of a single-stage numbers, Bernoulli numbers.

Consider the sum of the following view

$$S(n;m;t;a)=\sum_{k=1}^{n}\left(a+(k-1)m\right)^t=a^t+(a+m)^t+(a+2m)^t\ldots$$
$$+\left(a+(n-1)m\right)^t, \qquad (1)$$

which we call the full sum of the generalized arithmetic progression (SGAP) as the base of the numbers in the sum to form the AP. General properties of such sums: $S(n;m;0;a)=n; S(1;m;t;a)=a^t$. In (1) m and a random number, t is a nonnegative integer degree. Theory of calculation of such amounts has a long history. When $m=a=1$ they worked with 1617 Johann Faulhaber, who published the first book of the calculations of these amounts with powers up to "11" and after he published a second book with powers up to "17". Pierre Fermat to calculate such amounts suggested the squad-squares and cube-cubes in the letter to Mersenne. The main contribution made Jacob Bernoulli, who introduced the polynomials in his name. Later Euler found the generating function for the Bernoulli polynomials, and Appel indicated derivative for polynomials of Bernoulli. The calculation of these amounts worked well as Jacobi and other mathematicians [1]. In modern literature SGAP with $m=a=1$ is calculated using the Bernoulli polynomials $B_t(n)$ by the formula

$$S(n;1;t;1)=\frac{1}{t+1}\left[B_{t+1}(n+1)-B_{t+1}\right]. \qquad (2)$$

These polynomials are found by expansion in a power series generating function of the Euler

$$\frac{ke^{kn}}{e^k-1}=\sum_{t=0}^{\infty}\frac{k^t}{t!}B_t(n). \qquad (3)$$

B_t – Bernoulli numbers, $B_t=B_t(0)$. For small values of $t\le 10$ these polynomials we can take their spreadsheets [2]:

$$B_0(x)=1; B_1(x)=x-\frac{1}{2}; B_2(x)=x^2-x+\frac{1}{6};$$
$$B_3(x)=x^3-\frac{3}{2}x^2+\frac{1}{2}x;\ B_4(x)=x^4-2x^3+x^2-\frac{1}{30};$$
$$B_5(x)=x^5-\frac{5}{2}x^4+\frac{5}{3}x^3-\frac{1}{6}x.$$

For large values of t it is necessary to paint a number (3) next. The data to calculate the value of (1) with an arbitrary interval m and an arbitrary first element $a\ne 1$ using the Bernoulli polynomials do not exist. There are also other simple approaches to their analysis. In our article [3] we proposed a faster way of calculation of such amounts for arbitrary n,m,t, but $a=1$, using the integrals

$$S(n;m;t+1;1)=\left\{m(t+1)\int_0^n S(\zeta;m;t;1)d\zeta\right\}+ \qquad (4)$$
$$+n\left\{1-m(t+1)\int_0^1 S(\zeta;m;t;1)d\zeta\right\}.$$

In this article we generalize this formula to the case of arbitrary initial number a, i.e. give the full integral formula for calculating the sums $S(n;m;t;a)$

$$S(n;m;t+1;a)=a^{t+1}\left\{\frac{m}{a}(t+1)\int_0^n S\left(\zeta;\frac{m}{a};t;1\right)d\zeta\right\}+$$
$$+a^{t+1}n\left\{1-\frac{m}{a}(t+1)\int_0^1 S\left(\zeta;\frac{m}{a};t;1\right)d\zeta\right\}. \qquad (5)$$

The relation (5) obtained by the method of mathematical induction and is new, as in reference books and monographs[1,2,4,5], we can't find him. When $a=m=1$ (5) gives the same results as the Bernoulli polynomials (3). Show the effect of this ratio for $t=1$. As $S(n;1;0;1)=n$, then

$$S(n;m;1;a)=\sum_{k=1}^{n}\left(a+(k-1)m\right)=m\int_0^n\zeta\,d\zeta+an\left(1-\frac{m}{a}\int_0^1\zeta\,d\zeta\right)$$

$$=\frac{mn^2}{2}+\frac{(2a-m)n}{2}. \qquad (6)$$

When $a=m=1$, we $(n;1;1;1)=n(n+1)/2$ well-known formula for the sum of natural numbers. We give some specific formulas for the calculation of these amounts for the subsidiary (5)

$$S(n;m;2;a)=\frac{m^2n^3}{3}+m(2a-m)\frac{n^2}{2}+\frac{\left(6a^2-6am+m^2\right)}{6}n \quad ; \qquad (7)$$

$$S(n;m;3;a)=\frac{m^3n^4}{4}+m^2(2a-m)\frac{n^3}{2}+\frac{m\left(6a^2-6am+m^2\right)}{4}n^2+\frac{a\left(2a^2-3ma+m^2\right)}{2}n; \qquad (8)$$

$$S(n;m;4;a)=\frac{m^4n^5}{5}+m^3(2a-m)\frac{n^4}{2}+\frac{m^2\left(6a^2-6am+m^2\right)}{3}n^3+m\left(2a^3-3a^2m+am^2\right)n^2+\frac{\left(30a^4-60a^3m+30a^2m^2-m^4\right)}{30}n. \qquad (9)$$

For example, from (8) it is possible to obtain a new equality at $m=\frac{1}{2}$ and $a=2,t=2$

$$S\left(n;\frac{1}{2};2;2\right)=\sum_{k=1}^{n}\left(\frac{3}{2}+\frac{k}{2}\right)^2=\frac{2n^3+21n^2+73n}{24}. \qquad (10)$$

In $S(n;m;t;a)$ the first term is always equal to $\left(m^tn^{t+1}\right)/(t+1)$, second $\left(m^{t-1}(2a-m)n^t\right)/2$, and the third $\left(t\left(m^{t-2}n^{t-1}\right)\left(6a^2-6am+m^2\right)/12\right)$. If we take $m=a=1$, these results coincide with the formulas of Bernoulli [2].

Next, we write the analyzed amount in the form of the polynomial

$$S(n;m;t;a)=\sum_{k=1}^{t+1}c_n(m;t;k;a)n^k. \qquad (11)$$

Between the coefficients $c_n(m;t;k;a)$ of (5) implies the following recurrence relation

$$c_n(m;t+1;k+1;a)=\frac{m(t+1)c_n(m;t;k;a)}{(k+1)}. \qquad (12)$$

The last coefficient $c_n(m;t+1;1;a)$ is the equality

$$c_n(m;t+1;1)=a^t-\sum_{k=2}^{t+1}c_n(m;t+1;k). \qquad (13)$$

Also from (5) differential recurrent ligament

$$\frac{1}{m(t+1)}\left(\frac{\partial S(n;m;t+1;a)}{\partial n}\bigg|_0^n\right)=S(n;m;t;a). \qquad (14)$$

The formula $S(n;m;t;a)$ you can search not only by integration, but also using the recurrence relation (12,13,14).

The sum $S(n;m;t;a)$ can be differentiated by the variable m. Derivative with respect to m p-th order allows to calculate analytically the sum of view

$$\sum_{k=p}^{n}(k-1)^p\left(a+(k-1)m\right)^{t-p}=\frac{(t-p)!}{t!}\cdot\frac{\partial^pS(n;m;t;a)}{\partial m^p}. \qquad (15)$$

For example, the first derivative gives

$$\frac{\partial S(n;m;t;1)}{\partial m}=t\sum_{k=2}^{n}(k-1)\left(1+(k-1)m\right)^{t-1}. \qquad (16)$$

Indeed, when $m=2,n=4,\ t=3,a=4$

$$3\left(3^2+2\cdot5^2+3\cdot7^2\right)=\frac{\partial S(4;m;3;4)}{\partial m}=\frac{3m^2n^4}{4}+$$

$$+\left(4m-3m^2\right)\frac{n^3}{2}+\frac{\left(6-12m+3m^2\right)}{4}n^2+\frac{(2m-3)}{2}n=618.$$

The sum $S(n;m;t;a)$ can be differentiated on the variable a

$$\frac{\partial S(n;m;t;a)}{\partial a}=tS(n;m;t-1;a).$$

The sum $S(n;m;t;a)$ can also integrate on the variable m. The result is a new ratio

$$m+\sum_{k=2}^{n}\left\{\frac{\left[a+(k-1)m\right]^{t+1}-1}{(t+1)(k-1)}\right\}=\int_0^mS(n;\zeta;t;a)d\zeta. \qquad (17)$$

For example, taking $m=2,n=3,t=2$ and proindeksirovat $S(n;m;2;1)$ for m from zero to «m» obtained by direct calculation of the left part of the number «31,33..» and in the right part of the function

$$\int_0^mS(n;\zeta;2;1)d\zeta=\frac{m^3n^3}{9}+\frac{m^2n^2}{2}-\frac{m^3n^2}{6}+mn-\frac{m^2n}{2}+\frac{m^3n}{18},$$

which gives the same number.

The above formula for SGAP can drastically reduce the computer calculations for large amounts, analytically to work with amounts of a new kind, with sign-alternating amounts or amounts with a predetermined order of the «+» and «–».

Using the formula (5) are solved some difficult Diophantine and algebraic equations. For example, the algebraic equation of the fifth order

$$768x^5-640x^3+112x-19680=0 \qquad (18)$$

is the coefficients from unknown coincides with SGAP with $t=4,m=4,a=2$, and one solution is just $x=2$.

In the study of solutions to Diophantine equations with a large number of unknowns we found a long sequence of numbers like amounts of Farm

$$2^3+4^3+7^3+10^3+13^3+14^3+14^3+17^3+20^3+23^3+$$
$$+23^3+24^3+28^3+35^3+46^3+53^3+61^3+70^3=98^3 \quad .$$

The author thanks the editorial of the journal "Proceedings of Institute of mathematics and mechanics Ur RAS", recognized the basic formula of article (4) are correct and the obtained for the first time, and also thanks a member of.-Q. RAS A. A. Makhneva for reviewing the manuscript and valuable comments.

References:

1. Prasolov V. V., Polynomials. MZIMA, –2003, –P. 131.
2. Graham, Z., Knuth, D., Patashnik O. Concrete mathematics, –Moscow, "Mir", –P. 313, – 1998.
3. Druzhinin V. V.//NTVP, –No. 5, – P. 18–20, – 2016.
4. Gradshteyn I. S., Ryzhik I. M. Tables of integrals, sums, series and products. GIMPL, – Moscow, – 1962. – P. 15–16.
5. Korn G., Korn T. Handbook of mathematics, science, GIMPL, – M., – 1974, – P. 31, 135.

Section 4. Machinery construction

DOI: http://dx.doi.org/10.20534/AJT-16-9.10-18-28

Vasenin Valery Ivanovich,
Perm National Research Polytechnic University,
Associate Professor, Candidate of technical sciences,
Department of Materials, technologies and machinery design
E-mail: vaseninvaleriy@mail.ru

Bogomyagkov Aleksey Vasilyevich,
Assistant

Investigation of the operation of a ring-shaped gating system

Abstract: The description of laboratory ring-shaped gating system is provided. Results of theoretical and experimental determination of flow speed and liquid flow rate, depending on the quantity of simultaneously working feeders are stated. It is shown that the Bernoulli equation is suitable for calculating the gating systems with variable flow rate (mass), which varies manifold in the collector with the flow distribution to feeders. It takes stock of three loss pressure: by friction on length, in local resistances and on changing of pressure. The calculation is done by method of successive approximations until the desired value of difference of losses of the pressure from the opposite sides from the zero point is achieved. The decision is the method of successive approximations given the difference the loss head with opposition side from the zero point. A good agreement between the calculated and experimental data is obtained.

Keywords: pouring basin, sprue, collector, feeder, pressure, zero point, resistance coefficient, flow coefficient, stream velocity, fluid consumption.

Introduction

L-shaped, branched, combined and step gating systems (GS) were studied earlier. The difference between the calculated and experimental values of velocities, flow rates and pressures was several percent. The Bernoulli equation (BE) for the stream with variable flow rate (and mass) was used in the calculations. Although, it is established [1, P. 10; 2, P. 205] for a fluid flow with constant flow rate (mass) given the absence of the distribution of the stream to feeders, i. e. for GS with one feeder. It is not clear why BE works. And its use in the calculation of GS with the fluid flow rate in the collector (slag catcher) alternating from maximum to zero *is not proved theoretically*. Thus, it appears practical to study, experimentally and by way of calculations, the most complex GS – ring-shaped, in which there are 2 flows of fluid and the metal can be supplied to the feeder from two sides.

Method of research

The system (Fig. 1 and 2) consists of a pouring basin, sprue, collector and seven identical feeders I–VII. The inner diameter of the basin is 272mm, and the height of water in the basin is 103,5mm. Longitudinal axes of the collector and feeders are in one horizontal plane. The level of fluid H – the distance vertically from the section *1–1* in the basin to the longitudinal axes of the collector and feeders – was maintained by the constant way of undisrupted adding of water to the basin and discharge of its surplus through a special crack in the basin: $H = 0{,}363$ m. The fluid flows from top from the feeders into the mould. Piezometers, glass pipes with the length of 370mm and internal diameter of 4,5mm, were installed in the sections of the collector *5–5, … 16–16* to measure pressure. Piezometers bent by 90° (not shown in Fig. 1) were placed in the section of the sprue *2–2, 3–3* and *4–4.* The time of the fluid outflow from every feeder is 50–200s depending on the number of simultaneously operating feeders, and the volume of water outflowed from every feeder is about 9 liters. These time and weight limitations ensured the deviation from the mean value of the velocity $\pm 0{,}005$ m/s, not more. The outflow of fluid from every feeder was determined not less than 6 times.

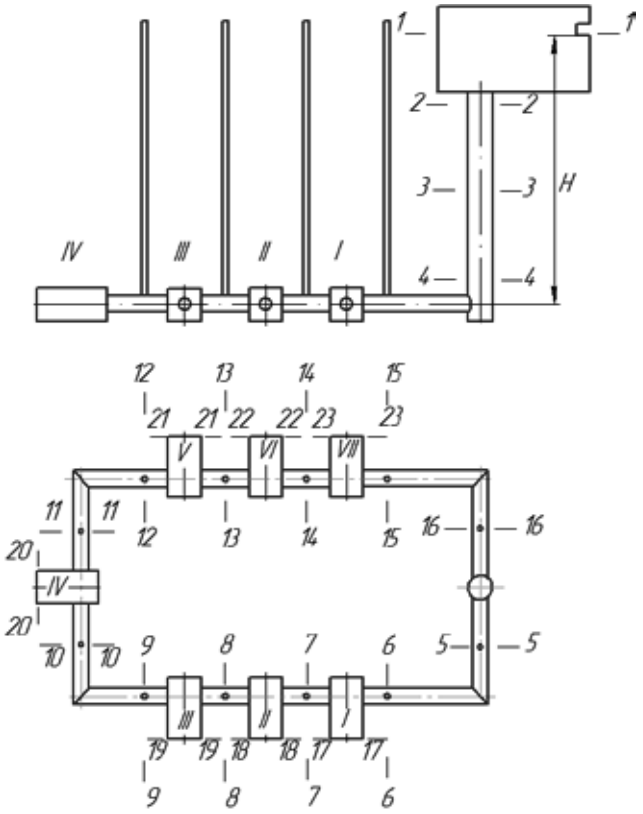

Figure 1. Ring-shaped gating system

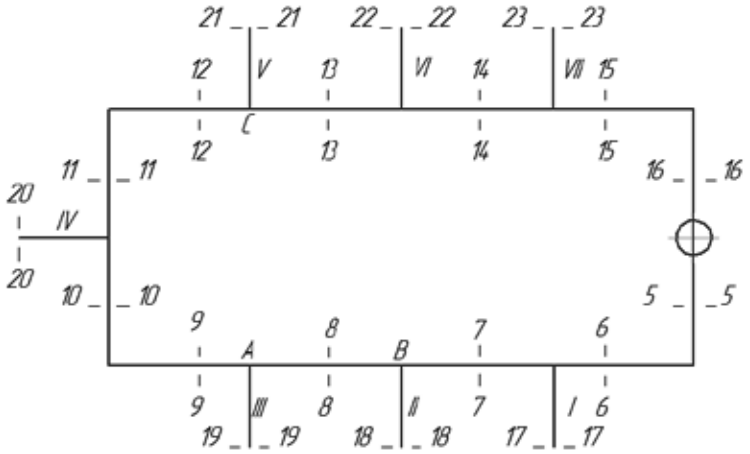

Figure 2. Scheme of a ring-shaped gating system

Main body

First, let us calculate the characteristics of GS during the operation of only one feeder for the case, when the hydraulic system is disconnected in the section *16–16* (no ring). Let's establish the Bernoulli equation (BE) for the sections *1–1* and *17–17* of GS (let's consider that only feeder I is operating):

$$\frac{p_1}{\gamma}+\alpha\frac{v_1^2}{2g}+H=\frac{p_{17}}{\gamma}+\alpha\frac{v_{17}^2}{2g}+h_{1-17}, \qquad (1)$$

where p_1 and p_{17} – pressures in the sections *1–1* and *17–17*, N/m^2 (equal to atmospheric pressure: $p_1 = p_{17} = p_a$); α – coefficient of inequality of distribution of velocity along the section of the stream (Coriolis coefficient); accept $\alpha = 1{,}1$ [2, p. 108]; g – acceleration of free fall; $g = 9{,}81$ m/s^2; v_1 and v_{17} – velocities of the metal in the sections *1–1* and *17–17*, m/s (due to a big difference in the areas of the basin S_1 in the section *1–1* and of the feeder S_n in the section *17–17*, one can accept $v_1 = 0$); γ – specific weight of liquid metal, N/m^3; h_{1-17} – loss of pressure during the movement of fluid from section *1–1* to section *17–17*, m. These losses of pressure are

$$h_{1-17}=\left(\zeta_{cm}+\lambda\frac{l_{cm}}{d_{cm}}\right)\alpha\frac{v_{cm}^2}{2g}+ \\ +\left(\zeta_{\kappa}+\zeta+\lambda\frac{l_{cm-1}}{d_{\kappa}}\right)\alpha\frac{v_5^2}{2g}+\left(\zeta_n+\lambda\frac{l_n}{d_n}\right)\alpha\frac{v_{17}^2}{2g}, \qquad (2)$$

where ζ_{cm}, ζ_{κ} and ζ_n – coefficients of local resistances of the entry of the metal from basin into sprue, turn from the

sprue into collector and turn from the collector into feeder I; ζ – coefficient of local resistance of the turn to 90° from section *5–5* to section *6–6* (without a change of areas without the sections of the collector); λ – coefficient of friction losses; l_{cm} – length (height) of the sprue, m; d_{cm}, $d_к$ and d_n – hydraulic diameters of the sprue, collector and feeder I, m; v_{cm} and v_5 – velocity of fluid in the sprue and in the collector in section *5–5*, m/s; l_{cm-I} – distance from the sprue to the feeder I, m; l_n – length of the feeder, m. Consumption in GS during the discharge from top is determined by the velocity of metal v_{17} in the output section *17–17* of the feeder I and area of its cross section: $Q = v_{17}S_n$. Other velocities of fluid in the channels of GS are determined from the equation of flow continuity:

$$Q = v_{cm}S_{cm} = v_5S_к = v_{17}S_n, \quad (3)$$

where S_{cm}, $S_к$ – areas of the sections of the sprue and collector, m^2. Let us express all velocities of metal in (2) through velocity v_{17}, using the equation of flow continuity (3):

$$h_{1-17(17)} = \alpha\frac{v_{17}^2}{2g}\left[\left(\zeta_{cm} + \lambda\frac{l_{cm}}{d_{cm}}\right)\left(\frac{S_n}{S_{cm}}\right)^2 + \left(\zeta_к + \zeta + \lambda\frac{l_{cm-I}}{d_к}\right)\left(\frac{S_n}{S_к}\right)^2 + \zeta_n + \lambda\frac{l_n}{d_n}\right]. \quad (4)$$

The expression in square brackets is specified as $\zeta_{1-17(17)}$ – it is a coefficient of resistance of the system from section *1–1* to section *17–17*, reduced to the velocity of fluid in the section *17–17*:

$$\zeta_{1-17(17)} = \left(\zeta_{cm} + \lambda\frac{l_{cm}}{d_{cm}}\right)\left(\frac{S_n}{S_{cm}}\right)^2 + \left(\zeta_к + \zeta + \lambda\frac{l_{cm-I}}{d_к}\right)\left(\frac{S_n}{S_к}\right)^2 + \zeta_n + \lambda\frac{l_n}{d_n}. \quad (5)$$

Now, (1) can be written as:

$$H = \alpha v_{17}^2(1 + \zeta_{1-17(17)})/2g. \quad (6)$$

And the coefficient of the flow rate of the system from section *1–1* to section *17–17*, reduced to the velocity v_{17},

$$\mu_{1-17(17)} = \left(1 + \zeta_{1-17(17)}\right)^{-1/2}. \quad (7)$$

The velocity

$$v_{17} = \mu_{1-17(17)}\sqrt{2gH/\alpha}. \quad (8)$$

We find flow rate Q according to the expression (3). In the given GS, the length of the sprue $l_{cm} = 0{,}2675$ m, the length of every feeder $l_n = 0{,}0495$ m, distance from the sprue to the first feeder $l_{cm-I} = 0{,}251$ m. The diameters of the feeder, collector and sprue: $d_n = 0{,}00903$ m, $d_к = d_5 = ... = d_{12} = 0{,}01603$ m, $d_{cm} = 0{,}02408$ m. Like in the works [3, 4], we accept that the coefficient of friction loss $\lambda = 0{,}03$. The coefficient of local resistance of the discharge from the basin into the sprue depending on the radius of rounding of the entering edge is defined according to the reference book [5, p. 126]: $\zeta_{cm} = 0{,}12$. The coefficients of local resistances are [6]: $\zeta = 0{,}885$, $\zeta_к = 0{,}396$, $\zeta_n = 0{,}334$. The results of calculations according to correlations (5), (7), (8) and (3): $\zeta_{1-17(17)} = 0{,}683710$, $\mu_{1-17(17)} = 0{,}770666$, $v_{17} = 1{,}960978$ m/s, $Q_{17} = 125{,}585114 \cdot 10^{-6}$ m^3/s.

During the calculation of the fluid outflow from the feeders II, III and IV, it should be taken into account that $l_{cm-II} = 0{,}370$ m, $l_{cm-III} = 0{,}489$ m, $l_{cm-IV} = 0{,}742$ m, and for the feeder IV – one more turn of fluid stream by 90° (without a change of the areas of the sections of the stream before and after the turn). The results of the calculations and experiments (in the denominator) are presented in Table 1.

Table 1. — Characteristics of GS during the operation of one feeder

Operating feeders	Characteristics of the system				
	ζ	μ	$\frac{v}{v^{эксп}}$, м/с	$\frac{Q}{Q^{эксп}}$, см^3/с	Q_0^*, %
1	***2***	***3***	***4***	***5***	***6***
I*	0,684	0,771	$\frac{1{,}961}{1{,}932}$	$\frac{125{,}59}{123{,}71}$	+1,5
I	0,631	0,783	$\frac{1{,}992}{1{,}976}$	$\frac{127{,}60}{126{,}51}$	+0,9
II*	0,706	0,766	$\frac{1{,}948}{1{,}925}$	$\frac{124{,}76}{123{,}26}$	+1,2
II	0,634	0,782	$\frac{1{,}991}{1{,}955}$	$\frac{127{,}48}{125{,}19}$	+1,8
III*	0,729	0,761	$\frac{1{,}935}{1{,}904}$	$\frac{123{,}95}{121{,}97}$	+1,6
III	0,637	0,782	$\frac{1{,}989}{2{,}010}$	$\frac{127{,}37}{128{,}71}$	–1,0

1	2	3	4	5	6
IV*	0,865	0,732	1,863 / 1,822	119,31 / 116,66	+2,3
IV	0,644	0,780	1,984 / 2,024	127,07 / 129,63	–2,0

*) $Q_o = \dfrac{Q - Q^{эксп}}{Q^{эксп}} \cdot 100$

*) *Hydraulic system is disconnected in the section 16–16.*

When the feeder I is in the ring, the loss of the pressure in parallel pipelines *5–6* and *16–13–10–7* are not summed up, and they are equal to one another. The BE for sections *4–4* and *17–17* (on the way through sections *5–5* and *6–6*):

$$\frac{p_4}{\gamma} + \alpha \frac{v_{cm}^2}{2g} = \left(\zeta^{\partial}_{4-5(5)} + \lambda \frac{l_{cm-I}}{d_к} + \zeta \right) \alpha \frac{v_5^2}{2g} + \left(\zeta_n + \lambda \frac{l_n}{d_n} + 1 \right) \alpha \frac{v_{17}^2}{2g} + \frac{p_{17}}{\gamma}. \quad (9)$$

The BE for sections *4–4* and *16–16* (through sections *16–16, 13–13, 10–10* and *7–7*):

$$\frac{p_4}{\gamma} + \alpha \frac{v_{cm}^2}{2g} = \left(\zeta^{\partial}_{4-16(16)} + \lambda \frac{l_{cm-I(16-7)}}{d_к} + 3\zeta \right) \alpha \frac{v_{16}^2}{2g} + \left(\zeta_n + \lambda \frac{l_n}{d_n} + 1 \right) \alpha \frac{v_{17}^2}{2g} + \frac{p_{17}}{\gamma}. \quad (10)$$

Here $\zeta^{\partial}_{4-5(5)}$ — coefficient of resistance on the division of the stream in the sprue in the section *4–4* between sections *5–5* and *16–16*, reduced to the velocity of metal in the section *5–5*; $\zeta^{\partial}_{4-16(16)}$ — coefficient of resistance on the division of the stream in the sprue in the section *4–4* between sections *5–5* and *16–16*, reduced to the velocity of fluid in the section *16–16*. We define these coefficients according to the following expression [5, p. 277]:

$$\zeta^{\partial} = \left[1 + \phi \left(v_{\partial} / v \right)^2 \right] / \left(v_{\partial} / v \right)^2, \quad (11)$$

where ϕ — coefficient depending on the rounding of the edges at the place of stream division; at big radius of rounding, $\phi = 0{,}3$; at zero radius of rounding, $\phi = 1{,}5$; for our GS, $\phi = 1{,}5$; v — velocity of the fluid before stream division, m/s; v_{∂} — velocity of the fluid in one of the channels after stream division, m/s.

Left parts of the expressions (9) and (10) are equal. We equate their right parts and, after transformations, we receive ($z = v_5 / v_{16}$, $l_{cm-I(16-7)} = 1{,}233$ m):

$$z = \sqrt{\frac{\zeta^{\partial}_{4-16(16)} + 4{,}962548}{\zeta^{\partial}_{4-5(5)} + 1{,}354744}}. \quad (12)$$

$v_{cm} S_{cm} = v_5 S_к + v_{16} S_к = z \cdot v_{16} \cdot S_к + v_{16} S_к = (z+1) v_{16} S_к$. It is apparent that $v_5 > v_{16}$, see equations (9) and (10).

Let us assume that $v_5 = 1{,}1 v_{16}$, i. e. $z = 1{,}1$. Then $v_{16} / v_{cm} = S_{cm} / (z+1) S_к = 1{,}074550$. According to (11), we find that: $\zeta^{\partial}_{4-16(16)} = 2{,}366058$.

$v_{16} = v_5 / z$, $v_{cm} S_{cm} = (v_5 + v_{16}) S_к = (v_5 + v_5 / z) S_к = (1 + 1/z) v_5 S_к$. And $v_5 / v_{cm} = S_{cm} / (1 + 1/z) S_к = 1{,}182005$. According to (11), we define: $\zeta^{\partial}_{4-5(5)} = 2{,}215750$.

We put received values $\zeta^{\partial}_{4-5(5)}$ and $\zeta^{\partial}_{4-16(16)}$ in (12) and get: $z = 1{,}432671$. We set $z = 1{,}1$. We do the following approximation – $z = 1{,}432671$ – and repeat the calculation. After some approximations given the established $z = 1{,}504590$, we find according to the calculation $z = 1{,}5045904$. The calculation of this relation can be finished because the difference between stablished and calculated values z is only 0,0000004. We accept that $z = v_5 / v_{16} = 1{,}504590$. Herewith, $v_5 / v_{cm} = 1{,}355587$, $\zeta^{\partial}_{4-5(5)} = 2{,}044183$, $v_{16} / v_{cm} = 0{,}900968$, $\zeta^{\partial}_{4-16(16)} = 2{,}731917$, $v_{16} = 0{,}664633 v_5$.

$v_{cm} = v_{17} S_n / S_{cm}$, $v_{cm} S_{cm} = (1 + 1/z) v_5 S_к = v_{17} S_n$, a $v_5 = v_{13} S_n / (1 + 1/z) S_к$. Coefficient of resistance of GS from section *1–1* to section *17–17*, reduced to velocity v_{17} in the feeder I [(see dependences (2) and (9)],

$$\zeta_{1-17(17)} = \left(\zeta_{cm} + \lambda \frac{l_{cm}}{d_{cm}} \right) \left(\frac{S_n}{S_{cm}} \right)^2 + \left(\zeta^{\partial}_{4-5(5)} + \lambda \frac{l_{cm-1}}{d_к} + \zeta \right) \left(\frac{S_n}{(1+1/z) S_к} \right)^2 + \zeta_n + \lambda \frac{l_n}{d_n}.$$

We put in the known values, and receive: $\zeta_{1-17(17)} = 0{,}631241$, $\mu_{1-17(17)} = 0{,}782964$, $v_{17} = 1{,}992266$ m/s, $Q_{17} = 127{,}588871 \cdot 10^{-6}$ m^3/s.

As it can be seen, the closure of the ring around feeder I led to the reduction of resistance coefficient $\zeta_{1-17(17)}$ from 0,684 to 0,631. The appearance of a parallel collector led to the fall of fluid velocities in each line, reduction of friction losses and in local resistances, which caused the reduction $\zeta_{1-17(17)}$, growth $\mu_{1-17(17)}$, v_{17} and Q_{17} compared to the case, when feeder I was working at the disruption of fluid ring in the section *16–16*.

When feeders II and III operate in GS (see Fig. 1), fluid from the sections *8–8* and *9–9* goes to feeder III, and to feeder II — only from the section *7–7*, and not

fully. In the considered ring, there are two different streams: one anti-clockwise (*16–13–9*), the other — clockwise (*5–7–8*). The movement of fluid in the section *8–8* is from right to left. In this case, it is easily defined during the operation of two feeders. The streams meet at the entry to feeder III at the point A (Fig. 3), which is called *the point of water division or zero point* [2, p. 216–217]. Mentally, we cut our ring along the intended line of water division and receive a net depicted in Fig. 3. Then, according to regular equations, we calculate the losses of pressure for the line *16–13–9* h_{16-9} and for the line *5–7–8* h_{5-8}. After this, we compare two found losses of pressure. If $h_{16-9} = h_{5-8}$, we conclude that pressures in points A' and A'' will be identical, which should be, because points A' and A'' represent physically one point A. Consequently, having obtained the indicated equation, we can state that we established the correct values of flow rates of Q_7, Q_8, Q_9, Q_{18} and Q_{19}. If the specified equation is not obtained, one has to change the values of these flow rates, and sometimes shift the point if water division, for instance, to point B — the point of fluid entry into feeder II (Fig. 3). Herewith, we refer to the 2nd, 3rd attempts making sure that the equation specified above had accurate precision.

Let us establish the BE for the sections *1–1* and *18–18* (for the path through sections *2–2, 5–5, 7–7*)

$$H = \left(\zeta_{cm} + \lambda\frac{l_{cm}}{d_{cm}}\right)\alpha\frac{v_{cm}^2}{2g} + \left(\zeta^{\partial}_{4-5(5)} + \zeta + \lambda\frac{l_{cm-II}}{d_к}\right)\alpha\frac{v_5^2}{2g} + \left(\zeta_{18} + \lambda\frac{l_n}{d_n} + 1\right)\alpha\frac{v_{18}^2}{2g}, \quad (13)$$

and for sections *1–1* and *19–19* (for the path through sections *2–2, 16–16, 13–13, 9–9*)

$$H = \left(\zeta_{cm} + \lambda\frac{l_{cm}}{d_{cm}}\right)\alpha\frac{v_{cm}^2}{2g} + \left(\zeta^{\partial}_{4-16(16)} + 3\zeta + \lambda\frac{l_{cm-III(16-9)}}{d_к}\right)\alpha\frac{v_{16}^2}{2g} + \left(\zeta_n + \lambda\frac{l_n}{d_n} + 1\right)\alpha\frac{v_{19}^2}{2g}. \quad (14)$$

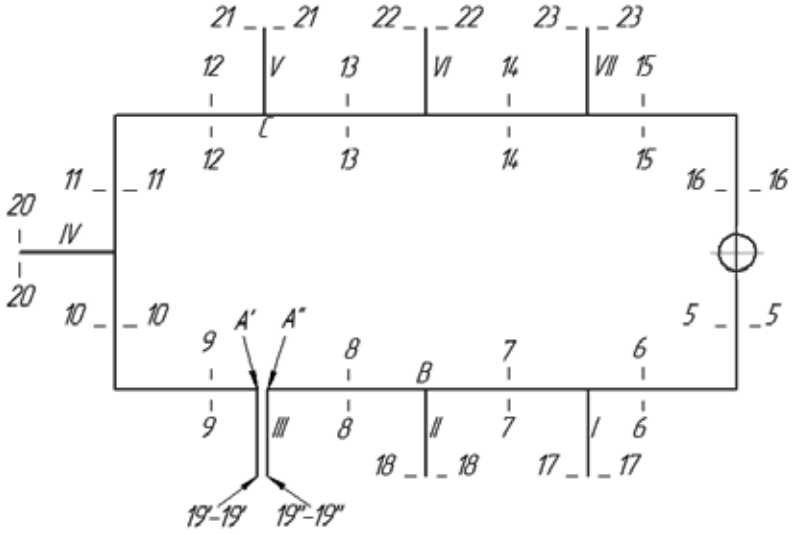

Figure 3. Scheme for the calculation during the operation of feeders II and III

In the expression (13), ζ_{18} — coefficient of resistance on the branching of a part of the stream from the collector into the feeder II with the output section *18–18*. ζ_8 — coefficient of resistance on the passage of fluid from section *7–7* into section *8–8* during the branching of a part of the stream from the collector into the feeder II. Coefficients of resistances determined by the branching of the stream from the collector into the feeder will be calculated according to the equations for three-way pieces [1, p. 112–115]. Coefficients of resistance on the passage in the collector during the branching of a part of the stream into the feeder

$$\zeta_{пр} = 0{,}4\left(1 - v_{пр}/v_к\right)^2 / \left(v_{пр}/v_к\right)^2, \quad (15)$$

and coefficient of resistance on the branching of a part of the stream into the feeder

$$\zeta_{отв} = \left[1 + \tau\left(v_n/v_к\right)^2\right] / \left(v_n/v_к\right)^2, \quad (16)$$

where $v_к$ and $v_{пр}$ — velocities of metal in the collector before and after the branching of a part of the stream into the feeder, m/s; v_n — velocity of fluid in the collector, m/s; τ — coefficient. For our case, at $S_n/S_к = 0{,}317$ $\tau = 0{,}15$ [7]. Coefficient $\zeta_{пр}$ is reduced to the velocity of passing stream $v_{пр}$, and $\zeta_{отв}$ — to the velocity in the feeder v_n.

Let us write down apparent equations:

$Q = v_{cm}S_{cm} = Q_5 + Q_{16} = v_5S_к + v_{16}S_к = Q_{18} + Q_{19} = v_{18}S_n + v_{19}S_n$, $Q_8 = v_8S_к = Q_7 - Q_{18} = v_7S_к - v_{18}S_n$, $Q_{19} = v_{19}S_n = Q_8 + Q_9 = v_8S_к + v_9S_к$.

Let us introduce the following notations: $x = v_{18}/v_{19}$, $y = Q_8/Q_7 = v_8S_к/v_7S_к = v_8/v_7$, $z = Q_5/Q_{16} = v_5S_к/v_{16}S_к = v_5/v_{16}$. And $Q_8 = yQ_7$, $v_7 = v_8/y$,

$Q_{16} = Q_5 / z$, $v_{16} = v_5 / z$, $v_5 = v_6 = v_7$, $v_9 = v_{10} = ... = v_{15} = v_{16}$.

The flow rate of fluid in the system $Q = (v_{18} + v_{19})S_n = (x \cdot v_{19} + v_{19})S_n = v_{19}(x+1)S_n = v_{19}S_{np(19)}$, where $S_{np(19)} = (1+x)S_n$ – reduced to the velocity v_{19} – area of the feeders (considers the operation of both feeders). And $v_{cm} = v_{19}S_{np(19)} / S_{cm}$. Similarly, we write down: $Q = (v_{18} + v_{19})S_n = (v_{18} + v_{18} / x)S_n = v_{18}(1+1/x)S_n = v_{18}S_{np(18)}$, where $S_{np(18)} = (1+1/x)S_n$ – reduced to the velocity v_{18} area of the feeders. And $v_{cm} = v_{18}S_{np(18)} / S_{cm}$.

We also have:

$$Q = v_{cm}S_{cm} = (v_5 + v_{16})S_к = (v_5 + v_5 / z)S_к = v_5(1+1/z)S_к,$$

$$v_5 = v_{cm}\frac{S_{cm}}{(1+1/z)S_к} = v_{18}\frac{S_{np(18)}}{S_{cm}}\frac{1}{1+1/z}\frac{S_{cm}}{S_к} = v_{18}\frac{S_{np(18)}}{(1+1/z)S_к}.$$

Now, the equation (13) can be written down as:

$$H = \alpha\frac{v_{18}^2}{2g}\left[\left(\zeta_{cm} + \lambda\frac{l_{cm}}{d_{cm}}\right)\left(\frac{S_{np(18)}}{S_{cm}}\right)^2 + \left(\zeta^{\partial}_{4-5(5)} + \zeta + \lambda\frac{l_{cm-II(5-7)}}{d_к}\right)\times\right.$$
$$\left.\times\left(\frac{S_{np(18)}}{(1+1/z)S_к}\right)^2 + \zeta_{18} + \lambda\frac{l_n}{d_n} + 1\right].$$

The expression in square brackets (except "1") is a coefficient of resistance from section *1–1* to section *18–18*:

$$\zeta_{1-18(18)} = \left(\zeta_{cm} + \lambda\frac{l_{cm}}{d_{cm}}\right)\left(\frac{S_{np(18)}}{S_{cm}}\right)^2 + \left(\zeta^{\partial}_{4-5(5)} + \zeta + \lambda\frac{l_{cm-II}}{d_к}\right)\left(\frac{S_{np(18)}}{(1+1/z)S_к}\right)^2 + \zeta_{18} + \lambda\frac{l_n}{d_n}. \quad (17)$$

We accept (randomly): $x = v_{18/19} = 1$, $y = v_8 / v_7 = 0{,}4$, $z = v_5 / v_{16} = 1{,}6$. At $x = 0{,}4$ $\zeta_8 = 0{,}9$, $\zeta_{18} = 0{,}429714$, see equations (15) and (16). For $z = 1{,}6$ according to (11), we find that $\zeta^{\partial}_{4-5(5)} = 2{,}018579$, and $\zeta^{\partial}_{4-16(16)} = 2{,}827562$. The results of calculations according to (17), (7), (8) and (3): $\zeta_{1-18(18)} = 1{,}178541$, $\mu_{1-18(18)} = 0{,}677512$, $v_{18} = 1{,}723946$ m/s, $Q_{18} = 110{,}405056 \cdot 10^{-6}$ m^3/s.

For the feeder III (line *1–16–19*), the following correlations are apparent:

$$Q = v_{cm}S_{cm} = v_5S_к + v_{16}S_к = (v_5 + v_{16})S_к =$$
$$= (zv_{16} + v_{16})S_к = v_{16}(z+1)S_к,$$

$$v_{16} = v_9 = v_{cm}\frac{1}{z+1}\frac{S_{cm}}{S_к} = v_{19}\frac{S_{np(19)}}{S_{cm}}\frac{1}{z+1}\frac{S_{cm}}{S_к} = v_{19}\frac{S_{np(19)}}{(z+1)S_к}.$$

And the equation (14) will look as:

$$H = \alpha\frac{v_{19}^2}{2g}\left[\left(\zeta_{cm} + \lambda\frac{l_{cm}}{d_{cm}}\right)\left(\frac{S_{np(19)}}{S_{cm}}\right)^2 + \left(\zeta^{\partial}_{4-16(16)} + 3\zeta + \lambda\frac{l_{cm-III(16-9)}}{d_к}\right)\left(\frac{S_{np(19)}}{(z+1)S_к}\right)^2 + \zeta_n + \lambda\frac{l_n}{d_n} + 1\right].$$

In the square brackets (except "1") — coefficient of resistance of the system from section *1–1* to section *19–19* (for line *1–16–9*):

$$\zeta_{1-19(19)} = \left(\zeta_{cm} + \lambda\frac{l_{cm}}{d_{cm}}\right)\left(\frac{S_{np(19)}}{S_{cm}}\right)^2 + \left(\zeta^{\partial}_{4-16(16)} + 3\zeta + \lambda\frac{l_{cm-III(16-9)}}{d_к}\right)\left(\frac{S_{np(19)}}{(z+1)S_к}\right)^2 + \zeta_n + \lambda\frac{l_n}{d_n}. \quad (18)$$

According to (18), (7), (8) and (3), we find: $\zeta_{1-19(19)} = 0{,}971933$, $\mu_{1-19(19)} = 0{,}712121$, $v_{19} = 1{,}812009$ m/s, $Q_{19} = 116{,}044835 \cdot 10^{-6}$ m^3/s.

The flow rate in the system $Q = Q_{18} + Q_{19} = 226{,}449891 \cdot 10^{-6}$ m^3/s. $v_{cm} = Q / S_{cm} = 0{,}497244$ m/s.

$Q_5 = \frac{Q}{1+1/z} = 139{,}353779 \cdot 10^{-6}$ m^3/s, $v_5 = Q_5 / S_к = 0{,}690497$ m/s.

$Q_{16} = \frac{Q}{1+z} = 87{,}096112 \cdot 10^{-6}$ m^3/s, $v_{16} = Q_{16} / S_{cm} = 0{,}431561$ m/s.

$Q_8 = Q_5 - Q_{18} = 28{,}948723 \cdot 10^{-6}$ m^3/s, $v_8 = Q_8 / S_к = 0{,}143441$ m/s.

In the ring-shaped hydraulic system, the losses of pressure h_{cm-A} from the sprue to point *A*, on the way through the sections *5–5*, *6–6*, *7–7* and *8–8*, should be equal in losses of pressure $h_{cm-A(16-9)}$ from the sprue to point *A* on the way through the section *16–16*, *13–13* and *9–9*. These losses of pressure can be found according to the following equations:

$$h_{cm-A} = \left(\zeta^{\partial}_{4-5(5)} + \zeta + \lambda\frac{l_{cm-II}}{d_к}\right)\alpha\frac{v_5^2}{2g} + \left(\zeta_8 + \lambda\frac{l}{d_к}\right)\alpha\frac{v_8^2}{2g}, \quad (19)$$

$$h_{cm-A(16-9)} = \left(\zeta^{\partial}_{4-16(16)} + 3\zeta + \lambda\frac{l_{cm-III(16-9)}}{d_к}\right)\alpha\frac{v_9^2}{2g}. \quad (20)$$

All values in (19) and (20) are known. $v_9 = v_{16}$, $h_{cm-III(16-9)} = 0{,}995$ m. We find that $h_{cm-A(16-9)} = 0{,}076692$, the difference between them is $h_A = 0{,}020729$ m.

Losses h_{cm-A} more than $h_{cm-A(16-9)}$, one should reduce the velocity of fluid on the way through the sections *5–5*, *6–6*, *7–7* and *8–8*. We accept $z = v_5 / v_{16} = 1{,}4$, and x and y remain same. We repeat the calculation and obtain: $h_{cm-A} = 0{,}087971$ m, $h_{cm-A(16-9)} = 0{,}087166$ m, $h_A = 0{,}000805$ m, and $y = v_8 / v_7 = 0{,}152813$.

The results of the calculations at $x = v_{18/19} = 1$, $y = v_8 / v_7 = 0{,}152813$ and $z = v_5 / v_{16} = 1{,}4$: $h_{cm-A} = 0{,}096260$ m, $h_{cm-A(16-9)} = 0{,}090155$ m, $h_A = 0{,}006104$ m, $x = 1{,}010657$, $y = 0{,}138314$.

Acting in such way, we receive that $x = v_{18/19} = 1{,}031010$, $y = v_8 / v_7 = 0{,}139022$ and $z = v_5 / v_{16} = 1{,}352501$ $h_{cm-A} = 0{,}09340484$ m, $h_{cm-A(16-9)} = 0{,}09324289$ m, $h_A = 4{,}91 \cdot 10^{-5}$ m.

Apparently, the difference h_A can be reduced to any earlier established infinitely small value. It is clear that the difference of pressures in 10^{-5} m is pointless. It was required to ensure the working capacity of the proposed method of GS calculation. The results of calculations and experiments (in the denominator) are presented Table 2.

Table 2. – Characteristics of GS during the operation of several feeders

Operating feeders	Characteristics of the system							
	$\zeta_{1-19(19)}$	$\mu_{1-19(19)}$	$\frac{v_{19}}{v_{19}^{эксп}}$, m/s	$\frac{v_{18}}{v_{18}^{эксп}}$, m/s	$\frac{v_{17}}{v_{17}^{эксп}}$, m/s	$\frac{Q_{19}}{Q_{19}^{эксп}}$, cm^3/s	$\frac{Q}{Q^{эксп}}$, cm^3/s	Q, %
II, III*	1,530	0,629	$\frac{1,600}{1,626}$	$\frac{1,514}{1,547}$		$\frac{102,46}{104,13}$	$\frac{199,36}{203,21}$	–1,9
II, III	1,069	0,695	$\frac{1,769}{1,770}$	$\frac{1,818}{1,752}$		$\frac{113,30}{113,35}$	$\frac{229,73}{225,56}$	+1,8
I–III*	2,470	0,537	$\frac{1,366}{1,374}$	$\frac{1,292}{1,319}$	$\frac{1,128}{1,166}$	$\frac{87,48}{87,99}$	$\frac{242,42}{247,10}$	–1,9
I–III	1,646	0,615	$\frac{1,564}{1,525}$	$\frac{1,557}{1,558}$	$\frac{1,516}{1,455}$	$\frac{100,17}{97,66}$	$\frac{295,76}{290,62}$	+2,2
I–III, VII**	2,319	0,549	$\frac{1,397}{1,390}$	$\frac{1,437}{1,362}$	$\frac{1,305}{1,270}$	$\frac{89,44}{88,99}$	$\frac{359,00}{349,29}$	+1,8
I–III, V, VI***	2,998	0,500	$\frac{1,273}{1,256}$	$\frac{1,258}{1,209}$	$\frac{1,118}{1,098}$	$\frac{81,50}{80,42}$	$\frac{390,57}{384,96}$	+1,5
I–VII****	4,775	0,416	$\frac{1,059}{1,004}$	$\frac{0,945}{0,954}$	$\frac{0,811}{0,830}$	$\frac{67,81}{64,31}$	$\frac{427,68}{422,62}$	+1,2

*) *Hydraulic system is disconnected in the section 16–16.*

**) $v_{23}=1,466$ m/s, $v_{23}^{эксп}=1,433$ m/s

***) $v_{21}=1,292$ m/s, $v_{21}^{эксп}=1,277$ m/s, $v_{22}=1,158$ m/s, $v_{22}^{эксп}=1,171$ m/s

****) $\zeta_{1-20(20)}=4,904$,

$\mu_{1-20(20)}=0,412$, $v_{20}=1,047$ м/с, $v_{20}^{эксп}=1,024$ m/s

During the operation of feeders I–III, the zero point will be located, apparently, in point B (Fig. 4). In this case, the fluid goes to feeder II from sections *7–7* and *8–8*, to feeder I — only from sections *6–6*, and not all fluid, and to feeder III — from section *9–9* (not all).

Let us establish the BE for sections *1–1* and *17–17*:

$$H=\left(\zeta_{cm}+\lambda\frac{l_{cm}}{d_{cm}}\right)\alpha\frac{v_{cm}^2}{2g}+\left(\zeta_{4-5(5)}^{\partial}+\zeta+\lambda\frac{l_{cm-I}}{d_к}\right)\alpha\frac{v_5^2}{2g}+$$
$$+\left(\zeta_{17}+\lambda\frac{l_n}{d_n}+1\right)\alpha\frac{v_{17}^2}{2g}, \quad (21)$$

for sections *1–1* and *18–18*:

$$H=\left(\zeta_{cm}+\lambda\frac{l_{cm}}{d_{cm}}\right)\alpha\frac{v_{cm}^2}{2g}+\left(\zeta_{4-5(5)}^{\partial}+\zeta+\lambda\frac{l_{cm-I}}{d_к}\right)\alpha\frac{v_5^2}{2g}+$$
$$+\left(\zeta_7+\lambda\frac{l}{d_к}\right)\alpha\frac{v_7^2}{2g}+\left(\zeta_n+\lambda\frac{l_n}{d_n}+1\right)\alpha\frac{v_{18}^2}{2g}, \quad (22)$$

and for sections *1–1* and *19–19* (for the way through sections *2–2, 16–16, 13–13, 9–9*):

$$H=\left(\zeta_{cm}+\lambda\frac{l_{cm}}{d_{cm}}\right)\alpha\frac{v_{cm}^2}{2g}+\left(\zeta_{4-16(16)}^{\partial}+3\zeta+\lambda\frac{l_{cm-III(16-9)}}{d_к}\right)\times$$
$$\times\alpha\frac{v_{16}^2}{2g}+\left(\zeta_{19}+\lambda\frac{l_n}{d_n}+1\right)\alpha\frac{v_{19}^2}{2g}. \quad (23)$$

Let us indicate: $x_1=v_{17}/v_{19}$, $x_2=v_{18}/v_{19}$. Then, $v_{17}=x_1v_{19}$, $v_{18}=x_2v_{19}$, $v_{19}=v_{17}/x_1$, $v_{19}=v_{18}/x_2$, $v_{17}=x_1v_{19}=v_{18}x_1/x_2$, $v_{18}=x_2v_{19}=v_{17}x_2/x_1$.

Let us introduce the following notations: $y_1=Q_7/Q_6=v_7S_к/v_6S_к=v_7/v_6$, $y_2=Q_8/Q_9=$ $=v_8S_к/v_9S_к=v_8/v_9$, $z=Q_5/Q_{16}=v_5S_к/v_{16}S_к=v_5/v_{16}$. And $v_6=v_7/y_1$, $v_9=v_8/y_2$, $v_{16}=v_5/z$, $v_5=v_6$, $v_9=v_{10}=...=v_{15}=v_{16}$.

Let us assume that $x_1=x_2=1$, $y_1=y_2=0,4$, and $v_5=1,6v_{16}$, i. e. $z=1,6$. The flow rate in the system $Q=v_{cm}S_{cm}=v_5S_к+v_{16}S_к=zv_{16}S_к+v_{16}S_к=(z+1)v_{16}S_к$. And the relation $v_{16}/v_{cm}=S_{cm}/(z+1)S_к=0,867906$. We calculate it according to (11): $\zeta_{4-16(16)}^{\partial}=2,827562$.

Similarly, we define: $Q=(v_5+v_{16})S_к=(v_5+v_5/z)S_к=(1+1/z)v_5S_5$, $v_5/v_{cm}=S_{cm}/(1+1/z)S_к=1,388649$, $\zeta_{4-5(5)}^{\partial}=2,018580$.

At $y_1=0,4$ $\zeta_7=0,9$ — according to the correlation (15). $v_{17}S_n=(1-y_1)v_6S_к$, $v_{17}/v_6=(1-y_1)S_к/S_n=$ $=1,890788$, $\zeta_{17}=0,429714$ — according to the dependence (16).

For $y_2=0,4$ $\zeta_8=0,9$, and $\zeta_{19}=0,429714$.

The flow rate of the fluid in the system

$$Q=v_{cm}S_{cm}=(v_{17}+v_{18}+v_{19})S_n=\left(v_{17}+v_{17}\frac{x_2}{x_1}+\frac{v_{17}}{x_1}\right)S_n=$$

$$= v_{17}\frac{x_1+x_2+1}{x_1}S_n = v_{17}S_{np(17)},$$

where $S_{np(17)} = \frac{x_1+x_2+1}{x_1}S_n$ — reduced to velocity v_{17} — the area of the feeders (considers the operation of all three feeders). And $v_{cm} = v_{17}S_{np(17)}/S_{cm}$.

Also, $Q = v_{cm}S_{cm} = (v_5+v_{16})S_к = (v_5+v_5/z)S_к =$

$= v_5(1+1/z)S_к$, $v_5 = v_6 = v_{cm}\frac{1}{1+1/z}\frac{S_{cm}}{S_к} =$

$$= v_{17}\frac{S_{np(17)}}{S_{cm}}\frac{1}{1+1/z}\frac{S_{cm}}{S_к} = v_{17}\frac{S_{np(17)}}{(1+1/z)S_к}.$$

And the correlation (21) will look as follows:

$$H = \alpha\frac{v_{17}^2}{2g}\left[\left(\zeta_{cm}+\lambda\frac{l_{cm}}{d_{cm}}\right)\left(\frac{S_{np(17)}}{S_{cm}}\right)^2 + \left(\zeta^{\partial}_{4-5(5)}+\zeta+\lambda\frac{l_{cm-l}}{d_к}\right)\times\right.$$
$$\left.\times\left(\frac{S_{np(17)}}{(1+1/z)S_к}\right)^2 + \zeta_{17}+\lambda l_n/d_n+1\right].$$

The expression in square brackets (except "1") is the coefficient of resistance of the system from section *1–1* to section *17–17* (for the line *1–5–17*)

$$\zeta_{1-17(17)} = \left(\zeta_{cm}+\lambda\frac{l_{cm}}{d_{cm}}\right)\left(\frac{S_{np(17)}}{S_{cm}}\right)^2 + \left(\zeta^{\partial}_{4-5(5)}+\zeta+\lambda\frac{l_{cm-l}}{d_к}\right)\times$$
$$\times\left(\frac{S_{np(17)}}{(1+1/z)S_к}\right)^2 + \zeta_{17}+\lambda l_n/d_n. \quad (24)$$

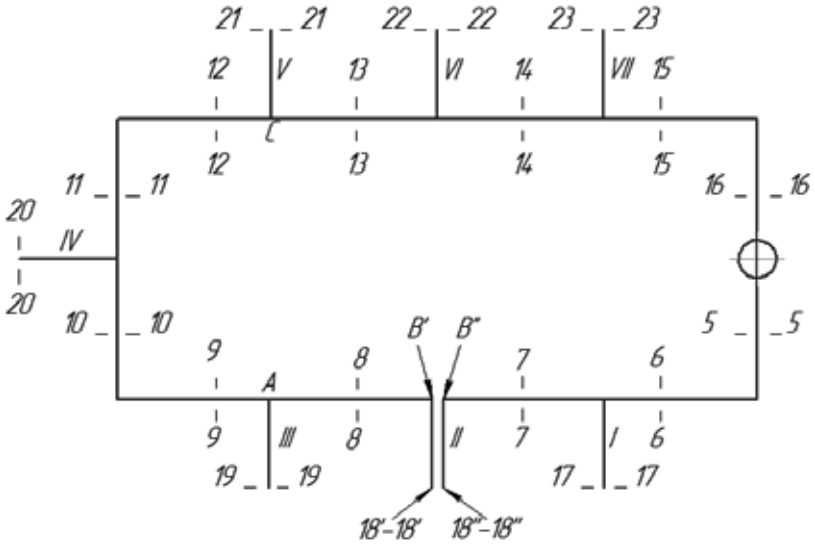

Figure 4. Scheme for the calculation during the operation of feeders I, II and III

According to the correlations (24), (7), (8) and (3), we find: $\zeta_{1-17(17)} = 1{,}832576$, $\mu_{1-17(17)} = 0{,}594168$, $v_{17} = 1{,}511874$ m/s, $Q_{17} = 96{,}823562\cdot10^{-6}$ m^3/s.

Let us calculate the outflow of fluid from feeder II. The flow rate of the fluid in the system

$$Q = v_{cm}S_{cm} = (v_{17}+v_{18}+v_{19})S_n = \left(v_{18}\frac{x_1}{x_2}+v_{18}+\frac{v_{18}}{x_2}\right)S_n =$$

$$= v_{18}\frac{x_1+x_2+1}{x_2}S_n = v_{18}S_{np(18)},$$

where $S_{np(18)} = \frac{x_1+x_2+1}{x_2}S_n$ — reduced to velocity v_{18} area of the feeders (considers the work of three feeders). $v_{cm} = v_{18}S_{np(18)}/S_{cm}$. We also have: $Q = v_{cm}S_{cm} = (v_5+v_{16})S_к =$

$= (v_5+v_5/z)S_к = v_5(1+1/z)S_к$, $v_5 = v_6 = v_{cm}\frac{1}{1+1/z}\frac{S_{cm}}{S_к} =$

$= v_{18}\frac{S_{np(18)}}{S_{cm}}\frac{1}{1+1/z}\frac{S_{cm}}{S_к} = v_{18}\frac{S_{np(18)}}{(1+1/z)S_к}$, $v_7 = y_1v_5 =$

$= y_1v_{18}\frac{S_{np(18)}}{(1+1/z)S_к}$. The dependence (22) will look as follows:

$$H = \alpha\frac{v_{18}^2}{2g}\left[\left(\zeta_{cm}+\lambda\frac{l_{cm}}{d_{cm}}\right)\left(\frac{S_{np(18)}}{S_{cm}}\right)^2 + \left(\zeta^{\partial}_{4-5(5)}+\zeta+\lambda\frac{l_{cm-l}}{d_к}\right)\times\right.$$
$$\times\left(\frac{S_{np(18)}}{(1+1/z)S_к}\right)^2 + \left(\zeta_7+\lambda\frac{l}{d_к}\right)\left(\frac{y_1S_{np(18)}}{(1+1/z)S_к}\right)^2 +$$
$$\left.+\zeta_n+\lambda\frac{l_n}{d_n}+1\right].$$

In the square brackets (except "1"), the coefficient of resistance of the system from section *1–1* to section *18–18* is written down:

$$\zeta_{1-18(18)} = \left(\zeta_{cm}+\lambda\frac{l_{cm}}{d_{cm}}\right)\left(\frac{S_{np(18)}}{S_{cm}}\right)^2 + \left(\zeta^{\partial}_{4-5(5)}+\zeta+\lambda\frac{l_{cm-l}}{d_к}\right)\times$$
$$\times\left(\frac{S_{np(18)}}{(1+1/z)S_к}\right)^2 + \left(\zeta_7+\lambda\frac{l}{d_к}\right)\left(\frac{y_1S_{np(18)}}{(1+1/z)S_к}\right)^2 + \zeta_n+\lambda\frac{l_n}{d_n}. \quad (25)$$

The results of calculations according to (25), (7), (8) and (3): $\zeta_{1-18(18)} = 1{,}798513$, $\mu_{1-18(18)} = 0{,}597773$, $v_{18} = 1{,}521048$ m/s, $Q_{18} = 97{,}411043\cdot10^{-6}$ m^3/s.

For the feeder III, the flow rate of fluid in the system

$$Q = v_{cm}S_{cm} = \left(v_{17} + v_{18} + v_{19}\right)S_n = \left(x_1 v_{19} + x_2 v_{19} + v_{19}\right)S_n =$$
$$= v_{19}\left(x_1 + x_2 + 1\right)S_n = v_{19}S_{np(19)},$$

where $S_{np(19)} = \left(x_1 + x_2 + 1\right)S_n$ — reduced to velocity v_{19} the area of the feeders. A $v_{cm} = v_{19}S_{np(19)} / S_{cm}$.

$$Q = v_{cm}S_{cm} = \left(v_5 + v_{16}\right)S_к = \left(zv_{16} + v_{16}\right)S_к = v_{16}\left(z+1\right)S_к,$$

$$v_{16} = v_9 = v_{cm}\frac{1}{z+1}\frac{S_{cm}}{S_к} = v_{19}\frac{S_{np(19)}}{S_{cm}}\frac{1}{z+1}\frac{S_{cm}}{S_к} = v_{19}\frac{S_{np(19)}}{\left(z+1\right)S_к}.$$

And the expression (23) will be written down as follows:

$$H = \alpha\frac{v_{19}^2}{2g}\left[\begin{array}{l}\left(\zeta_{cm} + \lambda\frac{l_{cm}}{d_{cm}}\right)\left(\frac{S_{np(19)}}{S_{cm}}\right)^2 + \\ + \left(\zeta^{\partial}_{4-16(16)} + 3\zeta + \lambda\frac{l_{cm-III(16-9)}}{d_к}\right)\times \\ \times\left(\frac{S_{np(19)}}{(z+1)S_к}\right)^2 + \zeta_{19} + \lambda\frac{l_n}{d_n} + 1\end{array}\right].$$

The correlation in square brackets (except "1") is the coefficient of resistance of the system from section *1–1* to section *19–19* (for the line *1–16–19*):

$$\zeta_{1-19(19)} = \left(\zeta_{cm} + \lambda\frac{l_{cm}}{d_{cm}}\right)\left(\frac{S_{np(19)}}{S_{cm}}\right)^2 + \left(\zeta^{\partial}_{4-16(16)} + 3\zeta + \lambda\frac{l_{cm-III(16-9)}}{d_к}\right)\times$$
$$\times\left(\frac{S_{np(19)}}{(z+1)S_к}\right)^2 + \zeta_{19} + \lambda\frac{l_n}{d_n}. \qquad (26)$$

According to the equations (26), (7), (8) and (3), we define: $\zeta_{1-19(19)} = 1{,}659498$. $\mu_{1-19(19)} = 0{,}613197$, $v_{19} = 1{,}560295$ m/s, $Q_{19} = 99{,}924513\cdot10^{-6}$ m^3/s.

The flow rate in the system of three feeders I, II and III $Q = Q_{17} + Q_{18} + Q_{19} = 294{,}159118\cdot10^{-6}$ m^3/s, and the velocity of fluid in the sprue $v_{cm} = Q / S_{cm} = 0{,}645921$ m/s.

$Q_5 = \frac{Q}{1+1/z} = 181{,}020995\cdot10^{-6}$ m^3/s, $v_5 = Q_5 / S_к =$
$= 0{,}896958$ m/s.

$Q_{16} = \frac{Q}{1+z} = 113{,}138122\cdot10^{-6}$ m^3/s, $v_{16} = Q_{16} / S_{cm} =$
$= 0{,}560599$ m/s.

$Q_7 = Q_5 - Q_{18} = 84{,}197434\cdot10^{-6}$ m^3/s, $v_7 = Q_7 / S_к =$
$= 0{,}417198$ m/s.

$Q_8 = Q_{16} - Q_{19} = 13{,}213610\cdot10^{-6}$ m^3/s, $v_8 = Q_8 / S_к =$
$v_8 = Q_8 / S_к =$ m/s.

In the ring-shaped hydraulic system, the losses of pressure $h_{cm◆B}$ from the sprue to point *B* on the way through sections *5–5*, *6–6* and *7–7* should be equal to the losses of pressure $h_{cm◆B(16-9)}$ from the sprue to point *B* on the way through sections *16–16*, *13–13*, *9–9* and *8–8*. These losses of pressure can be defined according to the following correlations:

$$h_{cm-B} = \left(\zeta^{\partial}_{4-5(5)} + \zeta + \lambda\frac{l_{cm-I}}{d_к}\right)\alpha\frac{v_5^2}{2g} + \left(\zeta_7 + \lambda\frac{l}{d_к}\right)\alpha\frac{v_7^2}{2g}, \qquad (27)$$

$$h_{cm-B(16-9)} = \left(\zeta^{\partial}_{4-16(16)} + 3\zeta + \lambda\frac{l_{cm-III(16-9)}}{d_к}\right)\alpha\frac{v_{16}^2}{2g} +$$
$$+\left(\zeta + \lambda\frac{l}{d_к}\right)\alpha\frac{v_8^2}{2g} \qquad (28)$$

All values in (27) and (28) are known. $v_9 = v_{16}$, $h_{cm-III(16-9)} = 0{,}995$ m. We find that $h_{cm-B} = 0{,}178106$, $h_{cm-B(16-9)} = 0{,}133188$, the difference between them $h_B = 0{,}044918$ m.

Losses h_{cm-B} are bigger than $h_{cm-B(16-9)}$, hence, one should reduce the velocity of fluid on the way through sections *5–5*, *6–6*, *7–7* and *8–8*. We accept $z = v_5 / v_{16} = 1{,}4$, and x_1, x_2, y_1 and y_2 remain unchanged. We repeat the calculation and receive: $h_{cm-B} = 0{,}156807$ m, $h_{cm-B(16-9)} = 0{,}149202$ m, $h_B = 0{,}007605$ m, $y_1 = 0{,}426329$, $y_2 = 0{,}206438$.

The results of calculations at $x_1 = 1$, $x_2 = 1$, $y_1 = 0{,}426329$, $y_2 = 0{,}4$ and $z = 1{,}4$: $h_{cm-B} = 0{,}155072$ m, $h_{cm-B(16-9)} = 0{,}148714$ m, $h_B = 0{,}006358$ m, $y_1 = 0{,}428153$, $y_2 = 0{,}205169$.

At $x_1 = 1$, $x_2 = 1$, $y_1 = 0{,}4$, $y_2 = 0{,}206438$ and $z = 1{,}4$, we have: $h_{cm-B} = 0{,}159007$ m, $h_{cm-B(16-9)} = 0{,}155007$ m, $h_B = 0{,}004000$ m, $y_1 = 0{,}430048$, $y_2 = 0{,}194150$.

Acting in such way, we receive that, at $x_1 = 0.966830$, $x_2 = 0.993380$, $y_1 = 0{,}440432$, $y_2 = 0{,}188701$ and $z = 1{,}393022$ $h_{cm-B} = 0{,}155951$ m, $h_{cm-B(16-9)} = 0{,}155918$ m, $h_B = 3{,}33\cdot10^{-5}$ m.

Acting similarly, we find the characteristics of GS during the operation of different numbers of feeders (Table 2).

Results of the research and their discussion

Experimental results differ from calculated ones by –2,0% to +2,2%, see Tables 1 and 2. The differences are small and it's difficult to make conclusions. In the whole, one can consider that a good correspondence of theoretical and experimental data was obtained. And the Bernoulli equation established for the specific case — for the system with one feeder, works in multi-feeder gating system, herewith, in the most complicated one — ring-shaped gating system.

Due to such small differences, there is a thought about a vicious circle when the data obtained in own experiments is used. Naturally, the coefficients of resistances on the turn in the collector by 90° and from the collector to the feeder and change of areas of the sections of the stream before and after the turn were found for same GS. However, there is no vicious circle. Firstly, not a new, but known dependence — the Bernoulli equation, was used in the experiments on the definition of this coefficient *during the operation of only one feeder* (there was no stream division).

Secondly, to define the specified coefficient, independent experiments were conducted [6]. And, mainly, the coefficients of resistances in the hydraulics cannot be calculated and are defined experimentally. Only the resistance of a sharp expansion of the stream as well as with some allowances, the resistance of sharp narrowing and the resistance of turn by 90° without the change of areas of sections before and after the turn, are calculated theoretically. And our primary resistances — the turn in the collector by 90° and the turn from the collector into the feeder with the change of areas of sections before and after the turn are defined only experimentally. As the coefficient of losses on friction λ, the coefficients of resistances on the division of the stream calculated according to (11) and passage and branching of a part of the stream defined according to (15) and (16), are also obtained by way of processing the results of experiments [1, 5]. Since hydraulics is calculation and experimental science, one will have to use experimental data in theoretical researches.

Regardless the number of operating feeders, the Bernoulli equation is same — it is equation (1). Or, one can write down the BE for section *1–1* and any section of GS or any two sections (along the stream), although the flow rates of the fluid in these sections can differ by many times. I. e. we *use the Bernoulli equation for the sections of the stream with different float rates* and, unsurprisingly, experiments prove this, seemingly, absurd allowance. And the calculation of GS became possible at this expense. Without any additional principles. Only obvious: $Q = \sum_{i=1}^{n} Q_i$, where Q_i — the flow rate of the fluid in i feeder. In any section of the hydraulic system, H acts in the form of a sum of velocity and piezometric pressures and losses of pressure.

Apart from two usual hydraulic losses — on friction along the length and in local resistances, the calculations take into account the losses on the change of pressure calculated according to the correlations (11), (15) and (16). The possibility to sum up losses on the change of pressure with the losses on friction along the length and in local resistances is not grounded theoretically. However, there is no experimental data contradicting this allowance.

The Bernoulli equation is established for the elementary spray of ideal («dry») fluid at the established movement strictly theoretically, without engagement of experimental data [2, P. 95–97]: $h + p/\gamma + v^2/2g = \text{const}$ (along the spray), where h is the excess of the section over the plane of comparison. However, for the stream of real (viscous) fluid at the established movement, one has to implement the losses of pressure on friction and in local resistances and the coefficient of inequality of distribution of velocity on the section of the stream α [2, P. 108–111]. Herewith, to define losses on the friction, they find the experimental coefficient of losses λ, and for the losses in local resistances — coefficients of local resistances ζ. The coefficients λ and ζ depend on the velocity of the movement of the stream, coarseness of the surface of the pipe etc. I. e. the Bernoulli equation becomes calculation-experimental. And the expansion of its work on the streams with alternate flow rate of fluid with the use of experimental equations (11), (15) and (16) should not cause protest.

Let us note that the feeders «know» about each other, because switching on and switching off of only one feeder leads to the change of work of the entire hydraulic system (see Tables 1 and 2). Herewith, experimentally, the process of the fluid outflow is established very quickly, for 5–10s, even at sharp «imbalance» in the system, when, only feeders I, II and III operate. Apparently, there is something that is yet to be understood.

Conclusion

Thus, the ring-shaped gating system is researched theoretically and experimentally with the definition of velocities and flow rates of fluid in each feeder and in the entire system. At the calculation of such hydraulic system with changing flow rate of the fluid, the Bernoulli equation was used, although, it was established theoretically and checked in practice for the stream of fluid with constant flow rate. The calculation is done by method of successive approximations until the desired value of difference of losses of the pressure from the opposite sides from the zero point is achieved. A good agreement between the calculated and experimental data is obtained.

References:

1. Меерович И. Г., Мучник Г. Ф. Гидродинамика коллекторных систем. – М.: Наука, – 1986. – 144 с.
2. Чугаев Р. Р. Гидравлика. – М.: изд-во "Бастет", – 2008. – 672 с.
3. Токарев Ж. В. К вопросу о гидравлическом сопротивлении отдельных элементов незамкнутых литниковых систем//Улучшение технологии изготовления отливок. – Свердловск: изд-во УПИ, – 1966. – С. 32–40.
4. Jonekura Koji (et al.) Calculation of amount of flow in gating systems for some automotive castings//The Journal of the Japan Foundrymen's Society. – 1988. – Vol. 60. – № 8. – P. 326–331.
5. Идельчик И. Е. Справочник по гидравлическим сопротивлениям. – М.: Машиностроение, – 1992. – 672 с.

6. Васенин В. И., Васенин Д. В., Богомягков А. В., Шаров К. В. Исследование местных сопротивлений литниковой системы//Вестник ПНИПУ. Машиностроение, материаловедение. – 2012. – Т. 14. – № 2. – С. 46–53.
7. Васенин В. И., Богомягков А. В., Шаров К. В. Исследования L-образных литниковых системы//Вестник ПНИПУ. Машиностроение, материаловедение. – 2012. – Т. 14. – № 4. – С. 108–122.

DOI: http://dx.doi.org/10.20534/AJT-16-9.10-28-30

Kuliev Sabir,
Azerbaijan University of Architecture and Construction
Kazymov Musa,
Azerbaijan State University of Oil and Industry
E-mail: rahimova_mahluqa@mail.ru

Study of cracks formation in curved bars and rocks

Abstract: As it is know, different load-gripping devices, so called hooks, are used in the performance of loading and unloading works of mobile installations, cranes.

Years-long use of load hooks showed that the wrong selection of the material, production technology as well as violations of the exploitation regime lead to the appearance of hollows, cracks, slag inclusions, which can cause the breakdown of hooks and emergency situations at production site. Hence, during the design of hooks, it is required to calculate its exact durability and crack-resistance**.**

Keywords: load-gripping devices, high curve bar, stress-intensity factor, cracks, buckling loads, normal fracture.

The work [1] presents the study of the stress condition of load-gripping devices, hooks, and defines total stress in critical points B and C of cross-section (Figure 1).

Having defined the maximal total stress in a critical point of the cross-section of the bar during the calculation of hook durability, it is required to determine critical values of external load (i. e. the weight of a lifted load) at which cracks formation and local or complete destruction of the body begin.

A principle moment consists in the condition of the limit equilibrium. The simplest variant of this condition, based on physical ideas of Griffith, was formulated by Irwin in case of a normal fracture [2; 3]. Irwin showed that the appearance of cracks in a brittle or quasi-brittle body takes place when stress intensity at the top of the crack (к) reaches some (constant, for this material) value.

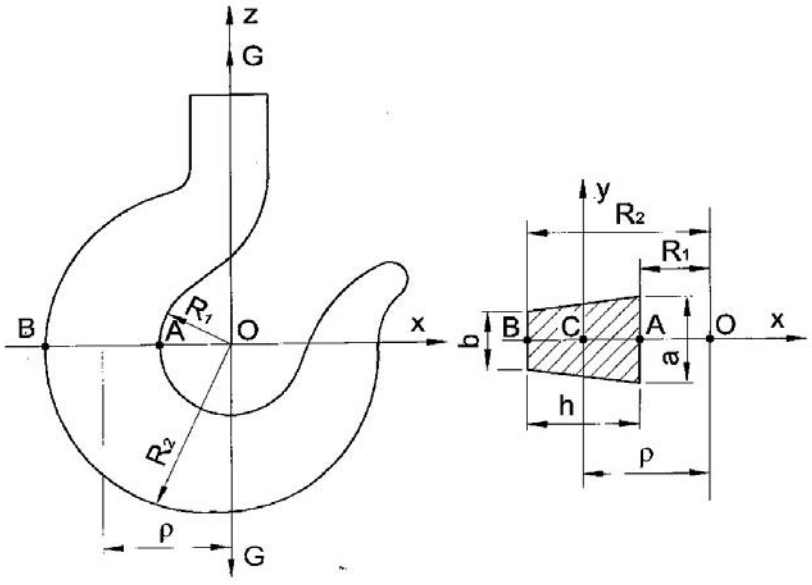

Figure1. Curved bar (hook)

$$k = \frac{K_C}{\sqrt{\pi}} \quad (1)$$

The constant k_c characterizes resistance of the material to destruction, which is determined experimentally. At uniaxial tension of the body, the value of the critical stress $P_{np} = \sigma_{np}$ is defined by the correlation

$$P_{np} = \frac{k_c}{\sqrt{\Pi l}} \quad (2)$$

P_{kp} is a mean value of technical durability of this material at uniaxial tension $[\sigma_b]$.

$$\min P_{kh} \cong 0{,}97P = [\sigma_b] \quad (3)$$

According to calculations obtained on the basis of accepted Griffith-Irwin hypothesis, the data about the spread of the crack accords well with experimental data [4].

Since our equation simultaneously includes bending moment (Mbend) and tension force, P we took into account the following criterion of brittle fracture specified in the works of Knowles, Vang, Engie and Williams [4; 5]:

$$K_{1calculated} + \frac{1+\nu}{3+\nu} \cdot K_{1bend} = K_C \quad (4)$$

Here, $K_{1calculated}$ is a coefficient of stress intensity at tension, which is defined on the basis of the following asymptotic formula (in polar coordinates r and θ):

$$\left.\begin{aligned} \sigma_r &= 5\cos\frac{\theta}{2} + \cos\frac{3\theta}{2} \\ \sigma_\theta &= \frac{K_1^{(calculated)}}{4\sqrt{2r}} 3\cos\frac{\theta}{2} + \cos\frac{3\theta}{2} \\ \sigma_{r\theta} &= \sin\frac{\theta}{2} + \sin\frac{3\theta}{2} \end{aligned}\right\}$$

$$\left.\begin{matrix} \sigma_r \\ \sigma_\theta \\ \sigma_{r\theta} \end{matrix}\right| = \frac{K_1^{(calculated)}}{4\sqrt{2r}} \left|\begin{matrix} 5\cos\frac{\theta}{2} + \cos\frac{3\theta}{2} \\ 3\cos\frac{\theta}{2} + \cos\frac{3\theta}{2} \\ \sin\frac{\theta}{2} + \sin\frac{3\theta}{2} \end{matrix}\right. \quad (5)$$

In numerical calculations, the value r is accepted as $r \cong 0{,}011l$, where θ is the angle between the axis ox and their polar radius vector r.

K_{1bend} is a coefficient of stress intensity at pure bending of the moment M_{bend}, which is defined according to the following asymptotic formula:

$$\sigma_p \quad \left|\left(3+5\nu\right)\cdot\cos\frac{\theta}{2} - \left(7+\nu\right)\cos\frac{3\theta}{2}\right.$$

$$\sigma_\theta = \frac{K_1^{bend}}{2\left(3+\nu\right)\sqrt{2r}} \cdot \frac{\delta}{h}\left(5+3\nu\right)\cdot\cos\frac{\theta}{2}$$

$$\sigma_{r\theta} = -\left(1-\nu\right)\cdot\sin\frac{\theta}{2} + \left(7+\nu\right)\sin\frac{3\theta}{2}$$

$$\left.\begin{matrix} \sigma_p \\ \sigma_\theta \\ \tau_{r\theta} \end{matrix}\right| = \frac{K_1^{bend}}{2(3+\nu)\sqrt{2r}} \left|\begin{matrix} (3+5\nu)\cos\frac{\theta}{2} - (7+\nu)\cos\frac{3\theta}{2} \\ (5+3\nu)\cos\frac{\theta}{2} + (7+\nu)\cos\frac{3\theta}{2} \\ -(1-\nu)\sin\frac{\theta}{2} + (7+\nu)\sin\frac{3\theta}{2} \end{matrix}\right. \quad (6)$$

where ν is a Poisson ration for many makes of steel $0{,}2'' \nu'' 0{,}3$ and coefficient $K_1^{(bend)}$ is defined by the following formula:

$$K_1^{(bend)} = \frac{6M_{bend}}{2h^2}[1-\cos 2\alpha]\cdot\sqrt{l} \quad (7)$$

M_{bend} is a moment defined by the formula:

$$M_{изг} = P\cdot x = \rho\left(\frac{d}{2} + h_1\right) \quad (8)$$

where, P is force applied to the hook (weight of the lifted load); d is the diameter of inner circumference of the hook (curved bar); h is the distance from inner circumference to the center of gravity of the cross-section of the bar (hook); l is the length of supposed crack (maximal length of the crack will be equal to the length of the base of trapezoid, i. e. $l_{\max} = a$).

In numerical calculations, the value of technical durability (durability limit of the bar material) $[\sigma_b]$ for different makes of steel is selected from respective reference books. Below is the values $[\sigma_b]$ for some makes of steel:

Material:

$[\sigma_b] = C_T - 10\,34$ kG/mm^2;

$[\sigma_b] = C_T - 25\,46$ kG/mm^2;

$[\sigma_b] = C_T - 40\,58$ kG/mm^2;

C4 ← (12–28) – grey cast iron 12 kG/mm^2 – of stree 50 kG/mm^2 – in compression

$[\sigma_b] = C_T - 20x - 80$ kG/mm^2

Final stress in the critical point of the section of the bar (hook) is defined according to the following formula

$$\sigma_\theta = \sigma_{\theta calculated} + \sigma_{\theta bend} \quad (9)$$

where $\sigma_{\theta calculated} = \frac{P}{F}$ is normal stress at the tension with the force P.

The stress of the bending is related to M_{bend} and defined by the formula

$$\sigma_{\theta bend} = \frac{M_{bend}}{F}\cdot k \quad (10)$$

where M_{bend} is bending moment defined by the formula

$$M_{bend} = P\left(\frac{d}{2} + h_1\right) \quad (11)$$

K is the ratio depending on typical sizes of section, which is defined as:

$$K = \frac{1}{z_0}\cdot\frac{z_0+z}{r_0+z};$$

At the section of tasks by the method of the theory of elasticity, the stress at bending σ_{bend} is defined by the formula

$$\sigma_{bend} = M\delta \cdot \left[\frac{a^2 b^2}{r^2} \cdot \ln \frac{b}{a} + b^2 \cdot \ln \frac{r}{b} + a^2 \ln \frac{d}{r} + b^2 - a^2 \right] (12)$$

$$\delta = \frac{4}{\varepsilon}$$

$$\varepsilon = \left(b^2 - a^2\right)^2 - 4a^2 b^2 \cdot \left(\ln \frac{b}{a} \right)^2;$$

Knowing the final stress σ_θ, we define the coefficient of stress intensity (K_1) and the value of critical load P_{cd}, at which the body starts destruction, according to the following formulas.

$$K_1 \left[\frac{10}{P\sqrt{l}} \right] = 4a \quad (13)$$

where *a* is a numerical value of stress δ_θ

Critical values of load P_{cd}

$$P_{cd} = \frac{10}{0{,}97 \cdot 4a} \cdot \left[\sigma_b\right] \quad (14)$$

Conclusions. Equations obtained by us for final stress allow defining the coefficient of stress intensity and the value of critical force at which the body start destruction.

References:

1. Кулиев С. А., Казимов М. И. Напряженное состояние грузоподъемных крюков. Восточно-Европейский журнал передовых технологий. – 1/1 (73) – 2015. – Украина, – С. 67–72.
2. The theory of rupture-Proc. First Intern. Congr. Appl. Mech. Delft – 1924. – 55–63.
3. Analysis of stresses and strains near the and of a crack traversing a plate. – t. Appl. Mech. – 1957, – 24, – № 3, – P. 361–364.
4. Эрдоган И. С. О развитии трещин в палстинках под действием продольной и поперечной нагрузок технической механики (труды Американское общество инженеров механиков) – 1963. – Т. 85. – д.4, – С. 49–51.
5. Math T.and Phys, – 1960, – V. 39, – No 3. – P. 223–236.
6. Appl T. Mech., – 1961, – V. 28, – No 3. – P. 372–378.

Section 5. Medical science

DOI: http://dx.doi.org/10.20534/AJT-16-9.10-31-35

Gushul Ivan Yaroslavovich,
Higher State Educational Establishment of Ukraine
"Bukovinian State Medical University", Chernivtsi
E-mail: ivanhushul@ukr.net

Some pathomorphological peculiarities of acute distress-syndrome in case of the large intestine cancer, complicated by acute prevalent peritonitis

Abstract: The results of experimental-clinical investigation of the pathomorphological changes of the lung tissue at acute respiratory distress-syndrome, the origin of which was due to acute extensive peritonitis, against a background of the large intestine cancer are presented in the article.

The obtained results of the research are evidence that the development of acute respiratory distress-syndrome in case of acute extensive peritonitis of cancerous genesis is characterized by more evident accumulation of the swollen tissue with great quantity of erythrocytes and a decreased fibrin formation that is manifested including the absence of the classical hyaline membranes.

Keywords: acute respiratory distress-syndrome, acute extensive peritonitis, cancer of the large intestine.

The main reason of unsatisfactory results of the patients' treatment suffering from acute prevalent peritonitis (AEP) is the onset of abdominal sepsis with the subsequent development of polyorganic insufficiency [1, 9].

For the most part, lungs are involved first to the development of polyorganic insufficiency syndrome with the following origin of acute respiratory distress-syndrome (ARDS) which is one of the main causes of the lethality of patients with AEP making 70–90% [5; 9].

In spite of a great number of investigations, devoted to diagnostics, optimization of the intensive therapy of ARDS, many aspects of this problem are insufficiently known, particularly against a background of AEP of oncogenous genesis, what is demonstrated by high lethality.

Study of patho-morphological specific characteristics of ARDS development at AEP, originated against a background of the large intestine cancer, will enable to understand better the role of oncogenous process in the development and clinical course of this complication [1; 3; 4; 8].

The aim of the research is to study experimentally and clinically patho-morphological peculiarities of ARDS in case of AEP development, which arisen against a background of the large intestine cancer.

Material and methods of the research Experiment was carried out on 14 sexually mature non-linear rats of middle age of both sexes with the weight not less than 180g, to whom AEP was simulated by means of intraperitoneal introduction of 30% fecal suspension in quantity of 1 ml per 100 g of the animal weight [2].

All animals under study were divided into two groups — a group of comparison and basic one. The basic group consisted of 8 animals to which Heren's tumor had been vaccinated into the large intestine two weeks before simulation of acute prevalent peritonitis according to the method proposed by us [7].The group of comparison was made up of 6 animals without Heren' tumor.

Biological material sampling was carried out during autopsy of animals, 24 and 48 hours after AEP simulation.

Surgical procedures were conducted under vivarium conditions of higher state educational establishment of Ukraine "Bukovinian state medical university" meeting the requirements standards "General ethical principles of the experiments on animals" (Ukraine, 2011), coordinated with regulations of the "European convention about protection of the spinal animals, used for experiments and other scientific purposes" (Strasburg, 1985).

Euthanasia of rats was realized according to the ethical standards and acting recommendations, in a state of deep narcosis, by means of introduction of surplus quantity of the narcotic preparation, in compliance with the law of Ukraine № 3447–1 of the 21.02.2006 "About the protection of animals from the cruel treatment".

Clinical investigations were conducted by means of autopsy of 16 physical bodies of the dead patients with acute prevalent peritonitis, where acute respiratory dysfunction took place in the structure of polyorganic insufficiency. The dead patients were divided into two groups — the group of comparison and the basic one. The basic group was composed of 9 persons with peritonitis as a result of complication of the large intestine cancer. The group of comparison consisted of 7 patients when not-tumor diseases of the large intestine were the source of peritonitis. Both groups were represented as to the age, sex, stage, degree of peritonitis severity, volume of the surgical procedures performed.

At histological research biopsy materials of the lungs were fixed in 10% neutral formalin for photooptical investigation. Paraffin sections were stained with hematoxylin and eosin.

Descriptive technique of the detected patho-morphological changes has been used.

The results of the research The conducted experimental investigations showed that on the 24 hour of observation patho-morphological picture of the lungs of the animals of the basic group and the group of comparison, was characterized by the presence of emphysematous areas, however, they had more expressed character, with focal hyperemia of medium and small size, diapedetic hemorrhages and irregular edemas, interstice and lumens of the respiratory parts of the lungs. Desquamation of epithelium and macrophages was also determined in small and medial bronchi as well as the respiratory parts of the lungs (figure1, figure 2).

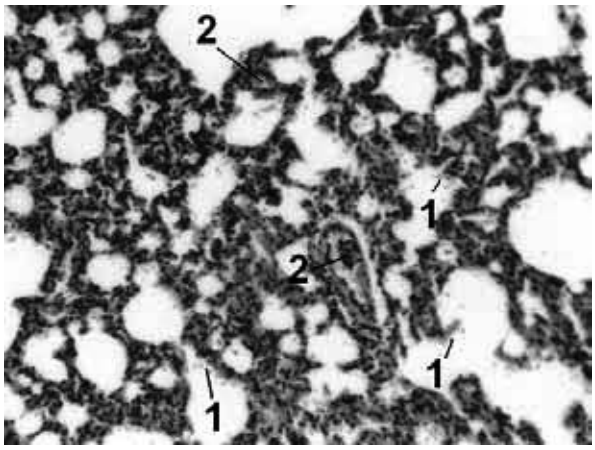

Figure 1. Histological section of the right lung of the laboratory rat with Heren's tumor, inoculated into the wall of the large intestine, on the 24hour after simulation of acute prevalent peritonitis. Emphysematous areas with diapededic hemorrhages (1), focal hyperemia of the veins (2). Staining was carried out using hematoxylin and eosin.Vol.10×.Oc.10×.

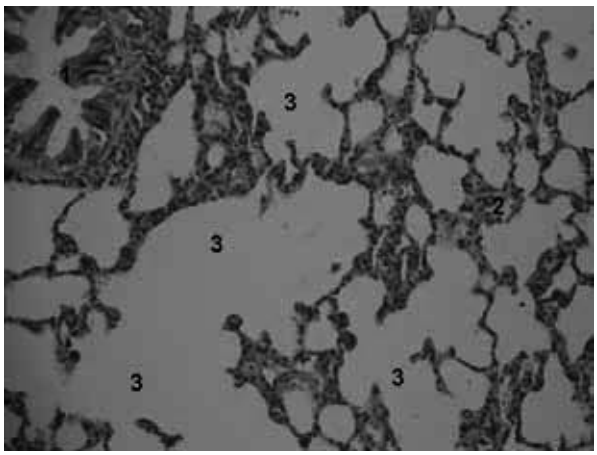

Figure 2. Histological section of the right lung of the laboratory rat with Heren's tumor inoculated into the wall of the large intestine, on the 48th hour after simulation of acute prevalent peritonitis. Dystrophy of epithelium of the bronchi (1). Dilatated blood vessels (2). Emphysematous areas of the pulmonary tissue (3). Staining with hematoxylin and eosin. Vol.10^{x}. Oc.10^{x}.

ARDS development, characterized by filling the respiratory parts of the lungs, approximately 40–60%, by erythrocytes, fibrin, hydropic fluid, peeled alveolocytes and condensed macrophages should be indicated when studying the pulmonary tissue of the patients of the group of comparison.

In contrast to the basic group, significantly more fibrin, but less erythrocytes is marked in hydropic fluid, and hyaline membranes' formation is also observed, in some places there are areas of dystalectase (figure 3, figure 4).

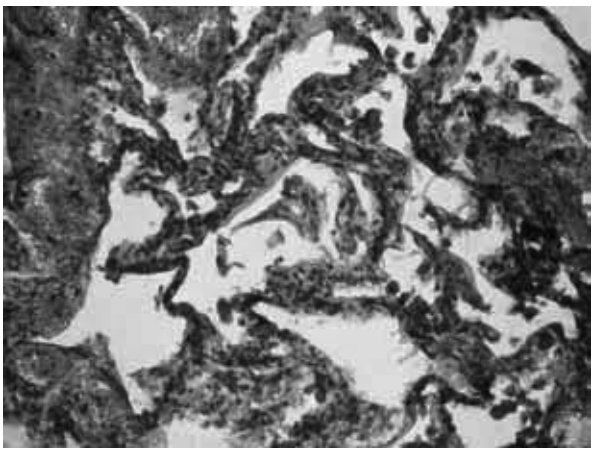

Figure 3. Histological section of the pulmonary tissue. Patient B., 60 years old, № 11. Diagnosis: perforation of the sigmoid colon. Diffuse fecal peritonitis. Respiratory part of the lung is filled with erythrocytes (1), fibrin (2). Peeled alveolocytes and condensed macrophages (3). Hyaline membranes (4). Hematoxylin and eosin.Vol. 10^x. Oc. 10^x.

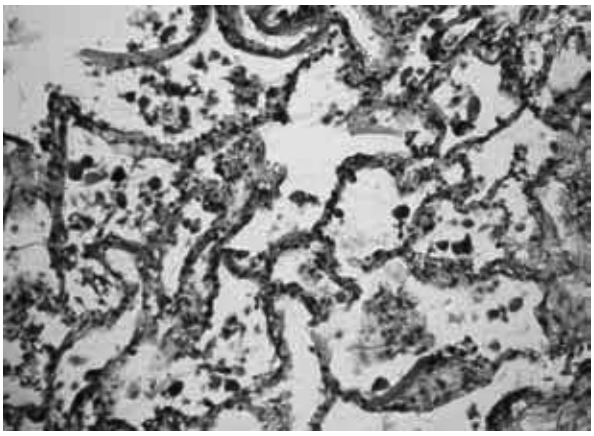

Figure 4. Histological section of the pulmonary tissue. Patient D., 67 years old, № 7. Diagnosis: perforation of the descending part of the sigmoid colon. Diffuse fibrinopurulent peritonitis. Respiratory part of the lung is filled with fibrin (1), erythrocytes (2). Peeled alveolocytes and condensed macrophages (3). Hematoxylin and eosin.Vol. 10^x. Oc. 10^x.

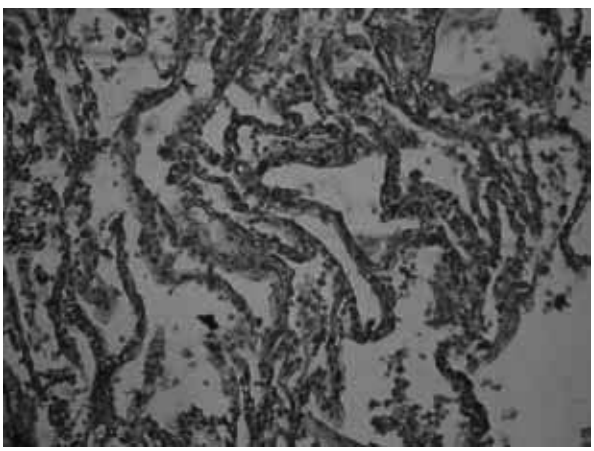

Figure 5. Histological section of the pulmonary tissue. Patient K., 73 years old, № 11. Diagnosis: cancer of rectosigmoid part of the rectum, $T_3N_1M_0$, III stage, II clinical group. Perforation of intestinal wall with tumor. Diffuse fecal peritonitis. Fibrin filaments (1), areas of dystalectase (2). Hematoxylin and eosin.Vol. 20^x. Oc. 10^x.

Pulmonary tissue of patients of the basic group, in the predominant majority of cases, was characterized by the development of the picture of exudative ARDS, namely, the respiratory parts of the lungs are filled with erythrocytes, hydropic fluid, fibrin approximately 85–95%, taking into account comparatively small quantity of fibrin. Microthrombosis and stasis of the blood were noticed (figure 5, figure 6).

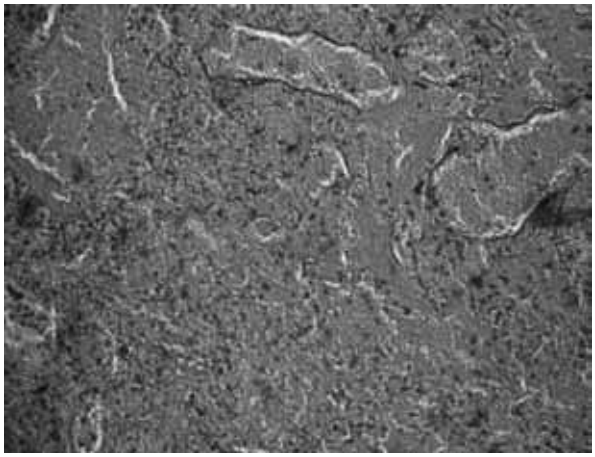

Figure 6. Histological section of the pulmonary tissue. Patient D., 75 years old, № 27. Diagnosis: cancer of the descending part of the colon $T_3N_2M_1$. Metastatic damage of the liver, IVstage, IVclinical group. Perforation of the intestinal wall with tumor. Diffuse fecal peritonitis. Respiratory part of the lung is predominantly filled with erythrocytes (1). Hematoxylin and eosin.Vol. 20^x. Oc. 10^x.

Discussion of the results of the research Summing up the results of the carried out investigations, it should be noted that similar changes, namely, ARDS development, arise in the pulmonary tissue at "oncogenous" and "non-oncogenous" peritonitis, however, at oncogenic pathology, into exudative phase, much more area of filling the respiratory part of the pulmonary tissue with hydropic tissue, erythrocytes is marked.

It should be noted that just at AEP of oncogenous etymology classical hyaline membranes are almost not formed, admixtures of erythrocytes in fibrinous exudates of the pulmonary tissue are marked, microaggregates, accompanied by the blood stasis, take place in the vessels.

Thus, the presence of oncogenous pathology at AEP, somewhat changes and complicates the development of ARDS, since comparatively more quantity of hydropic fluid with more expressed hemorrhagic component is marked, however, probably positive side — the absence of classical hyaline membranes should be marked.

Conclusion

The development of acute respiratory distress-syndrome at acute prevalent peritonitis of oncogenous genesis is characterized by more evident accumulation of hydropic fluids with great quantity of erythrocytes, but with the reduction of the fibrin formation, manifesting among them, by the absence of the classic hyaline membranes.

References:

1. Бойко В. В. Поширений гнійний перитоніт: монографія/В. В. Бойко, І. А. Криворучко, С. М. Тесленко, А. В. Сивожелізов. – Х.: Прапор, – 2008. – 280 с.
2. Василик В. М. Моделювання калового перитоніту у білих щурів/В. М. Василик//Вісн. пробл. біол. і мед. – 2006. – № 2. – С. 417–418.
3. Гресько М. М. Сучасні діагностичні критерії гострого перитоніту/М. М. Гресько, О. В. Стасишена, С. В. Колібаба//Науковий вісник міжнародного гуманітарного університету. – 2014. – № 7. – С. 13–14.
4. Гушул І. Я. Особливості перебігу гострого поширеного перитоніту онкологічного ґенезу/І. Я. Гушул, О. І. Іващук, В. Ю. Бодяка//Буковинський медичний вісник. – 2015. – Т. 19, – № 2 (74). – С. 62–65.
5. Давиденко І. С. Морфологічна діагностика гострого респіраторного дистрес-синдрому (клінічні лекції)/І. С. Давиденко//Неонатологія, хірургія та перинатальна медицинаю. – 2012. – Т. II, – № 1 (3). – Р. 84–89.
6. Моделювання раку товстої кишки/І. Я. Гушул, І. О. Іващук, І. С. Давиденко [та ін.]//Клінічна та експериментальна патологія. – 2015. – Т. XIV, – № 1 (51). – С. 44–46.

7. Патент України на корисну модель 98406, МПК A61 B 17/00. Спосіб моделювання раку товстої кишки/Гушул І. Я.; заявник та патентовласник Буковинський державний медичний університет. – № u 2014 12363; заявл. 17.11.14; опубл. 27.04.15, Бюл. – № 8.
8. Порівняльний аналіз результатів діагностики та лікування хворих на колоректальний рак/І. Д. Галайчук, В. І. Дрижак, М. І. Домбрович [та ін.]//Онкологія. – 2008. – Т. 10, – № 1. – С. 125–129.
9. Сучасні аспекти патогенезу, діагностики, хірургічного лікування перитоніту/Ю. Б. Куцик, В. П. Федоренко, Ю. І. Шаваров [та ін.]//Український Журнал Хірургії. – 2009. – № 4. – С. 92–97.

Section 6. Food processing industry

DOI: http://dx.doi.org/10.20534/AJT-16-9.10-36-40

Djahangirova Gulnoza Zinatullaevna,
Tashkent chemical-technological institute,
the PhD student, faculty "Foodstuff technology",
chair «Food technology»
E-mail: djaxangirova77@ mail.ru

Tursunkhodjaev Pulat Muhamedovich,
Tashkent chemical-technological Institute,
professor, faculty "Foodstuff technology", chair «Food technology»

Modern problems of quality formation of bread and way of their solution

Abstract: of actual in problems on the quality formation of bread is carried out. Additives which are used to improve the quality of the product are systematized. The feasibility of using natural supplements, including fruit and berry, vegetable raw-materials in bakery is proved.

Keywords: bread, quality, additives-improves, technological effect, functional orientation.

The basic functions of food consist not only in satisfaction of physiological requirements of an organism in food nutrients and energy, but also in the improvement of human health and preventive maintenance of alimentarno-dependent diseases. Thus, the special role is taken away to socially significant foodstuff, in particular, to bread and bakery products. Situation monitoring testifies to misfit of the quality of given products, especially from high-quality wheat flour, to demands of nutritiology to an adequate food. Baking production undergoes recently essential changes under the influence of sociopolitical, economic and market factors, namely as a result of an essential rise in prices for flour and energy carriers that should be reflected in the finished product price. Therefore instead of traditional production engineering everywhere the accelerated and express — production engineering providing considerable abbreviation of such stages of process, as maturation of flour half stuffs and proof. The given aspects cause decrease in consumer worth of bread: the maintenance of biologically valuable substances and their bioavailability decreases; expressiveness of grain aroma and taste decreases; curtailment of stability terms of physical and chemical and microbiological parameters of a finished product, there is mistrust of users to its safety [1, P. 25–33; 2, P. 24–27; 3, P. 24–26].

Iorgachevoj E. G., Lebedenko I. e. [4, P. 102–103] analyzed and systematized the basic actual problems of quality formation of the baking branch production (fig. 1).

It has been established that the basic problems connected with the quality formation of product in dynamical conditions of production, dare by means of application of the various additives positioned in the capacity of conditioners, in the core of an artificial origin. However, the fact of wide application of conditioners in breadmaking guards users and nutritiologists. As, with the account of constant and mass consumption of bakery products, even the insignificant maintenance of potentially dangerous joints of the chemical nature in them creates a steady load on a human body, though also small intensity that is one of the most important risk factors for his health.

It is known that foreign firms in the highly-developed countries manufacture conditioners, the containing components prohibited for local use, and deliver them in other countries by which legislation application of such additives is not regulated. For example, the firm Muhlenchemie GmbH produces conditioners which composition includes the bromate of potassium prohibited to use in Russia. The ascorbic acid, widespread in Germany for improving of the quality of flour, is prohibited in France, as it, in the core, a synthetic product. Besides ascorbic acid to raise baking properties of flour it is also applied such synthetic additives, as azodicarbomide, mono- and diglyceride diacetyl acids, benzoyl peroxide, phosphate and sodium carbonate, etc. [5, P. 34–35].

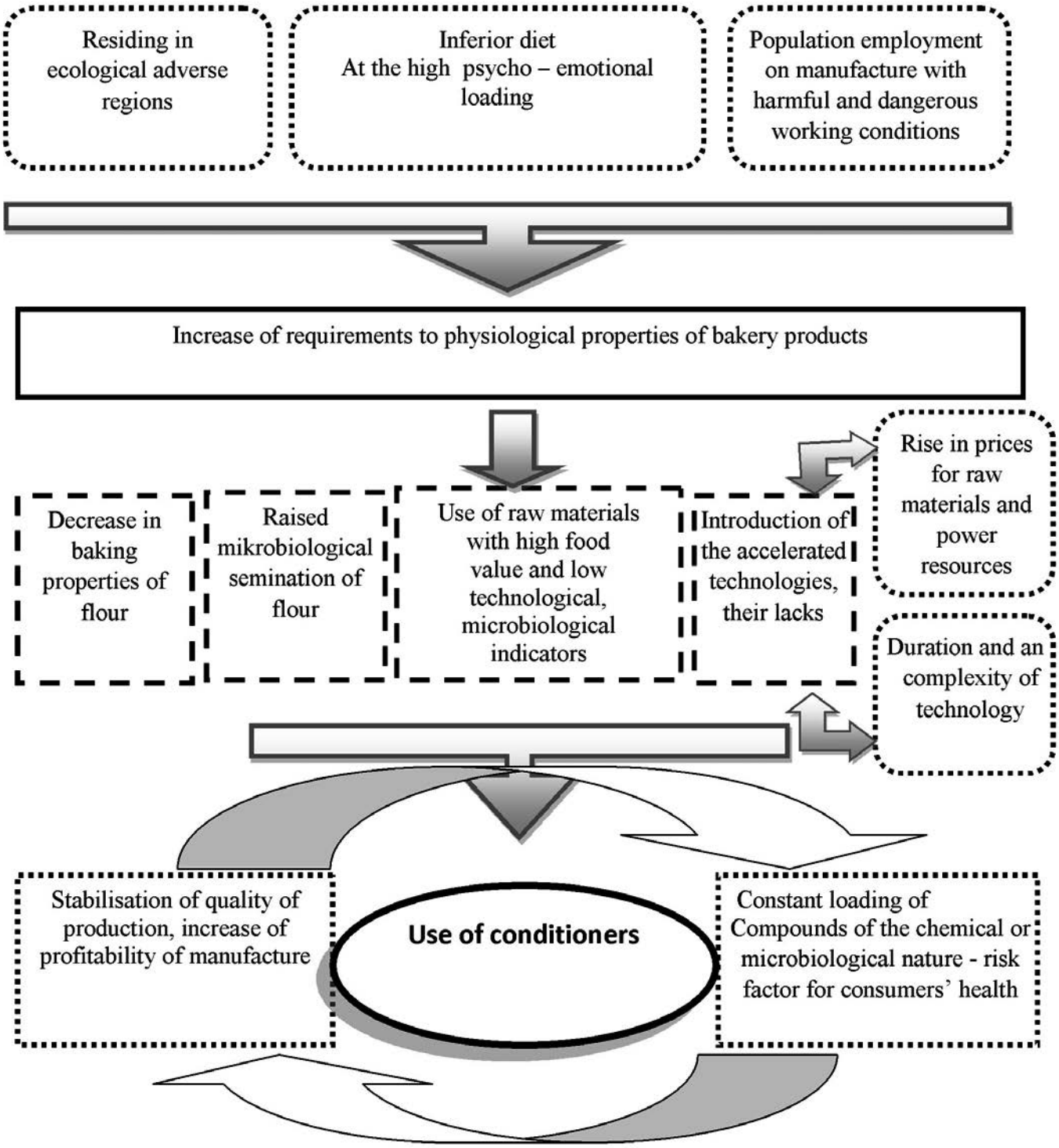

Fig. 1. The basic actual problems of quality formation of the baking branch production

Application and the food additives obtained in the biochemical way have been found. Such additives refer to artificial, for example, mushroom α-amilaza, glucooxidase and hemicellulose, which are obtained from specially, selected strains mold Aspergillus. Here it is possible to refer to the lecithin obtained from soybeans too. Necessity of the careful approach to artificial food additives proves that enzymes represent biological substances of high concentration and can cause an allergy, and lecithin is made from genetically inoculated raw materials which agency on human health remains disputable till now [5, P. 34–35; 6, P. 127–145; 7, P. 18–20].

Now all over the world stable trend of the growth of interest in the use of natural additives, including from a secondary material, in breadmaking is observed [8; 9, P. 15–32], systematized in the form of the circuit design represented in fig. 2.

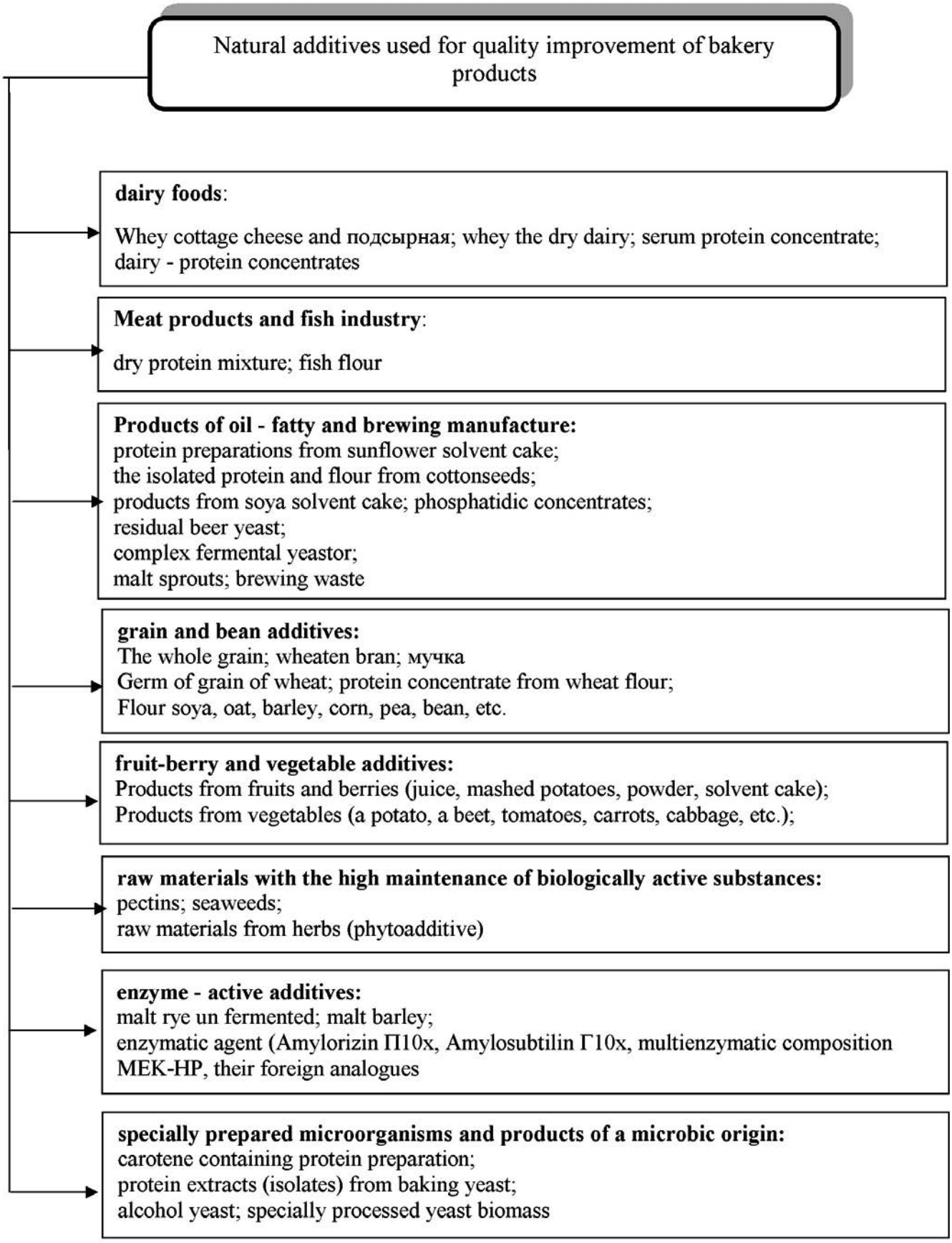

Fig. 2. Systematization of the additives used for expansion of assortment and quality improvement of bakery products

The technological effect and functional directivity on the use of separate natural additives at bread making and bakery products are resulted in tab. 1 [10, P. 46–47].

Table 1. – Technological effect and functional directivity of natural raw materials

The name of a raw component	Technological effect, functional directivity
Grain and leguminous raw materials: wheat and rye all-grinded; speltbean; corn; oat; barley; soya; buckwheat flour	Decrease in calorific value of bread; bread enrichment by food fibres; increase in the maintenance of fiber, mineral substances, vitamins; improvement of taste and aroma of bread; raise of bread yield
Wheat germ	Enrichment of bread by vitamins and mineral substances; raise of power worth of product
Wheat middlings	Decrease in calorific value of bread; bread enrichment by food fibres
Wheat, barley, rye, peas, corn, oat flakes	Bread enrichment by food fibres; decrease in calorific value of bread
Groats and grains of corn, soya, rye, buckwheat	Bread enrichment by micronutrient; calorific value decrease, improvement of flavoring qualities of products
Seeds of oil-yielding crops and products of their rehash: sunflower, flax, blue plant, gymnospermous pumpkins	Bread enrichment by polyunsaturated fatty acids; improvement of amino-acid score of bread on lysine, to methionine, tryptophan; increase in the maintenance of fiber; raise of energetic value of products
Processed products of fruits and vegetables: potato flakes, whitlow grass; powders of tomatoes, carrots	Delay of bread hardening; enrichment with vitamins, mineral substances and food fibers; decrease of energetic value of products
Herbs: thistle seeds, amaranthus flour, chicory, sea kale (sea girdle)	Improvement of taste and aroma of bread; enrichment of products with micronutrients
Spices: caraway seeds, anise, coriander	Improvement of taste and aroma of bread

Uzbekistan is one of the largest producers of fruit and vegetables. As a result of studying of the domestic market of functional foodstuff, raw sources and the marketing SWOT-analysis (tab. 2) it has been noted that to application of processing products of natural vegetative raw materials for nutrification of flour products do not appear proper attention.

Table 2. – The SWOT-analysis of application of nonconventional vegetative raw materials by manufacture of flour products

Potentially internal strength	Potentially internal weakness
• Engineering and working out of new aspects of products of the raised nutritive value. • Trade marks and positioning. • Skilled and qualified personnel. • Stable material resources. • Use of natural food raw materials, including secondary. • Independence of suppliers. • Possibility of a diversification of manufacture. • Resource-saving.	• Pricing. • Relative decrease in consumer advantages of products (volume decrease, crumb dim-out).
Potentially external possibilities	**Potentially external threats**
• Presence of legal acts. • Requirements of consumers in the market. • Accessibility, variety of raw sources.	Competitiveness of new aspects of products. Intensity of a competition. Pressure from producers of artificial additives and fillers.

At the same time use of the given additives allows to solve a row of technological problems: improvement of consumer advantages of products, raise of its biological worth, a process intensification of doughmaking, expansion of segment assortment of products of "a healthy food", the economy of basic raw materials (a flour, sugar, etc.).

Thus, there are almost unlimited natural food resources as by volume, and on a variety of the physiological affecting, allowing considerably to expand assortment and to raise the quality of flour products, in particular both bakery, and their treatment-and-prophylactic properties. Enrichment of bakery products by natural products has advantage before chemical specimens and their mixes. As a rule, the composition of these products, besides albumens, includes vitamins, mineral salts, other valuable food components, and, there are they in natural

relationships, in the form of natural joints, that is in that form which is better assimilated by an organism.

We have developed the receipt of grain products with addition of pulverous vegetative half-stuff from fruit (apples) and vegetable raw materials (a pumpkin, carrots, red sweet pepper, garlic, onions and fennel). The physiological effect and safety of the developed products has been investigated by the case study of morphofunctional characteristics of rats viscus (heart, a liver, gemmas, easy, a spleen, a brain, mother trees, adrenal glands) and the basic biochemical parametres of blood.

It has been determined that introduction in a ration of experimental animals of bread with investigated additives makes positive impact on behavioural reactions of rats, promotes a faster gain of their weight. The morphological both histologic data of an internal and biochemical parametres of blood of animals testified to the improvement of exchange processes in an organism of experiment groups of rodents. The positive physiological effect from use of vegetative additives in grain products for completion of diet of the person natural biologically active nutrient, in this case β — carotene, bioflavonoid and food fibres has been proved.

Thus, the expediency of use of processing products of vegetative raw materials, in particular fruit and vegetable, for bread enrichment biologically has been determined by active materials. Application of natural additives allows to reduce volumes of use of additives of not alimentary nature by manufacture of foodstuff and, hence, to raise level of safety and physiological effect from their application in a population food allowance.

References:

1. Соколов А. Правила игры меняются. Хлебобулочные изделия: обзор рынка / А. Соколов // Брутто. – 2011. – № 52. – С. 25–33.
2. Гагарина А. Хлебные моменты/А. Гагарина//Продукты & Ингредиенты. – 2011. – № 2. – С. 24–27.
3. Акинфиева И. Хлеб наш насущный/И. Акинфиева//Продукты & Ингредиенты. – 2008. – № 2. – С. 24–26.
4. Иоргачева Е. Г. Потенциал лекарственных, пряно- ароматических растений в повышении качества пшеничного хлеба/Е. Г. Иоргачева, Т. Е. Лебеденко//Технология и оборудование пищевых производств. Восточно –Европейский журнал передовых технологий. – 2014. – № 12 (68) –Т. 2. – С. 101–107.
5. Мелешкина Е. Пищевые добавки для муки/Е. Мелешкина//Хлебопродукты. – 2005. – № 12. – С. 34–35.
6. Матвеева И. В. Биотехнологические основы приготовления хлеба/И. В. Матвеева, И. Г. Белявская. – М.: Де Ли принт, – 2001. – 150 с.
7. Войно Л. И. Белковые добавки грибного происхождения для обогащения хлеба/Л. И. Войно, О. И. Коннова //Кондитерское и хлебопекарное производство. – 2011. – № 7. – С. 18–20.
8. Дробот В. И. Использование нетрадиционного сырья в хлебопекарной промышленности/В. И. Дробот. – К.: Урожай, – 1988. – 152 с.
9. Матвеева Т. В. Мучные кондитерские изделия функционального назначения. Научные основы, технологии, рецептуры: монография/Т. В. Матвеева, С. Я. Корячкина. – Орел: ФГОУ ВПО «Г осуниверситет – УНПК», – 2011. – 358 с.
10. Стабровская О. И. Анализ рынка многокомпонентных смесей для производства хлебобулочных изделий/О. И. Стабровская, А. С. Романов//Хлебопродукты. – 2011. – № 1. – С. 46–47.

DOI: http://dx.doi.org/10.20534/AJT-16-9.10-41-44

Djuraeva Nafisa Radjabovna,
Bukhara engineering-technological institute,
scientific researcher-applicant, faculty of chemical technology
E-mail: nafis101@mail.ru

Isabaev Ismail Babadjanovich,
Bukhara engineering-technological institute,
professor, faculty of chemical technology.
E-mail: isabayev_63@mail.ru

Influence of fat-flour mixes on sensor quality indicators of bread

Abstract: in article is considered the problem of expediency of use of the germinal product of wheat as flour fraction of fat-flour mixes. Efficiency of application of these mixes for improvement of sensor indicators of quality of bread is determined.

Keywords: fat-flour mix, fat, flour of the germinal product, bread, sensor indicators.

In the baking industry as a part of compounding of the majority of bakeries and rich products from the wheaten flour are widely used the high-quality margarine, animal and vegetable oils, baking fats, shortening agents, compounds various on structure and properties. Their addition in the dough improves quality of finished goods: the volume increases, porosity of a crumb improves, the freshness of bread remains longer [1, 35].

However, besides the traditional fats, nowadays raised demand of consumers and manufacturers has the production corresponding to the concept of a positive food, and that demands expansion of fundamental and applied researches to this group of products which should become the basic diet [2, 287–291].

One of key directions of the decision of the given problem in baking industry is development of fatty composite mixes with functions of modifiers, allowing purposefully coordinate the rheological properties of the dough and quality of bread in the set direction. Search of economically effective technologies of reception of fatty products of the functional purpose has shown expediency of application of the germinal product of wheat for preparation of the various mixes. The germinal product accumulates in itself the significant amount of biologically active substances, is characterized by integrated approach of a chemical compound and is biologically and technologically effective in making of fat-flour mixes [3, 9; 4, 32].

With the account of conservatism of tastes of consumers, that is the settled stereotypes to quality of food products, especially to bread and bakery products as socially significant, sensor indicators are the most important. Therefore at use of the various additives positioned as modifiers of quality of products, it is necessary to predetermine their influence on the above-stated indicators.

Objective of the research was development of fat-flour mixes with the crushed germinal product further called as the flour (flour from the germinal product of wheat), for use as receipt component at bread production.

For achievement of goal of the research following problems have been solved: selection and optimization of structure of fat-flour mixes; an estimation of influence of the offered semi-finished product on sensor (organoleptic) indicators of quality of bread.

As objects of research have been used samples of fat-flour mixes and ready bakery products with additives.

The technology developed by us provides application of composite mixes from waterless fats with flour from the germinal product of wheat. For preparation of a waterless mix as a fatty component can be used any firm, plastic or buttery (for prevention of the process of sedimentation of particles with the mixed flour) food waterless fats or the fatty mixes of various structure intended for a batch.

In work are used receipt culinary fat, consisting of 85% vegetative fat-oil of and 15% vegetable oil.

For an estimation of influence of various on structures fat-flour mixes quality of bread from wheat flour of 1st grade we carried out a series of trial laboratory batches by the standard technique with entering of respective alterations in the receipt in compliance with a matrix of mathematical planning of experiment. As samples of comparison were used the products prepared on above-stated margarine and the waterless fat without addition of flour from the germinal product of wheat. Quality of products analyzed in 3 hours after the batch.

Research program has been carried out by central composition uniform-routable planning, which includes following stages: factorial plan $2^{3.}$ constituent «the core» of the plan; «star-like» points on the factorial dimension and additional experiments in the center of plan [5, 5–11].

Matrix of planning and results of experiment are shown in Table 1.

Table 1. – Matrix for calculation of coefficient of regression equation for three-factorial experiment

Experiment system	№	Coded factors				Natural factors			$\bar{y}_u$, grade
		x_0	x_1	x_2	x_3	X_1	X_2	X_3	
Full factorial experiment of type 2^3	1.	+1	–1	–1	–1	1,0	30,0	40,0	14,3
	2.	+1	+1	–1	–1	7,0	30,0	40,0	10,7
	3.	+1	–1	+1	–1	1,0	70,0	40,0	10,1
	4.	+1	+1	+1	–1	7,0	70,0	40,0	9,4
	5.	+1	–1	–1	+1	1,0	30,0	46,0	18,3
	6.	+1	+1	–1	+1	7,0	30,0	46,0	15,2
	7.	+1	–1	+1	+1	1,0	70,0	46,0	16,3
	8.	+1	+1	+1	+1	7,0	70,0	46,0	16,0
Experiments in «star-like» points	9.	+1	–1,21	0	0	0,4	50,0	43,0	17,4
	10.	+1	+1,21	0	0	7,6	50,0	43,0	15,0
	11.	+1	0	–1,21	0	4,0	25,8	43,0	18,3
	12.	+1	0	+1,21	0	4,0	74,2	43,0	16,8
	13.	+1	0	0	–1,21	4,0	50,0	39,4	11,4
	14.	+1	0	0	+1,21	4,0	50,0	46,6	17,7
Experiments in planning center	15.	+1	0	0	0	4,0	50,0	43,0	18,5

In a general view required under the composite plan of secondary order the mathematical model is reliably enough approximated by the equation (1):

$$y=b_0+b_1x_1+b_2x_2+b_3x_3+b_{12}x_1x_2+b_{13}x_1x_3+b_{23}x_2x_3+b_{11}x_1^2+b_{22}x_2^2+b_{33}x_3^2 \quad (1)$$

As major factors are accepted: x_1 –receipt quantity of fat-flour mixes, in% to the receipt quantity of the flour; x_2-mass fraction of flour from the germinal product of wheat, in% to total quantity of the mix; x_3 — humidity of the dough, in%. For each factor were definedthe center, an interval of a variation and dependence of coded variable x_i from natural X_i. Target parameter (y) was the sensor indicators of quality, a point.

Complex factor of sensor indicators of quality of bread (y) represents the sum of products of individual indicators of quality on corresponding factors of weightiness. For the characteristic of the given indicators used the 20-point scale with the account of factors of the importance of indicators [6, 15–22].

Intervals of a variation of major factors are determined experimentally with the account of quality of received mixes and requirements to fatty products.

For definition of degree of a coordination of experts used the method of aprioristic ranging [7, 69–73]. Experts were offered to make ranged number on the sum of organoleptic indicators of the quality of investigated samples of bread for the purpose of allocation of the most qualitative samples. Then by experts the samples-leaders having the minimum total rank (table 2) have been allocated.

Table 2. – The normalized columns of ranks of individual indicators of the quality of bread

Number of the sample	Experts (n=7)							The sum of ranks	Deviation of the sum of ranks from average d	Squares of deviations d^2
	1	2	3	4	5	6	7			
1	*2*	*3*	*4*	*5*	*6*	*7*	*8*	*9*	*10*	*11*
1	11	11	10	11	11	11	11	76	20	400
2	13	13	13	13	12	13	13	90	34	1156
3	14	15	14	14	14	14	14	99	43	1849
4	15	14	15	15	15	15	15	104	48	2304
5	3	3	3	4	4	3	3	23	–33	1089

1	*2*	*3*	*4*	*5*	*6*	*7*	*8*	*9*	*10*	*11*
6	9	9	8	9	9	9	9	62	6	36
7	7	6	7	7	7	7	7	48	–8	64
8	8	8	9	8	8	8	8	57	–1	1
9	5	5	5	5	5	5	5	35	–21	441
10	10	10	11	10	10	10	10	71	15	225
11	2	2	2	1	2	2	2	13	–43	1849
12	6	7	6	6	6	6	6	43	–13	169
13	12	12	12	12	13	12	12	85	29	841
14	4	4	4	3	3	4	4	26	–30	900
15	1	1	1	2	1	1	1	8	–48	2304
Σ	–	–	–	–	–	–	–	–	–	**13628**

The sums of ranks on each indicator were defined:

$$\sum_{j=1}^{m=7} x_{ij} = x_{i1} + x_{i2} + ... + x_{i7} \qquad (2)$$

$i = 1 \div 15$.

where x_{ij} - a *rank of i — indicator of j — expert; m — number of experts* ($m=7$).

Deviation of the sum of ranks of each indicator from an average arithmetic for the whole matrix was determined under the formula (3):

$$d_{ij} = \sum_{j=1}^{m=7} x_{ij} - a = \frac{1}{2} \cdot 7 \cdot (15+1) = 56 \qquad (3)$$

where $a = \frac{1}{2} m(n+1)$ *– Average arithmetic value from the whole matrix, n — number of ndicators* (*15*).

The sum of squares of deviations is defined by dependence (4):

$$\sum_{i=1}^{15} d^2 = \sum_{i=1}^{15} \left(\sum_{j=1}^{m=7} x_{ij} - a \right)^2 \qquad (4)$$

Degree of a coordination of opinions of experts defined on Kendall's concordance factor, defined under the formula (5):

$$W = \frac{\sum_{i=1}^{15} d^2}{\frac{1}{12} m^2 (n^3 - n) - m \sum_{j=1}^{m=7} T_j} = \frac{13628}{\frac{1}{12} \cdot 7^2 (15^3 - 15)} = 0{,}99 \qquad (5)$$

where m — number of experts; n — quantity of variants, piece; T_j — an estimation of the connected ranks (it is defined in case the expert does not specify an order of decrease of two or several indicators and appropriates to each of them an identical average rank. In our case $T_i = 0$).

The coordination of opinions of experts confirmed with the concordance factor W=0,99 (at completely coordinated ranks *W=1,0*).

Experimental examples on anhydrous fat with M_{gp} have received the highest mark of tasters concerning control examples. The best ones were models with content of FFC 4% and M_{gp} 50% at humidity of dough 43%, which have received 18,5 grade concerning at 18,0 grade in control examples (with 2% fat without M_{gp}).

Statistical processing of experimental data has been executed with the help of correlation-regression analysis in Microsoft Excel 2013, and adequate mathematical models are derived as a result. Intervals of variation of factors are caused by technological indicators of quality of finished products.

On the basis of statistical processing of experimental data, calculation of estimations of regression factors, check of their importance, an estimation of reproducibility of experiences and determination of adequacy of the equations have been used statistical criteria of Student and Fisher. As a result were received the below-mentioned equations of the regress adequately describing dependences of chosen criterion *y* from the investigated factors:

$$y = 18{,}5 - 0{,}97x_1 - 0{,}78x_2 + 2{,}65x_3 - 1{,}52x_1^2 - 0{,}61x_2^2 - 2{,}64x_3^2 + 0{,}71x_1x_2 + 0{,}54\,x_2x_3; \qquad (6)$$

where x_i — the coded values of factors connected with natural values X_i, presented by correlations: $x_1 = (X_1 - 4{,}0)/3{,}0$; $x_2 = (X_2 - 50{,}0)/20{,}0$; $x_3 = (X_3 - 43{,}0)/3{,}0$.

The analysis of the received equations has shownthat on sensor indicators of quality of bakery products inversely proportional influence renders receipt quantity of fat-flour mixes — x_1 (regress factors «– 0,97»). It means that with reduction of factor x_1 value of the response will increase, and with increase of factor x_1 value of the response will decrease. As a whole the received results do not contradict known laws and are connected with features of structure of fat-flour mixes and test parameters.

On the basis of received relations were defined optimum dosages of FFC and the content of M_{gp} in them for bakery. Has been established that for receiving quality products receipt quantity of FFC on anhydrous fat shouldn't exceed 5% with content of M_{gp} no more than 50%.

Herewith [8, 23–25] recommended defining humidity of dough by formula (7):

$$W_m = 44{,}5 - 0{,}312 \cdot C_{fat}, \qquad (7)$$

where C_{fat} — receipt quantity of fat *(in our case quantity of FFC with account of oil content* M_{gp}*),%.*

We have to notice that because of rather high maintenance of flour from the germinal product of wheat, possessing raised water absorbing ability, at use of fat-flour mixes on waterless fat it is recommended to increase humidity of the dough on 0.5 … 1.0% concerning settlement value, and that will allow to increase an output of production of demanded quality and to lower its cost price.

Thereby, experimentally established optimal conditions of production of bread and bakery from wheat flour with use of FFC on anhydrous fat with content of M_{gp}. Received regress equation allows to predict and optimize the proportion of fat and flour fractions of mixture with aim of receiving of finished product of high quality according to the demands of consumers.

References:

1. Tarasova V. V. Application of physiologically functional components in manufacture of bakery products/V. V. Tarasova//Food-processing industry. – 2014. – 3. – P. 34–41.
2. Ipatova L. G. Fatty products for a healthy food. The modern opinion/L. G. Ipatova A. A. Kochetkova, A. P. Nechaev V. A. Tutelyan. – M: DeLi print, – 2009. – P. 396.
3. Ponomaryova O. I. Higher attention to use of by-products of grain-processing enterprises/O. I. Ponomaryova, I. M. Vasilinets//Baking of bread in Russia. – 2000. – 6. – P.19.
4. Paronyan, V. H. Products of processing of cereal cultures in fatty products/V. H. Paronyan, N. M. Skryabin, A. A. Popov//Fat-and-oil industry. – 2006. – 5. – P. 32.
5. Gaydadin A. N. Use of method of composition planning of experiment for description of technological processes: methodological instructions/A. N. Gaydadin, S. A. Yefremova. – Volgograd: VolgSTU, – 2008. – P. 16.
6. Koryachkina S.Ya. Method of research of quality of bakery products: tutorial-methodological textbook for higher educational institutions/S.Ya. Koryachkina H. A., Berezina E. V. Hmeleva//Orel: OrelSTU, – 2010. – P. 166.
7. Marchenko G. Carrying out of experiment with use of statistical methods of planning and information technologies/G. Marchenko, U. Mannanov, A. Boyarinov: Edited by N. Yusupbekov. – T: Mehnat, – 1991. – P. 264.
8. Puchkova L. I. Influence of sugar and fat on properties of the dough and structure of a crumb of white bread/L. I. Puchkova, I. D. Schegoleva, E. V. Golovach //Baking and confectionery industry. – 1981. – 5. – P. 23–25.

DOI: http://dx.doi.org/10.20534/AJT-16-9.10-44-46

Oltiev Azim Tuykulovich,
Bukhara engineering technological institute, Uzbekistan
Senior researcher, the Faculty of Chemical technology
E-mail: azim-10–86@mail.ru

On the resistance of different fat margarine emulsions

Abstract: In article questions of research of influence of the cotton and soy palmitin enriched with phospholipids of soy oil on firmness of margarine emulsions of various fat content are considered. Synergy influence of prescription emulsifier and a cotton and soy palmitin on firmness of margarine emulsions 60, 72 and 82% fat content is established. It promotes increase of firmness of margarine emulsions of various fat content and reduction of necessary amount of prescription emulsifier.

Keywords: cotton and soy palmitin, margarine, cotton oil, soybean oil.

Introduction: A number of the main criteria one of which is ability to keep physical stability (not to be stratified) defines quality of emulsion systems. Such emulsion products as spreads, margarine, some types of confectionery creams are fatty products based on the return emulsions. Tribune my physical stability of emulsion products is usually provided with introduction to their compounding of emulsifiers with use of the special equipment creating high degree of dispersion of system.

The cotton and soy palmation received by fractionation of a blend "the refined cotton oil — the refined soy oil — not refined soy oil", is and richen with phospholipids of soy oil [1, 3]. In this regard, its influence on firmness of margarine emulsions of various fat content was in vest gated.

When carrying out experiments fatty bases of margarine emulsions consisted of prescription fatty components of widespread margarine of prescription amount of vegetable oil, table with replacement of 10%, with the cotton and soy palmation containing in structure from 0, 1% to 0,4% of phospholipids. A gyro — the water and dairy emulsion of margarine was prepared according to technological instructions. Thus fat content of margarine emulsions of various options made 60, 72 and 82%.

Materials and methods: As criterion of an assessment of quality of the emulsion systems received during experiments the indicator of firmness of a margarine emulsion which values were defined according to GOST 976–81 [2; 4] served. Firmness of an emulsion is characterized by amount of the emitted fat at centrifugation of an emulsion in the set mode (5 min. at 1500 rpm). Thus, than the quantity, allocated (remaining not divided) is more than fatty layer and the quantity of the separated water (not fatty) phase in a test tube is less, the it is considered the best firmness of an emulsion [5].

Results and Discussion: For each option of fat content of margarine emulsions, the two-factorial four-level plan of experiments was separately used. The results of experiments presented in drawing demonstrate synergy influence of emulsifier (in this case based on the monoglycerides distilled) and a cotton and soy palmitin on firmness of margarine emulsions of various fat content. Apparently, inclusion in margarine of 10% of the cotton and soy palmitin containing 0,2–0,4% of phospholipids can promote substantial increase of firmness of a margarine emulsion and reduction of amount of emulsifier, especially for margarine emulsions 72 and 82% fat content. For such systems, the amount of emulsifier can be reduced almost twice at preservation of 100% firmness of an emulsion. It is obvious that ensuring 100% firmness of an emulsion in low-fatter margarine emulsion with fat content of 60% requires use of higher dosages of emulsifier. However and here inclusion in margarine of the cotton and soy palmitin containing 0,4% of phospholipids promoted reduction of amount of emulsifier for 12%. Possibly, addition of stabilizers of structure like hydrocolloids in low-fat margarine can increase even more effect of improvement of firmness of its emulsion.

Table 1. – Influence of a cotton and soy palmation on firmness of margarine emulsions 60% fat content — emulsion area with firmness not less 100% not destroyed emulsions

№	Indicators	
	The amount of emulsifier in margarine (%)	**Phospholipid content in cotton and soybean palmitin (%)**
1	0,5	0
2	0,48	0,1
3	0,43	0,2
4	0,41	0,3
5	0,40	0,4

Table 2. – Influence of a cotton and soy palmation on firmness of margarine emulsions 72% fat content — emulsion area with firmness not less 100% not destroyed emulsions

№	Indicators	
	The amount of emulsifier in margarine (%)	**Phospholipid content in cotton and soybean palmitin (%)**
1	0,42	0
2	0,39	0,1
3	0,30	0,2
4	0,27	0,3
5	0,22	0,4

Table 3. – Influence of a cotton and soy palmation on firmness of margarine emulsions 82% fat content — emulsion area with firmness not less 100% not destroyed emulsions

№	Indicators	
	The amount of emulsifier in margarine (%)	**Phospholipid content in cotton and soybean palmitin (%)**
1	0,3	0
2	0,27	0,1
3	0,19	0,2
4	0,15	0,3
5	0,13	0,4

Thus, use of the cotton palmitic enriched with soy phospholipids promotes increase of firmness of margarine emulsions of various fat content and reduction of necessary amount of prescription emulsifier.

References:

1. GOST 976–81. Margarine, fats the confectionery, baking culinary. Acceptance procedures and test methods. – M.: – 1988.
2. Oltiev A.T, Isabaev I.B, Majidov K.H. Fractionation of composition Vegetable oils. "Chemistry and Chemical Technology" journal ("Chemical and chemical technology"), TChTI, Tashkent, – № 1, – 2012, – P. 65–67.
3. Heading "From Uzbekistan". Oil and fat industry – No. 2, – 2011, – P. 16.

4. Oltiev A. T., Isabayev I. B., Saidakhmedov K. F. Fractionation of the blend refined the cotton and not refined soy oils for an intensification of process of receiving a cotton palmitin.//"Food technology and service". – 2009. – No. 4–5. – P. 4–7.
5. Ipatova L. G., Kochetkov A. A., Nechayev A. P., Tutelyan V. A. Fatty products for healthy food. Modern view. – M.: Put the Print, – 2009. – P. 287.

Section 7. Technical sciences

DOI: http://dx.doi.org/10.20534/AJT-16-9.10-47-52

Djiyanbaev Sirojiddin Valiyevich,
Institute of General and Inorganic Chemistry,
Academy of Science of the Republic of Uzbekistan,
Senior Research Associate, a doctorate candidate
E-mail: sdjiyanbaev@bk.ru, sdjiyanbaev@gmail.com

Hamidov Bosit Nabiyevich,
Institute of General and Inorganic Chemistry,
Academy of Science of the Republic of Uzbekistan,
Doctor of Engineering Science, Chief of Petrochemistry Laboratory
E-mail: khimiyanefti@mail.ru

Ubaydullaev Bakhtiyarulla Hamidovich,
Institute of General and Inorganic Chemistry,
Academy of Science of the Republic of Uzbekistan,
Candidate of Engineering Science, a senior research associate
E-mail: khimiyanefti@mail.ru

Yarbabaev Azamat Asrorovich,
Institute of General and Inorganic Chemistry,
Academy of Science of the Republic of Uzbekistan,
Senior Research Associate, a doctorate candidate
E-mail: axiles1985@mail.ru

Thermal properties of composition gearbox lubricant composition for railway transportation

Abstract: Thermal properties of a composition of gearbox greasing and their components have been studied in this article. Physical and chemical properties of the components are resulted as for consideration of thermal properties. The results of the researches proved that, the gearbox greasing can be used at temperatures of 380 to 400 degrees Centigrade. Increase of thermal properties of gearbox greasing for the tar and additive SD-7 account is proved.

Keywords: Conditional viscosity, temperature, tar, hydrogenated fat, additive, composition, reducer, differential-thermal analysis (DTA), thermal gravimetric analysis (TG), differential — thermal gravimetric analysis (DTG).

While developing modern lubricants, a special attention is paid to the estimates of their properties on thermoanalytical probes that allow to reveal frictions happening in the zone at temperature increase, physical changes connected with polymorphic transformations that is melting and evaporation of components of lubricants as well as thermal and thermal-oxidative processes. Determination of temperatures of polymorphic transformations the lubricants is especially important at developing the scientifically grounded technology of producing lubricant compositions and assessment of efficiency of their work at elevated temperatures. Therefore, the thermal analysis in the field of development of new innovative technologies of receiving various lubricant com-

positions is of great importance [1; 2]. In this regard, we carried out works on studying thermal properties of compositions of gearbox lubricant and its ingredients for railway transport [3; 4].

Gearbox lubricant of the following composition had been exposed to such thermoanalytical studies as differential thermal analysis (DTA), thermal gravimetric analysis (TG), differential thermal gravimetric analysis (DTG): tar (relative viscosity at 100 °C — relative degree) — 50%; dewaxed oil (relative viscosity at 100 °C-2.95 усл.град)-48.2%; hydrogenated fat — 1,.5%; "ЦД" (TsD) additive — 0.3 of %. Preliminarily, we studied the main physical and chemical characteristics of the ingredients which are a part of gearbox lubricant for traction reducers.

Physical and chemical characteristics and the chemical group composition of dewaxed oil and tar are given in Table 1.

Table 1. – Physical and chemical characteristics and chemical group composition of dewaxed oil and tar

Name of indicators	Dewaxed oil residual	Tar
Kinematic viscosity, at 100 °C, at 50 °C, cS	21.4	–
Relative viscosity, at 80 °C, sec	–	13.2
Sulphur content,%	0.8	3.16
Density at 20 °C, g/cu cm.	0.901	0.973
Freezing point, °C	–15	–
Flash point, °C	210	220
1. paraffin-naphtene,%	32.4	30.5
2. Aromatic hydrocarbons,%	65.8	50.2
3. Resins	1.7	12.0
4. Asphaltenes	–	7.2

TsD-7 is an antiwear, anti-oxidizing, anticorrosive additive. It is a 90%-solution of zinc dialkyldithiophosphate in mineral oil, derived on the basis of isopropyl carbinol and 2-ethylhexyl alcohols.

Hydrogenated fat is a solid fat produced in industry by means of hydrogenation of cotton oil. The essence of process of hydrogenation is the saturation of non-saturated fatty acids by hydrogen of nonsaturated fatty acids triacylglycerols at double bonds, resulting their transformation into saturated fatty acids, and turning fat state from liquid into solid.

Process of preparing this composition of gearbox lubricant consisted of the following stages:

– preparation of components (mixing tar with dewaxed oil);

– addition of the washing-dispersing component such as hydrogenated fat with an antiwear and anti-oxidizing additive TsD-7;

– thermochemical dispergation of a thickener adding 20% water solution of NaOH while continuously hashing with a mixer within 3 hours at the temperature of 128–130 °C (for carrying out process of saponification and mixture dehydration);

– cooling the received composition.

The derived composition, according to its physical, chemical, and operational characteristics corresponded with gearbox lubricant of Osp (Осп) of Russian Federation in compliance with TU 38.401–58–81–94 and specifications under Osp-Uz-Tsh 39.3–225:2012 of the Republic of Uzbekistan. The thermal analysis was registered on a derivatograph of Paulik F., Paulik J., Erdey L. System under a speed of 10 degrees per minute and with the weighed quantity of 0.128–0.134g and under sensitivity of weighed quantity of T-1200, TG-200, DTA-1/100, DTG-1/100 galvanometers. The record was taken under atmospheric conditions. Alumina crucible without cap with a diameter of 10 mm served as the holder. We used Al_2O_3 as the standard. The obtained results are given in Figure 1.

The graph of DTA composition of the gearbox lubricant is characterized by three endothermic effects at 135 °C, 270 °C, and 476 °C and two exothermic effects at 415 °C and 607 °C. The first endothermic effect is followed within the temperature range of 80–140 °C and the loss in weight at the same time makes 3,43%, that is, apparently, connected with transition of composition of lubricant from semi-fluid to liquid state. The first exothermic effect proceeds within the temperature range of 403–432 °C with loss of weight of 24.76%. At occurrence of endothermic effect at 476 °C and at 607 °C loss of weight makes respectively 62.3%. The total loss of weight at 600 °C makes 72.4%. At the same time, the loss of weight at the maximum speed occurs (according to graphs of TG and DTG) between 403 and 493 °C that can be explained by complex thermal-oxidative processes in the gearbox lubricant in the course of heating and, obviously, by stage-by-stage thermal-oxidative destruction of the soaps received on the basis of hydrogenated fat in hydrooxidation saponification process.

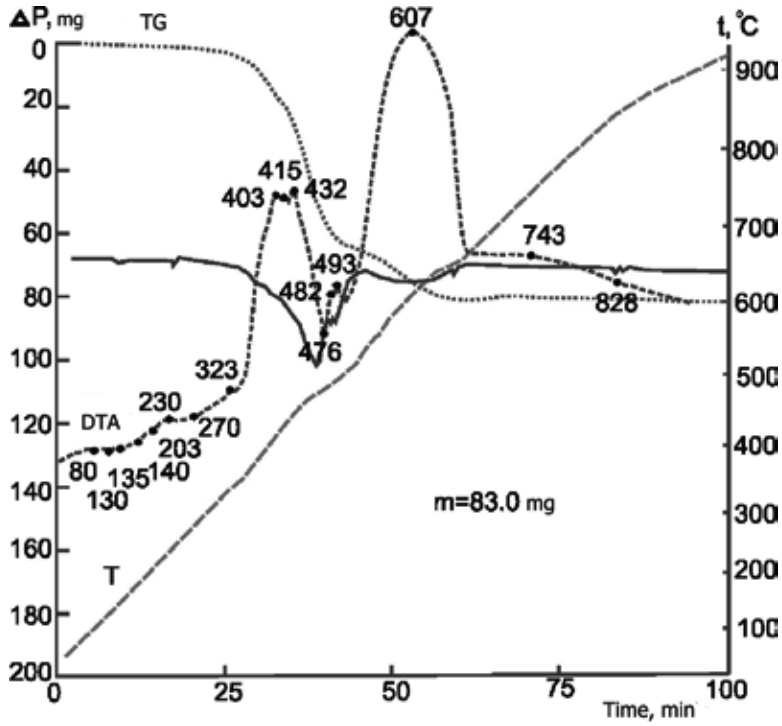

Figure 1. The graphs of thermoanalytical probes of a sample of gearbox lubricant compositions

For identification of the thermal-oxidative processes happening in the gearbox lubricant during heating, we have conducted thermoanalytical researches of structure of the lubricant's composition, on separate ingredients. The thermoanalytical analysis of the tar which is a part of tye gearbox lubricant is provided on the Figure 2.

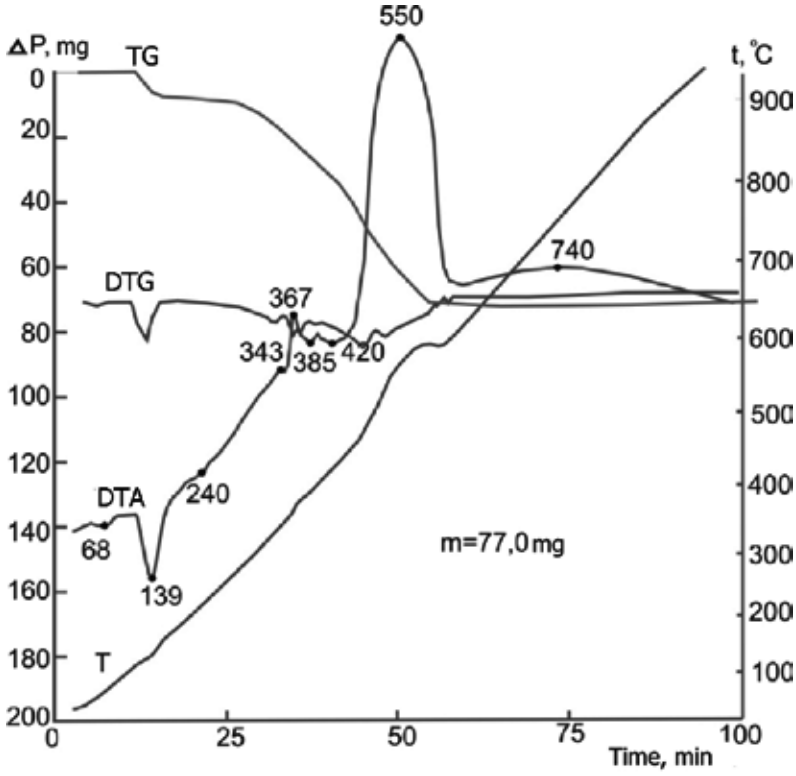

Figure 2. The graphs of thermoanalytical probes of the tar which is a part of the gearbox lubricant

DTA of tar is characterized by two endothermic effects at 68 °C and 139 °C as well as three exothermic effects at 367 °C, 395 °C, and 550 °C. The endothermic effect at 68 °C is explained by softening tar — teroxide in liquid state. The endothermic effect at 139 °C, obviosly, is explained by evaporation of the remains of more volatile solvents containing in tar. Besides, at these limits of temperatures, increase in speed of loss of weight up to

8–12% is observed that is reflected in DTG curve at temperature increase within the range of 120–200 °C.

Exothermic effects at 367 °C, 395 °C, and 550 °C, apparently, are explained by thermal-oxidative processes occurring in tar during heating. Maximum losses of weight, according to the graph of TG, during heating of tar, is within the range of 336–645 °C and makes 54–56%. Most significantly, different temperature increase of tar in comparison with that of gearbox lubricant (see Fig. 1) at heating up to 450 °C, where the temperature of the tar environment is increased up to 550 °C due to course of exothermic reactions and this exothermic effect in the composition of gearbox lubricant is displaced to higher temperatures up to 607 °C (see Figure 1), obviously, because of the resins and asfalten which are contained in tar (see Table 1).

The graphs of thermoanalytical probes of dewaxed oil are given Figure 3.

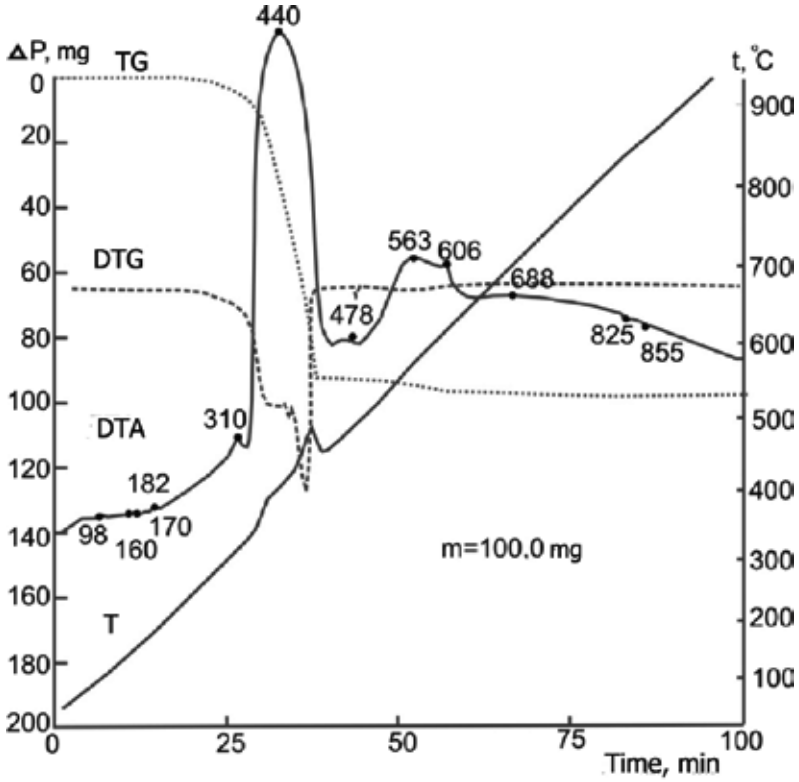

Figure 3. The graphs of thermoanalitycal probes of dewaxed oil

DTA of dewaxed oil is generally characterized by exothermic effects within temperatures of 98–310 °C, from which the weak endothermic effect at 318 °C, turns into exothermic effect of up to 440 °C. The next exothermic effect is shown at temperatures of 478–563 °C and 606 °C. The maximum loss of weight of 440 °C of TG appears within temperatures 310–455 °C, that is reflected by a peak in graphs of DTG that makes more than 90% and comes to the end with minor change of loss of weight of 2–4% at 540 °C. Loss of weight of 2–3% occurs at up to 310 °C. The processes happening during heating dewaxed oil up to 540 °C, apparently, can be explained with thermal-oxidative processes, but unlike tar (see Figure 2), the dewaxed oils show heat stability up to 310 °C.

Graphs of differential and thermal analysis of hydrogenated fat are characterized by six exothermic effects at 308 °C, 375 °C, 385 °C, 441 °C, 540 °C, and 600 °C, maximum loss of weight of TG from 8–62% is observed within temperatures of 220–390 °C that is distinctly reflected in the graphs of DTG. Endothermic effects are observed at temperatures of 479 °C and 610 °C. Displaying of exothermic and endothermic effects during heating the hydrogenated fat can obviously be explained with decomposition of various saturated fatty acids of triacylglycerol and development of various thermal-oxidative processes during heating.

Antiwear and antioxidative features of TsD-7 additive is appeared during DTA by exothermic by effects at 240 °C, 336 °C, 468 °C, and 540 °C and endothermic effects at 270 °C, 382 °C, 507.

Loss of weight on TG at/to 220 °C makes no more than 5%. Thermal-oxidative processes are displayed at temperatures higher than 220 °C, and maximum loss of weight according to TG grpah is shown within temperatures of 220–382 °C and makes 57–58.5%.

At assessment of thermal-oxidative stability of the studied objects which are gearbox lubricant and its components are, we paid attention to change of temperatures

of exothermic effects according to graphs of DTA; using thermogravimetric graph (TG) we determined temperatures of 10 and 50% of loss of weight at the set temperature, from the differential and using thermogravimetric graph (DTG), determined temperature of the maximum speed of loss of weight. As the phase-transition temperature we took the value of temperature corresponding to peak top on the thermogram of DTA.

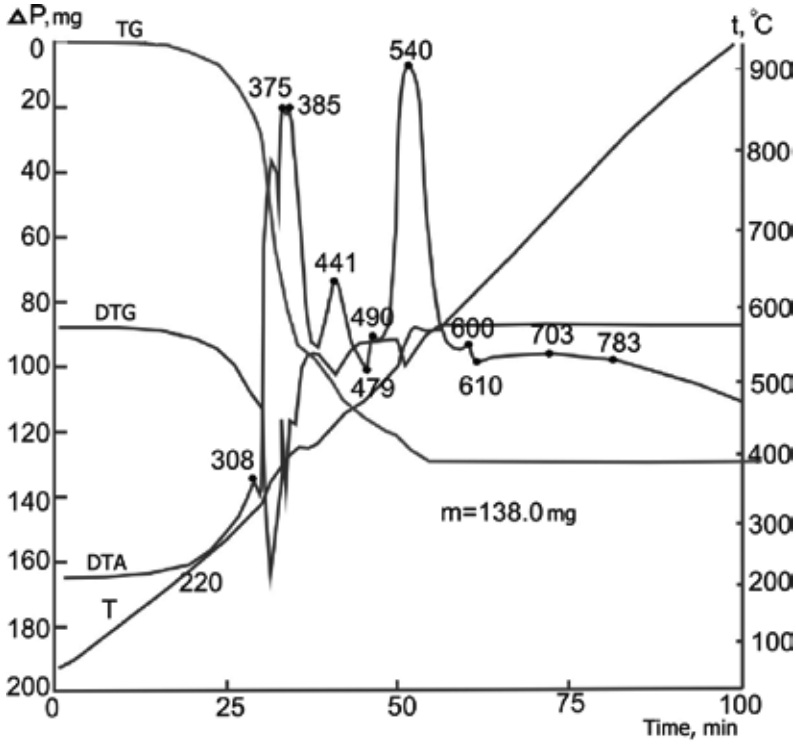

Figure 4. Thermonalytical graphs of hydrogenated fat

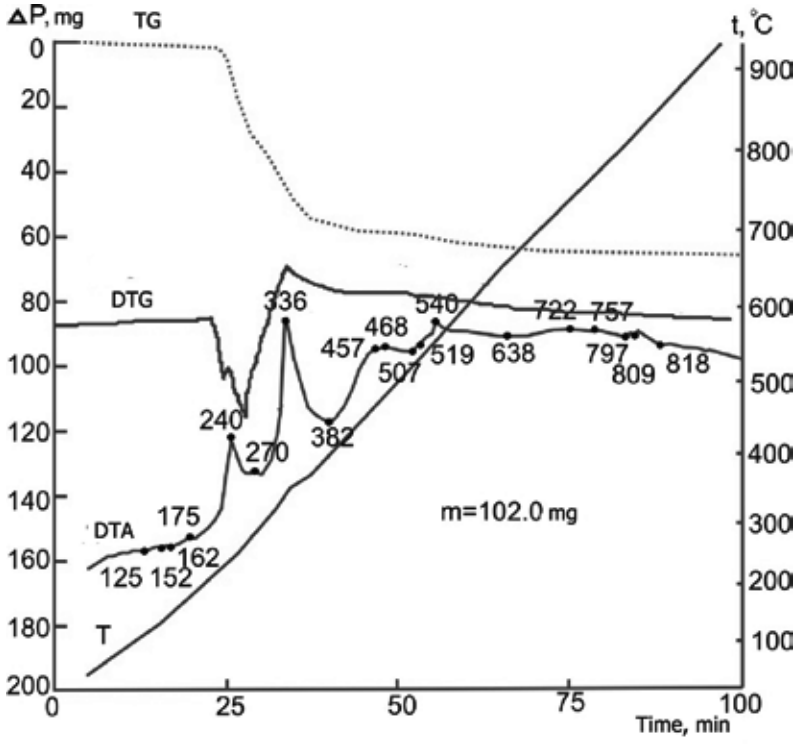

Figure 5. Thermoanalytical probes of TsD-7 additive

The comparative analysis of thermograms of composition of gearbox lubricant with its components, according to Figure 1–5, show that exothermic effects of tar at 367 °C and dewaxed oil appear on the DTA thermogram of the gearbox lubricant within temperatures of 403–432 °C; exothermic effects of tar at 550 °C and de-

waxed oil at 440 °C are shown on the DTA thermogram of composition of the gearbox lubricant at offset to the maximum temperature of exothermic effect at 607 °C that is, apparently, may be explained by thermal interaction where the main role is played by the resins and asfaltens which are part of dewaxed residual oil, and, in bigger quantity, are in composition of tar (see Table 1), respectively making 1.7, 12.0, and 7.2%. Use of these components as a part of composition of the gearbox lubricant, in combination with anti-oxidizing additive of TsD-7 and the saponified product of hydrogenated fat in the form of sodium soaps, leads to increase in thermal stability of lubricant composition of the gearbox lubricant in relation with temperatures of thermal decomposition.

Increase in thermal stability of composition of the gearbox lubricant is explained by offset of temperature at 10%-loss of weight at the set temperatures up to 380–390 °C, and for tar and dewaxed oil, this indicator is characterized, respectively, as 200–210 °C and 340–350 °C.

The maximum speed of loss of weight according to the DTG chart is displaced to the area of higher temperatures in the composition of the gearbox lubricant at 476 °C, and for tar, this indicator is within limits of 367–420 °C, and for dewaxed oil oil within limits of 442–456 °C.

Stability of properties of composition of the gearbox lubricant is shown also during operation that is at temperatures up to 40–45 °C. The gearbox lubricant keeps the properties of fluidity and doesn't flow down from reducers, when compared with "Nigrola" used as gearbox lubricant that favourably influences the solution of the problem of environmental protection. Here, a certain positive role is played by sodium soaps, which are in composition of the gearbox lubricant.

Thus, it is possible to claim that we have produced a thermostable composition of the gearbox lubricant which is possible to use in cars and traction reducers of locomotives within the temperature range of 380–400 °C without considerable changes of structure yet with increases in operational characteristics as well as with a solution of the problem of environmental protection. The greatest contribution in increase in heat stability of the gearbox lubricant is rendered by tar in combination with TsD-7, an anti-oxidizing and antiwear additive.

References:

1. Fuchs I. G., Melkovskaya N. K., Ishchuk D. L. et al. Differential and thermal analysis of lithium soaps and plastic lubricants//Oil processing and neftekhimiya-Moscow, Petrochemistry. – 1976. Issue II, – P. 17–28.
2. Ubaydullayev M.Zh., Hamidov B. N., Ubaydullayev B. H. Toshtemirov B. V., Azizov T. A. The thermal analysis of compositions of plastic rail lubricants and their components for railway transport.//Composite materials on the basis of technogenic waste and local raw materials: composition, properties, and application. Republican Scientific and Technical Conference. Tashkent, – 2010. – P. 36–38.
3. Sidorenko A. A., Pakina P. V., Savelyeva L. A. "Semi-fluid lubricants for reducers of all-machine-building appointment". Chemistry and technology of fuels and oils. – 2007. Issue 1. – P. 27–29.
4. Hamidov B. N., Saidahmedov Sh. M., Ubaydullayev B. H., Djiyanbayev S. V. "The main directions of production of lubricants with use of local raw material resources"//Uzbek magazine of oil and gas. Special release. – 2015. – P. 166–173.

DOI: http://dx.doi.org/10.20534/AJT-16-9.10-52-54

Amirov Sulton Fayzullaevich,
doctor of technical sciences,
professor, head of the Department "Railways Electricity"
Jurayeva Kamila Komilovna,
Assistant of the Department
"Railways Electricity" Tashkent institute of railway ingineering
E-mail: lade00@ bk.ru

Conceptual design of magneto stress sensors

Abstract: The stage of the energy of the information search method is the construction of new magneto elastic force sensors. The principle of the implementation of the generalized methods: in each row of the matrix of generalized receptions each new technical solution prefigures later, which improves the efficiency

of ongoing generalized methods. Shown that due to the design of the proposed ring magnet wires, the introduction of additional elastic taper bushes and mirror arrangement with the existing elastic sleeves provide simultaneous and bilateral efforts, resulting in increased sensitivity.

Keywords: the energy of the information search, generalized receptions, magneto elastic force sensors, ring magnet wires, elastic taper bushes, consistently counter connection, sensitivity.

Targeted improvement of magnetoelastic sensors, satisfying the ever-increasing requirements for controls systems, and the creation of new designs is impossible without analyzing the existing lessons learned in the design of magnetoelastic sensors.

For the analysis of known research and development of new designs of magnetoelastic sensors used energy-search method of constructing the sensitive elements of control systems [1, 17–31]. For a development of this method is reflected in the works [2, 93–110, 117–134, 201–223, 3, 259]. Distinctive features of the method are: the decomposition of complex physical processes occurring in the sensors, processes of different physical nature chains, the interaction between which is reflected by the presence of physical and technical effects. Either sensor can be divided into sections that include several successive elementary transformations. It allows you to organize the description of the operating principle of the sensor in the form of parametric structural diagrams. Each elementary unit of this scheme reflects one conversion. Comparative analysis of the structures of magnetoelastic sensors carried by the identification of generalized improvement techniques [1, 17–31]. It is widely used at the stage of exploratory design of electromagnetic systems and controls in stages analysis of inventions within the same subgroup of the International Classification of Inventions (ICI) [1, 17–31].

The effectiveness of implemented methods determined by the effectiveness of the generalized refined in the process of testing revealed generalized methods and values of the characteristics of new sensor designs.

However, the sequence of the implementation of the generalized receptions on the above principle will be ineffective. Therefore, we have proposed and used in the following sequence of generalized implementation techniques: in each row of the matrix of generalized techniques every new technical solution is the prototype of the next. In this case, the efficiency of ongoing generalized methods increases with the number of couples considered inventions.

We put the following task — using the foregoing method of conceptual design to increase the sensitivity of the magnetoelastic force sensor [4, 1–4].

The task of increasing the sensitivity of the magnetoelastic force sensor was decided to improve its design. Figure 1 shows the construction scheme developed magnetoelastic force sensor [5, 1–4]: in Figure 1, and — the sensor section A — A; in Figure 1, b — a top view of the sensor. Figure 2 shows the circuit diagram of the measuring section of the sensor windings.

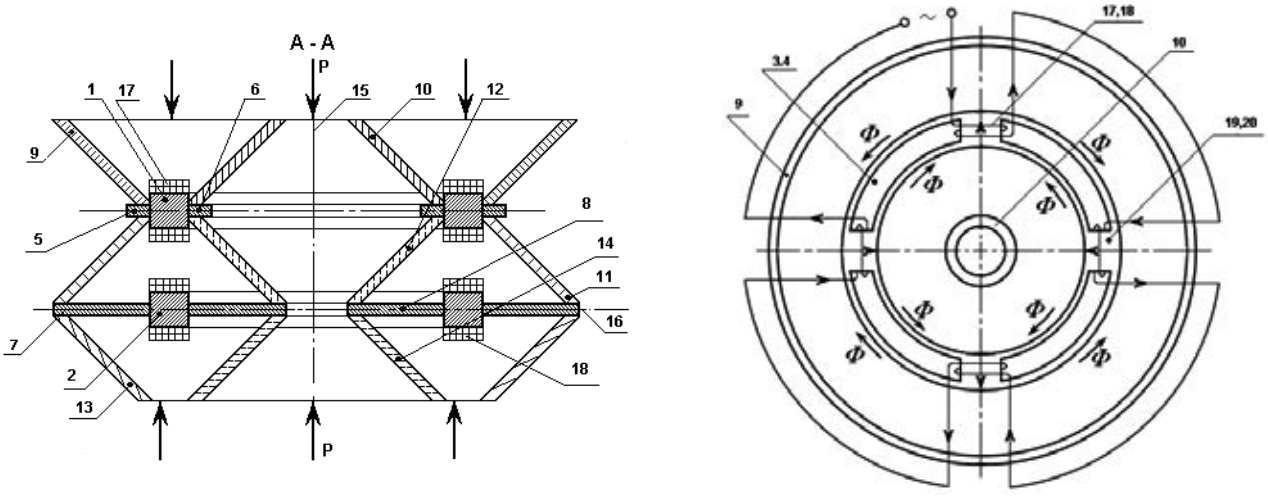

а) б)

Fig. 1. The design concept of the new magnetoelastic force sensor.

A magnetoelastic force sensor comprises two identical annular magnetic core 1 and 2 satisfied circumference through-slots 3 and 4. On the outer and inner circumferential surfaces of the magnetic cores 1 and 2 are annular protrusions 5–8 of inelastic material. Ring 1 and the yoke 2 via three pairs the power transmission elements in the

form of mutually concentric and arranged specularly 9–14 elastic conical sleeves mounted coaxially with the circular magnetic cores are arranged along the axis 15 in the serial number. In this series of sequential annular magnetic core 1 is covered without a gap end portions of two pairs of resilient conical bushes 9–12, and the free ends of the annular projections 7 and 8 are covered with no gap end portions of two pairs of resilient conical bushings 11–14. Any pair of two adjacent conical sleeves (11, 12 or 9,10 and 11, 12 and 13, 14) in a sequential row disposed symmetrically relative to the median plane 16 of the corresponding annular magnetic circuit. Sections measuring windings 17 and 18 comprise respective cores 19 and 20 disposed between adjacent through-slots 3 and 4 of ring cores 1 and 2. All sections of the measuring coil magnetic ring 17 are interconnected in series-counter. winding section 18 are also connected to the annular magnetic core 2. The thus obtained two-winding force sensor included in the adjacent shoulders bridge measuring circuit (Fig. 2).

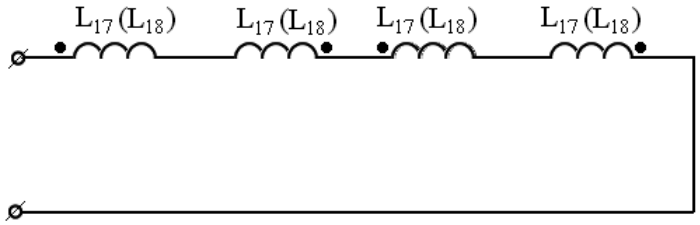

Fig. 2. Schematic diagram Connection sections measuring sensor windings:
L17, L18 — inductance winding sections measuring 17 and 18

Magnetoelastic force sensor operates as follows.

In the absence of measured force Φ acting to the extreme in a sequential series of pairs of elastic conical plugs 9, 10 and 13, 14. Bridge measuring circuit is balanced and the signal from the diagonal of the bridge is zero. Upon application of a compressive force along the axis of the tapered sleeve 15 is elastically deformed 9–14 follows. Larger diameter of the cone increases, and a smaller diameter — decreases (ie there is an elastic conical sleeves sludge 9–14). Such deformation causes the conical bushings 9–14 compressive stress in the annular yoke 1 and the tensile stress in the annular magnetic core 2. Consequently, the change of inductance of windings 17 and 18 of ring cores 1 and 2 (by changing the magnetic permeability of the magnetic material), the inductance of one of them, increases, and the inductance of the other — is reduced. Such a change in inductance of the windings 17 and 18 leads to unbalance the bridge measuring circuit and the appearance on the output signal, proportional to make efforts.

Due to the proposed Embodiment of magnetic ring, the introduction of additional elastic tapered sleeves and a mirror arrangement with the existing elastic bushings provided simultaneous and bilateral application of mechanical stress (the outer and inner surfaces of magnetic ring), thereby improving the sensitivity of the sensor.

Thus, we have shown the steps of the method of energy conceptual design of new magnetoelastic force sensors. The principle of the implementation of the generalized methods: in each row of the matrix of generalized techniques every new technical solution prefigures later, allowing to increase the effectiveness of ongoing generalized methods. It is shown that due to the proposed Embodiment of magnetic ring, the introduction of additional elastic taper bushings and the mirror arrangement with existing elastic bushings provided simultaneous and bilateral efforts of the application, thereby improving the sensitivity of the sensor.

References:

1. Zaripov M. F., Zaynullin N. R., I. Y. Petrov. Energy-method of scientific and technical creativity. – M.: VNIIPO SCCT, – 1988. – 124 p.
2. Design elements of information and measurement and control systems for intelligent buildings: a monograph/D. P. Anoufriev, M. F. Zaripov, Y. Lezhnina, I. Y. Petrova, T. V. Khomenko, O. Shikulska. – Astrakhan: GAOU JSC VPO "Astrakhan Institute of Civil Engineering", – 2015. – 231 p.
3. Amirov S. F., Kh. A. Sattarov On the question of energy-search method of designing sensors//"Innovation 2006": Proc. rep. Internat. scientific-practical. Conf. – Tashkent, – 2006. – P. 258–259.
4. AS № 1778559. Magnetoelastic force sensor/E. S. Agafonov – Publ. In BI, – 1992. – № 44.
5. Patent Uzbekistan. № IAP 04866. Magnetoelastic force sensor/S. F. Amirov, K. K. Juraeva, Z. G. Nazirova et al.//Rasmiy Ahborotnoma. – 2014. – № 4.

DOI: http://dx.doi.org/10.20534/AJT-16-9.10-55-57

Djandullaeva Munavara Saparbaevna,
Tashkent chemical-technological institute,
Senior staff scientist, Department of
Technology of inorganic substances
E-mail: djandullaeva@mail.ru.

Turabdjanov Sadritdin Mahamatdinovich,
Chancellor of Tashkent chemical-technological institute,
Doctor of technical sciences, professor

Atakuziev Temirjan Azim ugli,
Tashkent chemical-technological institute,
Doctor of technical sciences, professor, Department of
Technology of inorganic substances

Xusnitdinov Asomiddin Munnimovich,
Tashkent chemical-technological institute,
Senior staff scientist

Enhancement of adhesiveness of silicate brick on the basis of tuffit addition with masonry mortar

Abstract: Presented the results of research by investigation of possibilities enhancement of adhesiveness of silicate brick on the basis of barchan sands and steel making slag sand with masonry mortar due to introduction into the raw mixture hydraulic active addition — tuffit thermally processed at 600 °C in quantities of 10%, 20%, and 40%. It was established that the most effective is addition of tuffit 20% which enables enhancing its normal adhesion with masonry mortar already at 7 — day time of hardening, in more than 4-times as compared with brick without additions (0,115 MPa). Such brick has adhesion with masonry mortar almost 2 times more than requirements of Construction Rules and Regulations R ≥ 0,18 (0,309 MPa).

Keywords: Tuffit, hydraulic active addition, adhesiveness, silicate brick, masonry mortar, hardening.

It is well known, that residual hydraulic activity of silicate brick may change its properties via interactions of components which located inside of it with calcium hydroxide of masonry mortar, which affects technology of production of brick and on its basic construction and technical properties.

During autoclaving, first of all, occurs interaction between calcium hydroxide and active SiO_2 and Al_2O_3 contained in fired at 600 ° C tuffit, which introduced in mixture for production of silicate brick. From now on the thermally processed at 600 ° C tuffit we shall refer as tuffit.

Input in composition of silicate mixture of burned tuffit rock, as opposed to rock in natural condition, does not affect negatively in deformation, shrinkage and swelling of silicate brick. When 10–20% of tuffit introduced shrinkage does not change, but while there is addition of 30–40% tuffit, shrinkage reduces slightly as compared with mixture without additions of tuffit. Swellings of samplings practically do not change.

In laboratory mixer machine dry mixture with activity 8% were prepared from quicklime, tuffit addition, barchan sand and steel making slag sand (table. 1).

Table 1. – Content of components in investigated mixtures

Tuffit thermally processed at 600 °C	Quicklime	Steel-making slag sand	Barchan sand
10	10	20	60
20	10	20	50
40	10	20	30

Steel making slag sand with dimensions 0,35–0,60 mm we use as enlarger. Since barchan sands have homogenous granulometry (size 0,14 mm), which molded poor at currently functioning press machine.

Samples were molded in molds with sizes 4x4x4 mm by specific pressure — 20 MPa and different molding-moisture content. Optimal molding-moisture content of sample with addition of tuffit in quantities 10%; 20%; 40% accordingly is 10,5%; 11,5%; 13%, and molding-moisture content at samples without addition of tuffit is 9,5%. Addition of steel-making slag sand promotes reduction of moisture.

Molded samples were autoclaved at pressure of steam 0,8 MPa by cycle 2+8+2 hours. Before and after autoclaving physical and mechanical properties were measured (table 2).

Table 2. – Effect of tuffit addition on physical and mechanical properties of silicate samples

Quantity of tuffit	Before autoclaving			After autoclaving with pressure 0,8 MPa during 8 hours				
	Molding moisture,%	Compression strength, MPa	Volume-weight, g/sm^3	Compression strength, MPa	Volume weight, g/sm^3	Water absorption,%	Porosity,%	Frost resistance
0	9,5	0,4	1,940	12,8	1,682	17,8	35,02	25
10	10,5	0,6	1,990	20,0	1,678	16,9	35,3	30
20	11,5	0,8	1,930	27,0	1,646	16,0	35,9	35
40	13	0,12	1,920	21,0	1,593	18,1	37,8	30

Increasing the content of hydraulic active addition of tuffit in mixture causes a slight rise of optimal molding moisture. It is due to higher water absorption of tuffit addition as compared with barchan sand, and also due to lower volume weight.

There is very important moment in technological view the positive effect of tuffit addition on strength of pressed silicate samples (0,8–0,12 MPa). Presence in mixture of tuffit addition and slag enlarger increases removable strength of silicate samples in some cases up to 250%, without increasing activity of mixture. Removable strength of silicate samples to a large degree is defined by activity of tuffit addition. The hardness of structure of samples is affected not only by increase of the forces on which interacts on surface which is brought about by tuffit addition with high specific surface, but also by development especially at beginning period of chemisorptive bond.

Input of tuffit and steel making slag sand positively effects on hardening parameters of silicate samples, autoclaved at 175 ° C during 8 hours (Table 2). Maximal enhancement of strength of silicate samples corresponds to mixture with tuffit addition of 20–40% and steel-making slag sand 20% (21–27 MPa).

Crucial role of tuffit in forming of strength after autoclaving is due to its specific feature as hydraulic active addition, which affects not only speeding up of formation of calcium hydrocilicate by autoclaving, but also on crystallization of hydratation products.

Efficient effects of highly active (in absorption of CaO) addition such as tuffit, is center of crystallization new formation by autoclaving treatment of silicate materials. The properties of tuffit as crystallization priming may be due to more perfect structure of crystallite, formed in process cooling of alum silicate molten mass under high pressure.

Steel-making slag sand in given conditions also is active component participating in forming hard silicate rock. That obtained thanks to improving of fraction composition of barchan sand with steel-making slag with sizes 0,35–0,60 mm, which favors obtaining pressed silicate product with high grade strength by hydrothermal processing.

Autoclaved samples with tuffit addition have its optimum in content of addition from point of view of maximal mechanical strength (20%). With introduction of tuffit from 20% to 40% volume weight of autoclaved samples decreases.

Water absorption and porosity of autoclaved pressed silicate samples with tuffit addition and slag sand meets the qualifying standards to walling materials. Type of dependency of water absorption and porosity of autoclaved samples from their composition is analogous to changing of specific volume of samples.

Frost resistance is one of defining properties of material, which to large extent depends from structure and composition of samples. Autoclaved samples with tuffit addition containing up 20% has endured over 35 cycles of alternating freezing and thawing. Samples with tuffit addition — 10 и 40%, has endured less than 30 cycles of alternating freezing and thawing and proved that their sufficiently frost resistant (table 2).

Data obtained in principle corresponds to concept of effect of hydraulic active additions to frost resistance of autoclaved materials.

Introduction into mixture composition of hydraulic active addition — tuffit, even in relatively big quantities (up to 40%) enables to obtain autoclaved silicate materials with good physical mechanical parameters.

The research of normal adhesion of surface of silicate samples with tuffit addition which has residual hydraulic activity with masonry mortar as actual consequence of chemical interaction is of certain interest.

The adhesiveness has been studied on samples with sizes 4x4x16 mm; they were stuck together with the masonry mortar of the grade 50. We have applied complex masonry mortar from portlandcement M –100, hydrated lime (activity 70%) and beach sand with size modulus (micrometer) 1,24.

Water-solid ratio in masonry mortar is equal 0, 25 and in accordance with results earlier conducted researches and can be considered optimal.

Masonry mortar was prepared according to the requirements of standard.

After sticking samples during 28 days were stored in moisture-air conditions in bath with hydraulic valve and afterward were tested on normal adhesion.

In table 3 is given calculated value of normal adhesion of autoclaved silicate samples with residual hydraulic activity due to input of tuffit addition.

Table 3. – Normal adhesion with masonry mortar, MPa

Content of tuffit,%	**Samples after**				
	7days	**28 days**	**3 months**	**6 months**	**12 months**
0	0,029	0,034	0,039	0,041	0,046
10	0,093	0,205	0,238	0,246	0,287
20	0,115	0,214	0,253	0,265	0,309
40	0,121	0,210	0,245	0,254	0,290

From the results of the research it is evident, that normal adhesion of 1 sm^2 of surface of silicate materials with tuffit addition, which has residual hydraulic activity, is far above, than of silicate material without addition. Obtained parameters of normal adhesion not in direct proportion with residual hydraulic activity of investigated materials. Quite the contrary, when the quantity of tuffit addition in composition is raised up 40% the normal adhesion with masonry mortal has slightly decreased.

Introduction of tuffit in silicate mass is due to the presence of residual hydraulic activity of autoclaved material and this contributes to enhancement of normal adhesion with masonry mortar.

Application of tuffit thermally processed at 600 ° C for the production of silicate material enhances the technology of its production and vastly improves qualitative parameters of these materials.

References:

1. GOST 7025–91. Bricks and ceramic and silicate stones. Methods of defining of water absorption, hardness and control of frost resistance.
2. GOST 379–95. Bricks and silicate stones.
3. Kabulova L. B., Djandullaeva M. S., Atakuziev T. A. Atmospheric stability of Portland cement with 20 and 30% of tuffte additives which were burnt under 600 °C.//Austrian Journal of Technical and Natural Sciences. – Vienna. – 2015, – 110–113 p.
4. Tairov A. A., Nudelman B. I. Improvement of adhesion of silicate bricks with masonry mortar.//Construction materials. – M.:– 1969.

DOI: http://dx.doi.org/10.20534/AJT-16-9.10-58-60

Karimov Rasul Ishakovich,
Tashkent State Technical University
named after Abu Raykhan Beruni,
professor of the department
"Theoretical mechanic's and the theory of mechanisms and machines"

Nematov Erkinjon Hamroevich,
Tashkent State Technical University
named after Abu Raikhan Beruni, senior staff scientist of the Department
"Theoretical mechanic's and the theory of mechanisms and machines"

Baratov Nortoji Baratovich,
Tashkent State Technical University
named after Abu Raikhan Beruni,
associate professor of the Department
"Theoretical mechanic's and the theory of mechanisms and machines"

Axmedov Azamat Xaitovich,
Tashkent State Technical University
named after Abu Raikhan Beruni,
senior staff scientist of the Department
"Theoretical mechanic's and the theory of mechanisms and machines"

Shaxobutdinov Rustam Erkinbayevich,
Tashkent State Technical University
named after Abu Raikhan Beruni,
senior staff scientist of the Department
"Theoretical mechanic's and the theory of mechanisms and machines"
E-mail: azam0602@mail.ru

Determination of kinematic parameters, the redused moment of inertia and its derivative of the planetary mechanism with the variable moment of inertia of the planet pinion

Abstract: The article presents the analytical expressions for the determination of kinematic parameters of planetary gear with variable moment of inertia of the PLANET PINION. The influence of the mass, the mean radius of the center of mass of the processed material at the given laws of the change of inertia and its derivative.

Keywords: The planetary mechanism, the planet pinion, carrier, kinematics, the given moment of inertia, working drum, the processed material.

The planetary mechanisms are widely used in modern technological machines, in particular mixers, grinding machines and raw materials of minerals etc.

To determine the actual laws and loading of units necessary to investigate these mechanisms for quality actuating mechanisms of machine aggregates. It is known that at probe of aggregate of machine with variable moment of inertia essential to define the given moment of inertia and its derivative [1].

In this regard, the authors considered the guiding planetary gear in figure 1, which consists of a fixed central wheel 1, the planet pinion 2 carrier of h, *working drum* 3. here ω_H – the angular speed of the carrier, the "c" — the center of mass of the material is being processed $R_м$ – variable radius center of mass of the material is being processed.

The planet pinion makes difficult rotary the movements around two axes:

1. However, a carrier with the carrier around a rotational axis;

2. Around own axis of planet pinions.

As a rule, the working member is connected with the planet pinion and makes the same movement as the planet pinion. Due to the fact that during the operation of the above-stated machines at rotation of working body the center of mass of the processed material changes in relation to a planet pinion axis, the planet pinion has variable moment of inertia.

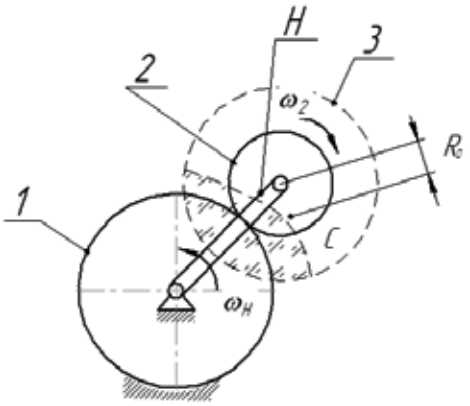

Figure 1. The kinematic scheme of the planetary gear traim with the variable moment inertia of the planetarium pinion.

The importance of the study of machines of this class is the definition of the center of mass of the kinematic parameters of the material is being processed. To determine the center of mass of the kinematic parameters of the material is being processed by the authors, based on the results of the study presented in the paper [2], proposed the following analytical expressions

$$x_c(t) = A\cos(\omega_H \cdot t) - R_м(t)\cos(u_{2H}\omega_H \cdot t),$$
$$y_c(t) = A\sin(\omega_H \cdot t) - R_м(t)\sin(u_{2H}\omega_H \cdot t), \quad (1)$$

where

$$R_м(t) = K_1 \cdot R_0 + K_2 \cdot R_0 \sin(K_3\omega_2 t),$$
$$A = (R_1 + R_2),$$

$R_м(t)$ – Variable radius center of mass of the material is being processed;

R_1, R_2 – The radii of the pitch circle of gear wheels;

R_0 – The average radius of the center of mass of the processed material;

K_1, K_2, K_3 – The constant coefficients whose values depend on the composition of the processed material and structural parameters of the drum;

$\omega_2 = \omega_H(1 + \frac{R_1}{R_2}) = \omega_H u_{2H}^{(1)}$ – The angular velocity of the planet pinion;

$x_c(t), y_c(t)$ – The coordinates of the center of mass of the processed material.

$$\vartheta_{cx}(t) = u_{2H} \cdot \omega_H \sin(u_{2H} \cdot \omega_H \cdot t)(K_1 \cdot R_0 + K_2 \cdot R_0 \sin(K_3\omega_2 t)) -$$
$$-A \cdot \omega_H \sin(\omega_H t) - K_2K_3R_0\omega_2 \cos(u_{2H}\omega_H t),$$
$$\vartheta_{cy}(t) = A \cdot \omega_H \cos(\omega_H t) - u_{2H} \cdot \omega_H \cos(u_{2H} \cdot \omega_H \cdot t) \times$$
$$\times(K_1R_0 + K_2 \cdot R_0 \sin(K_3\omega_2 t)) - \quad (2)$$
$$-K_2K_3R_0\omega_2 \cos(K_3\omega_2 t)\sin(u_{2H}\omega_H t).$$

$\vartheta_{cx}(t), \vartheta_{cy}(t)$ – projection of speed of the center of mass of the processed material onto the coordinate axes.

$$a_{cx}(t) = u_{2H}^2 \cdot \omega_H^2 \cos(u_{2H} \cdot \omega_H \cdot t)(K_1 \cdot R_0 + K_2 \cdot R_0 \sin(K_3\omega_2 t)) -$$
$$-A\omega_H^2 \cos(\omega_H t) - K_2K_3^2R_0\omega_2^2 \sin(K_3\omega_2 t)\cos(u_{2H}\omega_H t) +$$
$$+2K_2K_3R_0u_{2H}\omega_2\omega_H \cdot \cos(K_3 \cdot \omega_2 t) \cdot \sin(u_{2H}\omega_H t),$$
$$a_{cy}(t) = u_{2H}^2 \cdot \omega_H^2 \sin(u_{2H} \cdot \omega_H \cdot t)(K_1 \cdot R_0 + K_2 \cdot R_0 \sin(K_3\omega_2 t)) -$$
$$-A \cdot \omega_H^2 \sin(\omega_H t) + K_2K_3^2R_0\omega_2^2 \sin(K_3\omega_2 t)\sin(u_{2H}\omega_H t) -$$
$$-2K_2K_3R_0u_{2H}\omega_2\omega_H \cdot \cos(K_3 \cdot \omega_2 t) \cdot \cos(u_{2H}\omega_H t). \quad (3)$$

$a_{cx}(t), a_{cy}(t)$ – acceleration projection center of mass of the processed material onto the coordinate axes;

For the definition given to a shaft carrier moment of inertia of the planetary gear with variable moment of inertia is possible to use the following expression

$$J_{пр.H}(t) = J_H + J_c \cdot (u_{2H}^{(1)})^2 + J_б \cdot (u_{2H}^{(1)})^2 + m_c \cdot (R_1 + R_2)^2 + \quad (4)$$
$$+(m_б + m_м) \cdot (R_1 + R_2)^2 + m_м \cdot (u_{2H}^{(1)})^2 \cdot R^2{}_м(t),$$

where:

$J_{пр.H}$ – given to the carrier shaft moment of inertia of the planetary gear;

J_H – moment of inertia of the carrier relative to its axis of rotation;

J_c – moment of inertia of the planet pinion relative its own axis;

$J_б$ – moment of inertia of the drum relative its own axis of planet pinions;

$m_м$ – the mass of the material is being processed;

$m_б$ – the weight of drum;

m_c – the mass of the planet pinion;

$u_{2H}^{(1)} = (1 + \frac{R_1}{R_2})$ – the transmission ratio between the shaft of planet pinion and the shaft of carrier.

Derivative of the given inertia moment on time determined by the following expression

$$\frac{dJ_{\text{пр.Н}}}{\text{dt}} = m_м R_м (u_{2H}^{(1)})^2 \cdot \frac{dR_м}{dt} = \theta(t), \qquad (5)$$

$$\theta(t) = 2K_2K_3 \cdot R_0 \cdot u_{2H} m_c \omega_2 \cos(K_3 \cdot \omega_2 \cdot t) \times$$

$$\times (K_1 \cdot R_0 + K_2 R_0 \sin(K_3 \omega_2 t).$$

It should be noted that derivative of the given inertia moment on time and an angle of rotation carrier are connected among themselves by the following ratio

$$\frac{dJ_{\text{пр.Н}}}{\text{dt}} = \omega_H \cdot \frac{dJ_{\text{пр.Н}}}{d\phi}.$$

Analytical expressions (1–5) have been realized on the computer in the environment of MathCAD.

Study of the effect $m_м$, R_0, on the change in given moment of inertia $H_{J_{пр.Н}}$, and its derivative $H_{\frac{dJ_{пр.Н}}{dt}}$, for this mechanism were determined under variation the mass of the processed material from 5 to 20 kg in steps of 5 kg and the average radius of the center of mass from 0.2 to 0.35 m in steps of 0.05 m. The results of calculations are shown in the table.

Table 1. – Results of calculations of scope of fluctuations of the given moment of inertia, his derivative for the planetary mechanism at a variation of mass and average radius of the processed material

Variation of mass of the processed material $m_м$							
№	$m_м$, кг	$J_{пр.H\max}$, $кгм^2$	$J_{пр.H\min}$, $кгм^2$	$H_{J_{пр.Н}}$, $кгм^2$	$\left(\frac{dJ_{пр.H}}{dt}\right)\max$, $кгм^2$	$\left(\frac{dJ_{пр.H}}{dt}\right)\min$, $кгм^2$	$H_{\frac{dJ_{пр.Н}}{dt}}$, $кгм^2$
1	5	14,66	11,96	2,7	35,13	–35,13	70,26
2	10	18,72	13,32	5,4	70,26	–70,26	140,52
3	15	22,77	14,67	8,1	105,39	–105,39	210,78
4	20	26,83	16,03	10,8	140,52	–140,52	281,05
Variation of average radius of the center mass of the processed material R_0							
№	R_0, м	$J_{пр.H\max}$, $кгм^2$	$J_{пр.H\min}$, $кгм^2$	$H_{Jпр.H}$, $кгм^2$	$\left(\frac{dJ_{пр.H}}{dt}\right)\max$, $кгм^2$	$\left(\frac{dJ_{пр.H}}{dt}\right)\min$, $кгм^2$	$H_{\frac{dJ_{пр.Н}}{dt}}$, $кгм^2$
1	0,2	12,55	11,35	1,2	15,62	–15,62	31,23
2	0,25	13,5	11,63	1,87	24,4	–24,4	48,8
3	0,3	14,66	11,96	2,7	35,13	-35,13	70,26
4	0,35	16,04	12,36	3,67	47,81	-47,81	95,63

According to the results of calculations on a computer determined laws of change the oscillation scope given moment of inertia, its derivative, which is calculated by the following formula (6):

$$H_{Jпр.H} = J_{пр.H\max} - J_{пр.H\min},$$

$$H_{\frac{dJ_{пр.Н}}{dt}} = \left(\frac{dJ_{пр.H}}{dt}\right)\max - \left(\frac{dJ_{пр.H}}{dt}\right)\min. \qquad (6)$$

The analysis of results of calculations has shown that in this range of change of mass of the processed material scope of fluctuations of the given moment of inertia increases with 2,7 to 10,8 $кгм^2$ and scope of fluctuations, derivative of the given inertia moment, increases with 70,26 to 281,05 $кгм^2$.

Besides that, it was investigated the influence of value of the average radius of the center of mass the processed material at the given laws of the change of the given moment of inertia and its derivative. The average radius of the center of mass the processed material was changed from 0.2 to 0.35 m in steps of 0.05 m

It was established that the scope of fluctuation of the given inertia moment increases from 1.2 to 3.67 $кгм^2$, and the scope of fluctuation derivative from given moment of inertia increases with 31.23 to 95.63 $кгм^2$.

Thus, it is set that unlike the normal planetary mechanism this planetary mechanism with a variable inertia moment of the planet pinion has the variable given inertia moment. this feature of the researching mechanism needs to be considered in case of determination of the valid laws of movement of the mechanism.

References:

1. Артоболевский И. И. Теория механизмов и машин. – М.: «Наука», – 1988. – 640 с.
2. Каримов Р. И. Теоретические основы и конструкции планетарного и бипланетарного приводов рабочих органов тестомесильных машин. Монография, Таш ГТУ, – 2013–38,5 п. л.

DOI: http://dx.doi.org/10.20534/AJT-16-9.10-61-64

Kabulova Lola Baltamuratovna,
Tashkent chemical-technological institute,
Senior staff scientist, Department of
Technology of inorganic substancestment
Atakuziev Temirjan Azim ugli,
Tashkent chemical-technological institute,
Doctor of technical sciences, professor, Department of
Technology of inorganic substances
E-mail: ais-qr@mail.ru

Pilot batch of the mixed cements with the additive of composition of tuffite and SWSM

Abstract: In this work the technology of obtaining mixed portland cement with use as an active mineral additives of tuffite in the Karmana deposit and solid waste of soda manufacture (SWSM) has been investigated. The received data shows that tuffite breed burnt at 600 °C positively influences on the physical-mechanical properties of cements. The best results have been received at test of various cements at input of 20% and 30% of burnt tuffite additive.

Mixed portland cement containing simultaneously tuffites and SWSM are characterised concerning high grindability and less-water consumption than cements without additives.

Keywords: tuffite, solid waste of soda manufacture, portland cement, an active mineral additive.

Possibility of obtaining mixed Portland cements of rather high quality has been tested in laboratory with use as an active mineral additive of Karmaninsk deposit tuffite. Definition of band indicators of cements with additives has been carried out on standard sample-beam structure 1:3, made of a solution of a plastic consistence.

It is known that portland-pozzolana cements differ with their heavy-water consumption. The same it is possible to tell and about the mixed cements containing 20–50% of tuffite in the structure: with the increase of tuffite maintenance their water consumption increases too, the increase of spread of tuffite cone is testified in figure 6. This factor negatively reflects and on strength characteristics of a cement stone: the additive of tuffite to 20% reduces the durability of initial Portland cement on compression order on 4–10%, but durability increases by a bend a little. Considerable decrease of stone strength indicators on the basis of tuffite containing portland cements is noted at 30%-s' dose of tuffite (on 20–45%), especially it is appreciable by 28 days (tab. 1).

Hence, earlier drawn conclusions that with a view of maintenance of enough high durability of a stone on the basis of tuffitecontaining cements, the maintenance of tuffite in them should not exceed 15%, since specified additive in the big doses sharply reduces durability of cement. It is established that at the presence of tuffite grindability of clinker considerably raises: in the presence of 15% tuffite in 15 minutes the grinding residue on the sieve № 02 makes 20% that it is less on 5%, than in free-additive cement (fig. 1). The increase in time of grinding to 30 minutes reduces quantities of the residue on the sieve to 12,0% that it is less on 3%. 1,5 hours duration of grinding promotes to obtain cement with a subtlety of crushing of the residue of 4% on the sieve whereas this quantity for free-additive cement makes 8%.

At replacement of 15% tuffite with equal quantity of SWSM grindability deterioration of mixes is observed, however, it is much better, than free-additive clinker mixes (fig. 2). Mixed portland cement containing simultaneously tuffites and SWSM are characterised concerning high grindability grindability and lower water consumption than cements with tuffite: the size of normal density of the cement paste has considerably decreased, it is obvious on the account of increase in the maintenance of small fractions at input of SWSM.

Portland cements with tuffite at combined grinding with carbonate waste containing small amount of $CaCl_2$ are enriched with small fractions that leads to increase of activity of cements on the account of their optimisation of granulation, especially it is appreciable at a separate grinding of portland cement clinker, and SWSM with their subsequent mixing; at these hardening of cement as it is specified above, it is accelerated in initial stages of hydration.

Intensity of carbonate interaction with hydration products of portland cement clinker and a hydraulic additive — unequal tuffite, also depends on set of factors, in particular on crystal structure of calcium carbonate of and presence of impurity substances.

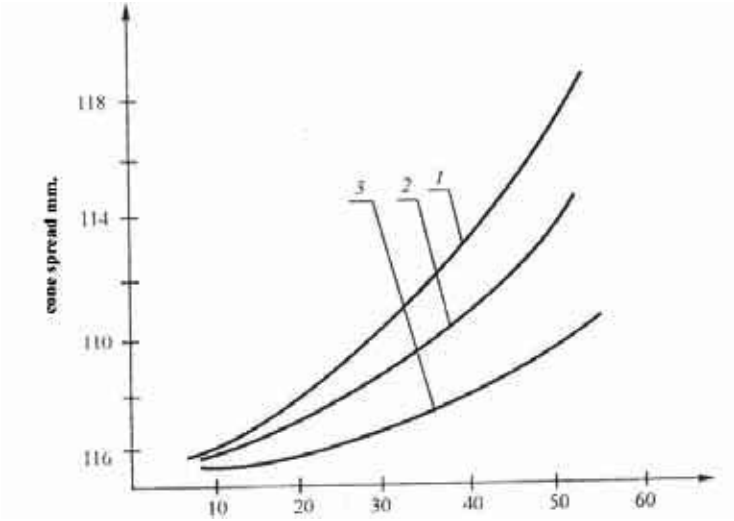

Fig. 1. The influence of quantity of tuffite on the cone spread

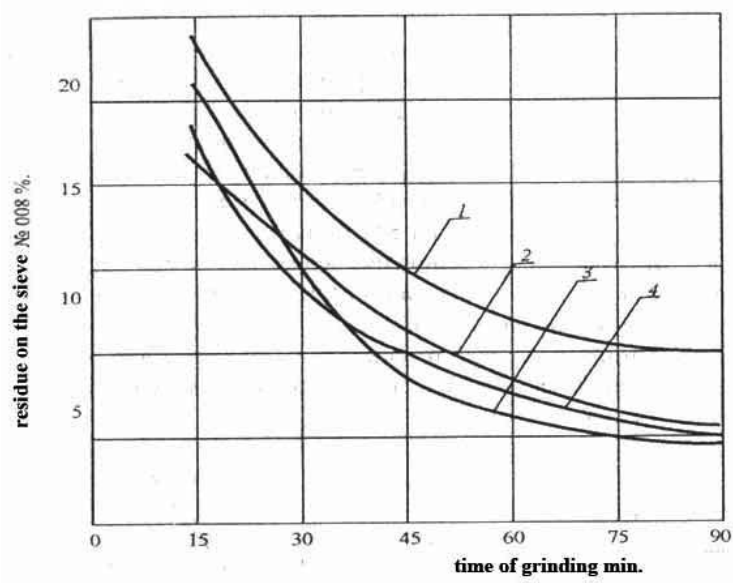

Fig. 2. The influence of a kind of an additive on grindability of clinkers

1 – clinker of Navoiy cement plant (NCP) +5% of gypsum; 2 – clinker of NCP + 5% of gypsum +15% SWSM; 3 – clinker of NCP +5% of gypsum + 15% of tuffite; 4 – clinker of NCP + 5% of gypsum +13% of tuffite + 15% SWSM.

Table 1. – The influence of natural tuffite additives on the physical-mechanical properties of Navoiy portlandcement

№ п/п	Composition of cement,%			Normal density,%	Limit of strength at a bend/compression, MPa					
	clinker	gypsum	tuffite		day 1	day 3	day 7	day 28	day 90	Heat moist curing
1	*2*	*3*	*4*	*5*	*6*	*7*	*8*	*9*	*10*	*11*
1	95	5	-	24,0	3,8/30	4,3/33	4,6/41	7,2/54	8,0/58	5,4/38
2	85	5	10	29,7	3,4/20	3,7/28	4,4/39	7,2/49	7,1/52	4,5/34
3	75	5	20	34,4	3,3/19	3,3/22	4,0/31	5,2/34	5,7/36	4,0/33
4	65	5	30	34,4	3,2/18	3,3/20	3,8/27	4,5/31	5,2/22	3,7/29

1	*2*	*3*	*4*	*5*	*6*	*7*	*8*	*9*	*10*	*11*
5	60	5	35	35,9	2,9/16	2,9/20	3,5/24	3,9/26	4,3/29	3,5/25
6	55	5	40	40,1	2,9/15	2,9/18	3,3/23	3,7/25	3,5/26	3,3/22
7	50	5	45	46,1	2,6/14	3,2/14	3,2/19	3,4/22	3,7/23	2,6/18
8	45	5	50	47,0	2,2/13	2,7/13	3,1/16	3,3/19	3,3/19	2,3/15

The note: numerator — durability on a bend; a denominator — durability on compression.

Table 2. – The influence of natural tuffite additives on the physical-mechanical properties of cements

№ п/п	Composition of cement,%		Normal density,%	Cementation time, hour-minute		Limit of strength at a bend/compression, MPa				
	clinker	tuffite		start	finish	day 1	day 28	day 90	day 180	day 360
Bekobod portland cement										
1	100	–	25,0	2–05	4–15	3,4/19	5,8/45	6,3/45	6,5/49	7,1/54
2	90	10	28,5	2–20	4–10	3,3/20	6,3/45	6,7/47	7,3/52	7,2/54
3	80	20	32,4	2–25	4–40	3,1/19	5,4/35	5,7/44	6,5/48	5,8/49
4	70	30	36,5	2–35	4–35	2,6/16	4,6/32	5,5/38	5,6/40	7,5/61
Ohangaron portland cement										
1	100	–	24,0	3–10	5–15	3,4/20	6,0/46	6,9/49	7,0/52	6,8/56
2	90	10	32,0	2–50	5–35	3,2/20	4,9/46	6,0/48	6,2/51	6,0/52
3	80	20	35,5	2–40	5–55	2,5/18	4,4/40	5,7/43	5,8/43	5,7/39
4	70	30	38,5	3–05	6–10	2,1/16	3,9/30	4,5/34	4,6/36	4,9/38

Table 3. – The influence of tuffite additives, burnt at 600 °C on physical-mechanical properties of Navoiy portland cement

№ п/п	Composition of cement,%			Normal density,%	Limit of strength at a bend/compression, MPa					
	clinker	gypsum	tuffite		day 1	day 3	day 7	day 28	day 90	HMC
1	95	5	–	24	4,0/31	4,5/34	4,8/42	7,5/56	8,4/61	5,6/44
2	85	5	10	26	4,4/25	4,6/34	4,8/46	7,8/56	7,8/57	5,5/40
3	75	5	20	28	4,5/29	4,8/41	5,4/44	5,4/48	6,1/53	4,4/45
4	65	5	30	30	4,5/42	4,6/44	4,9/46	5,5/57	5,6/63	4,6/53
5	60	5	35	33	4,1/34	4,5/36	4,8/42	7,5/53	7,5/57	5,5/45
6	55	5	40	35	3,4/22	4,0/31	4,6/42	5,7/46	7,0/48	4,7/38
7	50	5	45	36	3,3/21	3,6/23	4,0/31	4,7/32	5,2/34	3,8/32
8	45	5	50	37	2,8/16	3,3/17	3,3/21	3,6/23	3,9/25	2,8/21

Table 4. – The influence of tuffite additives, burnt at 600 °C on physical-mechanical properties of cements

№ п/п	Composition of cement,%			Normal density,%	Cementation time, hour-minute		Limit of strength at a bend/compression, MPa				
	clinker	tuffite	gypsum		start	finish	day 1	day 28	day 90	day 180	day 360
1	*2*	*3*	*4*	*5*	*6*	*7*	*8*	*9*	*10*	*11*	*12*
Bekobod portland cement											
1	100	–	5	24,1	2–05	4–10	3,4/20	5,8/45	6,5/45	6,5/40	7,1/56
2	90	10	5	25,3	2–20	4–00	4,0/30	5,6/48	7,0/61	7,6/68	7,6/57

1	*2*	*3*	*4*	*5*	*6*	*7*	*8*	*9*	*10*	*11*	*12*
3	80	20	5	26,4	2–25	4–20	4,1/31	6,0/51	6,2/64	6,9/67	7,1/69
4	70	30	5	27,5	2–35	4–30	4,4/34	6,3/60	6,9/68	7,0/67	7,8/67
Ohangaron portland cement											
1	100	–	5	24,0	3–10	3–15	3,4/21	6,0/48	6,9/49	7,0/50	6,8/56
2	90	10	5	26,0	2–40	5–20	3,6/32	6,3/56	6,4/57	6,5/58	6,3/61
3	80	20	5	27,0	2–39	5–50	3,8/34	5,7/60	6,0/61	6,1/63	6,1/64
4	70	30	5	28,0	3–05	4–10	4,0/40	6,4/65	7,0/67	7,1/68	7,4/69

The best results have been received at test of the various cements being made with burnt tuffite additive in the republic. Thus the adverse effect of montmorillonite impurity is eliminated, the water consumption of cement decreases, its strength indicator raises.

Under the active maintenance SiO_2 and Al_2O_3 burnt tests differ from breeds in natural state a little. Activity on absorption of lime from solutions for the burnt tests has increased, their swelling capacity has raised.

The recieved data shows that tuffite breed burnt at 600 °C influences physical-mechanical properties of cements positively. Cements is characterised by intensive increase of durability by 28 days, its hardening and steady growth in longer terms.

The best results are received at input of 20% and 30% of an additive. It has been shown as earlier by us that tuffites burnt at 600 °C make positive impact on grindability of clinker.

Clinker, gypsum, tuffite, SWSM are delivered supply bunker (fig. 3) by means of belt conveyors, whence they arrive on disk feeders where are dosed out in a certain parity. Dosed components blends arrive in a funnel of the cement mill.

Cement mill in the size 4,0x13,5mm, two-chamber where the first chamber is filled with spheres (balls), and the second with tsilpebs. The mill works in an open cycle with number of turns of 16,2 pour a minute. Movement is run by means of the central drive consisting of the electric motor, a reducer; half couplings and the central shaft.

The arrived components are exposed to a high milling, by means of grinding bodies, to grinding [milling] fineness with the residue on a sieve № 008 to 12–15%. The fine powder is portland cement with the composite additives, obtained on the bases of clinker, gypsum, tuffite and SWSM.

The obtained mixed cement by means of the pneumochamber pump on cement wires is transported in the cement silo, for storage and shipment to consumers. The obtained cement is shipped in wagon in railway cars or in cement truck.

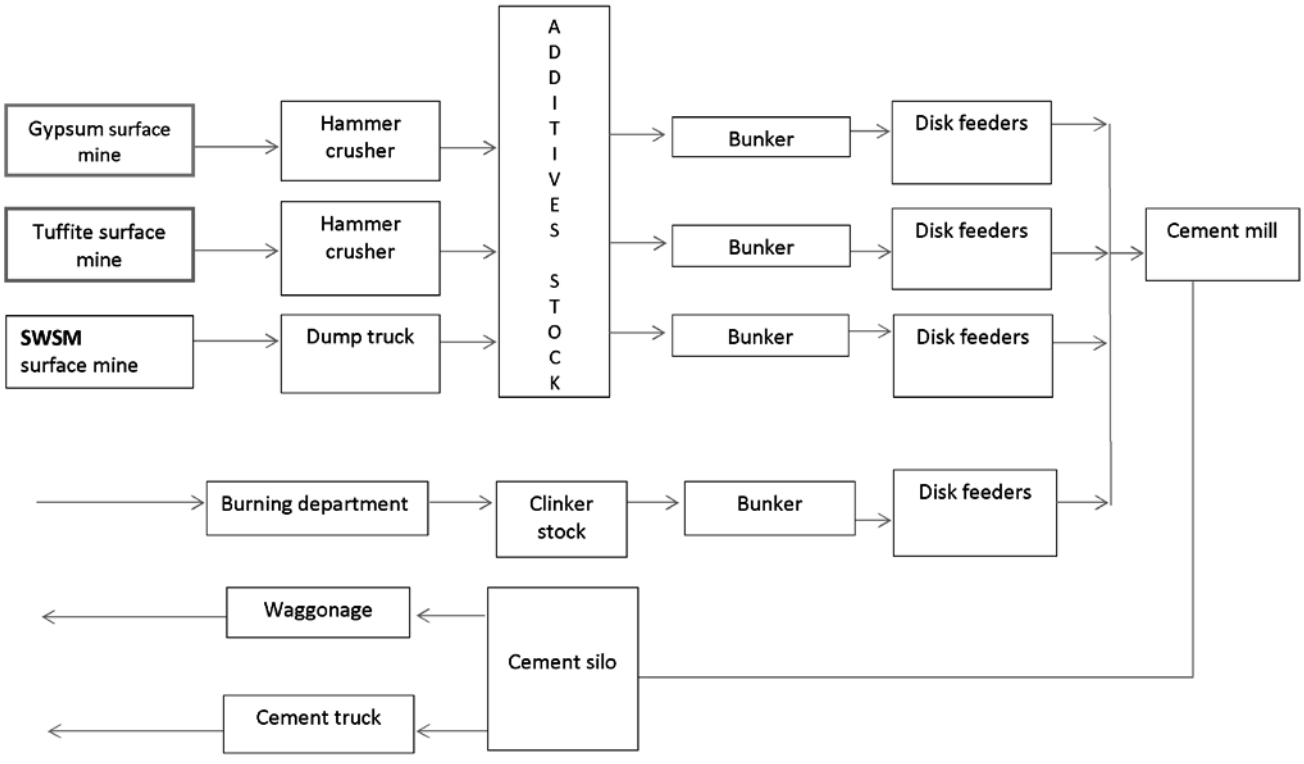

Fig. 3. Process flowsheet of manufacture

DOI: http://dx.doi.org/10.20534/AJT-16-9.10-65-68

Matkarimov Zaynobiddin Turdalievich,
Tashkent chemical-technological institute,
Department of «Technology of silicate materials and rare, noble metals», Assistant
E-mail: zaynobiddin1986@mail.ru

Aripova Mastura Khikmatovna,
Tashkent chemical-technological institute,
department «Technology of silicate materials and rare, noble metals»,
Doctor of technical sciences, Professor
E-mail: aripova1957@yandex.ru

Mkrtchyan Ripsime Vachaganovna
Tashkent chemical-technological institute,
Innovative center, Candidate of technical sciences
E-mail: mk_hripsime@mail.ru

Formation of the ceramic body structure with the use of steel industy slag

Abstract: The composition of ceramic body was developed with the use of the metallurgical slag and steel industry waste. The dependence of water absorption and shrinkage on the ceramic body composition was investigated. The appearance of anorthite and mullite phases in the process of heat treatment was established by X-ray diffraction analysis.

Keywords: ceramics, metallurgical slag, water absorption, shrinkage, anorthite, mullite.

The use of production wastes is a relevant task of modern times. The goal of our research was to develop and study the structure of ceramic floor tiles with the use of metallurgical slag of steel industry in its composition. Rich mineral raw material base of Uzbekistan allows solving the established task by different ways.

At this stage of technological development, the problem of disposal of man-caused wastes is urgent. The use of wastes for building material production is a promising direction [1, 10–11; 2, 22; 3, 3–6]. It is noted [4] that the use of metallurgical wastes leads to the enhancement of strength and durability of ceramic tiles.

Considering positive effect of metallurgical slags on ceramic tiles, the slag of steel-making production of APO «Uzmetkombinat» is implemented in the composition of the developed ceramic floor tiles. To obtain ceramic body, usually used natural materials such as clay and kaolin, the chemical compositions of which are presented in Table 1, were chosen apart from metallurgical slag.

Table 1. – Chemical compositions of raw material components

Name of raw material	Bulk quantity of oxides,%								
	SiO_2	Al_2O_3	TiO_2	CaO	MgO	K_2O	Na_2O	Fe_2O_3 + FeO	loi
Clay of the deposit of Maiskoe	50,48	12,37	0,58	10,79	3,23	2,33	0,52	4,88	14,82
Angren kaolin, secondary, grey	67,38	21,36	0,25	0,28	0,22	1,07	0,75	1,18	7,51
Metallurgical slag of steel making production	27,34	6,9	–	25,11	9,65	–	–	27,05	3,95

Table 2. – Parameters of mold powder of experimental masses

Mold powder humidity,%	Bulk weight of mold powder, g/cm^3	Granulometric composition of powder,%				
		Over 2 mm	2–1 mm	1–0,5 mm	0,5–0,25 mm	Less than 0,25 mm
6–7	1,0	0,5–0,6	22–25	20–22,9	15,0 –16,8	37,7–40,0

36 experimental masses were prepared in laboratory conditions. The de-watering of slip masses was performed in laboratory conditions. Preparation of ceramic body was done in ball mill to the residue of 2–3% at the sieve № 006; the humidity of the slurry was 38–42%. The parameters of ceramic body powder are presented in Table 2.

To choose an optimal composition for ceramic tiles, the change of water absorption and shrinkage depending on the body composition was studied (Fig. 1, 2).

Obtained data allowed selecting optimal compositions of the bodies according to water absorption (3,3–3,9) and shrinkage of the ceramic body (7,34%): 30% of clay; 50–60% of kaolin and 10–20% of slag. For these compositions, mean indicators of compressing strength were 141 Mpa and flexing strength — 85 MPa.

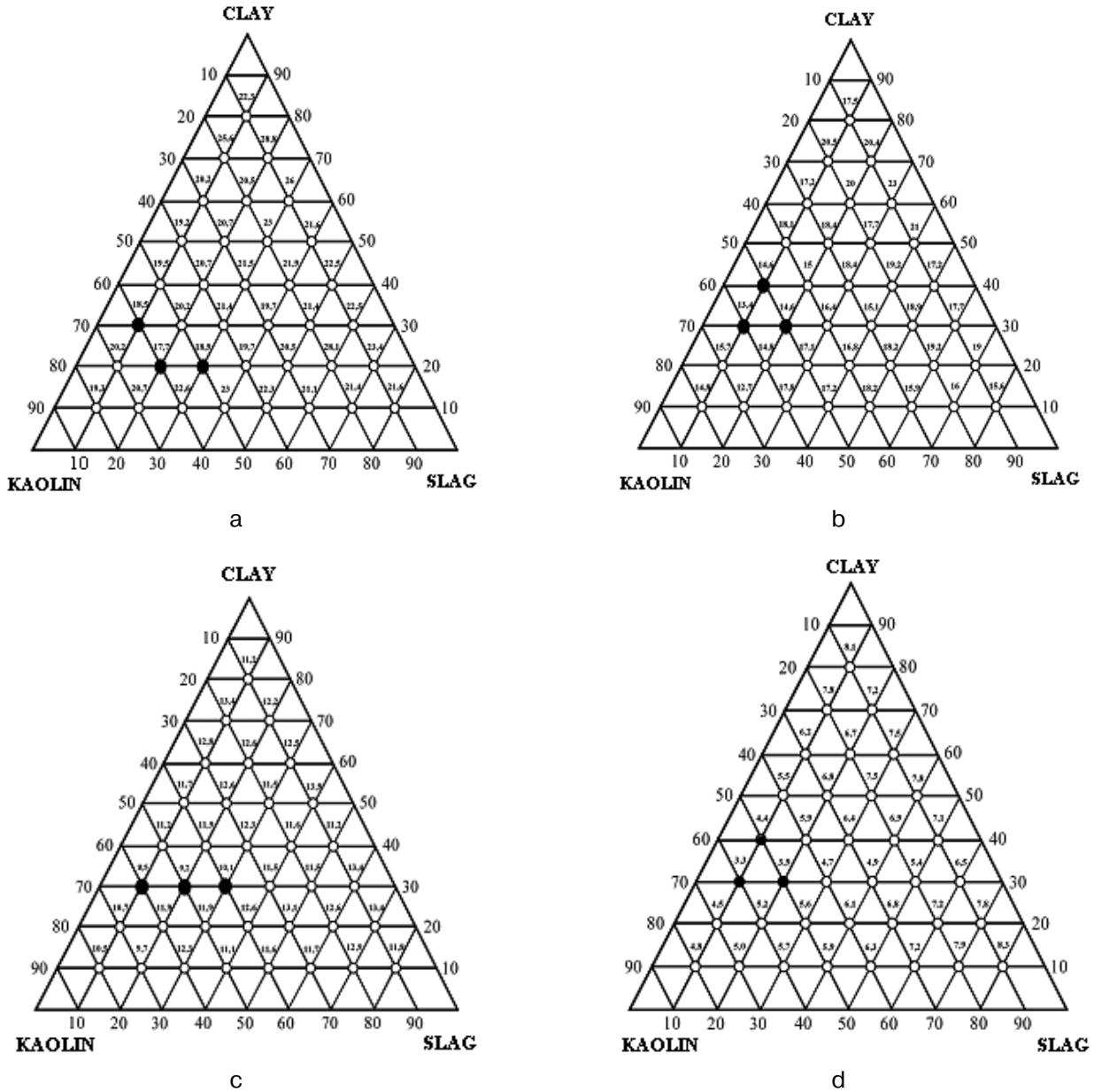

Figure 1. Dependence of water absorption on the composition of ceramic body burnt at the following temperature: a – 900 °C; b – 1000 °C; c – 1100 °C; d – 1180 °C

The changes in the phase composition of ceramic bodies in the process of heat treatment were studied. X-ray diffraction analysis was performed on the Shimadzu installation at Cu Kα radiation. The surveying of X-ray patterns was done with the step of 0,02 grad, voltage of 30 kV, current of 30 mA. Diffraction patterns recorded the appearance of new formations at 1100 °C (Fig. 3). Considering that the main peak of mullite is shadowed by quartz peak, the reflexes 3,42 and 2,690 Å are referred to the phase of mullite. The reflexes 4,08, 3,20, 2,507 Å certify about the formation of anorthite.

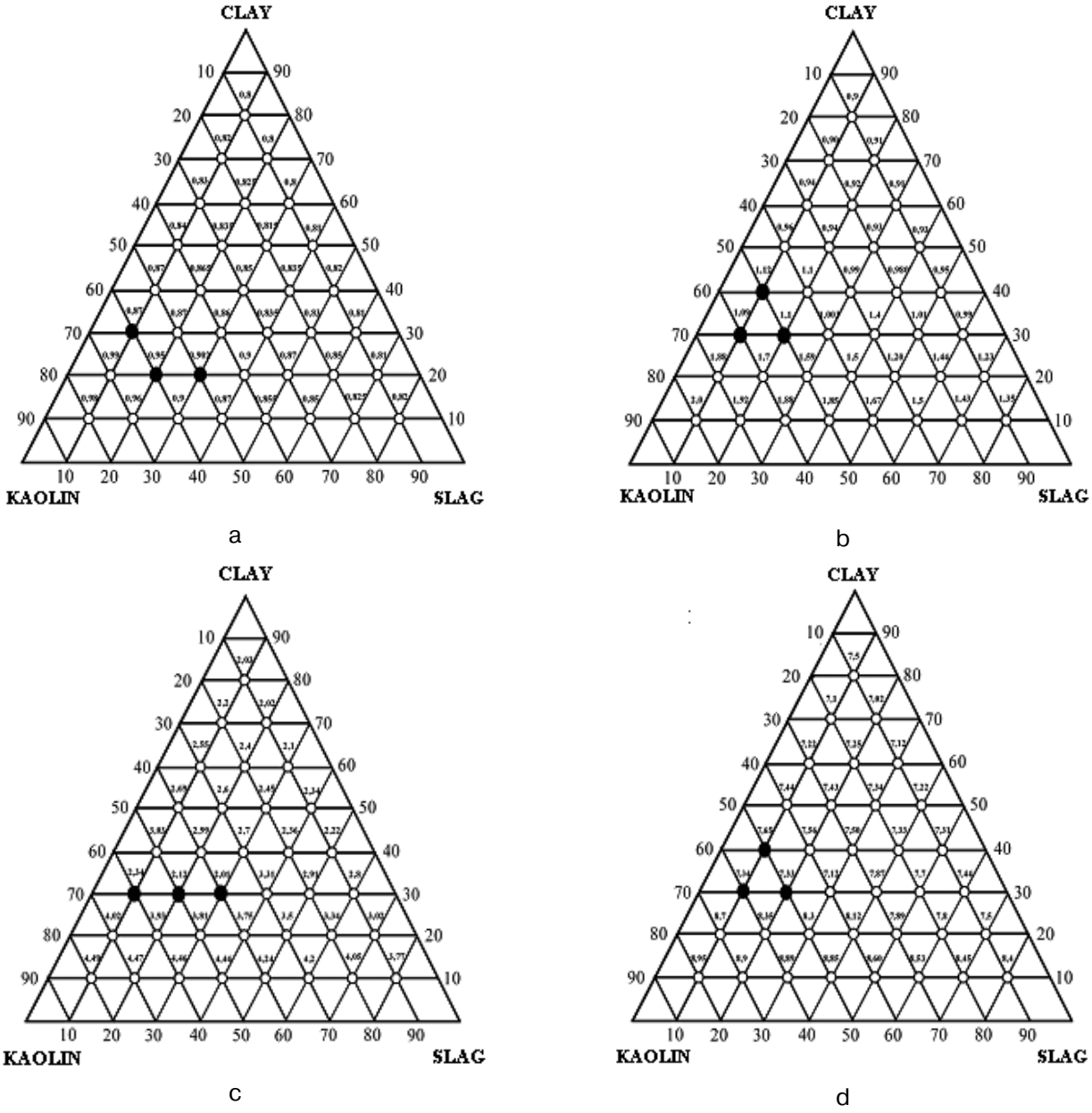

Figure 2. Dependence of shrinkage on the composition of ceramic body burnt at the following temperature: a – 900 °C; b – 1000 °C; c – 1100 °C; d – 1180 °C

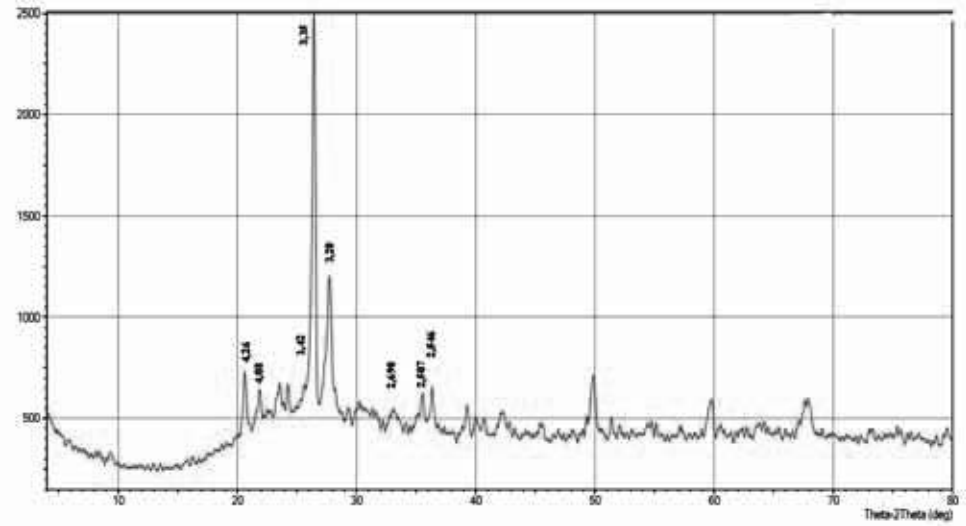

Figure 3. Diffraction pattern of the ceramic body burnt at the temperature of 1100 °C

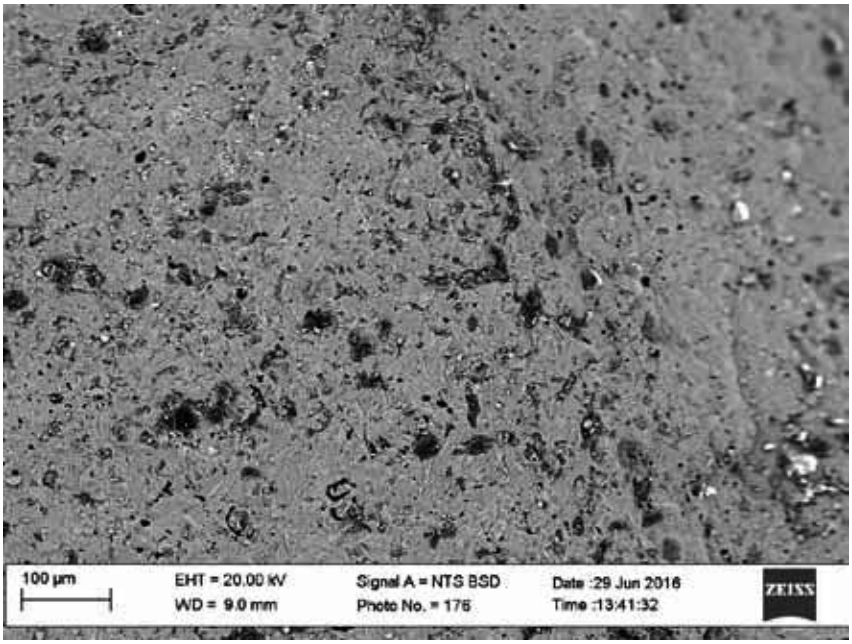

Fig. 4. Electronic-microscopic image of ceramic body heat-treated at 1100 °C

Heat-treated patterns were studied by the method of electronic microscopy (Fig. 4) at the scanning electronic microscope (SEM-EDX).

The implementation of metallurgic slag of steel-making production in the composition of ceramic body contributed to the intensification of mineral formation and obtaining of homogenous compact structure.

Based on the obtained data, ceramic floor tile was developed and its approbation was performed at the Tashkent ceramic plant. According to all indicators, received items met the specified requirements.

References:

1. Халматов М. М., Калинин В. П. Проблемы переработки техногенных отходов//Горный вестник Узбекистана, – 2003, – № 4. – С. 10–11.
2. Козубская Т. Г. Использование техногенных отходов в производстве строительных материалов // Строительные материалы. – М.: 2002, – № 2. – С. 22.
3. Залыгина О. С., Баранцева С. Е. Утилизация гальванического шлама в производстве стройматериалов //Стекло и керамика. – Москва, – 2002, № 4. – С. 3–6.
4. Патент RU 2345039. C04B 33/138. Керамическая масса для изготовления плитки для полов /Щепочкина Ю. А. Опуб. – 20.04.2014 Бюл. – № 11.

DOI: http://dx.doi.org/10.20534/AJT-16-9.10-68-71

Salimova Nigar Azizaga qizi,
Azerbaijan State University of Oil and Industry,
professor, faculty of "Chemical technology"
E-mail: nigar_08@mail.ru

Huseynova Matanet Arif qizi,
Azerbaijan State University of Oil and Industry,
associate professor, faculty of "Chemical technology"

Rational utilization of wastes of sulphuric acid propylene hydration

Abstract: The alkylation reaction of benzene by fraction 140–250 °C, separated from waste of production of isopropyl alcohol by sulphuric acid propylene hydration have been conducted. The waste is the cube resi-

due of the column dehydration of diisopropyl ether-being by product of isopropyl alcohol production. The results of experiments indicated possibility production of alkylbenzenes: dodecil and pentadecil-benzenes. The structure of synthesized products have been identified on base of spectral, gas chromatography analysis and results of physical-chemical investigations.

Keywords: waste, alkylation, alkylate, alkylbenzenesulphonate.

The most prevalence among the anion synthetic washing agents the alkylbenzene sulphonates of sodium $RC_6H_4SO_2Na$ received, which with some additives are known as sulphonol. In industry these substances received wide use that is explained by good washing properties of alkylbenzenesulphonates in composition with active additives, low cost and excellent technological qualities. These are unhygroscopic and uncaked powders that have the great significance by it is production by the method of spraing drying which is the base in production of synthetic washing agents.

One of the stage alkylbenzenesulphonates production is production of alkylbenzens by use of different alkylating agents.

In present work by purpose expansion of more available by its raw material base cost for production of alkylsulphonates, it is offered use as alkylatng agent the waste of isopropyl alcohol production by sulphuric acid propylene hydration.

In works [1,2] the results investigations of composition of the above-mentioned waste and method of its use have been presented. The waste of isopropyl alcohol production is the cube residue of column dehydration of diisopropyl ether received as by product of isopropyl alcohol production by sulphuric acid propylene hydration.

There are 76–78% of propylene oligomers (three-, tetra-, penta) in cube residue of column dehydration of diisopropyl ether of the distillation of the last and return it in process, which have been determined on base spectral, gas chromatography analysis and results of physical-chemical investigations [1, 2].

In present work the research by receiving of alkylbenzenes on base of waste of isopropyl alcohol production have been introduced.

In reaction alkylation of benzene as an alkylating agent the fraction 140–250^{0}C of cube residue of the column dehydration of diisopropyl ether, containing three-, tetra- and pentamers of propylene have been used. As an catalyst the catalytic complex on base of $AlCl_3$ have been used.

Method of experiment and analysis of received products.

The necessary device and reagents: three-throat flask by volume 250sm^3 with mechanical mixer, water bath, return cooler, dropping funnel, thermometer, dry benzene chemically pure, fraction 140–250^{0}C of cube residue of the column dehydration of diisopropyl ether (DIE) waterless, chloride aluminium, cationit CU-2, calcinated calcium chloride.

Table 1. – Conditions of experiment conducting

Have been put in reactor	mol
Benzene	2.65
Fraction 140–250 ^{0}C	0.4
Chloride aluminium	0.1
Mol correlation benzene: fraction (140–250 ^{0}C) DIE	6:1
Reaction temperature, ^{0}C	50–55

The catalytic complex — is suspension of chloride aluminium in benzene — has been loaded in reaction flask, then the rest of amount of benzene, necessary for reaction according to calculation and further from dropping funnel the alkylating agent a drop at a time have been added.

After addition in reaction zone the whole amount of the fraction 140–250^{0}C, the mixture has been mixed some more 45 minutes, then the mixture has been separated in dropping funnel on two layer: upper — hydrocarbon and lower — complex. The complex may be keep under of alkylate layer in tightly closed flask and may be used in another experiments as catalyst. Received alkylate have been put current through the cationit CU-2 layer, then from purified alkylate a sample has been taken for gas-chromotography, then the alkylate have been dried and have been distillated.

Benzene and part of unreacted fraction 140–250 ^{0}C have been distillated under atmospheric pressure up to 200^{0}C temperature, then the product have been distillated under vacuum, by that the following fractions have been distillated: the rest amount of unreacted fraction 140–250^{0}C; the first fraction have been distillated. By temperature 70 ^{0}C and residual pressure 1 mm mercury column, that correspond to temperature 265 ^{0}C by pressure 760mm mercury column; the second fraction have been distillated by temperature 110–120 ^{0}C and residual

pressure 1mm mercury column, that correspond to temperature 328–355 ^{0}C by pressure 760mm mercury column. The residue in flask had a more high boiling point and therefore haven't been distillated.

Discussion of experiments results.

In table 2 the material balance of one of numerous experiments of reaction alkylation of benzene by fraction 140–250^{0}C of waste of DIE have been presented.

Table 2. – Material balance of reaction alkylation of benzene by fraction 140–250^{0}C of waste of DIE

Have been taken	Qram	%, mas.	Have been received	Qram	%, mas.	yield of alkylbenzene
Benzene	225	69.23	Benzene	207.5	63.85	–
Fraction 140–250^{0}C of waste DIE	100	30.77	Unreacted fraction 140–250^{0}C	53.3	16.40	–
In all	325	100.0	I fraction of alkylbenzenes	21.7	6.68	58.96
			II fraction of alkylbenzenes	37.5	11.54	54.30
			Residue	5.0	1.54	–
			In all	325	100.0	–

Yield of alkylbenzenes fractions from theoretically possible have been calculated according to percentage content of three-, pentamers of propylene in fraction 140–250^{0}C of waste of DIE, equal correspondingly 33.1 and 66.9% mas. [1,2]. The material balance have been calculated on base of gas chromatography analysis, carried out on chromatograph LKHM — 8 MD in following conditions: phase-polysorb, length of column 2 metre, temperature 110–120^{0}C. The physical-chemical properties of alkylbenzenes (I and II fractions) have been presented in table 3. Identification of alkylbenzenes (I and II fractions) have been made on base of physical-chemical properties and spectroqram, made on apparatus FT-02.

The IR — spectrum of alkylbenzenes have been presented in figure 1.

In spectroqram the following are displayed: intensive peak 1462.72 distinctive for virbartion of aromatic ring; peak 1721.24, presenting overtones and combinative tones of benzene derivatives; peak 1377.68, is related to symmetrical deformations of alkyl groups and presenting the alkyl derivatives of benzene peak 2880–2860-is methyl group, added to benzene ring.

There is peak 1160 sm^{-1}, is related to deformative vibrations of CH in monosubstituted aromatic hydrocarbons.

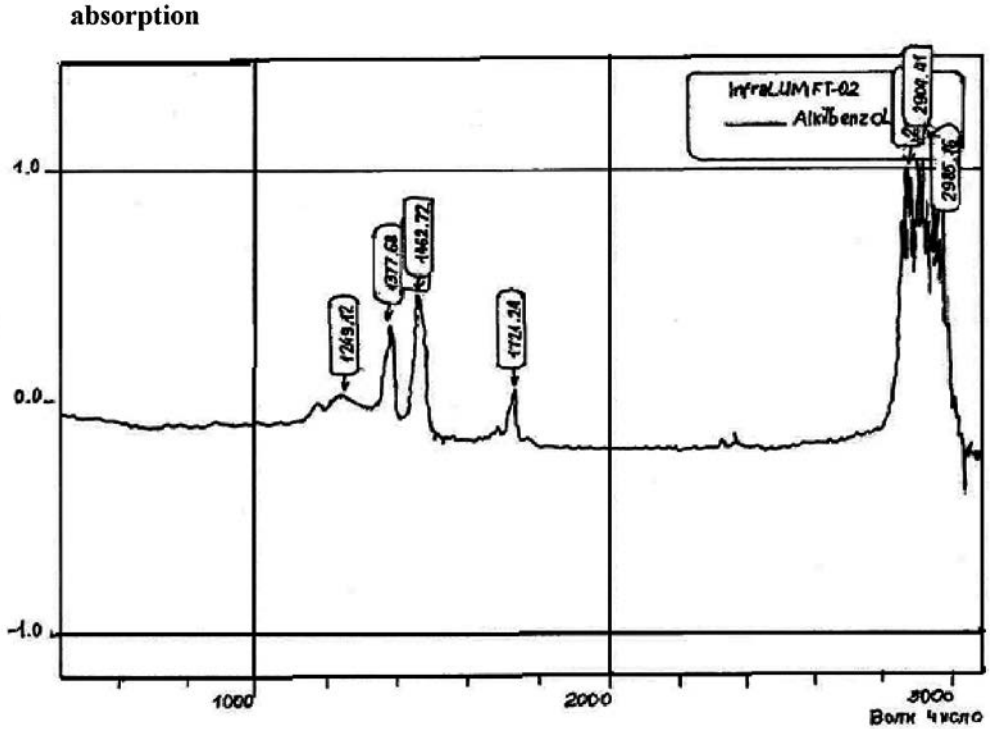

Figure 1. Spectrogram of alkylbenzenes

Table 3. – Physical-chemical properties of alkylbenzenes

Name	Yield on alkylate,% mas.	Mol. mas.	Coefficient of refraction	Pensity, kq/m^3	Molecular refraction MRD	
I fraction					Experimental	Calculated
II fraction	32.4	246	1.4589	837.3	80.19	77.62
Residue	17.6	408	1.4705	857.5	93.78	89.28
	50.0	>618	–	–	–	–

Analyzing the data of table 3 and spectrogram (figure 1) it can be suppose, that in fraction I, there is dodesilbenzene and in fraction II — pentadesilbenzene. Small difference between experimental and calculated molecular refractions to all appearances is explained by indistinct rectification by distillation with dephlegmator, in result of which, in first fraction the pentadesilbenzene is taken and in second fraction dipentadesilbenzene is taken. Presence of dialkylbenzenes is confirmed by availability on spectrogram peaks 2985.16 and 2904.41.

From literary references [3] it is known, that according to consecutive mechanism proceeding of reaction alkylation of benzene by olefins not only monoalkylbenzenes, also di- and polyalkylbenzenes are formed and olefines polymerization take place. Received highmolecular compound, boiling by more high temperature, have been presented in material balance as residue.

The I and II fractions of alkylbenzenes, present itself correspondingly dodesil-and pentadesilbnezenes may be recommended as alkylating agents for synthesis of alkylbenzenesulphonates.

Residue of reaction mass, containing according to literary references (3, 4) di-, three- and more highmolecular polyalkylbenzenes it is not to considered as undesirable by-product.

At present time on base of high-molecular alkylbenzenes soluble in oil sulphonates and washing additions for lubricating oils are received and therefore "rear" fractions of alkylbenzenes are also valuable product.

Conclusion

Reaction alkylation of benzene by fraction 140–250 ^{0}C separated from waste of isopropyl alcohol production by sulphur acid hydration of propylene have been conducted. The waste is cube residue of the column dehydration of diisopropyl ether-being by-product of isopropyl alcohol production. The results of experiments indicated the possibility synthesis of alkylbenzenes: dodesil- and pentadesilbenzenes.

The structure of synthesized products have been identified on base of spectral, gas chromatography analysis and results of physical-chemical research.

References:

1. Salimova N. A., Shakhverdiyeva F. M., Huseynova M. A. Ecologically harmless technology of sulphur acid production of isopropyl alcohol//Engineering ecology. – Moscow, – 2004, – № 5, – P. 30–36.
2. Salimova N. A., Shakhverdiyeva F. M., Huseynova M. A. Analysis of waste of sulfur acid production of isopropyl alcohol//News of higher technical institutions of Azerbaijan. – 2005, – № 1, – P. 35–37.
3. Lebedyev N. N. Chemistry and technology of base organic and oil chemical synthesis. Publishing house. Chemistry. – Moscow, – 1988, – P. 735.
4. Paushkin Y. M., Vishnyakov T. V., Belov P. S. Practical work by oil chemical synthesis. – M. Chemistry, – 1965, – P. 341.

DOI: http://dx.doi.org/10.20534/AJT-16-9.10-72-75

Siddikov Ilkhomjon Khakimovich,
Tashkent University of Information Technologies,
Head of the chair «Power supply systems»
E-mail: ikhsiddikov@mail.ru

Sattarov Khurshid Abdishukurovich,
Tashkent University of Information Technologies,
Ass.Prof., of the chair «Power supply systems»
E-mail: sattarov.khurshid@mail.ru

The transducers of the primary current to secondary voltage with flat measuring windings for combined control of reactive power

Abstract: Purpose of research is development of theories and designing the electromagnetic transducers one and multi-phases primary current to secondary voltage with flat measuring windings for multifunction control source of reactive power and creation of their base of power and resource saving in power systems. The classical methods of research of the magnetic circuits do not provide necessary accuracy due to the asymmetries of the three-phase primary currents of electric network, which do not possess the sufficient generality, covering here with only main varieties of the circuits of electric and magnetic nature.

Keywords: magnetic circuit, accuracy, electric nets, magnetic system, non-linear parameter, electromagnetic transducers, primary current, secondary voltage, reactive power, power and resource saving, power systems.

The development of the complex approach, providing power and resource saving on base of efficiently control sources of reactive power, expansion of the functional possibilities, simplification of designs, reduction of weight and volume factors, improvement of the technologies of fabrication, provision of the remote measuring processes, transformation of the current based on the usage of the modern primary measuring transducers is actual problem of the control devices and elements of power system.

Herewith, the primary measuring current transducers, being the main section information-measuring and controlling systems, completely define the technical and economic factors of power system. At present employment of the electromagnetic transducers of three-phase current with unified output value, expansion of the spectrum converted electric values is limited, because of the insufficient development of the methods of calculation and research of portioned magnetic systems of the transducers.

The classical methods of research of the magnetic circuits do not provide necessary accuracy due to the asymmetries of the three-phase primary currents of electric network, which do not possess the sufficient generality, covering here with only main varieties of the circuits of electric and magnetic nature. The magnetic systems of the transformation with non-linear parameters and features of the primary current of electric network of power system during calculations have been taken as an object with concentrated parameters. The Complex analysis of the elements and control system of source of reactive power and their mode, principle of their buildings, is indicative of insufficient research of problems in the field of electromagnetic transformation current and combined control of source of reactive power of power system. However shaping the priority methods of the contraction and researches of the electromagnetic transducers of the primary current in secondary voltage, providing adequacy of the value of the output voltage to primary current, algorithm of three-phase current in system of multifunction control reactive power systems require undertaking comprehensive research. This circumstance is connected with greater inaccuracy at transformation of the values primary current power systems, which bring about irrational use the sources to electric powers, obstruct checking and control mode their work, bring about excessive financial loss of powers.

The System analysis of the electromagnetic transducers of primary current has allowed also to install that classical designs of the transducers of the current managerial system by reactive power — a transformers of the current provide on output current by value 5 A under nominate of primary, have: restriction on range of the converted current; significant inaccuracy; complex and non-technological to designs; the greater size; the mass; specific consumption of materials and cost.

The Fact just cited limited using the classical electromagnetic transducers of the current in corresponding to managerial system of the values and parameter of the electric networks. So development, study and practical introducing the electromagnetic transducers with flat measuring winding primary one and three-phase current in secondary voltage with extended functional possibility and unified output value, taking into account non-symmetry of three-phase current and creation on their base of the systems of multifunction control reactive power is a decision of the problem of the improvement and developments existing technologies of control value and parameter of powers is actual problem of the power system.

Purpose of research the development of theories and designing the electromagnetic transducers one and multi-phases primary current to secondary voltage with flat measuring windings for multifunction control source of reactive power and creation of their base of power and resource saving in power systems.

In the fig.1. presented of the electrical network of power system with combined auto-control system of devices of production, transmissions, distribution and consumptions to reactive electric power [1].

In the tabl.1 references of electromagnetic transducer of the current to voltage, are classified main forms of the flat measuring windings and motivated formulas for determination area sections S different flat measuring windings. The Analysis of the conditions of the functioning the transducers of the current and requirements have shown that in power system it is advisable to use the electromagnetic transducers of the current and voltages with flat measuring windings and development principle transformations and design electromagnetic transducers of the current and voltages with flat measuring windings three-phase electric network, providing account non-symmetry, unification of the output values and possessing extended functional possibility for multifunction control source to reactive power of power system.

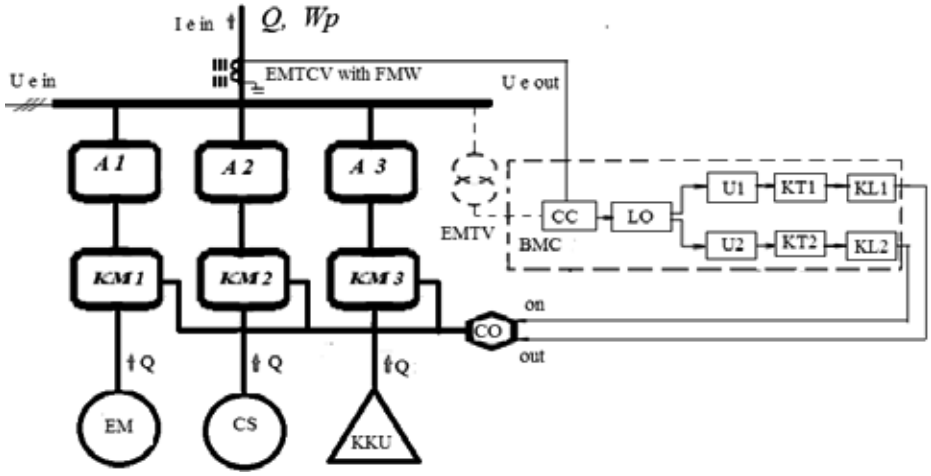

Figure 1. Functional scheme of the combined auto-control sources of reactive power of power system

A1, A2, A3 – an automatic breakers, KM1, KM2, KM3 – an commutation devices; CC – a block of current compensation; LO – logical organ; U1, U2 – an amplifiers; KT1, KT2 – an elements of the endurance on time; Kl1, Kl2 – an executive organs; CO – a control organ – BMC – bloc of microprocessors control – a digital automatic regulator of the source of reactive power; EM – a synchronous machine (the generator, motor and synchronous compensator), KKU – a source of reactive power – cosines capacitors installation, EMTCV with FMW and EMCV – an electromagnetic transducers of the current to voltage with flat measuring windings.

Figure 1. Functional scheme of the combined auto-control sources of reactive power of power system

Table 1. – The Principle of the design of flat measuring windings for electromagnetic transducers the current to voltage

№	Type of flat measuring windings	Form of flat measuring windings	Area of the section
1	*2*	*3*	*4*
1.	Triangular	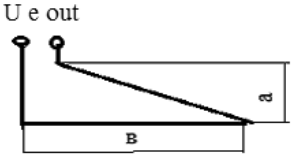	$S_{tr} = ab/2$

1	*2*	*3*	*4*
2.	**Square-wave**	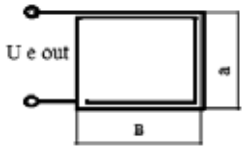	$S_{sq} = kab$
3.	**Round**	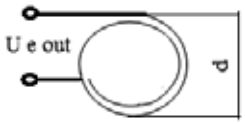	$S_r = k\pi D^2 / 4$

The principle of construction of the electromagnetic transducers of the current to voltage with flat measure winding for combined auto-control of source of reactive power of power system given in figure -2 and 3 [2–3].

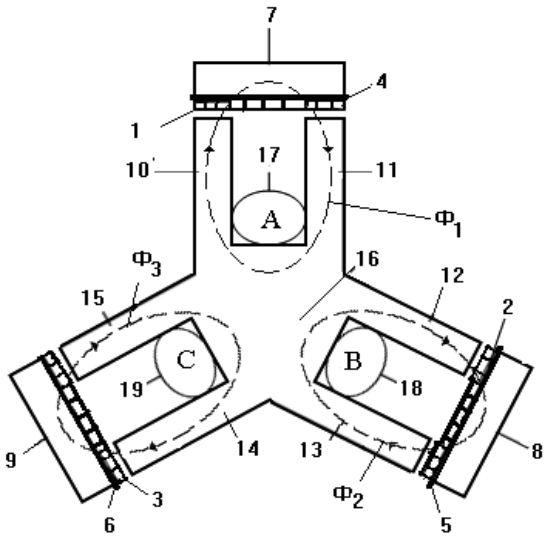

1, 2, and 3 – FMW, 4, 5 and 6 – insulation plates, 7,8 and 9 – additional Cores, 10 and 11, 12 and 13, 14 and 15 – pairs if parallel cterjens,16– base of core, 17, 18 and 19-primary windings

Fig.2 The Electromagnetic transducers of the current to voltage with flat measure winding with three magnetic cores

(Patent RUz № 04185)

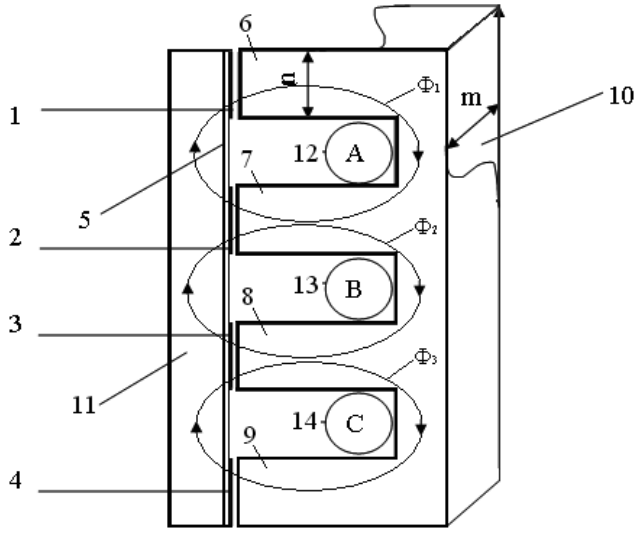

1, 2, 3 and 4 – FMW, 5 – insulation plates, 6, 7, 8 and 9 – four Cores, pairs 10 – base of core, 11 – core, 12 (phase A), 13 (phase B) and 14 (phase C) – primary winding

Fig.3. The Electromagnetic transducers of the current to voltage with flat measure winding and four magnetic cores

(Patent RUz № 04475)

In the fig. 4 given the principle schemes of the electromagnetic transducers of the current to voltage with flat measure winding for combined auto-control of source of reactive power of power system.

Conclusion

Motivated, that using of the flat measuring windings in electromagnetic transducer of current to voltage as detector elements, provides unified out signal with parameter: voltage — 20 V, current — 100 mA and allows develop of construction a new electromagnetic transducer of the current to voltage with flat measuring windings, being up to quality of combined auto-control system of reactive power of power systems.

Installed that influence of the secondary current e_{out} flat measuring windings of the current to voltage transducers of the forms 0,017% from normalized importance in primary current e_{in}. When change a temperature surrounding ambiences, inaccuracy of the transformation increases 0,03%, wrong fabrication form flat measuring windings — 0,07%. Accounting entropy inaccuracy of the transducers of the current to voltage does not exceed 0,2%, but experimental importance of inaccuracy electromagnetic transducer of the current to voltage with flat measuring windings forms 0,21%.

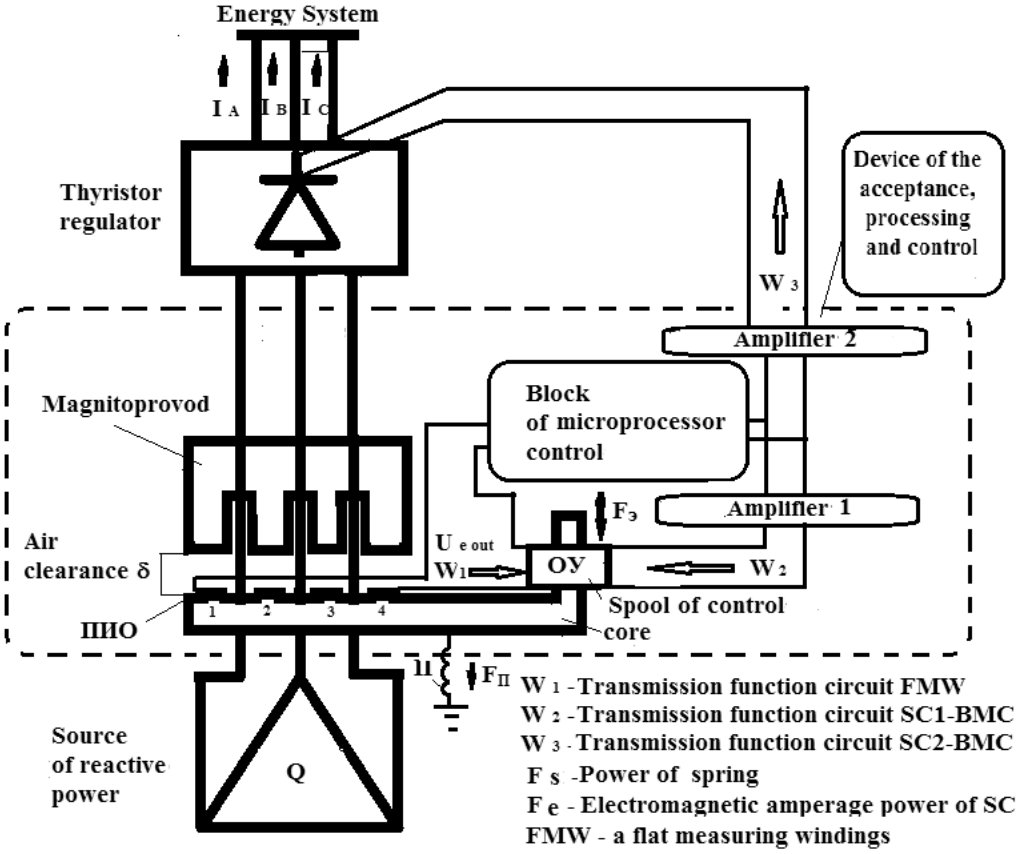

Fig.4. The principle schemes of the electromagnetic transducers of the primary current to secondary voltage with flat measure winding for combined control of source of reactive power of power system

References:

1. Siddikov I.Kh., Khakimov M.Kh., Anarbaev M., Bedritskiy I. M., Research of the electromagnetic transducers of the primary current to secondary voltage//Science and Education. Materials of the II International Research and practice conference. Vol. I, Publishing office of «Vela Verlag Waldkraiburg», Munich, Germany, December, – 18–19, – 2012. – P. 222–225.
2. Amirov S. F., Azimov R. K., Siddikov I.Kh., Khakimov M.Kh., Khushboqov B.Kh., Sattarov Kh., A. Patent RUz. № 04185. The Transducer of the non-symmetry of three-phases current//Patents Agency of RUz, Byul. – 2010. – № 6.
3. Azimov R. K., Siddikov I.Kh., Kurbanova M. J., Anarbaev M. A., Siddikov O. I., Mamatkulov A. N. Patent RUz. № 04907. The transducer of the current//Patents Agency of RUz, Byul. – 2014. – № 6.

Section 8. Chemistry

DOI: http://dx.doi.org/10.20534/AJT-16-9.10-76-79

Bekturdiyev Gulomboy Mavlonberdiyevich,
Ph.D., Senior Researcher of Laboratory of Chemical Technology of Institute of general and inorganic chemistry of Uzbekistan Academy of sciences;
E-mail: bekturdiev2015@mail.ru

Yusupov Farhod Maxkamovich,
Doctor of technical science., Head of the Laboratory of Chemical Technology of Institute of general and inorganic chemistry of Uzbekistan Academy of sciences;
E-mail: f.yusupov@yandex.ru

Kurbanov Elmurod Narzullayevich,
Director of the "Mubareksky gas processing plant" Ltd., NHC "Uzbekneftegaz"

Nurmukhammadov Jaloliddin Shermuxammad ogli,
Junior Researcher of Laboratory of Chemical Technology of Institute of general and inorganic chemistry of Uzbekistan Academy of sciences;

Yusupov Shaxzod Farhodovich
Engineer of the "Shurtaneftegaz" Ltd., NHC "Uzbekneftegaz"

Synthesis of Sulphanole on the basis of low-molecular polythene SGCC

Abstract: For the first time the technology of obtaining technical sulphanole has been developed based on a local source of raw materials from Shurtan gas chemical complex (low molecular polyethylene) and semi-products of the chemical enterprises. There are studied the temperature influence, mass parities of reagents and duration (time) of reaction on the product outlet. In laboratory conditions tests of the derived novel samples of sulphanole were conducted at preparation of the facilitated drilling solutions.

Keywords: Sulphanole, sulfonation, oleum, drilling, surface active substance (SAS), low-molecular polyethylene (LMP), reagent, sulphonate s.

Introduction. During the independence of the Republic dramatically increased range of import substitution, export-oriented chemical reagents, as well as new principles and methods of their treatment were developed. As additives to drilling solutions for revelation of the productive formations, water-soluble anionic surfactants — sulphanole is used. Of these, the greatest practical importance are alkylbenzenesulphonates, alkanesulphonates, lignosulphonates, naphthalenesulphonates, alkensulphonates, petroleum sulphonates and salts of sulphocarboxylicacids. Sulphonates are organic compounds containing one or more groups of SO_3M, where M is general cation of metal, ammonium substituted ammonium. Depending on the amount and structure of the radical, cation type and number of sulpho groups they are solid or liquid substances. Sulphonic acid is isolated from more water-soluble and organic solvents and identified as salts. On the basis of the synthesis alkensulphonates by sulfonation of olefin with subsequent neutralization and hydrolysis with an alkaline, the mixture of sulphonic acid and sulphonate isomers is obtained [1]. An important property of alkensulphonates is their high biodegradability in nature.

Petroleum sulphonates are mainly produced by direct sulfonation of petroleum products (distillate and residual oils) subsequent with purification and neutralization of the resulting sulphonic acid mixtures. The composition of the sulphonate depends on the hydrocarbon feedstock and the method of sulfonation.

It should be noted that alkaline earth metal salts of amines are of considerable importance among the oil-soluble petroleum sulphonates [2; 3]. World production of alkyl benzene (sulphonate) was 2580 thousand ton (1987). However, more than 80% of which is consumed for the production of domestic detergents. Besides, the amount of sulphanole consumption increases in the Republic each year.

Objects and methods. The objects of research are unsaturated aliphatic mixture of sulfonation waste and low-molecular polyethylene and their sulfonation. The methods of research is the pH-metry, viscometry, comparative analysis methods.

Results and discussion. It is known that sulfonation of unsaturated aliphatic compounds, depending on the reaction conditions, sulpho groups is bonded on the double bond or replaces a hydrogen atom one of the carbon atoms forming the double bond. The latter is actually sulfonation process. As a result of the action of chlorine sulphonic acid at a temperature of about 0 °C alkene sulphonic acid is formed on higher olefins. Alkenes easily sulfonated with oleum according to the following overall reaction:

$$RCH{=}CH_2 + H_2SO_4 = RCH(CH_3)OSO_3H\ (R{=}C_{12} - C_{20})$$

Technical sulphanole is to a series of anionic surfactants, used in oil and gas production to increase oil, gas and condensate return of bed by processing bottom-hole zones.

We first synthesized technical sulphanole and developed its technology based on local chemical intermediate product. In the technology housing of Institute of General and Inorganic Chemistry under Academy of Sciences of the Republic of Uzbekistan a pilot plant producing sulphanole has been developed (Figure 1).

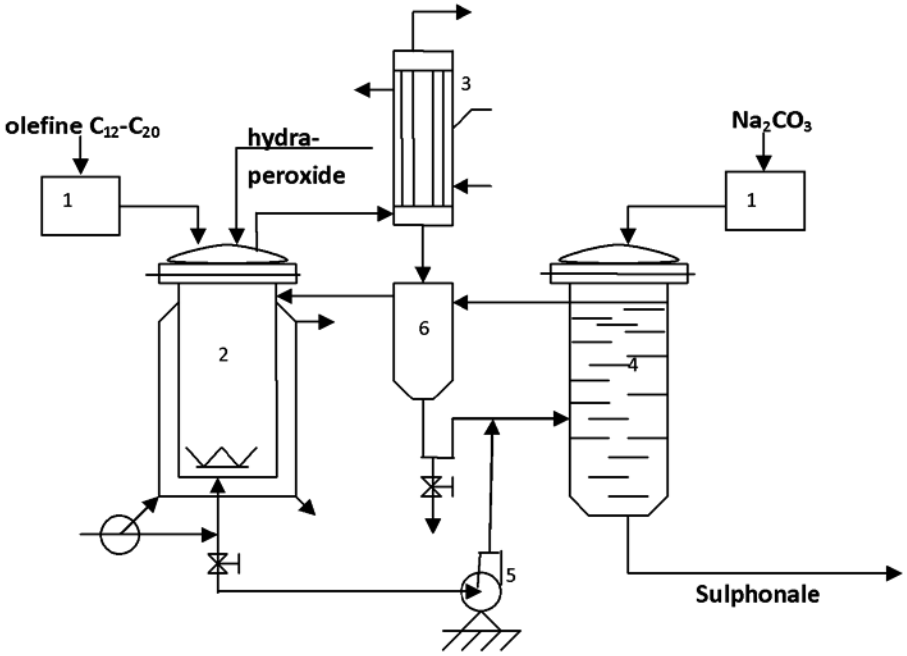

Fig. 1. Flow sheet of obtaining technical sulphanole: 1. The hopper; 2. Sulfurator; 3. Refrigerator; 4. Neutralizer; 5. Pump; 6. Separator

We have developed a method of synthesis sulphanole (Table 1) by sulfonation fractions of low-molecular polyethylene subsequent by neutralization (with $Na_2CO_3 * 10H_2O$, Na_2CO_3 and urea).

Table 1. – Data on synthesis sulphanole

№	Waste composition isolated from LMP	Molar ratio of reagents (mole): LMP sulfonating agent: additives	Sulfonating agent	Reaction tempe-rature (°C)	Reaction duration (hour)	Yield (%)
1	*2*	*3*	*4*	*5*	*6*	*7*
1	The first fraction	10:1:0.01	Oleum (40%)	–5–0	6	24
2	The second fraction	10:1:0.01	Oleum (40%)	–5–0	6	51
			H_2SO_4 (98%)	–5–0	6	39

1	*2*	*3*	*4*	*5*	*6*	*7*
3	The third fraction	10:1:0.01	H_2SO_4 (98%)	–5–0	6	61
			Oleum (40%)	–5–0	6	78
			Oleum (40%)	–5–0	5	73
4	The third fraction	10:1:0.01	H_2SO_4 (98%)	0–5	6	24
			Oleum (40%)	0–5	6	55
			Oleum (40%)	–10–(–5)	5	78
5		10:2:0.01	Oleum (40%)	–5–0	5	78

As it is seen from the data in Table 1, a result of sulphanole synthesis from waste of LMP by sulfonation 40% of oleum separated from fraction 3, the weight ratio of substances 10: 1: 0.01, temperature –5–0 °C, the reaction continuing time 6 hours was the highest yield.

Sulphanole synthesized readily dissolved in water and reveals anion-active properties; the surface tension of its is 1.5% aqueous solution $\sigma_{125}^{20} = 41.0 - 42.5\,\text{dun/cm}^2$, creates a volume-stable foam ($h_{0.125\%-100\,\text{ml}}^{20} = 7.0 - 8.4$ cm) and a hydrophilic-lipophobic balance of sulphanole obtained does not exceed 0.6. Thus, sulphanole obtained is a light brown liquid. The reaction duration is 6 hours temperature: –5–0 °C. Laboratory test results of sulphanole (OS series) for the preparation of facilitated drilling fluids are presented in Tables 2 and 3. To prepare the drilling fluids two types clay powder — bentonite: PBG brand and brand PBMB were used.

Table 2. – Composition and technological properties of the drilling solutions (bentonite grade PBG)

	Drilling solution's composition	**Process-dependent parameters**				
		Density, g/cm³	**Conditional viscosity, sec.**	**Water yeild, cm³/30 min.**	**Crust, mm.**	**pH**
1	Initial solution	1.07	33	6	0.4	10
2	Initial solution + 3.5% sulphanole OS-2	0.75	80	6	0.4	11
3	Initial solution + 3.5% sulphanole OS-3	0.80	38	6	0.4	10
4	Initial solution + 3.5% sulphanole OS-7	0.80	42	4	0.3	11
5	Initial solution + 7% sulphanole OS-7	0.70	42	4	0.3	11
6	Initial solution + 3.5% sulphanole OS-8	0.70	70	4	0.3	11

As it is seen from Table 2 sulphanole OS-8 and OS reduced density drilling fluid to 0.7 g/cm³, while increasing its conventional viscosity from 33 to 70 and 80 sec., i. e. adding sulphanole observed improvement of some physical and chemical characteristics of the drilling fluid.

Table 3. – Composition and technological properties of the drilling solutions (bentonite grade PBMB)

	Drilling solution's composition	**Process-dependent parameters**				
		Density, g/cm³	**Conditional viscosity, sec.**	**Water yeild, cm³/30 min.**	**Crust, mm.**	**pH**
1	Initial solution	1.09	36	6	0.4	10
2	Initial solution + 3.5% sulphanole OS-2	0.75	53	6	0.4	11
3	Initial solution + 3.5% sulphanole OS-3	0.76	37	6	0.4	10
4	Initial solution + 3.5% OS-3 + 50 g of clay PBMB	0.90	48	6	0.4	11
5	Initial solution + 3.5% sulphanole OS-7	0.75	47	5	0.3	11
6	Initial solution + 7% sulphanole OS-7	0.70	47	5	0.3	11
7	Initial solution + 3.5% sulphanole OS-8	0.70	56	5	0.3	11

On the basis of laboratory test all the samples sulphanole obtained reduced the density of drilling fluids, which are listed in the above tables. A simple way to obtain technical sulphanole and low cost allow to efficiently introduce it in production, as well as to use it in drilling wells for oil and gas.

Conclusion

Thus, the import-substituting sulphanole has been synthesized based on local raw materials and intermediates. The optimal conditions for the synthesis have been defined as following: reaction temperature was studied, initial substance and reaction time and the influence of the sulfonating agent to yield.

References:

1. Shexter Yu. N., Kreyn S.E., Poverxnostno-aktivnie veshestva iz neftyanogo sirya. M:., 1971, 112–116 p.
2. Shexter Yu.N., Kreyn S.E., Teterina L. N., Maslorastvorimie poverxnostno-aktivnie veshestva. M., 1978, 224–226 p.
3. Poverxnostno-aktivnie veshestva. Spravochnik. pod red. A. A. Abramzona i G. M. Gayevogo. L. Ximiya, 1979. 376 p.

DOI: http://dx.doi.org/10.20534/AJT-16-9.10-79-82

Daminova Shahlo Sharipovna,
Tashkent Chemical Technological Institute,
Department of "Technology of silicate materials and rare precious metals",
Scientific Researcher
E-mail: daminova-sh@mail.ru

Kadirova Zukhra Chingizovna,
Tashkent Chemical Technological Institute, Center of Excellence,
Dr. Engineering, PhD in Chemistry,
E-mail: zuhra-kadirova@yahoo.com

Sharipov Kasan Turabovich,
Tashkent Chemical Technological Institute,
Department of "Technology of silicate materials and rare precious metals",
Professor
E-mail: sharkhas@yandex.ru

Investigation of copper, nickel (II) and iron (III) ions sorption on sir by using FTIR and DRS methods

Abstract: The solvent impregnated resins (SIRs) based on Porolas resin impregnated with diisipropyldithiophosphoric acid were studied by Fourier transform infrared (FTIR) and electronic diffuse reflectance spectroscopic (DRS) methods. Physical sorption of diisopropyldithiophosphoric acid on macroporous Porolas resin in impregnation and sorption of metal ions on SIR were confirmed. The prepared SIR can be very useful for extraction of metals from hydrometallurgical solutions.

Keywords: Solvent impregnated resin, dialkyldithiophosphoric acid, infrared spectroscopy, electronic spectroscopy.

1. Introduction

Organophosphorus compounds are well known agents for impregnation of polymeric sorbents used for sorption of metal ions [1, 174–175]. Literature describes liquid phase sorption of Pb, Cd, Cu and Hg (II) ions by dialkyldithiophosphorous acids without detailed investigation of solid phase and effects of solid phase in solvent impregnated resins (SIR) [2, 1641]. The solvent impregnated resins (SIR) can be modeled as a "liquid complexing agent dispersed homogeneously in a solid polymeric medium" [3, 353]. The impregnated should behave as in the liquid state but exhibit strong affinity to the matrix. It is known different acidic organophosphorus extractants: di (2-ethylhexyl)phosphoric acid (DEHPA) [4, 126] used for extraction of Zn, Cu and Cd (II) [5, 131], V (IV) [6, 109], La and Ce (III) [7, 511]; di (2-ethylhexyl) dithiophosphoric acid (DEHTPA) [8, 201] applied for extraction of Pd (II) [9, 545], Cu [10, 149].

The aim of work is study Porolas resin impregnated by diisopropyldithiophosphoric acid $(i\text{-}PrO)_2PS_2H$ by Fourier transform infrared (FTIR) and electronic diffuse reflectance spectroscopic (DRS) methods. The FTIR method permits to describe a solid phase after impregnation while the diffuse reflectance spectroscopy (DRS) method permits to trace changing concentration of metal ions in the solid phase. Therefore, both methods are suitable for possible application to study sorption of Cu, Ni (II) and Fe (III) on the $(i\text{-}PrO)_2PS_2H$ solvent impregnated resin.

2. Experimental

Porolas is a commercial resin (Ukraine) with a macroporous structure and styrene-divinylobenzene skeleton. Diisopropyldithiophosphoric acid was purchased from Sigma Aldrich GmbH. Before impregnation Porolas was rinsed with methanol and then with water to remove impurities. 10 g of potassium diisopropyldithiophosphate dissolved in 250 cm^3 of methanol was added to 10 g of Porolas, all ingredients were shaken for 3 h at 293 K. After impregnation, SIR was rinsed by deionized water. The concentration of diisopropyldithiophosphoric acid in Porolas was determined by using gravimetric method. The content of $(i\text{-}PrO_2PS)_2H$ in Porolas was ~ 50%. The prepared SIR was used in further metal sorption studies in batch reactor. The metal ions contents were analyzed by using atomic absorption spectroscopy after sorption from 0.05–0.02–0.04 mol/l solutions.

The FTIR absorption spectra recorded by means IRAffinity-1 spectrometer (Shimadzu, Japan) over the 4000–400 cm^{-1} range at the resolution of 4 cm^{-1} in KBr pellet. The DRS spectra were measured by using the UV-2600 spectrometer (Shimadzu, Japan) equipped with a diffuse reflectance attachment.

3. Results and discussion

The Porolas resins (analogues of XAD-2, XAD-4 Amberlite resins) are macroporous (macroreticular) hydrophobic syrene-divinylbenzene copolymer resins, having a rigid three-dimensional structure suitable to incorporate large amounts of extractants due to the high specific surface area (~900 m^2/g, average pore diameter of 4~9 nm, and a pore volume of 1.1 cm^3/g), high mechanical strength, and rather low solvent swelling during the impregnation process.

The FTIR spectra of Porolas were recorded before and after impregnation to estimate the efficiency of the applied procedure. The broad band with the maximum located at 3430 cm^{-1} (Fig. 1) can be attributed to the stretching vibrations of adsorbed water. The bands of carbon–hydrogen strong stretching vibrations from alkyl groups of $(i\text{-}PrO)_2PS_2H$ were observed in the range 2900–2800 cm^{-1}. This part of spectrum is very similar to that for free diisopropyldithiophosphate, and gives an undeniable proof that the surface of resins is modified after the impregnation. The absence of SH vibration bands at 2550–2600 cm^{-1} confirmed impregnant anion state. The region of spectra between 1200 and 400 cm^{-1} is the most significant and informative because signals at 677 and 559 cm^{-1} are related to PSS ions. The signal at 559 is shifted to 548 cm^{-1} after sorption and it can be interpreted that metal ions are coordinated (Table 1).

Table 1. – Spectral data of Porolas impregnated with $(i\text{-}PrO)_2PS_2H$

Sample	FTIR spectra				DRS spectra
	n	Δ	n	Δ	
$(i\text{-}PrO)_2PS_2K$	679		587, 560		226
$(i\text{-}Pro)_2PS_2K$ — Porolas	677	2	559	28	226
$(i\text{-}PrO)_2PS_2$ — Porolas+ Cu^{2+}	710	31	548	39	255 (226)*, 421 (416)*
$(i\text{-}PrO)_2PS_2$ — Porolas+ Fe^{3+}	–	–	–	–	259, 426
$(i\text{-}PrO)_2PS_2$ — Porolas+ Ni^{2+}	–	–	–	–	262, 325, 528, 702

* – *spectra in ethanol solution*

The DRS spectra of Porolas impregnated with diisopropyldithiophosphoric acid after sorption of metal ions at different concentration in the range 1200–400 nm are shown in Fig.2. The DRS was used in order to improve the results obtained by using the FTIR method. The DRS method permits to trace changing of metal ions in time during experiment.

In Figure 2 the signal at 255 nm is related to dithiophosphoric acid ions in the solid phase of SIR from delocalized P=S double bond. The shift signal of dialkyldithiophosphate in solution from 226 nm to 255 nm in solid states confirmed physical interaction between resin and impregnated ligand. The reflectance spectra of the solid Ni complexes exhibit two broad bands in the visible

region (Table 1). The reflectance spectra of the solid Fe, Cu complexes exhibit one broad band in the visible region (Figure 2, Table 1) based sulphur to metal charge-transfer transition. The band profile look similar for both Fe, Cu complexes, but band maxima are observed to be sensitive to Cu ions.

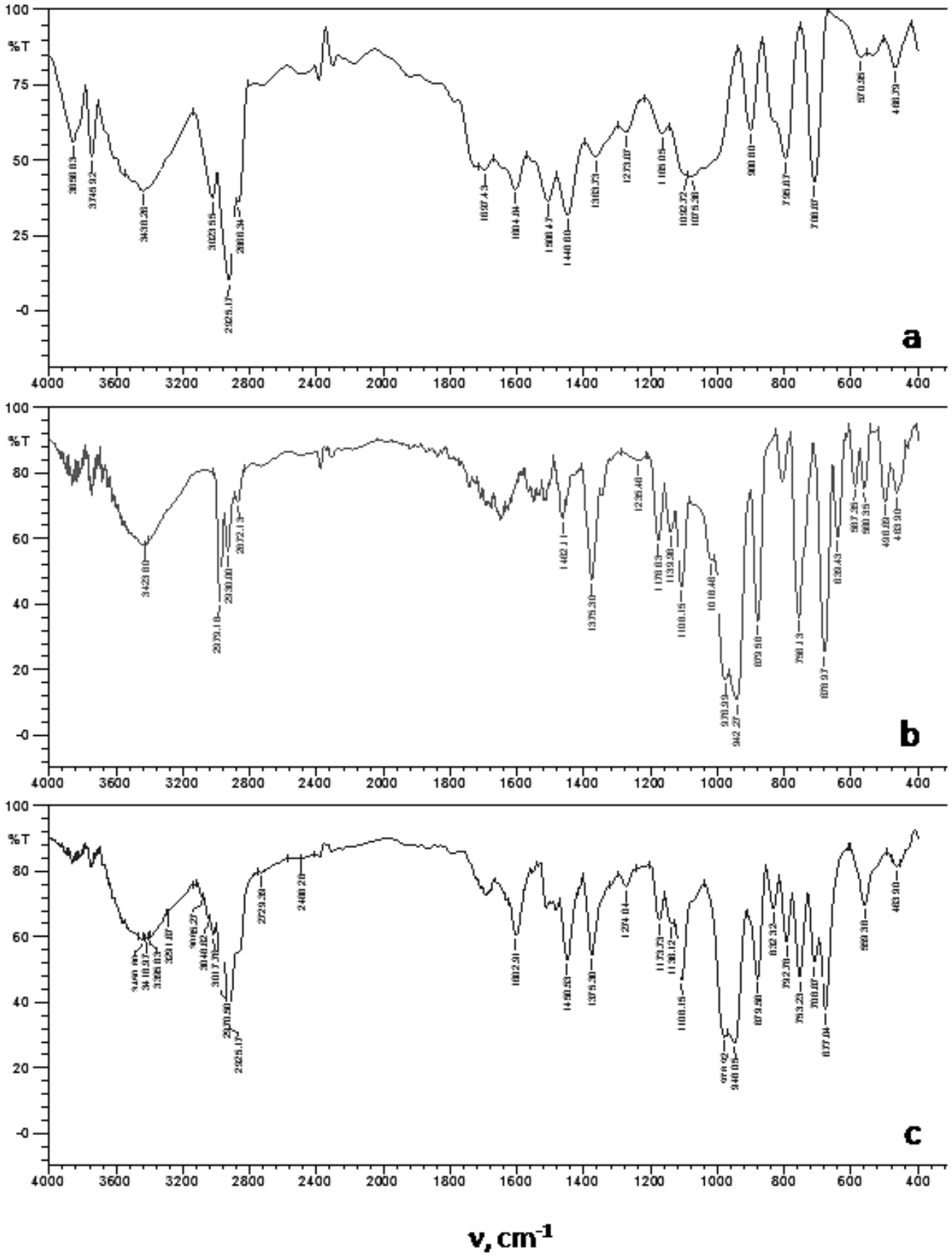

Figure 1. The FTIR spectra of Porolas (a) and $(i\text{-}PrO)_2PS)_2K$ (b) SIR (c)

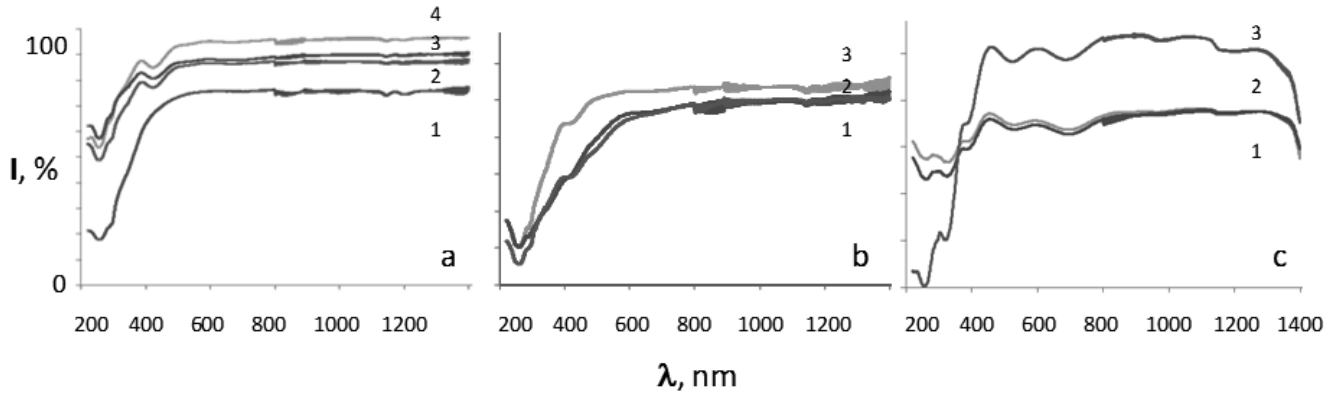

Figure 2. The DRS spectra of Porolas impregnated with $(i\text{-PrO})_2PS)_2H$ after sorption of metal ions measured after 24 h (a — Cu sorption (1–0.05, 2–0.1, 3–0.25. 4–0.4 mol/l); b — Fe sorption (1–0.05, 2–0.25. 3–0.4 mol/l); c — Ni sorption (1–0.05, 2–0.25. 3–0.4 mol/l))

4. Conclusion

Both FTIR and DRS methods are very useful in the investigations of SIRs based on Porolas resin and diisopropyldithiophosphoric acid. The FTIR spectra provide information about physical sorption of diisopropyldithiophosphoric acid on macroporous Porolas in impregnation and sorption of metal ions on SIR, while the DRS electronic spectra give the data about sorption of metal ions on the resin.

References:

1. Van Nguyen N., Lee J. C., Jeong J., Pandey B. D. Enhancing the adsorption of chromium (VI) from the acidic chloride media using solvent impregnated resin (SIR)//Chemical engineering journal. – 2013. – T. 219. – C. 174–182.
2. Ying X., Fang Z. Experimental research on heavy metal wastewater treatment with dipropyl dithiophosphate//Journal of hazardous materials. – 2006. – T. 137. – №. 3. – C. 1636–1642.
3. Juang R. S. Preparation, properties and sorption behavior of impregnated resins containing acidic organophosphorus extractants//Proc natl sci counc repub china part a phys sci eng. – 1999. – T. 23. – №. 3. – C. 353–364.
4. Akita S., Maeda T., Takeuchi H. Metal Sorption Characteristics of a Macromolecular Resin Containing D2EHPA//Journal of chemical engineering of Japan. – 1994. – T. 27. – №. 1. – C. 126–129.
5. Cortina J. L., Miralles N., Aguilar M., Sastre A. M. Extraction studies of Zn (II), Cu (II) and Cd (II) with impregnated and Levextrel resins containing di (2-ethylhexyl) phosphoric acid (Lewatit 1026 Oc)//Hydrometallurgy. – 1994. – T. 36. – №. 2. – C. 131–142.
6. Liang L., Bao S., Zhang Y., Tang Y. Separation and recovery of V (IV) from sulfuric acid solutions containing Fe (III) and Al (III) using bis (2-ethylhexyl) phosphoric acid impregnated resin//Chemical Engineering Research and Design. – 2016. – T. 111. – C. 109–116.
7. Nishihama S., Kohata K., Yoshizuka, K. Separation of lanthanum and cerium using a coated solvent-impregnated resin//Separation and Purification Technology. – 2013. – T. 118. – C. 511–518.
8. Jerabek K., Hankova L., Strikovsky A. G., Warshawsky A. Solvent impregnated resins: relation between impregnation process and polymer support morphology I. Di- (2-ethylhexyl) dithiophosphoric acid//Reactive and Functional Polymers. – 1996. – T. 28. – №. 2. – C. 201–207.
9. Rovira M., Hurtado L., Cortina J. L., Arnaldos J., Sastre A. M. Impregnated resins containing di (2-ethylhexyl) thiophosphoric acid for extraction of palladium (II). I. Preparation and study of the retention and distribution of the extractant on the resin//Solvent extraction and ion exchange. – 1998. – T. 16. – №. 2. – C. 545–564.
10. Strikovsky A. G., Jerabek K., Cortina J. L., Sastre A. M., Warshawsky A. Solvent impregnated resin (SIR) containing dialkyl dithiophosphoric acid on Amberlite XAD-2: extraction of copper and comparison to the liquid-liquid extraction//Reactive and Functional Polymers. – 1996. – T. 28. – №. 2. – C. 149–158.

DOI: http://dx.doi.org/10.20534/AJT-16-9.10-83-90

Soliev Lutfullo,
Department of General and Inorganic Chemistry,
Faculty of Chemistry, Tajik State Pedagogical University,
Dushanbe, Tajikistan

Jumaev Maruf,
Department of General and Inorganic Chemistry,
Faculty of Chemistry, Tajik State Pedagogical University,
Dushanbe, Tajikistan

Tursunbadalov Sherali,
Department of Chemistry, Faculty of Natural
and Applied Sciences, Nigerian Turkish Nile University,
Plot 681, Cadastral Zone C-OO, Research & Institution Area,
Abuja, Nigeria,
E-mail: sheerchem@gmail.com

Usmonov Mahmadsalim, Department of General and Inorganic
Chemistry, Faculty of Chemistry,
Tajik State Pedagogical University,
Dushanbe, Tajikistan

Avloev Shohiddin,
Department of General and Inorganic Chemistry,
Faculty of Chemistry, Tajik State Pedagogical University,
Dushanbe, Tajikistan

Structure of solubility diagram of the quaternary Na, Ca//So_4, Co_3-H_2O water-salt system at 25°C

Abstract: The results of the solubility investigation in the quaternary Na, Ca//SO_4, CO_3-H_2O water salt system along with its solubility diagram at 25°C are considered in this work. There are 4 invariant points, 8 monovariant curves and 6 divariant fields which are saturated with 3, 2 and 1 solid phases and their relevant equilibrium liquid phases respectively. The crystallization field of the calcite $CaCO_3$ covers most of the part of solubility diagram of investigated quaternary water-salt Na, Ca//SO_4, CO_3-H_2O system at 25°C, which signifies the low solubility of the latter salt in the given conditions.

Keyword: solubility, quaternary system, equilibrium, XRD.

The considered quaternary water-salt Na, Ca//SO_4, CO_3-H_2O system is a part of more complex six-component Na, Ca//SO_4, CO_3, HCO_3, F-H_2O system whose phase equilibria knowledge determine the conditions of exploitation of liquid wastes released from the aluminum production. Wastewater outlets of regeneration of cryolite in aluminum smelters contain fluorides, carbonates, bicarbonates and sulfates of sodium and calcium [1–4]. The crystallization and dissolution processes of salts in aqueous solutions of these wastes are determined by the laws of phase equilibria in the six-component Na, Ca//SO_4, CO_3, HCO_3, F-H_2O system and its constituent five — and four-component subsystems.

In the present work; the results of investigation of quaternary Na, Ca//SO_4, CO_3-H_2O system at 25°C by means of solubility method are deliberated with the purpose of establishing the concentration parameters at the geometrical figures of the system along with determining the ratio of the individual equilibrium crystallization fields of existing solid phases in the system.

Literature review shows that; the title quaternary system has not been investigated on the overall composition that is with the involvement of all its four components

simultaneously at 25°C. There are data on some more complex [5–10] systems at 25°C each of which also includes the quaternary Na, Ca//SO_4, CO_3-H_2O system as a subsystem. But those data are unlikely employable on the system under our consideration; as the phase equilibria and a closed phase equilibria diagram is required in order to fully exploit the system ingredients.

The mineral solubilities to high ionic strengths in the multicomponent Na-K-Mg-Ca-H-Cl-SO_4-OH-HCO_3-CO_3-CO_2-H_2O system which also involves the Na, Ca//SO_4, CO_3-H_2O quaternary system as well have been predicted by Charles E. Harvie et al at 25 °C [9]. Unfortunately, neither the phase equilibria diagram has been deliberated thereby nor has the solubility diagram in the considered quaternary Na, Ca//SO_4, CO_3-H_2O system at 25° been presented by the authors.

A chemical equilibrium model of solution behavior and solubility in the H-Na-K-Ca-OH-Cl-HSO_4-SO_4-H_2O system to high concentration and temperatures are published by Christomir Christov and Nancy Moller [10]. Although the three; Na^+, Ca^{2+} and SO_4^{2-}components of our considered quaternary system exist in the this multicomponent H-Na-K-Ca-OH-Cl-HSO_4-SO_4-H_2O system and as the third CO_3^{2-}component is missing; it is already insufficient data for the determination of the phase equilibria in the quaternary water-salt Na, Ca//SO_4, CO_3-H_2O system and do not enable one to construct its solubility diagram at 25°C.

As it is evident; the title quaternary Na, Ca//SO_4, CO_3-H_2O system has not been tackled as an independent system in the latter two literature data [9,10]; they are far from enabling one the construction of the closed phase equilibria diagram of the system at 25°C and presenting the complete phase equilibria data at the geometrical figures of the diagram.

The two available data on the entire quaternary system where all its four Na^+, $Ca2^+$, $SO_4^{2-}$and CO_3^{2-}components are dealt as a single set were published in J. Phys. Chem., 11, 415, (1907) and Z. Anorg. Chem., 71, 206, (1911) by F. K. Cameron et al. [11, 13] and W. Herz respectively [12, 13]. The unfortunate case of these works is that; the authors have characterized the system with the presence of the just $CaCO_3$ as the single solid phase which crystallizes in the system at 25°C. As it is dictated by the third basic principle of physicochemical analysis [14] along with the translation method [15; 16]; the geometrical figures of the n-component subsystems are transformed into a unit higher versions; that is the points to curves, the curves to fields and the fields to volumes etc. of the global system and translated to the (n+1) – component overall composition. Hence the title quaternary system cannot be characterized with the presence of the only one solid phase when its entire composition is considered. Briefly, according to the founder of third fundamental "compatibility principle" of the physicochemical analysis — Goroshenko Ya. G.; all the solid phases which participate in the composition of the one component less subsystems are expected to take part in the structure of the global system which involves them. This criterion of the physicochemical analysis thus reveals the incompleteness of the latter [11; 12] works better.

The need for recourse on the ternary subsystems of the title quaternary system hence emerges hereby. Earlier the phase equilibria in the title system were investigated [17] by our team members and its schematic closed phase diagram was constructed by means of the translation method [15, 16]. The considered quaternary water-salt Na, Ca//SO_4, CO_3-H_2O system is composed of the following four; Na_2SO_4-$CaSO_4$-H_2O, Na_2 CO_3-$CaCO_3$–H_2O, Na_2SO_4-Na_2 CO_3-H_2 O, and $CaSO_4$-$CaCO_3$-H_2O ternary subsystems. The data on the latter ternary subsystems [18–22] of the considered quaternary system were used in order to fully predict the phase equilibria and construct schematic phase equilibria diagram for the considered quaternary water-salt Na, Ca//SO_4, CO_3 — H_2O system [17].

The system at 25°C has been characterized to involve 4 invariant points, 8 monovariant curves and 6 divariant fields which are saturated with 3, 2 and 1 equilibrium solid phases and relevant liquid phases respectively in latter work [17].

As we intend to determine the solubility at the previously predicted geometrical figures [17] and construct the comprehensive solubility diagram of the system in the present study; the experimental procedures have proceeded according to the solution saturation method [23] as follow below:

Initially, the composition of the saturated solutions at the ternary invariant points in; Na_2SO_4-$CaSO_4$-H_2O, Na_2 CO_3-$CaCO_3$-H_2O, Na_2SO_4-Na_2 CO_3-H_2 O and $CaSO_4$-$CaCO_3$-H_2O subsystems at 25^0 C of the investigated quaternary Na, Ca//SO_4, CO_3-H_2O system were prepared on the basis of the solubility data in literature [18–22]. There are the following six equilibrium solid phases: $Na_2SO_4 \cdot 10H_2O$ — mirabillite (Mb); $CaSO_4 \cdot 2H_2O$ — gypsum (Gp); $Na_2SO_4 \cdot CaSO_4$ — glauberite (Gb); $Na_2CO_3 \cdot CaCO_3 \cdot 5H_2O$ — geylussite (Gl); $CaCO_3$ — calcite (Cl) and $Na_2CO_3 \cdot 10H_2O$ — C·10 which crystallize in the quaternary Na, Ca//SO_4,

CO_3-H_2O system at 25°C. The following chemical reagents were used in the experiments: $Na_2SO_4 \cdot 10H_2O$ (chemically pure); $CaSO_4 \cdot 2H_2O$ (chemically pure); Na_2CO_3 (pure) $CaCO_3$ (pure).

Next, the simulated mixtures of the quaternary invariant points which generate according to the translation schemes [17] of the relevant ternary invariant points to the quaternary composition were stirred until the equilibrium states have been reached. The temperature was controlled in G-8 type ultratermostate. The mixtures were stirred by a magnetic stirrer PD — 09 during 50 –100 hours. The temperature was maintained within ± 0,10 °C using contact thermometer. The crystallization of the solid phases was observed through the "POLAM P-311" microscope. The equilibrium solid phases were photographed with a digital camera «SONY-DSC-S500». The equilibrium achievements were followed on the immutability of the phase compositions of precipitates. Separation of the liquid phase from the solid phases was carried out by a vacuum pump through ashless (blue ribbon) filter paper on a Buchner funnel. The precipitates which are obtained by the filtration were washed with 96% ethanol and dried at 120°C. The chemical analysis of the product was carried out by the known methods [24–26].

The obtained results from the crystal optical analyses [27] of the equilibrium solid phases (photomicrographs) are shown in Figure 1.

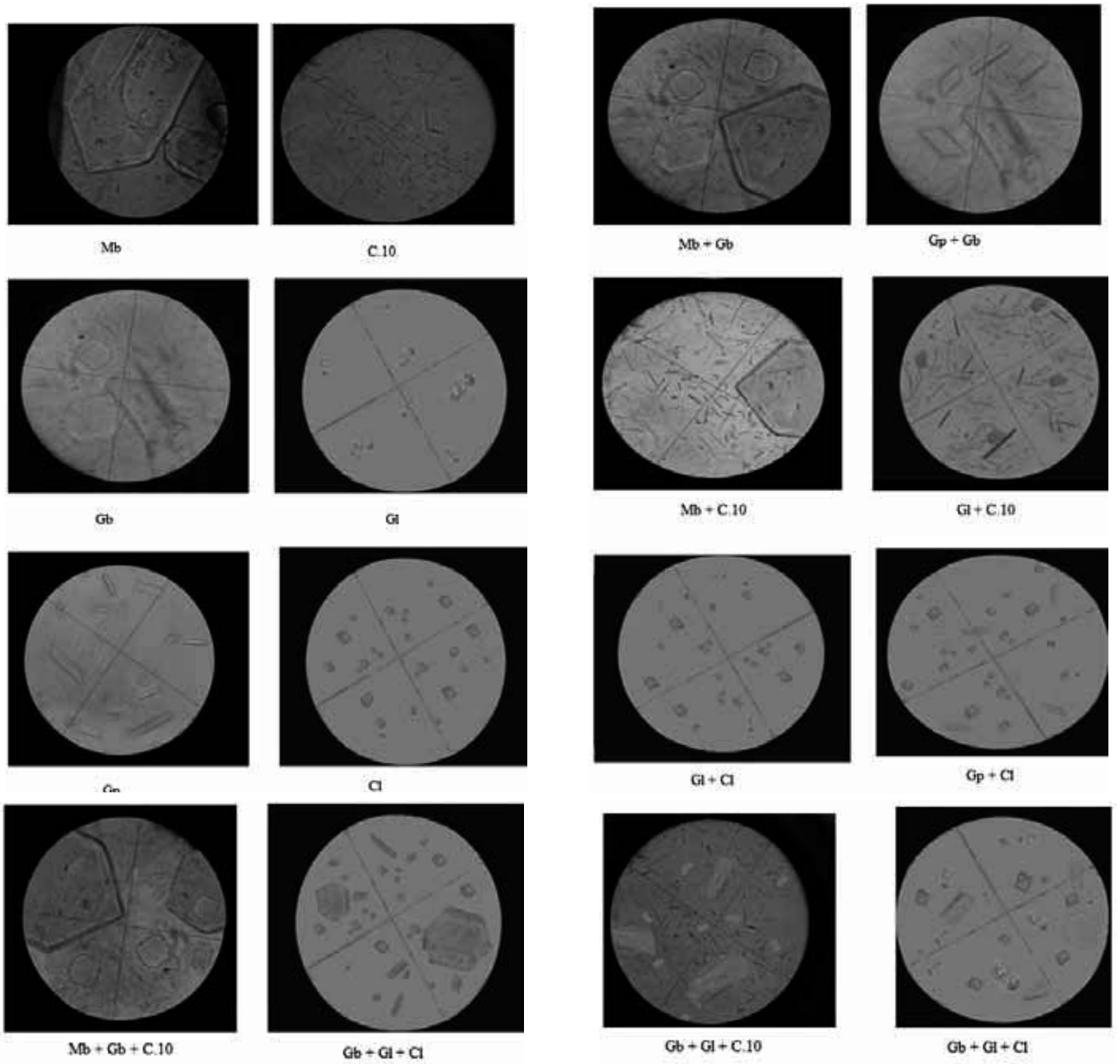

Figure1.The photomicrographs of the equilibrium solid phases in the quaternary Na, Ca//SO_4, CO_3-H_2O system at 25°C.

The results of the chemical analysis of the saturated solutions are shown in Table 1.

Table 1. – Solubility at knot (invariant) points of the quaternary Na, Ca//SO_4, CO_3-H_2O system at 25°C

Point No	Composition of the liquid phase, W.%					Phase composition of precipitates
	Na_2SO_4	$CaSO_4$	Na_2CO_3	$CaCO_3$	H_2O	
e_1	21.9	–	–	–	78.1	Mb
e_2	–	0.209	–	–	99.791	Gp
e_3	–	–	22.95	–	77.05	C·10
e_4	–	–	–	0.0048	99.9952	Cl
E_1^3	21.75	0.197	–	–	78.05	Mb + Gp
E_2^3	25.78	0.188	–	–	74.032	Gp + Gb
E_3^3	16.40	–	18.40	–	65.30	Mb + C·10
E_4^3	–	–	5.649	0.00349	94.347	C·10 + Gl
E_5^3	–	–	4.5	0.0024	95.497	Gl + Cl
E_6^3	–	0.213	–	0.0048	99.782	Gp + Cl
E_1^4	14.2	0.273	19.6	–	65.927	Mb + C·10 + Gb
E_2^4	–	0.408	18.55	0.00547	80.987	Gp + Gb + Cl
E_3^4	12.52	–	19.45	0.00521	64.977	C·10 + Gl + Gb
E_4^4	–	0.328	20.7	0.00431	78.928	Cl + Gb + Gl

The solubility diagrams of the quaternary Na, Ca//SO_4, CO_3-H_2O system at 25°C, which are shown in Figure 2 are obtained based on the obtained data.

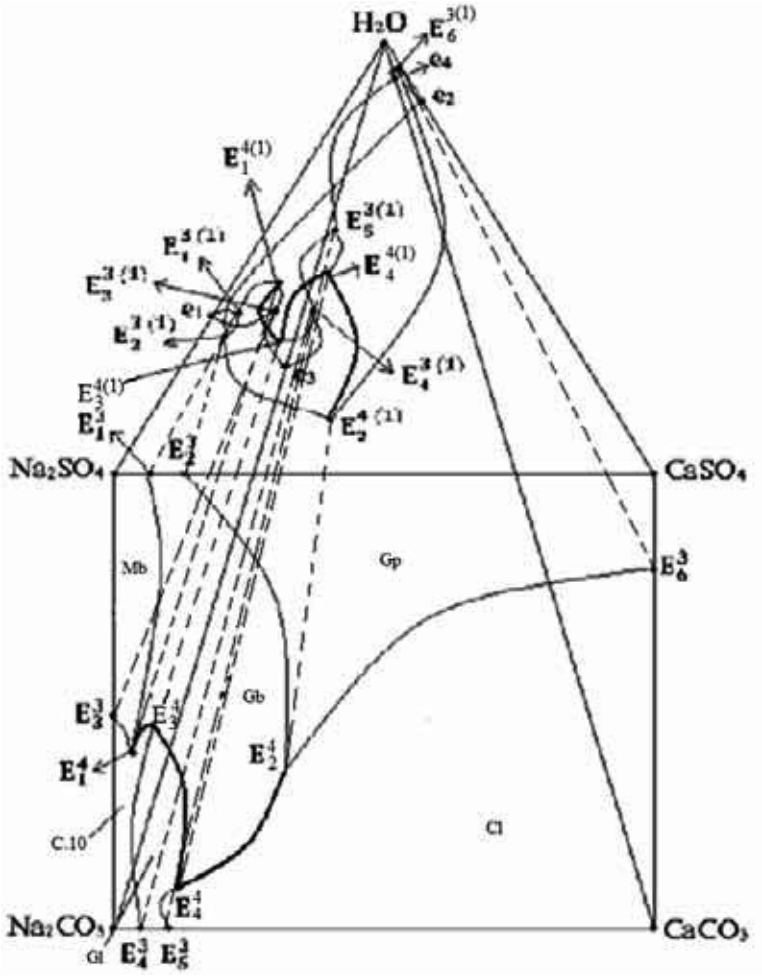

Figure 2 (a). Solubility diagram of the quaternary Na, Ca//SO_4, CO_3-H_2O system at 25°C

The locations of the ternary (E_n^3) and quaternary (E_n^4) invariant points in the diagrams where the "*n*" denotes the serial number of the relevant point are set by means of the centroid method [14].

Figure 2 (a) and Figure 2 (b) show the "comprehensive" and the "dry-salt" parts of the solubility diagram of the quaternary Na, Ca//SO_4, CO_3-H_2O system respectively, where the reciprocal locations of the invariant points and the monovariant curves along with the relative areas of the crystallization fields of equilibrium solid phases are reflected.

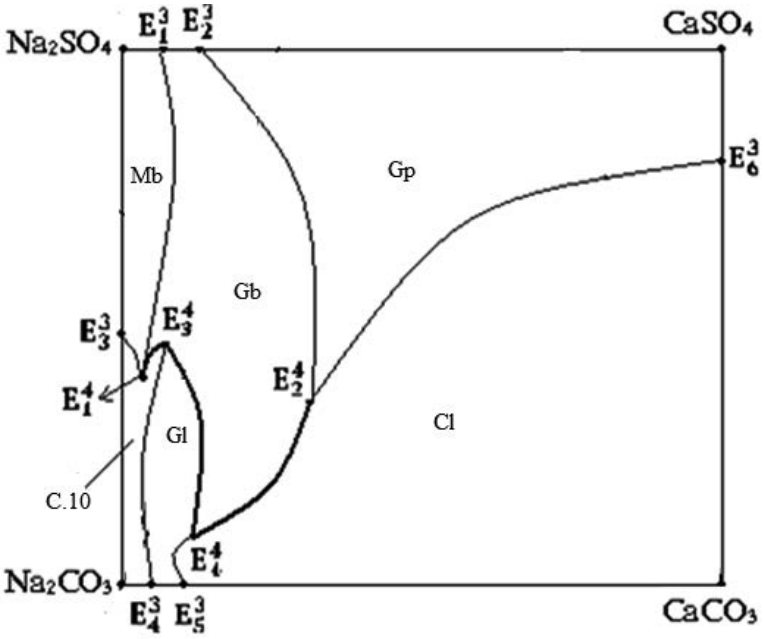

Figure 2 (b). Dry-salt part of solubility diagram of quaternary Na, Ca//SO_4, CO_3-H_2O system at 25°C

As is it shown in the Figure 2; the crystallization field of the calcite $CaCO_3$ covers the significant part of the diagram which signifies the low solubility of the latter salt in the given conditions. The compositions of the geometrical figures (fields, curves, points) of the diagram in Figure 2 are described in Table 2.

Table 2. — Composition of geometric figures in Figure 2

Notation of geometrical figures	**Composition**
1	***2***
e_1	Solubility of Na_2SO_4 phase in water
e_2	Solubility of $CaSO_4$ phase in water
e_3	Solubility of Na_2CO_3 phase in water
e_4	Solubility of $CaCO_3$ phase in water
E_1^3	The common crystallization point of $Na_2SO_4 \cdot 10H_2O$ and $Na_2SO_4 \cdot CaSO_4$ phases in the ternary Na_2SO_4–$CaSO_4$–H_2O system
E_2^3	The common crystallization point of $Na_2SO_4 \cdot CaSO_4$ and $CaSO_4 \cdot 2H_2O$ phases in the ternary Na_2SO_4–$CaSO_4$–H_2O system
E_3^3	The common crystallization point of $Na_2SO_4 \cdot 10H_2O$ and $Na_2CO_3 \cdot 10H_2O$ phases in the ternary Na_2SO_4– Na_2CO_3–H_2O system
E_4^3	The common crystallization point of $Na_2CO_3 \cdot 10H_2O$ and $Na_2CO_3 \cdot CaCO_3 \cdot 5H_2O$ phases in the ternary Na_2CO_3–$CaCO_3$–H_2O system
E_5^3	The common crystallization point of $Na_2CO_3 \cdot CaCO_3 \cdot 5H_2O$ and $CaCO_3$ phases in the ternary Na_2CO_3–$CaCO_3$–H_2O system
E_6^3	The common crystallization point of $CaSO_4 \cdot 2H_2O$ and $CaCO_3$ phases in the ternary $CaSO_4$–$CaCO_3$–H_2O system

1	*2*
E_1^4	The common crystallization point of $Na_2SO_4 \cdot 10H_2O$, $Na_2CO_3 \cdot 10H_2O$ and $Na_2SO_4 \cdot CaSO_4$ phases in the quaternary Na, Ca//SO_4, CO_3-H_2O system
E_2^4	The common crystallization point of $CaCO_3$, $CaSO_4 \cdot 2H_2O$ and $Na_2SO_4 \cdot CaSO_4$ phases in the quaternary Na, Ca//SO_4, CO_3-H_2O system
E_3^4	The common crystallization point of $Na_2SO_4 \cdot CaSO_4$, $Na_2CO_3 \cdot 10H_2O$ and $Na_2CO_3 \cdot CaCO_3 \cdot 5H_2O$ phases in quaternary Na, Ca//SO_4, CO_3-H_2O system
E_4^4	The common crystallization point of $Na_2SO_4 \cdot CaSO_4$, $CaCO_3$ and $Na_2CO_3 \cdot CaCO_3 \cdot 5H_2O$ phases in quaternary Na, Ca//SO_4, CO_3-H_2O system
$E_1^3\ E_1^4$	The common crystallization curve of $Na_2SO_4 \cdot 10H_2O$ and $Na_2SO_4 \cdot CaSO_4$ phases in the ternary Na_2SO_4–CaSO–H_2O system
$E_2^3\ E_2^4$	The common crystallization curve of $Na_2SO_4 \cdot CaSO_4$ and $CaSO_4 \cdot 2H_2O$ phases in the ternary Na_2SO_4–CaSO–H_2O system
$E_3^3\ E_1^4$	The common crystallization curve of $Na_2CO_3 \cdot 10H_2O$ and $Na_2SO_4 \cdot 10H_2O$ phases in the ternary Na_2SO_4–$CaCO_3$–H_2O system
$E_4^3\ E_3^4$	The common crystallization curve of $Na_2CO_3 \cdot 10H_2O$ and $Na_2CO_3 \cdot CaCO_3 \cdot 5H_2O$ in the ternary Na_2CO_3–$CaCO_3$–H_2O system
$E_5^3\ E_4^4$	The common crystallization curve of $CaCO_3$ and $Na_2CO_3 \cdot CaCO_3 \cdot 5H_2O$ phases in the ternary Na_2CO_3–$CaCO_3$–H_2O system
$E_6^3\ E_2^4$	The common crystallization curve of $CaCO_3$ and $CaSO_4 \cdot 2H_2O$ phases in the $CaSO_4$–$CaCO_3$–H_2O system
E_1^3 Na_2SO_4 $E_3^3E_1^4E_1^3$	Crystallization field of the $Na_2SO_4 \cdot 10H_2O$ phase
E_3^3 Na_2CO_3 $E_4^3E_3^4E_1^4E_3^3$	Crystallization field of the $Na_2CO_3 \cdot 10H_2O$ phase
$E_4^3E_3^4E_4^4E_5^3E_4^3$	Crystallization field of the $Na_2CO_3 \cdot CaCO_3 \cdot 5H_2O$ phase
$E_1^3E_1^4E_3^4E_4^4E_2^4E_2^3E_1^3$	Crystallization field of the $Na_2SO_4 \cdot CaSO_4$ phase
E_5^3 $CaCO_3$ $E_6^3E_2^4E_4^4E_5^3$	Crystallization field of $CaCO_3$
$E_2^3E_2^4E_6^3$ $CaSO_4$ E_2^3	Crystallization field of $CaSO_4 \cdot 2H_2O$

XRD analysis of the solid phased were performed on DRON-3 (filtered $CuKa_\alpha$ radiation Ni - filter) diffractometer. The shooting speed of diffractogram was kept at 30 ang.s/min. Diffractogramms have been prescribed by 0.1 degrees. The interplanar distance (dhkl), corresponding to the reflection angles (θ), were found in reference tables [28]. The obtained results are shown in Table 3.

Table 3. – The results of XRD patterns of solid phases in quaternary Na,Ca//SO4,CO3-H2O system at 25°C

q	**d,$^\circ_A$**	**θ, grad**	**d,$^\circ_A$**	**θ, grad**	**d,$^\circ_A$**	**θ, grad**	**d,$^\circ_A$**
1	*2*	*3*	*4*	*5*	*6*	*7*	*8*
10.2	4.3532	12.04	3.6956	15.06	2.9669	14.03	3.1798
10.04	4.4219	11.31	3.9308	14.12	3.1600	13.09	3.4038
8.21	5.3983	10.28	4.3197	12.04	3.6956	11.40	3.9001
8.13	5.4511	9.35	4.7450	11.29	3.9376	11.31	3.9308
7.11	6.2282	7.38	6.0015	10.29	4.3156	10.30	4.3114

1	*2*	*3*	*4*	*5*	*6*	*7*	*8*
6.33	6.992	7.16	6.1849	9.34	4.7500	9.33	4.7500
–	–	7.05	6.2803	8.37	5.2958	8.41	5.2708
–	–	5.39	8.207	7.11	6.2282	7.33	6.0422
–	–	–	–	–	–	7.17	6.1763

The presence of the corresponding solid phases in precipitates is determined by the existence of the diffraction patterns of the following; Mb, Gp, C.10, Cs, Gl and Gb most characteristic diffraction reflections [28, 29] in diffractogramms. The diffractograms of the individual equilibrium solid phases along with their mixtures at the; divariant fields, monovariant curves and invariant points are shown in Figure 3.

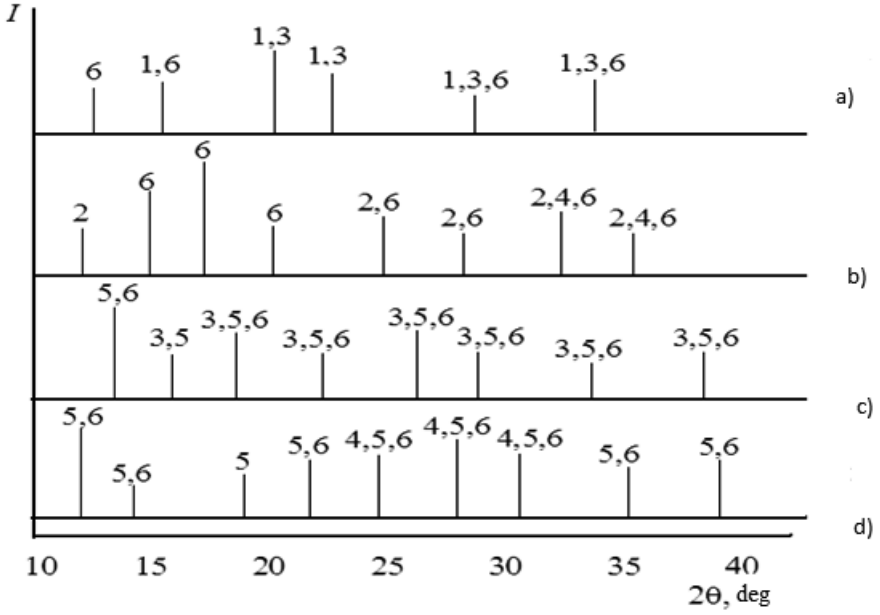

Figure 3.Schemes of the X-ray diffraction at equilibrium solid phases in quaternary Na, Ca//SO_4, CO_3-H_2O system at 25°C:

a) Mb + Gb + C.10 (point E_1^4); b) Gp + Gb + Cl (point E_2^4); c) C.10 + Gb + Gl (point E_3^4); d) Cl + Gb + Gl (point E_4^4); 1 – Mb, 2 – Gp, 3 – C·10, 4 – Cl, 5 – Gl, 6 – Gb

References:

1. Ermatov A. G., Mirsaidov U. M., Safiyev H. S., Azizov B. Recycling of wastes of aluminum smelters. Dushanbe, – 2006.
2. Mirsaidov U. M., Ismatdinov M. E., Safiyev H. S. Environmental issues and complex processing of raw materials and wastes of manufacturing. Dushanbe. Donish, – 1999.
3. Morozova V. A., Rzhechitsky E. P. Russian Journal of Applied Chemistry, – V. 49. – № 5. – 1976. – P. 1152.
4. Morozova V. A., Rzhechitsky E. P. Russian Journal of Inorganic Chemistry, – V.22, – № 3, – 1977, – P. 873.
5. Cameron F., Seidell A., Phys J. Chem., – 5, 653, – 1901.
6. Cameron F., Seidell A., Phys J. Chem., – 6, 53, – 1902.
7. Cameron F. K., Bell J. M., Robinson W. O., Phys J. Chem., – 11. – 416, – 1907.
8. Cameron F. K., Bell J. M., Robinson W. O., Phys J. Chem., – 11. 417, – 1907.
9. Harvie C. E., Moller N.and Weare J. H., Geochimica Cosmochimica Acta, – 48, – P. 723–751, – 1984.
10. Christomir Christov and Nancy Moller, Geochimica Cosmochimica Acta, – 68, – No.18, – 3717–3739, – 2004.
11. Cameron F. K., Bell J. M., Robinson W. O., Phys J. Chem., – 11. – 415, – 1907.
12. Herz W., Z.anorg. Chem., – 71, – 206, – 1911.
13. Handbook of experimental data on solubility of multicomponent water – salt systems. – Vol. II., Book 1&2. Saint Petersburg, Khimizdat, – 2004, – 1247 p.
14. Goroshchenko, Ya. G., The centroid method for imaging multicomponent systems. Naukova Dumka, – Kiev, – 1982.
15. Soliev L. Available from VINITI, – No. 8990-V87, – 1987.

16. Soliev L. Prediction of Marine-Type Multicomponent Systems' Phase Equilibria by Means of Translation Method. Dushanbe, Book 1 [in Russian], – 2000.
17. Soliev L., Usmonov M. Phase equilibria in the quaternary Na, Ca//SO_4, CO_3-H_2O system at 25°C. Proceedings of Tajik Branch of International Academy of Higher Education – TB IHEAS, – 2010, – № 1, – P. 77–81.
18. Caspari W. A., Chem J. Soc., – 125, – 2383–2385, – 1924.
19. Strakhov N. M., Zarubickaya A. N., Trudi Ins. Geo. Nauk AS USSR, – Vol 124, Geo. Series (№ 45), – 20, – 1951.
20. Hill A. E., Wills J. H., J. Am. Chem. Soc., – 60, – 1650–1653, – 1938.
21. Bury C., Redd R., Chem.Soc. J., – 1161, – 1933.
22. Handbook of experimental data on solubility of multicomponent water – salt systems. – Vol. 1, Book 1&2. Saint Petersburg, Khimizdat, – 2003, – 1151 p.
23. Goroshchenko Y. G., Soliev L., Gornikova Y. I. Ukrainian Journal of Chemistry. – 1987, – Vol. 53, – № 6, – P. 568.
24. Kreshkov A. P. Fundamentals of Analytical Chemistry, Saint Petersburg, Chemistry, – 1970, – Vol. 2, – 456 p.
25. Analysis of the mineral raw materials (under the general editorship of Knipovich Yu. N., Morachevsky Yu. V.). Goskhimizdat, Saint Petersburg, – 1959, –947 p.
26. Reznikov A. A., Mulikovskaya E. P., Sokolov I.Yu. Analytical methods of natural waters. Nedra, – Moscow, – 1970, – 488 p.
27. Tatarskiy V. B., Crystal optical and immersion methods of analyzing of substances. Saint Petersburg, Saint Petersburg State University. – 1948, – 268 p.
28. Giller Ya. L. Interplanar spacing tables. – Vol.2. Nedra, – 1966.
29. Mikheev V. I., Roentgenometric determinant of minerals. – Moscow, Gosgeoltekhizdat, – 1975, – 478 p.

DOI: http://dx.doi.org/10.20534/AJT-16-90-95

Nazirova Raxnamo Muxtarovna,
Junior researcher scientist,
Institute of General and Inorganic Chemistry
of the Academy of Sciences of the Republic of Uzbekistan
Tashkent, Uzbekistan

Tadjiev Sayfuddin Mukhtarovich,
PhD in chemistry science,
chief of "Complex fertilizer" laboratory,
Institute of General and Inorganic Chemistry
of the Academy of Sciences of the Republic of Uzbekistan
Tashkent, Uzbekistan
E-mail: raxnamoxon@mail.ru

Tukhtayev Saydiaxral,
Doctor of Science, academician,
Institute of General and Inorganic Chemistry
of the Academy of Sciences of the Republic of Uzbekistan
Tashkent, Uzbekistan

Phosphorus-potassium and nitrogen-phosphorus-potassium fertilizer based on washed and dried concentrate from central Kyzylkum phosphorite

Abstract: In this article the findings on the production of complex phosphorus-potassium and nitrogen-phosphorus-potassium fertilizer by decomposition of washed and dried phosphoconcentrate from Central

Kyzylkum phosphorite with incomplete norms of sulfuric acid with the addition of potassium chloride, sulfate, ammonium nitrate and urea have been given. It has been revealed that the addition of potassium chloride and ammonium salts significantly affect on expansion coefficient and NP and NPK fertilizer generated are quite suitable for use in agriculture.

Keyword: Phosphorus-potassium fertilizer, nitrogen-phosphorus-potassium fertilize, phosphoriteIntroduction.

Mineral fertilizers play an important role in the growth and development of crops. Uzbek research institute of cotton has been already presented that cotton crop yields by 12/ga without fertilizer application but when application 225 kg/ha of nitrogen, 150 kg/ha P_2O_5 and 100 kg/ha of K_2O under the cotton plant can be yielded a guaranteed yield [1]. Science-based need of Agriculture of the Republic of Uzbekistan is 839.6 thousand tons of nitrogen fertilizers, 518.3 thousand tons of phosphorus and 278.9 thousand tons of potash fertilizers (based on 100% of nutrients). In 2015, the chemical industry of Uzbekistan produced 942.8 thousand tons of nitrogen, 153.8 thousand tons of phosphorus, 120 tons of potash fertilizer (calculated as 100% of nutrients). Nitrogen fertilizers cover the needs of agriculture completely. Deficiency of phosphorus and potash fertilizers is aggravated by the fact that the harvest is removed from the soil a large amount of nutrients.

It is known that one ton of raw cotton takes out annually 45 kg of nitrogen, 15 kg P_2O_5 and 45 kg K_2O from the soil. In addition one ton of wheat takes annually 35kg of N, 10kg of P_2O_5 and 24 kg of K_2O from the soil [2].

It should be noted, because other cultures also carry out of the soil a large amount of nutrients. Therefore, they must be filled in the soil. For that it is necessary rev up production of phosphorus and potassium fertilizers. However, the prospect of increasing the production of potash fertilizers is obvious that is connected with an increase in production capacity of Dehkanabad potash plant with 120 tons of K_2O per year to 360 thousand tons per year of K_2O, or in kind, to 200 tons of KCl a year to 600 thousand tons in year of KCl.

The prospect of increasing phosphate fertilizers production on the Kyzylkum phosphorite combine (KPP) increased from 400 to 716 tones per year of washed calcined phosphoconcentrate containing 26% of P_2O_5. However, these figures cover the needs of agriculture by only 30–35%. The disadvantages of the processing plant KPP is the generation of a huge number of poor, low-grade phosphate rock containing 12–16% of P_2O_5 due to lack of rational processing technology on fertilizer that pilled and stored in the waste piles.

Central Kyzylkum phosphorites have unique structural features that characterize their high reactivity.

Therefore, scientific and practical interest is the processing of this kind of phosphorite by incomplete normal of mineral acids, salts, used in agricultural production as standard mineral fertilizer in the novel forms of complex fertilizers, such as phosphorus-potassium, and nitrogen-phosphorus-potassium fertilizer.

Matter of phosphorus-producing and phosphorus-nitrogen-potassium fertilizer is that Kizilkum phosphorite is treated by incomplete sulfuric acid, followed by addition of potassium chloride, ammonium sulfate (nitrate) ammonium and carbamide. The high reactivity of calcareous phosphorite and in principle the possibility of transferring phosphorous of phosphorite in acceptable form in the presence of potassium chloride, ammonium sulfate (nitrate) and urea with minimum acid reagent flow yields novel types of compound fertilizers with different ratios of nutrients that meet the agricultural requirements.

The introduction of superphosphate type fertilizers potassium chloride, ammonium sulfate (nitrate) and urea not only promotes for obtaining complex fertilizers, but also improves the product properties.

As advantages proposed development are the following:

– development of intensive technology allows saving difficult –to-obtain sulfuric acid, energy supply to production;

– reduction of solid and dust-gas emissions;

– increase of phosphorous-potash and nitrogen-phosphorus-potassium fertilizer production;

– reduce of the fertilizer cost.

Proposed results of the studies are based on the study of the regularities of interaction of components in sulfuric acid processing of carbonate rock phosphate in view of features of their chemical and mineralogical composition in the presence of potassium chloride, ammonium sulfate, ammonium nitrate and urea, will allow to base scientifically and develop a rational technology of obtaining effective complex phosphorus-potassium and nitrogen-phosphorus-potassium fertilizer with minimum energy and resource costs.

There are well-done the technology [3–5] of nitric acid benefication of phosphorite from Central Kyzylkum and generation of PK- and NPK fertilizer. The studies are preliminary carried out, have shown the fundamental

possibility of applying this method to enrich high calcareous phosphorite. For isolation of calcium nitrate from nitric acid slurry organic solvent was used.

Development of intensive technologies for production of phosphorus-potassium and nitrogen-phosphorus-potassium fertilizer with low consumption of mineral acids and with the involvement of the local phosphorite from Kyzylkum in processing is an urgent task for currently.

Materials and Methods

To study the technology of novel kinds of complex phosphorus-potassium and nitrogen-phosphorus-potassium fertilizer it was used that washed and dried phosphorite concentrate with the chemical composition (wt,%): P_2O_5 22.74; CaO 42.9; MgO 2.26; CO_2 9.4; SO_3 2.24; F 1.71; R_2O_3 2.76; insoluble residue 8.23; H_2O 1.04 and physical and mechanical properties, and potassium chloride (K_2O 60%) Dehkanabad potash fertilizer plant (Table. 1).

Table 1. – Physico-chemical properties of washed and dried phosphorite concentrate and potassium chloride

Sample	Humidity, %	Density, g/см^3	Bulk weight, г/см^3	Angle of slide, °C	Fluidity, %
Washed and dried phosphorite concentrate	1.67	2.51	1.24	38	15
	2.11	2.63	1.32	45	23
	3.59	2.71	1.64	50	no fluidity
Potassium chloride	2.45	–	1.12	37	10

For determination of the optimum process conditions of the sulfuric acid decomposition of washed dried phosphorite concentrate from Kyzylkum phosphate was used sulfuric acid concentration of 93.0% in its rate of 60%. Norma acid calculated on the decomposition of phosphate and carbonate minerals phosphate mineral to generation of calcium monobasic phosphate and calcium sulfate.

Interaction of phosphorite with sulfuric acid proceeds very easily and practically no foam and is completed in 5–10 minutes. The process is exothermic, the temperature depending on the concentration and rates of sulfuric acid rises to 120 °C.

In order to develop the intensive technology of complex phosphorus-potassium fertilizer nutrients various ratios of sulfuric acid decomposition products of washed dried phosphorite concentrate are mixed thoroughly with fine-grained potassium chloride.

When a phosphorus-potassium fertilizer ratio of P_2O_5: K_2O = 1: (0.3–1), mixture was made of 100 grams of the product of the sulfuric acid decomposition phosphorite concentrate (acid norm is 60%) and 8.10–27.00 grams of potassium chloride. Granulation was carried out in the presence of water (moisture content 13–15% of H_2O).

To study the effect of potassium chloride on the degree of decomposition of washed dried phosphorite concentrate depending on the weight ratio of P_2O_5: K_2O = 1: (0.3–1) at a concentration of sulfuric acid is 93% and 60% of norm, homogeneous products obtained were granulated in a laboratory plate granulator and dried at a temperature of 100–105 °C.

As the synthesis of complex NPK-fertilizer intermediate is wet phosphorous-potassium fertilizer (P_2O_5: K_2O = 1:1), produced by mixing sulfuric acid decomposition products of washed dried concentrate (H_2SO_4 is 93%, the rate of 60% from stoichiometry) with potassium chloride, treated with nitrogen-containing compounds — ammonium sulphate, ammonium nitrate and urea.

The starting raw material and the products analyzed for the following components: nitrogen, phosphate, calcium, magnesium, sulfur, aluminum, iron, fluoride, carbonate, insoluble residue, water. Total nitrogen was determined by [6, 7]. The method based on the reduction of nitrate to ammonia nitrogen Devarda alloy, followed by distilling off the ammonia and titrimetric determination.

Determination of phosphate conducted differential photometric method [8]. The method is based on the formation of a yellow-colored complex phosphorus vanadium molybdenum and photometric absorbance measurements of the complex at a wavelength of λ = 430–450 nm. Extraction of total phosphate was performed with nitric acid, acceptable phosphate — citric acid, water-soluble phosphates was carried out. Calcium and magnesium were determined by complexometric [6, 9]. The method is based on the change in color of the indicator (calcein in determining the calcium and the acid chrome dark blue in the determination of magnesium) in the interaction of calcium ions and magnesium Trilon B. Sulphate is determined gravimetrically [6]. The method is based on the precipitation of barium sulphate chloride in acidic

Table 2. — Chemical composition of PK- and NPK- fertilizer based on washed and dried phosphorite concentrate (H_2SO_4 93%, norm 60%)

Weight ratio	$P_2O_{5\%}$			Content,%									
	Total	Acceptable	Water	CO_2	N	NO_3	SO_3	CaO	K_2O	KCl	$CaSO_4$	Nitrogen manner	H_2O
P_2O_5: K_2O	With KCl												
1:03	16.13	11.17	1.63	2.59	–	–	19.67	30.41	4.82	8.05	33.30	–	2.77
1:0.,5	15.14	10.57	1.62	2.43	–	–	18.47	28.56	7.48	12.61	31.30	–	2.61
1:0.7	14.51	10.18	1.65	2.31	–	–	17.71	27.37	10.07	16.65	30.00	–	2.50
1:.1	13.40	9.47	1.67	2.23	–	–	16.34	25.26	13.24	22.30	30.00	–	2.31
P_2O_5: K_2O: N	With $(NH_4)_2SO_4$												
1:1:0.3	13.93	9.77	1.42	2.32	4.15	–	17.00	26.28	13.91	23.20	28.80	19.68	2.40
1:1:0.5	12.26	8.76	1.33	2.04	6.02	–	15.38	23.13	12.20	20.42	25.35	28.87	2.81
1:1:0.7	10.95	7.83	1.25	1.82	7.64	–	13.68	20.66	10.85	18.24	22.64	36.16	2.51
1:1:1	9.46	6.83	1.09	1.57	9.40	–	11.54	17.85	9.25	15.76	19.56	44.60	2.17
P_2O_5: K_2O: N	With NH_4NO_3												
1:1:0.3	15.01	10.37	1.39	2.45	4.55	10.02	18.31	28.31	14.95	25.00	31.03	12.93	2.50
1:1:0.5	13.82	9.59	1.40	2.03	6.81	15.37	16.83	26.06	13.75	23.00	28.57	19.84	2.38
1:1:0.7	13.03	9.08	1.41	2.12	8.95	19.87	15.56	24.06	13.00	21.24	26.37	25.64	2.93
1:1:1	11.72	8.24	1.31	1.90	11.65	25.49	13.98	21.61	11.68	19.07	23.68	32.90	2.63
P_2O_5: K_2O: N	With $(NH_2)_2CO$												
1:1:0.3	15.93	11.03	1.57	2.58	4.63	–	18.98	28.30	15.88	25.89	32.14	9.82	2.67
1:1:0.5	14.51	10.29	1.51	2.41	7.20	–	17.70	27.30	14.51	24.16	30.00	15.80	2.50
1:1:0.7	14.29	10.68	1.64	2.48	10.24	–	18.22	28.20	14.29	24.89	30.90	22.74	2.57
1:1:1	12.44	8.98	1.46	2.07	12.55	–	15.18	23.46	12.42	20.71	25.71	27.14	2.85

medium and subsequent weighing of the precipitate. Iron and aluminum content was adjusted complexometric method [6]. The method is based on the titration of the iron in the presence of Trilon B sulfosalicylic acid as an indicator and back-titration of excess Trilon B solution of zinc sulfate to determine the presence of aluminum in the xylenol orange as indicator.

The fluorine content in the feedstock and products of decomposition was determined after nitric acid samples potentiometric method [6]. The method is based on measuring the concentration of fluoride in the solution using a fluoride selective electrode without fluorine extraction.

Carbon dioxide carbonates determined rapid volumetric method [6]. The method is based on the decomposition of carbonates hydrochloric acid and determining the amount of carbon dioxide emissions.

Results and discussion

The results of experimental data, both types of product phosphorus-potassium and nitrogen-phosphorus-potassium fertilizer (PK- and NPK are summarized in Table 2 in above.

As the results of the analysis of phosphorus-potassium and nitrogen-phosphorus-potassium fertilizer, obtained under optimum conditions from washed and dried concentrate phosphorus-potassium fertilizer, derived by the intensive method depending on the rate of potassium chloride contain 13.40–16.13% of total phosphorus of them 9.47–11.17% is in the form of acceptable for plants, 4.82–13.24% of K_2O. The amount of nutrients is 51.36–51.90%.

In the case of nitrogen-phosphorus-potassium fertilizers, you can see the following:

Depending on the rate of ammonium sulfate, the compound fertilizer contents 9.46–13.93% of P_2O_5, 4.15–9.40% of nitrogen and 6.25–9.20% of K_2O when moisture 2.17–2.40%. The amount of nutrients is about 43%.

In the application of ammonium nitrate there are 11.72–15.01% of P_2O_5, 4.55–11.65% of nitrogen and 7.57–9.92% of K_2O. The amount of nutrients is 56%.

As carbamide containing nitrogen-phosphorus-potassium fertilizer, depending on the rate of the additive contains 12.73–15.93% of total phosphorus, of which 8.98–11.03% are in acceptable form, 4.63–12.55% of the nitrogen in the amide form, 10.77–12.22% of potassium. The amount of nutrients is 58%.

As the analysis results show that addition of potassium chloride and nitrogen compounds significantly affect on expansion coefficient of washed and dried phosphorite concentrate that is to phosphorus-potassium fertilizer in the range 69.25–70.67%, and in case the application of ammonium salts lies in a range 69.09–72.20%.

Conclusion

Thus, there has been presented the possibility of obtaining phosphorus-potassium and nitrogen-phosphorus-potassium fertilizers on the basis of the sulfuric acid processing of washed dried phosphorite concentrate subsequent by addition of potassium chloride and ammonium sulphate and nitrate and urea. The products have a high amount of nutrients and expansion coefficient. These kinds of products can be recommended as a complex of PK- and NPK fertilizer for different cultures, where their performance will display even rather.

References:

1. Beglov B. M., Namazov Sh. S. Phosphorites Central Kyzylkum and processing. Tashkent. – 2013. – 460 p.
2. Handbook of chemicals used in agriculture. Moscow. Publishing House "Kolos". – 1980. – 560 p.
3. Nazirova R. M., Tadjiev S. M., Akbarova M. G., Ahmedova D. H., Mahsudova Z. I., Hayrullaev Ch. K. iintensive technology for production of PK and NPK fertilizer on the basis of local raw materials/In materials engineering and Republican Bukhara technological Institute of scientific and technical conference "Actual problems of chemical technology". Bukhara 8–9 April – 2014. – P. 3–4.
4. Tadjiev S. M., Tuhtaev S., Hayrullaev Ch. K., Shukurov I. D. Rational technology for producing stabilized complex fertilizers/The materials of Republican scientific-technical conference "Actual problems of chemical technology" Bukhara Engineering Technology Institute. Bukhara 8–9 April – 2014. – P. 5–6.
5. Tadjiev S. M., Tuhtaev S., Hayrullaev Ch. K., Shukurov I. D. The new stabilized nitrogen fertilizer – "bentoselitra"/The materials of Republican Bukhara Engineering Technology Institute of Scientific and Technical Conference "Actual problems of chemical technology". Bukhara 8–9. April – 2014. – P. 7–8.
6. Nazirova R. M., Tadjiev S. M., Akbarova M. G., Ahmedova D. H., Mahsudova Z. I., Hayrullaev Ch. K. Intensive technology for production of RK and NPK fertilizers on the basis of local raw materials/In materials engineering and Republican Bukhara technological Institute of scientific and technical conference "Actual problems of chemical technology". Bukhara 8–9. April – 2014 – P. 3–4.

7. Methods of analysis of phosphate rock, phosphate and compound fertilizers, feed phosphates./M. Vinnik, Erbanova LN etc. – M.: Chemistry. – 1975–218.
8. GOST 30181.4–94. Mineral fertilizer. Method for determination of total mass fraction of nitrogen in compound fertilizers and nitrate in ammonium and nitrate forms (Devarda method). – M.: Publisher IPC Standards, – 1996. – 8 p.
9. GOST 20851.2–75. Mineral fertilizer. Methods for determination of phosphate. – M.: Publisher IPC Standards, – 1997. – 37 p.

DOI: http://dx.doi.org/10.20534/AJT-16-9.10-95-100

Sobirov Mukhtorjon Mahammadjanovich,
Junior scientific researcher Academy
of Sciences Republic of Uzbekistan
Institute of General and inorganic chemistry,
Tashkent, Uzbekistan,
E-mail: fcb-m-2011@mail.ru

Tajiev Sayfuddin Muhitdinovich,
PhD in chemistry, Head of laboratory of Complex fertilizers,
Academy of Sciences Republic of Uzbekistan
Institute of General and inorganic chemistry,
Tashkent, Uzbekistan,
E-mail: sayf49@rambler.ru

Sultonov Bokhodir Elbekovich,
PhD in technique, senior reseacher of Laboratory of Phosphorous fertilizers,
Academy of Sciences of the Republic of Uzbekistan,
Institute of General and inorganic chemistry, Tashkent, Uzbekistan.
E-mail: bse-chemist-68@mail.ru

Obtainment of suspended phosphorus-potassium containing nitrate

Abstract: In this study, process of obtaining suspended phosphorus-potassium containing fertilizers based on decomposition phosphorite from Central Kyzylkum in nitric acid subsequence mixing potassium chloride and ammonium nitrate obtained by neutralization of nitric acid with gaseous ammonia, has been studied. It is determined that decomposition coefficient of phosphorite flour depending on the norm of nitric acid. Triple N: P_2O_5: K_2O fertilizer was obtained when ratio from 1:0.5:0.5 to 1:1:2.

Keywords: phosphorite flour, nitric acid, potassium chloride, processing phosphorite, and ammonium nitrate.

Introduction. There are some ways of producing complex fertilizers based on ammonium nitrate with phosphorus additives [1], potassium [2] or sulfur [3]. A drawback of known methods consists in using scarce and expensive reagents such as thermal phosphoric acid and potassium nitrate, and fine-dispersed ammonium sulphate.

In [4] the way for producing complex fertilizer based on ammonium nitrate containing, except nitrogen, has additionally another nutrient, namely phosphor comprising mixing the ammonium nitrate melt with a phosphorus reagent. For that way nitrogen-phosphate fertilizer is used as component which contents from 13 to 21% P_2O_5 and it is obtained by granulation method. The resulting complex fertilizer contents 32–34% of nitrogen and 2–6% P_2O_5, but drawback of the method is limited possibility of expanding the range of produced fertilizers. Besides, the method can not produce a triple NPK-fertilizer with potassium component in form potassium chloride that is available, as the introduction of the latter in the ammonium nitrate melt with a temperature of 170 °C will be result in decomposition of the explosive mixture.

A new trend in the improvement of fertilizer is to create suspended fertilizers, i. e. liquids, in which a supersaturated solution, the crystals of soluble salt nutri-

ent are in suspended condition. Application of fertilizers suspended allows obtaining any ratio of nutrients. The production does not require large capital investments, and can be as close as possible to the places of consumption. Using suspended fertilizer makes possible to organize individual providing nutrients to any particular field. Flexibility in the choice of the ratio between the nutrients components avoids making excessive doses of the mineral fertilizer, which not only reduces the cost of their purchase, but also improve the ecological environment clean and products.

Complex suspended fertilizers are convenient and profitable for farmers for several reasons. Advantage of fertilizers is complete absence of manual labor when using these fertilizers. There is the possibility of applying fertilizers with irrigation during preparation of soil for sowing, their combination with pesticides and other necessary ingredients. Farmers appreciate them for the benefits connected with uniformity of their application, and therefore, the synchronization of maturation of plant due to absence of caking and dissipation, characteristic for dry fertilizer mixtures.

Suspended fertilizer is also well-tested in the practice of the method and subsequent agrochemical effective for their application in various soils and for different crops. Notably it is widespread of this method has received in the United States and in countries Western Europe. Over 65% of liquid fertilizers are used in 10 leading agricultural states such as Iowa, Illinois, Nebraska, Californium, Texas, Indiana, Kansas, Ohio, Minnesota and Georgia [5].

It is well known that method of producing liquid nitrogen fertilizer by mixing urea, ammonium nitrate and the subsequent introduction in the composition of microelements [6]. The disadvantage of this fertilizer is the introduction of micronutrient is carried out by coarse dissolving them in a melt of ammonium nitrate, which complicates production technology. Moreover, it does not include other nutrients as phosphorus and potassium.

There is also a liquid nitrogen fertilizer, and its production method comprising urea, ammonium sulfate, ammonium nitrate and water. Fertilizer was created in order to maximize the use of ammonium sulfate solution, while maintaining the nitrogen content at a level that provides agrochemical efficiency of fertilizers and maintaining its properties during transportation and storage. The disadvantage of this fertilizer is that it contains only sulfur and nitrogen, does not include other macronutrients [7].

As it is from the above noted that development of rational technology of complex suspended nitrogen, phosphorus, potassium, and calcium-containing fertilizers based on nitric acid decomposition of phosphorite flour from Central Kyzylkum at a reduced norm of acid, potassium chloride and ammonia is a topical object.

Objects and methods. Experiments were conducted in a laboratory apparatus consisting of a tubular glass reactor equipped with helical stirrer driven by an electric motor. In the synthesis of new types of suspended fertilizers high calcareous containing phosphorite flour was used with composition (weight.%.): 17.55 — P_2O_5; 43.68 — CaO; 14.83 — CO_2; 1.68 — MgO; 2.47 — R_2O_3; 1.01 — SO_3; 2.17 — F; 1.19 — H_2O; 3.80 — insoluble residue, potassium chloride from Dehkanabad plant potassium fertilizers (K_2O — 60%), gaseous ammonia and 58.50% of nitric acid. Norma of nitric acid was varied in the range of 30–70% of the stoichiometry on the decomposition of carbonate and phosphate minerals of phosphorite flour to form calcium phosphate and calcium nitrate.

To obtain complex suspended phosphorus-potassium-nitrate the phosphorite flour was decomposed by first part of the nitric acid. The remainder of the nitric acid is neutralized with gaseous ammonia; this result in a 64.16% ammonium nitrate solution is formed. The decomposition process of phosphorite flour by acid is easily feasible. Interaction of the components is virtually completed within 15–20 min. The temperature of the process ranges at 30–45 °C according to the norm acid. To improve the quality and properties of the compound suspended fertilizer the calculated amount of 64.16% solution of ammonium nitrate and potassium chloride was added into obtained nitrogen phosphoric slurry under constant stirring. The water content of the slurry was maintained at 30% H_2O.

The contents of all forms of P2O5 (total, acceptable, water-soluble) in the products obtained was determined by photocalorimetric as a yellow complex phosphorus-vanadium- molybdenum complex on photo calorimeter CPC-3 (λ = 440 nm) [8]. The nitrogen content is by the distillation of ammonia on Kjeldahl and chloramine method [9]. Determination of potassium content in the obtained samples was determined as described in [10]. Determination of the content of all forms of calcium was carried out by complexometric titration volume Trilon B in the presence of calcein or chrome dark blue indicators [11]. Expansion coefficient (Ec) was calculated using the formula, where - P2O5acc. is an acceptable form of 2% citric acid, P2O5tot. is a total phosphorus content of the fertilizer samples. The water content in the obtained fertilizer samples was determined by calculation.

Results and discussion. The suspended nitrogen-phosphorus-potassium-calcium-containing fertilizer (N: P2O5: K2O = 1: 1: 1) obtained at 30% norm of nitric acid contains 7.10% of total nitrogen, of which 35.07% is in the ammonium and the remainder of 64.93% is in the nitrate form, 7.11% of P2O5total., of which 34.88% is in acceptable form, 7.10% of K2O, 17.67% of CaOtot. of which 34.52% of CaO is in acceptable form (Table. 1). It mainly consists of calcium nitrate – 12.46% ammonium nitrate – 14.21% of mono- and dicalcium phosphate, as well as phosphorite flour in activated form – 28.32% and potassium chloride – 11.83%. The amount of nutrients N + P2O5 + K2O + CaO is 38.98%.

Table 1. – Chemical composition of suspended phosphorus-potassium-containing nitrate, %

N: P_2O_5: K_2O	N			P_2O_5		CaO		K_2O	H_2O	Ec
	total	nitrate	ammo-nium	total	accep.	total	accep.			
When norm of HNO_3 30%										
1:0.5:0.5	11.01	6.33	4.68	5.5	1.99	13.70	4.79	5.50	27.25	36.18
1:0.7:0.5	9.29	5.61	3.67	6.50	2.31	16.21	5.63	4.64	27.68	35.54
1:0.7:0.7	9.02	5.46	3.57	6.31	2.25	15.72	5.47	6.31	26.84	35.66
1:1:1	7.10	4.61	2.49	7.11	2.48	17.67	6.10	7.10	26.45	34.88
1:1:2	6.34	4.11	2.22	6.35	2.23	15.80	5.46	12.69	23.65	35.12
When norm of HNO_3 40%										
1:0.5:0.5	10.97	6.58	4.39	5.48	2.53	13.65	6.22	5.48	27.26	46.17
1:0.7:0.5	9.25	5.92	3.33	6.48	2.96	16.13	7.32	4.62	27.69	45.68
1:0.7:0.7	8.98	5.75	3.23	6.29	2.88	15.66	7.11	6.29	26.86	45.79
1:1:1	7.06	4.94	2.12	7.07	3.19	17.59	7.94	7.07	26.47	45.12
1:1:2	6.32	4.41	1.89	6.32	2.86	15.74	7.11	12.63	23.68	45.25
When norm of HNO_3 50%										
1:0.5:0.5	10.93	6.81	4.11	5.46	3.11	13.60	7.66	5.46	27.27	56.96
1:0.7:0.5	9.21	6.22	2.99	6.45	3.63	16.06	9.04	4.60	27.70	56.28
1:0.7:0.7	8.94	6.04	2.91	6.26	3.53	15.59	8.77	6.26	26.87	56.39
1:1:1	7.03	5.27	1.76	7.02	3.9	17.51	9.79	7.03	26.48	55.56
1:1:2	6.29	4.71	1.57	6.29	3.51	15.67	8.76	12.58	23.71	55.80
When norm of HNO_3 60%										
1:0.5:0.5	10.94	7.11	3.83	5.46	3.65	13.61	9.06	5.47	27.27	66.85
1:0.7:0.5	9.23	6.54	2.67	6.46	4.28	16.08	10.66	4.61	27.69	66.25
1:0.7:0.7	8.96	6.35	2.60	6.27	4.16	15.61	10.35	6.27	26.86	66.35
1:1:1	6.66	5.32	1.33	6.65	4.36	16.58	10.96	6.66	26.67	65.56
1:1:2	5.99	4.78	1.20	5.99	3.94	14.92	9.87	11.99	24.01	65.78
When norm of HNO_3 70%										
1:0.5:0.5	10.95	7.4	3.55	5.47	4.13	13.63	10.50	5.47	27.26	75.50
1:0.7:0.5	9.24	6.88	2.36	6.47	4.86	16.11	12.34	4.62	27.69	75.12
1:0.7:0.7	8.97	6.68	2.29	6.28	4.72	15.63	11.97	6.28	26.86	75.16
1:1:1	6.31	5.37	0.94	6.32	4.72	15.73	12.07	6.31	26.84	74.68
1:1:2	5.70	4.85	0.85	5.71	4.27	14.23	10.92	11.42	24.29	74.78

With increasing amounts of ammonium nitrate to 26.75% in the composition of the slurry, i. e. with change the ratio of N: P_2O_5: K_2O of from 1: 1: 2 to 1: 0.5: 0.5, the decomposition coefficient of phosphorite flour is increased from 34.88% to 36.18%.

With an increase the norm of nitric acid from 40% to 70%, the content of acceptable phosphorus and calcium raised from 2.86% to 4.27%, from 7.11% to 10.92% respectively. The decomposition coefficient of phosphate flour increased from 45.25% to 74.78%.

We have also studied the change of water-soluble forms of calcium and phosphorus in the resulting phosphorus-potassium containing suspended nitrate (Fig. 1) depending on the norms of nitric acid and the ratio of nutrients. It is found that with increasing nitric acid water-soluble form of calcium and phosphorus increases. For example, at a ratio of N: P_2O_5: K_2O from 1: 1: 2 and a nitric acid norm of 30%, content water-soluble forms of phosphorus and calcium is 0.23% and 3.79% and the acid norm of 70% is equal to 1.23% and 8.04%, i. e. increased 5.35 and 2.12 times, respectively.

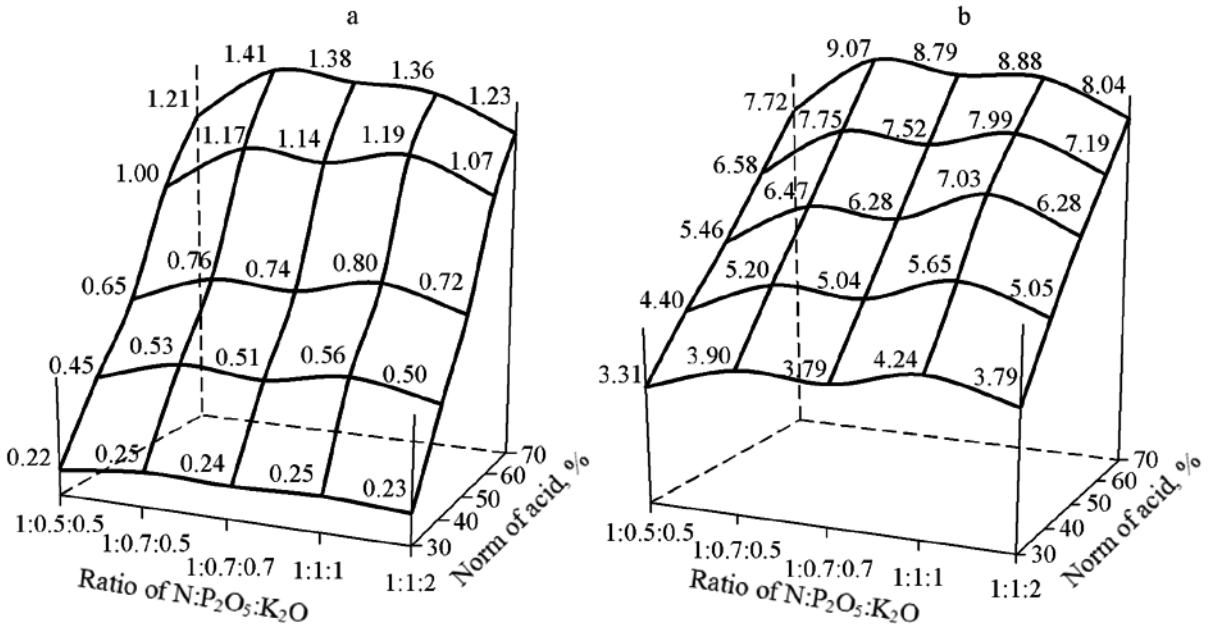

Figure 1. Changing water-soluble content of P_2O_5 (a) and CaO (b) depending on the norm of HNO_3 and ratio of N: P_2O_5: K_2O

Table 2. – Salt composition of suspended phosphorus-potassium –containing nitrate,%

N: P_2O_5: K_2O	NH_4NO_3	$Ca(NO_3)_2$	Mono-dicalcium phosphate	Activated phosphorite	H_2O	KCI
1	*2*	*3*	*4*	*5*	*6*	*7*
When norm of HNO_3 30%						
1:0.5:0.5	26.75	9.63	3.75	21.95	27.25	9.16
1:0.7:0.5	21.00	11.44	4.36	25.98	27.68	7.74
1:0.7:0.7	20.37	11.06	4.25	25.20	26.84	10.52
1:1:1	14.21	12.46	4.68	28.32	26.45	11.83
1:1:2	12.71	11.12	4.21	25.32	23.65	21.15
When norm of HNO_3 40%						
1:0.5:0.5	25.09	12.81	4.73	18.75	27.26	9.13
1:0.7:0.5	19.07	15.15	5.53	22.17	27.69	7.71
1:0.7:0.7	18.5	14.70	5.38	21.50	26.86	10.48
1:1:1	12.14	16.52	5.96	24.16	26.47	11.78
1:1:2	10.86	14.77	5.34	21.62	23.68	21.05
When norm of HNO_3 50%						
1:0.5:0.5	23.44	15.95	5.78	15.57	27.27	9.09
1:0.7:0.5	17.15	18.85	6.75	18.40	27.70	7.68
1:0.7:0.7	16.64	18.29	6.56	17.85	26.87	10.44
1:1:1	10.07	20.51	7.26	20.04	26.48	11.72
1:1:2	9.01	18.38	6.53	17.94	23.71	20.96

1	*2*	*3*	*4*	*5*	*6*	*7*
When norm of HNO_3 60%						
1:0.5:0.5	21.9	19.14	6.72	12.47	27.27	9.10
1:0.7:0.5	15.32	22.65	7.89	14.73	27.69	7.69
1:0.7:0.7	14.87	21.98	7.66	14.29	26.86	10.45
1:1:1	7.63	23.31	8.03	15.18	26.67	11.10
1:1:2	6.87	21.05	7.26	13.67	24.01	19.97
When norm of HNO_3 70%						
1:0.5:0.5	20.33	22.38	7.59	9.28	27.26	9.12
1:0.7:0.5	13.43	26.47	8.93	10.96	27.69	7.70
1:0.7:0.7	13.04	25.69	8.67	10.64	26.86	10.46
1:1:1	5.37	25.86	8.68	10.68	26.84	10.52
1:1:2	4.86	23.36	7.85	9.66	24.29	19.02

As it is seen from the tabulated data that with a change in a N: P_2O_5: K_2O salt composition of the complex suspended fertilizer changed considerably. For example, at a ratio of N: P_2O_5: K_2O = 1: 0.5: 0.5, and 30% norm of nitric acid, the suspended fertilizer composition is the following: calcium nitrate — 9.63% ammonium nitrate — 26.75% and mono- dicalcium phosphate — 3.75% and phosphorite flour in an activated form — 21.95% (Table 2.). By changing the ratio of N: P_2O_5: K_2O from 1: 0.5: 0.5 to 1: 1: 2 in one and the same norm of nitric acid in the obtained complex suspended fertilizer content of the main component is increased except the ammonium nitrate. For example, at a 50% norm of nitric acid with a change the ratio of N: P_2O_5: K_2O from 1: 0.5: 0.5 to 1: 1: 2 content of calcium nitrate, mono- and dicalcium phosphate, phosphorite flour in activated form is increased from 15.95 to 20.51 from 5.78 to 7.26, and from 15.57 to 20.04%, respectively, ammonium nitrate content is decreased from 23.44 to 9.01%.

The rheological properties of the suspended fertilizer: density, viscosity, and crystallization temperature are important as they determine the conditions of production, storage, transportation and application into the soil. Therefore, we was studied the rheological properties of the suspended complex fertilizers. Research shows that with an increase the temperature, decrease of viscosity and density of the fertilizer suspension are observed. The crystallization temperature of the suspended fertilizer varied from –6 to 7 °C. The suspended fertilizer containing higher concentrations of calcium nitrate, i. e. obtained at raised norm of nitric acid has higher crystallization temperature. pH of the suspended complex fertilizer depending on norm of acid and ratio of nutrients in the range 4.5–6.5.

Increasing the norm of nitric acid promotes increase of the acceptable forms of phosphorus and calcium, but it is unsuitable to increase the norm of acid from this point of view, since in this case there is overspending acid. Therefore, we consider that the optimal norm of nitric acid is 50–60%. The most common a N: P_2O_5: K_2O in the complex fertilizer for the main crops — cereals, sugar beet, cotton, potatoes, vegetables, fodder root crops — are the following: 1: 0.7: 0.5; 1: 1: 1, 1: 1: 2 ratio and these are optimal.

Conclusion. The principal possibility of obtaining new effective forms of suspended fertilizer universal action on the basis of local raw materials experimental way has been obtained. The proposed suspended complex NPK-fertilizer in comparison with standard solid mineral fertilizer is characterized by simple production and meets the basic requirements established in agricultural production.

References:

1. Production of ammonium nitrate in aggregates with high unit capacity/under editor V. M. Olevsky, second ed., – M.: Chemistry, – 1990, – 130–164 p.
2. RF patent № 2182144, IPC 7 S05G 1/001, publ. 10, 05, – 2002.
3. RF Patent № 2279416, publ. 10.07.2006.
4. RF patent № 2253639, IPC 7 S05S 1/02, publ. 10.06.2005.
5. Levin BV On the state and prospects for the production of mixed mineral fertilizers (fertilizer mixtures) in Russia//World of sulfur, N, P and K – 2009, – No3. 3–13 p.
6. Author's certificate USSR 1279982, MKI S05D 9/02 1983.
7. Patent RB TA (11) 3173 C1, S05S 9/00, S05S13/00, publ. 12.30. – 1999.

8. GOST 20851.2.75. Methods for determination of phosphorus content. – M.: Ed. standards, – 1983. – 22 p.
9. GOST 30181.4–94 Methods for determination of total mass fraction of nitrogen in compound fertilizers and nitrate in ammonium and nitrate forms (Devard method).//Intergovernmental Council for Standardization, Metrology and Certification – Minsk – 1996. – 7 p.
10. GOST 20851.3–93 Mineral fertilizers. Methods for determination of potassium. Intergovernmental Council for standarizatsii, Metrology and Certification – Minsk – 1995. – 11–18 p.
11. Vinnik M., Erbakova L. I., Zaitsev G. I. Methods for analysis of phosphate raw materials, phosphate and compound fertilizers, feed phosphates/ – M.: Chemistry, – 1975. – 218 p.

DOI: http://dx.doi.org/10.20534/AJT-16-9.10-100-104

Choriev Azimjon Uralovitch,
Karshi State University,
Senior Lecturer the Faculty of Natural Sciences,
Department of Chemistry
E-mail: azimjon-organik@mail.ru
Abdushukurov Anvar Kabirovitch,
National University of Uzbekistan
named after Mirzo Ulug'bek,
professor the Department of Organic Chemistry
E-mail: abdushukurov-ximik@mail.ru

Synthesis of 4-hydroxy-ω-chloracetophenones

Abstract: This paper reports a synthesis of 4-hydroxy-ω-chloracetophenone as a catalyst using $MoCI_5$, WCI_6, $SnCI_4$, VCI_3. The mechanism has not been studied. It was studied the influence of the ratio of reactants, catalysts' concentration and the time of synthesis in the reaction of obtaining 4-hydroxy-ω-chloracetophenone from phenol and chloride chloracetyl. The purified 4-hydroxy-ω-chloracetophenone is characterized in terms of physical-chemical properties.

Keywords: 4-hydroxy-ω-chloracetophenone, chloracetyl chloride, small quantities Lewis acids, IR spectrum.

4-Hydroxy-ω-chloracetophenone is an aromatic ketone formula $C_8H_7O_2CI$ and an important photochemical reaction used in perfumery and as a reagent in organic chemistry. 4-Hydroxy-ω-chloracetophenone acts as an optical filter being able to use the energy of UV radiation (promoting electrons into an excited state) and release this energy as heat to the environment (electrons returning to the initial state). This is possible because 4-hydroxy-ω-chloracetophenone singlet and triplet have close states in terms of energy.

4-Hydroxy-ω-chloracetophenone is used as a flavor ingredient, a flavor enhancer, perfume fixative in perfumery industry. In the composition of perfumes, cologne and scented soaps and UV light does not degrade the smell and color of these products. It is used as an additive for plastics, coatings and adhesive formulations [1, 5005–5010]. It is a component of sunscreen products and a plastic packaging can be added to block UV rays, protecting products within them [2, 3909–3916]. It is used in textile to protect them against degradation under the action of ultraviolete radiation [3, 53–62]. In preparations for solar protection, 4-hydroxy-ω-chloracetophenone is intended to absorb UV-A and UV-B, protecting the skin from the negative effects of tanning (sun). It is known that structure is unstable in terms of photochemical because under the influence of sunlight it forms reactive radicals, aggressive, in which scientists associates with oxidative stress in human cells, skin damage, etc. 4-hydroxy-ω-chloracetophenone and its derivatives are used as intermediates for dyes, in the manufacture of insecticides and pharmaceuticals, etc. [4, 145–149]. In the pharmaceutical industry are used for their anesthetic [5, 4818–4825] and anti-inflammatory properties [6, 3505–3514] etc. [7, 4046–4051]. It is a white solid

with the smell of rose, insoluble in water but soluble in benzene, tetrahydrofuran, methanol, and propylene glycol. 4-hydroxy-ω-chloracetophenone and its derivatives are synthesized by Friedel-Crafts reaction of aromatics. Acylation is done with acid chlorides or anhydrides. The reaction is catalyzed by Lewis acids, BF_3, $AlCl_3$, $FeCl_3$, $TiCl_4$ or $ZnCl_2$ [8, 1609–1610]. Nowadays, restrictions are imposed for waste minimization requiring the development of new catalytic technologies often based on solid catalysts. Various research groups have reported the use as a catalyst of the Friedel-Crafts acylation of phenole derivatives of various different metal oxides, for example a mixture of thorium dioxide, magnesium oxide, ZnO, etc. [9, 3442–3447].

Friedel-Crafts reaction of phenole and chloracetyl chloride in the presence of Lewis acid type catalysts ($AlCl_3$) or $MoCI_5$, WCI_6, $SnCI_4$, VCI_3 is used for the preparation of ω-chlor-para-hydroxyacetophenone (Scheme 1).

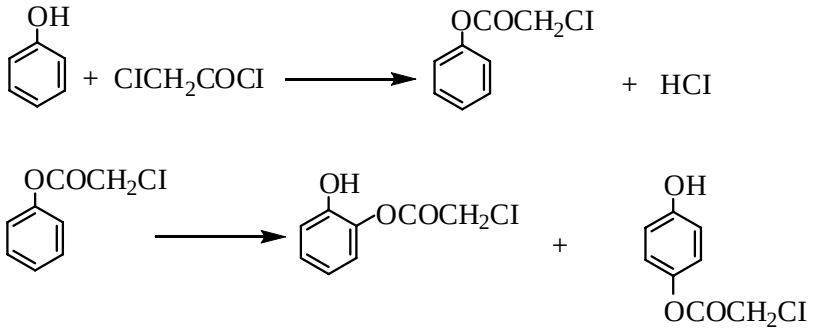

Scheme 1.

Reagents and materials

The reagents used were: phenole (99.5%), chloracetyl chloride (98%), $MoCI_5$ (98.5%), WCI_6 (99%), $SnCI_4$ (99%), VCI_3 (99.5%). Merck, Sigma Aldrich. In this paper reagents are used as such without further purification. Concentrated hydrochloric acid (37%) Sigma Aldrich, carbonyl sulphide and other materials are used without special treatment. Melting point determination is made using the device "Melting Point Meter" KRS-P1, the company Kruss Optronic GmbH. The IR spectrum was carried out using a Perkin Elmer FT-IR spectrophotometer — Spectrum 100.

Syntheses

In the syntheses with Lewis catalysts was used the classical method of synthesis. The work was done with phenole, chloracetyl chloride, carbon disulfide, anhydrous aluminum chloride and the mixture was heated at 40–45 °C. In the syntheses where $MoCI_5$, WCI_6, $SnCI_4$, VCI_3 was used it was also used a catalyst system for stirring the reaction mixture in order to obtain the most intimate contact between the catalyst and the reactants. After completion of the synthesis the catalyst is removed by filtration ($MoCI_5$, WCI_6, $SnCI_4$, VCI_3). $MoCI_5$, WCI_6, $SnCI_4$, VCI_3 powder is reused after washing it with dichloromethane and dried. Crude 4-hydroxy-ω-chloracetophenone obtained after syntheses was purified by recrystallization from ethanol, filtered and dried under vacuum.

Getting 4-hydroxy-ω-chloracetophenone is achieved by Friedel-Crafts reaction in the presence of $AlCl_3$ catalyst in good yields, and we tested the $MoCI_5$, WCI_6, $SnCI_4$, VCI_3 as catalyst. Laboratory syntheses were carried out in order to determine the influence of various parameters on the efficiency of the reaction of 4-hydroxy-ω-chloracetophenone: the variation ratio of the reactants, the variation in the catalyst concentration, reaction time, type of catalyst reaction.

The influence of the variation ratio of reactants

The syntheses were conducted with different molar ratios of the reactants chloracetyl chloride phenole, ratios ranging from 1:1 to 1:2 and 1:3. The chloracylation is generally used, working at reflux. The reaction temperature is 130–135 °C. The concentration of $MoCI_5$, WCI_6, $SnCI_4$, VCI_3 catalyst was 0.2% compared with chloracetyl chloride. The reaction is given by the excess phenole. The duration of the synthesis is 3 hours. In Table 1 is shown the variation of the yield depending on the ratio of reactants. As may be seen in Table 1 the yield increases with the increasing molar ratio of reactants. By working with a large excess of phenole (molar ratio chloracetyl dechlorinated phenole) of 1: 3 is obtained a high yield of 85.6% of 4-hydroxy-ω-chloracetophenone. Using a large excess of one reactant leads to increased reaction yields, but increases are not very spectacular and taking into account the need for recovery of phenole leading to increased costs it would be preferable to work with a ratio of chloracetyl chloride: phenole 1:2.

Influence of changes in concentration of the catalyst

To track variation's influence the concentration of $MoCI_5$, WCI_6, $SnCI_4$, VCI_3 catalyst use the following values: 0.001%, 0.002%, 0.005%, 0.01% (percentage by mass) from chloracetyl chloride. Synthesis duration is

two hours. Temperature is 130–135 °C. All syntheses were carried out with a molar ratio of chloracetyl chloride: phenole 1:2. The results are shown in Table 1.

Watching the graph in Table 1 shows that with increasing concentration of catalyst ($MoCI_5$, WCI_6, $SnCI_4$, VCI_3) increases the reaction yield, but the yield is very small increased after increasing the concentration from 0.2 to 1% yield increase by only 9%. It is therefore preferred to work with a concentration of catalyst ($MoCI_5$, WCI_6, $SnCI_4$, VCI_3) of 0.002%.

Table 1. – Chloracetylation of phenol in the presence of small quantities of $MoCI_5$, WCI_6, $SnCI_4$, VCI_3

№	Molar ratio of phenole: chloracetyl chloride: katalysator	Reaction time, hour	Temperature, °C	Yield,%	Reaction product by column chromatography,%	
					PCA*	4-HCA**
	$MoCI_5$					
1	$1:1:2{,}5.10^{-3}$	3	118–120	80	15	85
2	$1:1:5.10^{-4}$	2	118–120	85	23	77
3	$3:1:1{,}2.10^{-2}$	2	130–135	74	28	72
	WCI_6					
4	$1:1:1{,}5.10^{-3}$	3	118–120	78	30	70
5	$1:1:3.10^{-3}$	3	118–120	82	20	80
6	$3:1:7{,}4.10^{-3}$	2	130–135	73	32	68
	$SnCI_4$					
7	$1:1:1{,}1.10^{-3}$	3	118–120	81	24	76
8	$1:1:2{,}2.10^{-3}$	3	118–120	83	35	65
9	$3:1:7{,}4.10^{-3}$	2	130–135	66	51	49
	VCI_3					
10	$1:1:1{,}4.10^{-3}$	3	118–120	60	31	69
11	$1:1:2{,}8.10^{-3}$	3	118–120	72	36	64
12	$3:1:1{,}6.10^{-3}$	2	130–135	55	38	62

* – *phenylchloracetate*

** – *4-hydroxy-ω-chloracetophenone.*

The influence of reaction time

The observation of the influence of reaction time on the 4-hydroxy-ω-chloracetophenone synthesis by the Friedel-Crafts reaction in the presence of catalytic $MoCI_5$, WCI_6, $SnCI_4$, VCI_3 synthesis was accomplished by carrying out the reaction at different times. It increases the reaction time from 1, 2, 3 and 5 hours. The concentration of catalyst working with is 0.002% $MoCI_5$, WCI_6, $SnCI_4$, VCI_3 related to the amount of chloracetyl chloride. Synthesis temperature is the reflux (130–135 °C). The synthesis was carried out with a molar ratio of the reactants: Chloracetyl chloride: phenole 1:2. Low yield of the reaction is observed after one hour of synthesis. With increasing reaction time and yields are higher, but the increase is not significant. After 5 hours of synthesis the yield of 4-hydroxy-ω-chloracetophenone obtained practically is 88.20%. The influence of the catalyst type on the yield of reaction The influence of catalyst type synthesis by the reaction of 4-hydroxy-ω-chloracetophenone Friedel-Crafts acylation has been found by working with the acylation catalysts $AlCl_3$ as compared to the catalytic action of $MoCI_5$, WCI_6, $SnCI_4$, VCI_3. The reaction time is 3 hours. The concentration of catalyst which is employed is 0.002% related to the amount of chloracetyl chloride. Synthesis temperature is the reflux. The $MoCI_5$, WCI_6, $SnCI_4$, VCI_3 synthesis with synthesis temperature is 130–135 °C. When working with $AlCl_3$ catalyst, the reaction temperature is 40–45 °C, because it is currently working in the reaction of solvent carbon disulfide. (40% by mass in relation to the reaction mixture). The syntheses were carried out with a molar ratio of the reactants: Chloracetyl chloride: phenole 1:2.

Synthesized 4-hydroxy-ω-chloracetophenone was processed. In the first stage of the reaction mixture is filtered to remove the catalyst $MoCI_5$, WCI_6, $SnCI_4$, VCI_3. Then the clear solution is treated with water. Solution is treated with hydrogen chloride and passed into a separating funnel to separate the organic layer containing 4-hydroxy-ω-chloracetophenone. The solution is heated to remove the excess phenole. The resulting crude in the synthesis of 4-hydroxy-ω-chloracetophenone was made subject to a process of recrystallization for obtaining a pure compound. As the recrystallization solvent used is ethanol. 4-hydroxy-ω-chloracetophenone obtained and puri-

fied by recrystallization has been characterized from the physical-chemical point of view, the results are as follows: white crystals m. p. 58 °C, density 1.1 g/cm^3. 4-hydroxy-ω-chloracetophenone is soluble in alcohol, chloroform, ether, and very slightly soluble in water. In the IR spectrum can be observed some characteristic absorption bands (Figure 1).

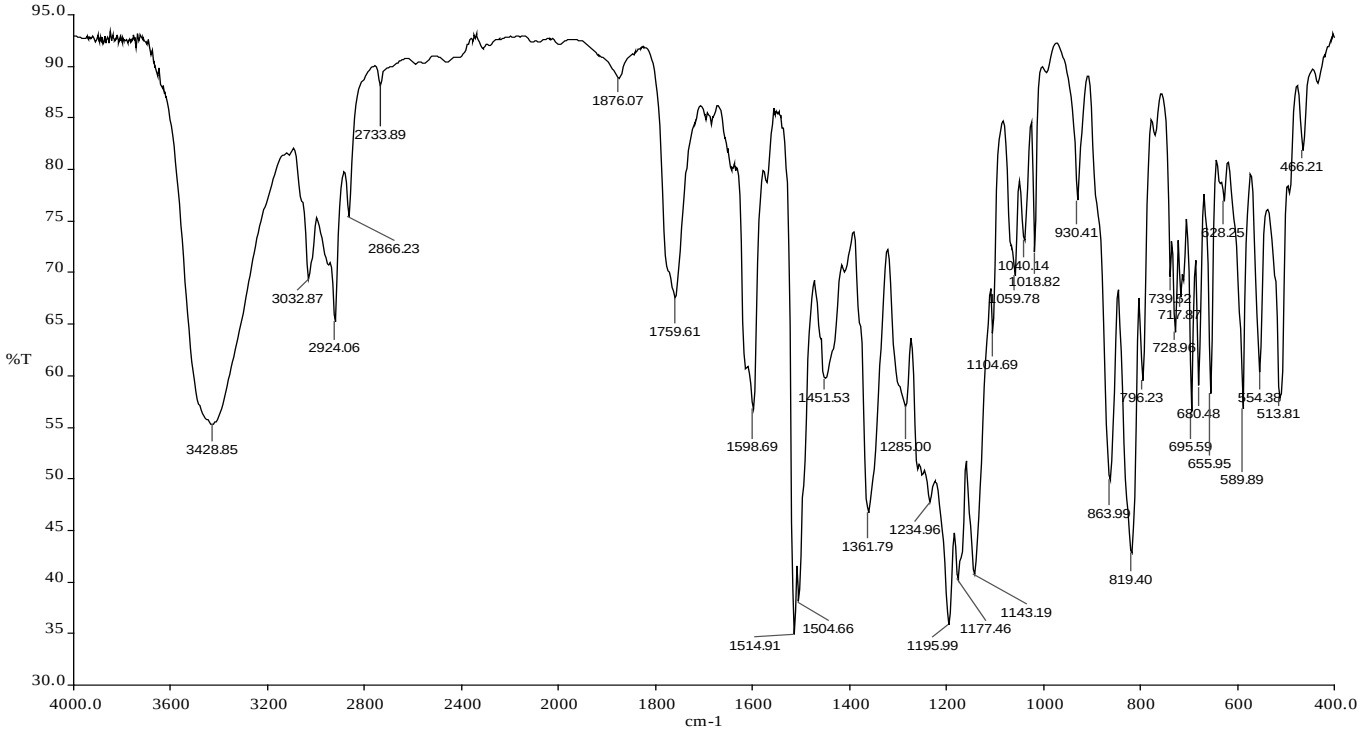

Figure 1. Is shown the IR spectra of 4-hydroxy-ω-chloracetophenone purified

The FT-IR spectrum of crystal ω-chlor-para-hydroxyacetophenone shows bands characteristic to υC-H stretching vibration at 3056 cm-1 aromatic (m) and 3010 cm-1 (m) respectively the characteristic band of deformation at δC-H 1447 cm-1 (s). Bands characteristic to υC=C stretching vibrations assigned to aromatic ring at 1594 cm-1 were confirmed at 1594 cm-1 (i) and 1493 cm-1 (vi), and between 944–764 cm-1 appears characteristic bands to δC-H bending vibrations (characteristic to aromatic nucleus). At 1759 cm-1 band appears very intense band attributed to υC=O stretching vibration (for ketones). In the spectrum appear intense and very intense bands at 1275–1135 cm-1range, assigned to the stretching vibrations υC-O.

Interesting results have been obtained in the synthesis of 4-hydroxy-ω-chloracetophenone as a catalyst using $MoCI_5$, WCI_6, $SnCI_4$, VCI_3. It is a heterogeneous catalyst which may be easily separated from the reaction mixture and re-used. It is not corrosive and does not produce secondary products. The mechanism has not been studied. It was studied the influence of the ratio of reactants, catalysts' concentration and the time of synthesis in the reaction of obtaining 4-hydroxy-ω-chloracetophenone from phenol and chloride chloracetyl. A comparison was made between the catalyst and catalysts' Friedel-Crafts chloracetylation classics: aluminum chloride, respectively. Under the same reaction conditions as those used in the synthesis of $MoCI_5$, WCI_6, $SnCI_4$, VCI_3 the yield was smaller than classical catalysts, which can be explained by a too low concentration of catalyst. The purified 4-hydroxy-ω-chloracetophenone is characterized in terms of physical-chemical properties.

References:

1. Kim J. K., Kim W. H., Lee D. H., "Adhesion properties of UV crosslinked polystyrene-block-polybutadieneblock-polystyrene copolymer and tackifier mixture", Polymer, 43 – (2002) – 5005–5010.
2. Zhang Z., Ren N., Li Y. F., Kunisue T., Gao D., Kannan K., "Determination of benzotriazole and benzophenone UV filters in sediment and sewage sludge.", Environmental Science &Technology, 45 (9) – (2011) – 3909–3916.
3. Saravanan D., "UV Protection Textile Material", Autex Research Journal, 7 (1) – (2007) – 53–62.
4. Cheng L., Zhang Y., Shi W., "Photoinitiating Characteristics of Benzophenone Derivatives as Type II Macromolecular Photoinitiators Used for UV Curable Resins", Chem. Res. Chinese Universities, 27 (1) – (2011) – 145–149.

5. Husain S. S., Nirthanan S., Ruesch D., Solt K., Cheng Q., Li G. D., Arevalo E., Olsen R. W., Raines D. E., Forman S. A., Cohen J. B., Miller K. W., "Synthesis of trifluoromethylaryl diazirine and benzophenone derivatives of etomidate that are potent general anesthetics and effective photolabels for probing sites on ligand-gated ion channels", J. Med. Chem., 49 (16) – (2006) – 4818–4825.
6. Venu T. D., Shashikanth S., Khanum S. A., Naveen S., Firdouse A., Sridhar A. M., Prasad J. S., "Synthesis and crystallographic analysis of benzophenone derivatives – The potential anti-inflammatory agents", Bioorganic & Medicinal Chemistry, 15 – (2007) – 3505–3514.
7. Ferris R. G., Hazen R. J., Roberts G. B., Clair M. H. S., Chan J. H., Romines K.R, Freeman G. A., Tidwell J. H., Schaller L. T., Cowan J. R., Short S. A., Weaver K. L., Selleseth D. W., Moniri K. R., Boone L. R., "Antiviral Activity of GW678248, a Novel Benzophenone Nonnucleoside Reverse Transcriptase Inhibitor", Antimicrobial Agents and Chemotherapy, 49 (10) – (2005) – 4046–4051.
8. Manivel P., Roopan S. M., Khan F. N., "Synthesis of o-Substituted Benzophenones by Grignard Reaction of 3-Substituted Isocoumarins", J. Chil. Chem. Soc., 53 (3) – (2008) – 1609–1610.
9. Ashoka S., Chithaiah P., Thipperudaiah K. V., Chandrappa G. T., "Nanostructural zinc oxide hollow spheres: A facile synthesis and catalytic properties", Inorganica Chimica Acta, 363 (13) – (2010) – 3442–3447.

DOI: http://dx.doi.org/10.20534/AJT-16-9.10-104-107

Yuldasheva Mukhabbat Razzoqberdievna,
National university of Uzbekistan,
the Faculty of Chemistry
E-mail: ymuxabbat@bk.ru

Synthesis and analysis of aryl methyl amines

Abstract: Synthesis of alkyl amines derivatives of aromatic hydrocarbons. The structure of the obtained 2,4-demethylbenzylamine, 2,5- dimethybenzylamine, 2,4,6-threemethyl 3,5-di (N-aminomethyl) nitrobenzene was determined by means of IR spectroscopy and chromato-mass-spectrometry**.**

Keywords: aromatic hydrocarbons, xylenes, nitro-mesitylene, amidoalkylation, N-hydroxyalkylimide, alkyl amines of aromatic hydrocarbons.

Aromatic compounds and their functional derivatives are the most widen and important class of organic compounds on the base of the chemical transformations of which can be solved the fundamental problems influential ability reflectional reactivity of aromatic substrates and alkylating reagents by using various catalysts.

Continuing systematically investigation of reaction amidoalkylation of aromatic hydrocarbons [1-3], we have studied the amidoalkylation of xylenes and nitromezitilena in the presence of proton catalysts, also synthesized aryl alkyl amines.

We investigated synthesis arylalkylimides from amidalkyl reaction using from m-xylene which is substitutents of the aromatic ring methyl groups in a consistent orientation and easy reacts with N-hydroxymethylftalimide (N-MFI) by electrophilic substitution. Starting materials for this reaction: m-xylene, N-MFI, cons H_2SO_4:H_3PO_4 were taken 6:1:2:1 mol and reaction was continued by string at 120 °C for four hours. The result of this reaction 1,3-dimethyl-4-(N-phthalimidomethyl)benzene is obtained in yield 73%. Experimental section contains the IQ-spectrum of compound and H^1spectra were obtained 2,29d (6H, $2CH_3$), 4,6 s (2H, CH_2), 6,9d (3H, Ar_3H_3), 7,75 m (4H, ArR_2H_4). Subsequent treatment with β-hydroxoethylphthalimide under the usual reaction conditions afforded substance in 76% yield.

Similarly, the compound of p-xylene's with phthalimidialkyl synthesized as an ordered stages above. The reaction of para- xylene's with N-MFI, H_3PO_4 and H_2SO_4 is prolonged for six hours. The result of this reaction 1,4-dimethyl 2-(N-phthalimidomethyl) benzene is obtained in yield 78%.

The reaction of nitrogen mezitilen with N-methylolphthalimid is carried by one mol out. Phosphoric acid is used as a catalysis. It is defined that in this reaction all substitutents of benzene ring have obtained consistent orientation so that reason it gives a opportunity to make bis-amidalkyle and separate 2,4,6- threemethyl 3,5-di-(N-phthalimidomethyl) nitro benzene by string at 120 °C in 65% yield.

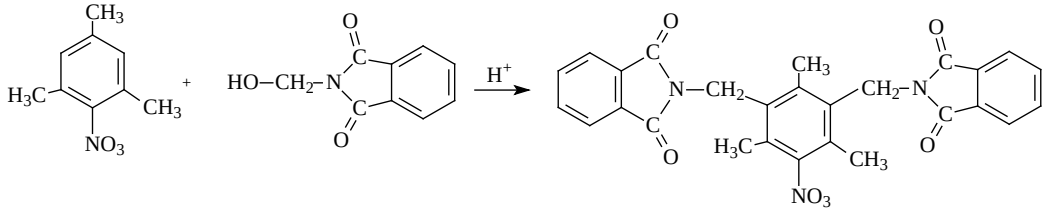

In it's IR-spectrum the following characterical bands (ν, sm^{-1}) were observed: 890 (substituted benzene), 1605 (C-C в ArH), 3030 (=C-H в ArH), 1439 (CH_3), 2933 ($\nu_s CH_2$), 1400,1460(δCH_2) 2873($\nu_s CH_2$), 2980($\nu_{as} CH_3$).

Next experiments associated with hydroxylation of amidoalkyl products of nitromezethylen and m-, p- xylenes with ammonia and NaOH. It is defined that different products can be taken from hydroxylation according to type and quantity of reagents. The hydroxylation reaction of 1,3-dimethyl 4-(N-phthalimidomethyl) benzene is carried out with 25% ammonia water. If ammonia is taken 1:1 mol it would produce arylalkylamine and amide of phthalic acid.

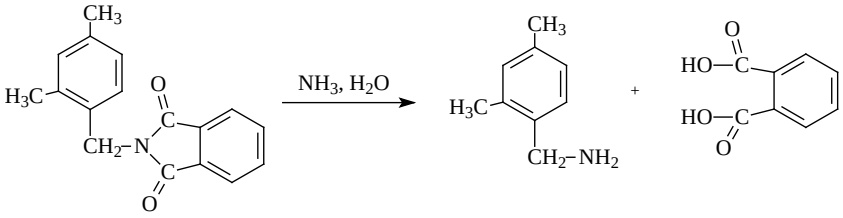

When 2,4-demethylbenzylamine is put to chromato-mass-spectra in a condition which we have chosen after 16.001 minutes we can see ions of 2,4- dimethylbenzyl. In addition, the particular reorientation of xenon on aromatic nuclear leads to create ammonia ions which can be seen at chromato-mass-spectrometry.

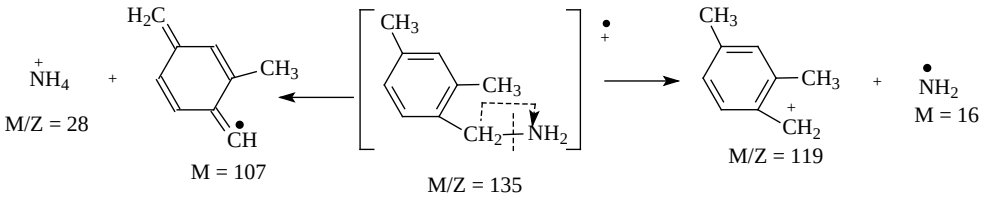

In MS molecules are broken apart and produced narrow piece of ions [128]. Breaking apart ions of 2,4- dimethylbenzyl are illustrated below. First of all, the ions of 3- methylbenzyl are created at 105 M/Z. These ions reorientated like an aromatic compounds which contain methylen group and produced benzyl ions removing a small amount of methene at 91 M/Z, while the breaking apart higher amount of ethelen compare to benzyl ions amount produces phenyl ions at 77 M/Z.

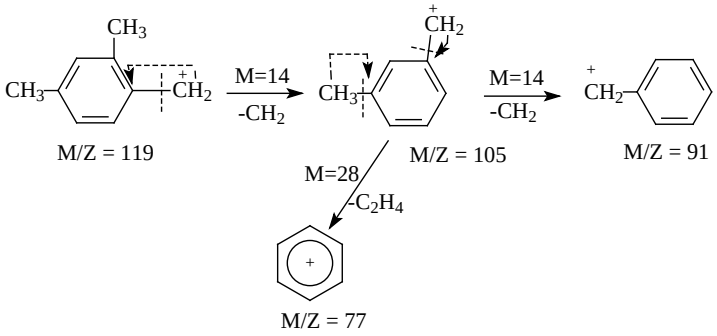

It is obvious that the ion of benzyl at 91M/Z produces phenyl ions at 77M/Z.

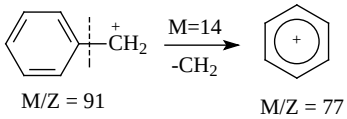

Generally view of direction of fragmetation in chromato-mass-spectrium is represented below:

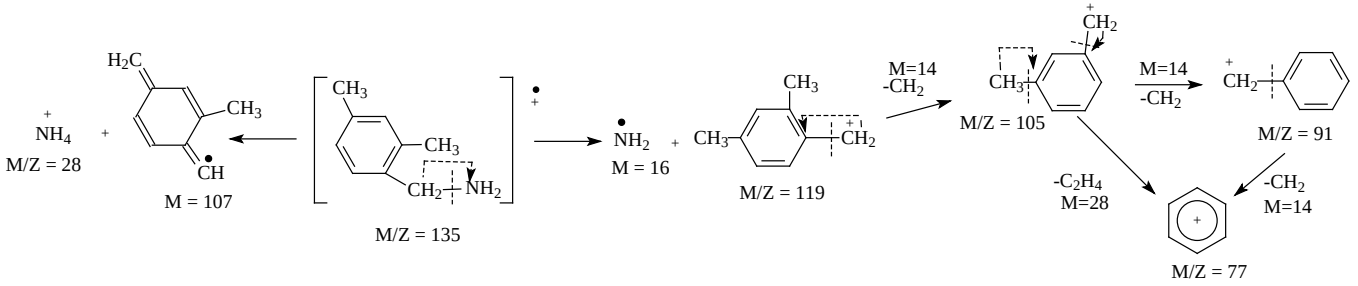

In it's IR-spectrum there are following typical bands of absorption (ν, sm^{-1}): 979, 942 (1,2,4- threesubstituted benzene), 1615, 1599 (C-C в ArH), 3030 (=C-H в ArH), 1717, 3488 ($-NH_2$), 2900 ($\nu_S CH_3$), 2951 ($\nu_{as} CH_3$), 1392 (δCH_3), 2845 ($\nu_S CH_2$), 1465 (δCH_2).

The molecular ions of phthtalic acid which synthesized by hydroxylation of 2,4-dimethylbenzyl amine's are demonstrated after 16,708 minutes at 166 M/Z in mass-spectra.

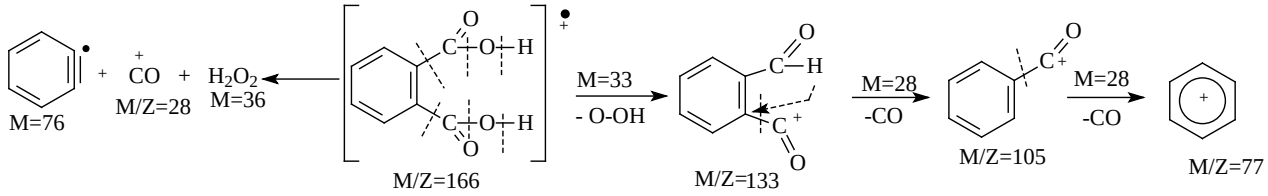

From this picture you can see fully view of producing ion fragments from the molecular ions.

Hydroxylation of 1,4-dimethyl 2-(N-phthalimidomethyl) benzene is occurred in the mixture of kalium hydroxyl's with water and ethanol 1:2 molls. After separating water from mixture, remnants are melted in the methanol. The residue of phthalic acid salt doesn't melt in the methanol. The amine which melted in the methanol can be separated with the help of evaporation method. The hydroxylation afforded 2,5- dimethybenzylamine in 98% yield:

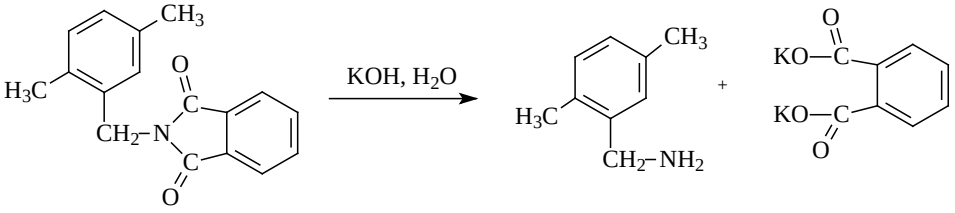

In 2,5-dimethybenzylamine's IR-spectrum there are following typical bands of absorption (ν, sm^{-1}): 958, 802 (1,2,4- threesubstituted benzene), 1600 (C-C в ArH), 3005 (=C-H в ArH), 1708, 3114 ($-NH_2$), 2906 ($\nu_S CH_3$), 2951 ($\nu_{as} CH_3$), 1392 (δCH_3), 2845 ($\nu_S CH_2$), 1467 (δCH_2).

1,3,5-Threemethyl 2,6-di (N-phthalimidomethyl) nitrobenzene is hydrolysed by 25% ammonia aqua. Hydroxylation process is carried out since boiling temperature of water and 1,3,5-threemethyl 2,6-di (N-phthalimidomethyl)nitro benzene in 98% yield. Due to ammonia takes excessive amount the arylalklylamine and amide of phthalic acid are produced. The equation of hydrolysis reaction:

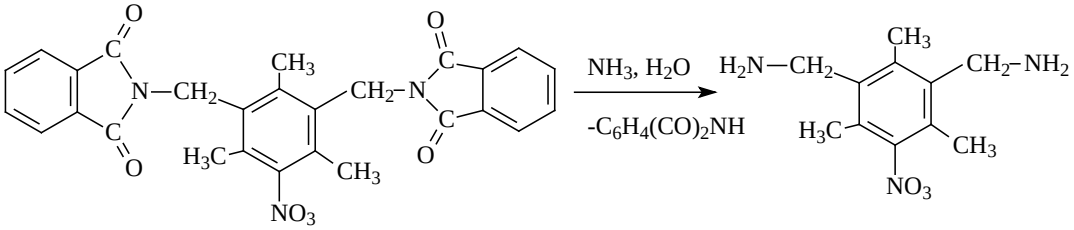

The molecular ions of 2,4,6-threemethyl 3,5-di (N-aminomethyl) nitrobenzene demonstrates after 25,802 minutes at 224 M/Z.

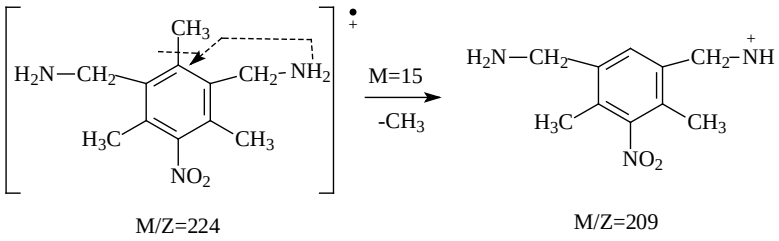

The piece of ions is produced from ordered disintegration of CH_2, NH_2, and NO_2 molecular ions at 209 M/Z.

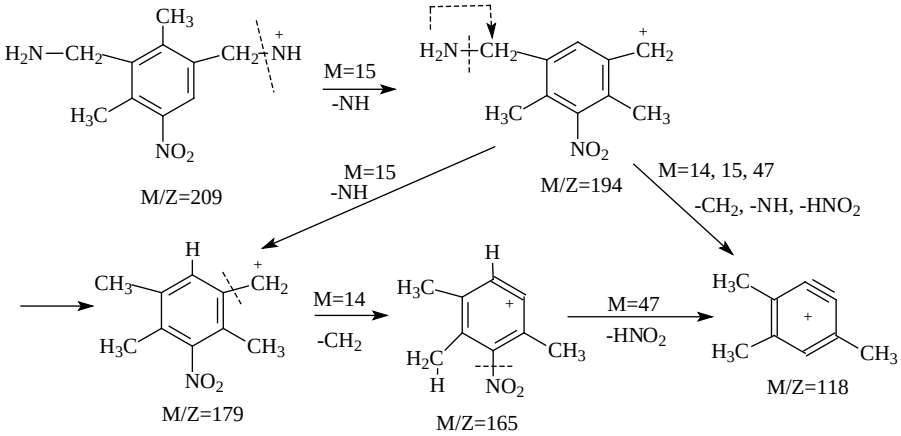

The main part of these ions are produced at 118 M/Z and they also disintegrated more small piece of ions.

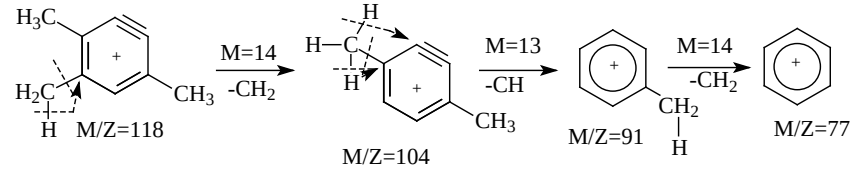

The general view of reaction

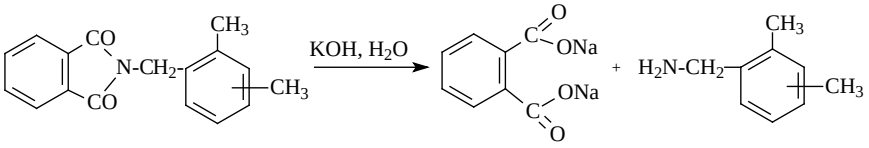

Initially, the bond of carbon-nitrogen is broken cause of hydroxyl group connected with carbonyl group. Due to breaking C-N bond, redistribution electrons of the second carbonyl group which is strong positive charged and easy attack of hydroxyl group.

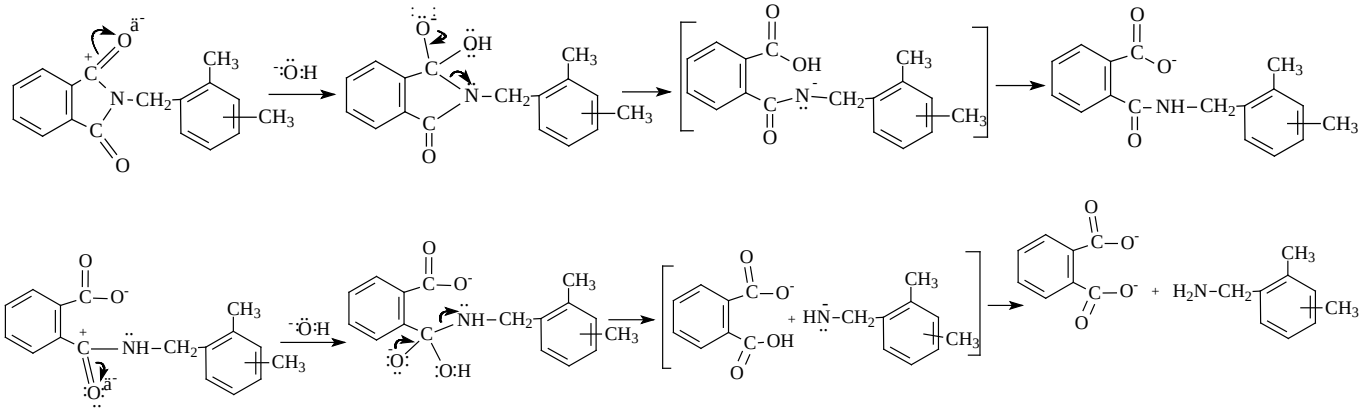

It is possible synthesis the highest yield of amines by hydroxylation the products of phthalimidoalkylaryl in a base condition.

– If ammonia is taken 1:1 mol (ekvimolar) it would produce arylalkylamine and amide of phthalic acid, if it takes in an excessive 1:2 mol it would produce arylmethylamine and amide of phthalic acid.

– Hydrolysis of phthalimidoalkylarys with kalium hydroxide produces kalium salt of phthalic acid and arylalkylamines.

References:

1. Axmedov Q.N., Okmanov R.Y. Yuldasheva M.R. Benzodioqsan-1,4ni β-gidroksi- va β-brometilftalimid bilan amidoalkillash. – 2009. Вестник НУУз – No 3. – С.67–69.
2. Ахмедов К.Н., Юлдашева М.Р., Турсунова М.Р. Взаимодействие изомерных ксилолов с N-бром-метилфталимидом в присутствии каталитических количеств катализаторов. Узб.Хим. Журн. – 2006 – №2. С. 28–32.
3. Axmedov Q.N., Yuldasheva M.R. Mezitilen va psevdokumolning ftalimidoalkil hosilalari sintezi. O'z RFM. – 2013. – №4. – С.42–45.

Contents